

Sensor and Simulation Notes

Note 207

January 1975

Analysis of Periodic Structures for Trapping Electrons
in EMP Simulators

Shyam H. Gurbaxani
Donald E. Jones
The University of New Mexico
College of Engineering
Bureau of Engineering Research
Albuquerque, New Mexico 87131

CLEARED
FOR PUBLIC RELEASE
PL/PA 5/15/87

Abstract

In the System Generated Electromagnetic Pulse (SGEMP) simulators a flux of high energy photons is introduced into a vacuum chamber. These photons strike the walls of the chamber, producing Compton electrons. As this effect is not present in the environment to be simulated, it is desirable to prevent these electrons from entering the working volume of the chamber.

In this paper a method of containing these electrons is considered. It is proposed that a grid of wires be placed parallel to the chamber wall and raised to a high negative potential, thus repelling the electrons and containing them between the chamber wall and the grid. The results of a computer study undertaken to evaluate this approach are presented.

The electrostatic potential is determined by the use of a line charge approximation for grids consisting of wire of small cross section. For wires of larger cross section a series solution is employed; the coefficients of the series are determined using a least squares fit. Finally, the effectiveness of the grids as electron traps is evaluated by calculating the trajectories of electrons having various kinetic energies, positions, and angles of departures.

This study was performed under subcontract to

The Dikewood Corporation
1009 Bradbury Drive, S.E.
University Research Park
Albuquerque, New Mexico 87106

PL 9/6-1000

TABLE OF CONTENTS

<u>Section</u>	<u>Page</u>
INTRODUCTION	12
I. LINE CHARGE APPROXIMATION	18
1. Simplifying Assumptions	18
2. Single Grid of Wires	18
3. Double Grid of Wires	22
4. Limits on Wire Size for Line Charge Approximation	24
II. GRIDS OF LARGE RADII CONDUCTORS	30
1. Need for Series Solution	30
2. Parallel Cylindrical Conductor Case	30
3. Crossed Cylindrical Conductor Case	36
4. Application of the Line Charge Solution to the Large Radii Cylindrical Conductor Cases	41
5. Least Squared Error Fitting	42
III. ELECTRON TRAJECTORIES	54
1. Need for Electron Trajectories	54
2. Calculation of Electron Trajectories	54
3. Some Approximations for Determining Whether an Electron Will Escape	57
IV. COMPUTER SOLUTIONS	59
1. Preliminaries	59
2. Single Grid of Small Radii Conductors	60
3. Double Grid of Small Radii Conductors	116
4. Parallel Cylindrical Conductors Case	128
5. Crossed Cylindrical Conductors Case	138
6. High Energy Approximation	159

<u>Section</u>	<u>Page</u>
V. CONCLUSIONS AND FUTURE WORK	164
1. Conclusions	164
2. Future Work	165
REFERENCES	167
APPENDICES	168
A. SERIES COEFFICIENTS	168
1. General	168
2. Parallel Cylindrical Conductor Case	168
3. Crossed Cylindrical Conductor Case	174
B. COMPUTER PROGRAMS	182

LIST OF FIGURES

<u>Figure</u>		<u>Page</u>
1	A SGEMP Simulator	14
2	A Wire Grid Near a Ground Plane	15
I-1	A Single Grid of Line Charges	19
I-2	A Set of Parallel Line Charges	20
I-3	A Double Grid of Line Charges	23
I-4	A Set of Parallel Line Charges with a Point on a Circle of Radius δ	25
II-1	A Set of Parallel Cylindrical Conductors	31
II-2	A Set of Crossed Cylindrical Conductors	37
II-3	Crossed Cylindrical Conductors--Top View	39
II-4	A Set of Parallel Cylindrical Conductors	44
II-5	A Set of Crossed Cylindrical Conductors	50
IV-1	Coordinate System and Angles	60
IV-2a	Normalized Potential Contour Plot for $b/a = 1.0$ and $z = 0$	61
IV-2b	Normalized Potential Contour Plot for $b/a = 1.0$ and $z = a/4$	62
IV-2c	Normalized Potential Contour Plot for $b/a = 1.0$ and $z = a/2$	63
IV-2d	Normalized Potential Contour Plot for $b/a = 1.0$ and $z = 3a/4$	64
IV-2e	Normalized Potential Contour Plot for $b/a = 1.0$ and $z = a$	65
IV-3a	Normalized Potential Contour Plot for $b/a = .5$ and $z = 0$	66
IV-3b	Normalized Potential Contour Plot for $b/a = .5$ and $z = a/4$	67
IV-3c	Normalized Potential Contour Plot for $b/a = .5$ and $z = a/2$	68

<u>Figure</u>	<u>Page</u>
IV-3d Normalized Potential Contour Plot for $b/a = .5$ and $z = 3a/4$	69
IV-3e Normalized Potential Contour Plot for $b/a = .5$ and $z = a$	70
IV-4a Electron Trajectories for $b/a = 1.0$, Normalized Energy of 1.1, $B = 0$ radian and $\theta = 0^\circ$	72
IV-4b Electron Trajectories for $b/a = 1.0$, Normalized Energy of 1.1, $B = 0$ radian and $\theta = 10^\circ$	73
IV-4c Electron Trajectories for $b/a = 1.0$, Normalized Energy of 1.1, $B = 0$ radian and $\theta = 20^\circ$	74
IV-4d Electron Trajectories for $b/a = 1.0$, Normalized Energy of 1.1, $B = 0$ radian and $\theta = 30^\circ$	75
IV-4e Electron Trajectories for $b/a = 1.0$, Normalized Energy of 1.1, $B = \pi/8$ radians and $\theta = 10^\circ$	76
IV-4f Electron Trajectories for $b/a = 1.0$, Normalized Energy of 1.1, $B = \pi/8$ radians and $\theta = 20^\circ$	77
IV-4g Electron Trajectories for $b/a = 1.0$, Normalized Energy of 1.1, $B = \pi/8$ radians and $\theta = 30^\circ$	78
IV-4h Electron Trajectories for $b/a = 1.0$, Normalized Energy of 1.1, $B = \pi/4$ radians and $\theta = 10^\circ$	79
IV-4i Electron Trajectories for $b/a = 1.0$, Normalized Energy of 1.1, $B = \pi/4$ radians and $\theta = 20^\circ$	80
IV-4j Electron Trajectories for $b/a = 1.0$, Normalized Energy of 1.1, $B = \pi/4$ radians and $\theta = 30^\circ$	81
IV-5a Electron Trajectories for $b/a = 1.0$, Normalized Energy of 1.3, $B = 0$ radians and $\theta = 0^\circ$	82
IV-5b Electron Trajectories for $b/a = 1.0$, Normalized Energy of 1.3, $B = 0$ radians and $\theta = 10^\circ$	83

<u>Figure</u>	<u>Page</u>
IV-5c Electron Trajectories for $b/a = 1.0$, Normalized Energy of 1.3, $B = 0$ radians and $\theta = 20^\circ$	84
IV-5d Electron Trajectories for $b/a = 1.0$, Normalized Energy of 1.3, $B = 0$ radians and $\theta = 30^\circ$	85
IV-5e Electron Trajectories for $b/a = 1.0$, Normalized Energy of 1.3, $B = \pi/8$ radians and $\theta = 10^\circ$	86
IV-5f Electron Trajectories for $b/a = 1.0$, Normalized Energy of 1.3, $B = \pi/8$ radians and $\theta = 20^\circ$	87
IV-5g Electron Trajectories for $b/a = 1.0$, Normalized Energy of 1.3, $B = \pi/8$ radians and $\theta = 30^\circ$	88
IV-5h Electron Trajectories for $b/a = 1.0$, Normalized Energy of 1.3, $B = \pi/4$ radians and $\theta = 10^\circ$	89
IV-5i Electron Trajectories for $b/a = 1.0$, Normalized Energy of 1.3, $B = \pi/4$ radians and $\theta = 20^\circ$	90
IV-5j Electron Trajectories for $b/a = 1.0$, Normalized Energy of 1.3, $B = \pi/4$ radians and $\theta = 30^\circ$	91
IV-6a Electron Trajectories for $b/a = 1.0$, Normalized Energy of 2.0, $B = 0$ radians and $\theta = 0^\circ$	92
IV-6b Electron Trajectories for $b/a = 1.0$, Normalized Energy of 2.0, $B = 0$ radians and $\theta = 10^\circ$	93
IV-6c Electron Trajectories for $b/a = 1.0$, Normalized Energy of 2.0, $B = 0$ radians and $\theta = 20^\circ$	94
IV-6d Electron Trajectories for $b/a = 1.0$, Normalized Energy of 2.0, $B = 0$ radians and $\theta = 30^\circ$	95
IV-6e Electron Trajectories for $b/a = 1.0$, Normalized Energy of 2.0, $B = \pi/8$ radians and $\theta = 10^\circ$	96

<u>Figure</u>		<u>Page</u>
IV-6f	Electron Trajectories for $b/a = 1.0$, Normalized Energy of 2.0, $B = \pi/8$ radians and $\theta = 20^\circ$	97
IV-6g	Electron Trajectories for $b/a = 1.0$, Normalized Energy of 2.0, $B = \pi/8$ radians and $\theta = 30^\circ$	98
IV-6h	Electron Trajectories for $b/a = 1.0$, Normalized Energy of 2.0, $B = \pi/4$ radians and $\theta = 10^\circ$	99
IV-6i	Electron Trajectories for $b/a = 1.0$, Normalized Energy of 2.0, $B = \pi/4$ radians and $\theta = 20^\circ$	100
IV-6j	Electron Trajectories for $b/a = 1.0$, Normalized Energy of 2.0, $B = \pi/4$ radians and $\theta = 30^\circ$	101
IV-7a	Electron Trajectories for $b/a = .5$, Normalized Energy of 1.1, $B = 0$ radians and $\theta = 0^\circ$	102
IV-7b	Electron Trajectories for $b/a = .5$, Normalized Energy of 1.1, $B = 0$ radians and $\theta = 10^\circ$	103
IV-7c	Electron Trajectories for $b/a = .5$, Normalized Energy of 1.1, $B = 0$ radians and $\theta = 20^\circ$	104
IV-7d	Electron Trajectories for $b/a = .5$, Normalized Energy of 1.1, $B = 0$ radians and $\theta = 30^\circ$	105
IV-7e	Electron Trajectories for $b/a = .5$, Normalized Energy of 1.1, $B = \pi/8$ radians and $\theta = 10^\circ$	106
IV-7f	Electron Trajectories for $b/a = .5$, Normalized Energy of 1.1, $B = \pi/8$ radians and $\theta = 20^\circ$	107
IV-7g	Electron Trajectories for $b/a = .5$, Normalized Energy of 1.1, $B = \pi/8$ radians and $\theta = 30^\circ$	108
IV-7h	Electron Trajectories for $b/a = .5$, Normalized Energy of 1.1, $B = \pi/4$ radians and $\theta = 10^\circ$	109

<u>Figure</u>	<u>Page</u>
IV-7i Electron Trajectories for $b/a = .5$, Normalized Energy of 1.1, $B = \pi/4$ radians and $\theta = 20^\circ$	110
IV-7j Electron Trajectories for $b/a = .5$, Normalized Energy of 1.1, $B = \pi/4$ radians and $\theta = 30^\circ$	111
IV-8a Fraction of Electrons Escaping (F_e) for $b/a = 1.0$	113
IV-8b Fraction of Electrons Escaping (F_e) for $b/a = 1.0$	113
IV-8c Fraction of Electrons Escaping (F_e) for $b/a = 1.0$	114
IV-9a Fraction of Electrons Escaping (F_e) for $b/a = .5$	114
IV-9b Fraction of Electrons Escaping (F_e) for $b/a = .5$	115
IV-9c Fraction of Electrons Escaping (F_e) for $b/a = .5$	115
IV-10a Normalized Potential Contour Plots for $b/a = 1.0$ and $z = 0$	118
IV-10b Normalized Potential Contour Plots for $b/a = 1.0$ and $z = a/4$	119
IV-10c Normalized Potential Contour Plots for $b/a = 1.0$ and $z = a/2$	120
IV-10d Normalized Potential Contour Plots for $b/a = 1.0$ and $z = 3a/4$	121
IV-10e Normalized Potential Contour Plots for $b/a = 1.0$ and $z = a$	122
IV-11 Electron Trajectories for $b/a = 1.0$, Normalized Energy of 1.1, $B = 0$ radians and $\theta = 0^\circ$	124
IV-12a Fraction of Electrons Escaping (F_e) for $b/a = 1.0$	126
IV-12b Fraction of Electrons Escaping (F_e) for $b/a = 1.0$	126
IV-12c Fraction of Electrons Escaping (F_e) for $b/a = 1.0$	127

<u>Figure</u>	<u>Page</u>
IV-13 Normalized Potential Contour Plot for $b/a = 1.0$ and $c/a = .25$	130
IV-14 Normalized Potential Contour Plot for $b/a = 1.0$ and $c/a = .1$	131
IV-15 Normalized Potential Contour Plot for $b/a = .5$ and $c/a = .25$	132
IV-16 Normalized Potential Contour Plot for $b/a = .5$ and $c/a = .1$	133
IV-17 Fraction of Electrons Escaping (F_e) for $b/a = 1.0$ and $c/a = .25$	136
IV-18 Fraction of Electrons Striking Conductor (F_c) for $b/a = 1.0$ and $c/a = .25$	136
IV-19 Fraction of Electrons Escaping (F_e) for a Normalized Energy of 1.1	137
IV-20a Normalized Potential Contour Plot for $b/a = 1.0$, $c/a = .25$ and $z = 0$	139
IV-20b Normalized Potential Contour Plot for $b/a = 1.0$, $c/a = .25$ and $z = a/4$	140
IV-20c Normalized Potential Contour Plot for $b/a = 1.0$, $c/a = .25$ and $z = a/2$	141
IV-20d Normalized Potential Contour Plot for $b/a = 1.0$, $c/a = .25$ and $z = 3a/4$	142
IV-20e Normalized Potential Contour Plot for $b/a = 1.0$, $c/a = .25$ and $z = a$	143
IV-21a Normalized Potential Contour Plot for $b/a = .5$, $c/a = .25$ and $z = 0$	144
IV-21b Normalized Potential Contour Plot for $b/a = .5$, $c/a = .25$ and $z = a/4$	145
IV-21c Normalized Potential Contour Plot for $b/a = .5$, $c/a = .25$ and $z = a/2$	146
IV-21d Normalized Potential Contour Plot for $b/a = .5$, $c/a = .25$ and $z = 3a/4$	147
IV-21e Normalized Potential Contour Plot for $b/a = .5$, $c/a = .25$ and $z = a$	148
IV-22a Normalized Potential Contour Plot for $b/a = 1.0$, $c/a = .1$ and $z = 0$	149

<u>Figure</u>	<u>Page</u>
IV-22b Normalized Potential Contour Plot for b/a = 1.0, c/a = .1 and z = a/4	150
IV-22c Normalized Potential Contour Plot for b/a = 1.0, c/a = .1 and z = a/2	151
IV-22d Normalized Potential Contour Plot for b/a = 1.0, c/a = .1 and z = 3a/4	152
IV-22e Normalized Potential Contour Plot for b/a = 1.0, c/a = .1 and z = a	153
IV-23a Normalized Potential Contour Plot for b/a = .5, c/a = .1 and z = 0	154
IV-23b Normalized Potential Contour Plot for b/a = .5, c/a = .1 and z = a/4	155
IV-23c Normalized Potential Contour Plot for b/a = .5, c/a = .1 and z = a/2	156
IV-23d Normalized Potential Contour Plot for b/a = .5, c/a = .1 and z = 3a/4	157
IV-23e Normalized Potential Contour Plot for b/a = .5, c/a = .1 and z = a	158
IV-24a Fraction of Electrons Escaping (F_e) for b/a = 1.0 and c/a = .25	160
IV-24b Fraction of Electrons Escaping (F_e) for b/a = 1.0 and c/a = .25	160
IV-25a Fraction of Electrons Striking the Conductors (F_c) for b/a = 1.0 and c/a = .5	161
IV-25b Fraction of Electrons Striking the Conductors (F_c) for b/a = 1.0 and c/a = .5	161
IV-26a Fraction of Electrons Escaping (F_e) for a Normalized Energy of 1.1	162
IV-26b Fraction of Electrons Striking Conductor (F_c) for a Normalized Energy of 1.1	162
IV-27 High Energy Approximation Comparison	163

LIST OF TABLES

<u>Table</u>		<u>Page</u>
I-1	Fractional Variation of Potential	28
IV-1	Ratio of Voltages Required on Conductors to be Approximated by Equal Charge Densities	116
IV-2	Mean Squared Error for Various Solutions	128
IV-3	V_0/V_∞ for Various Spacings of Conductors	135
IV-4	Mean Squared Error for Two Solutions	138
IV-5	V_0/V_∞ for Various Dimensions	159
A-1	Series Coefficients for $b/a = 1$ and $c/a = .25$	170
A-2	Series Coefficients for $b/a = 1$ and $c/a = .1$	171
A-3	Series Coefficients for $b/a = .5$ and $c/a = .25$	172
A-4	Series Coefficients for $b/a = .5$ and $c/a = .1$	173
A-5	Series Coefficients for $b/a = 1$ and $c/a = .25$	176
A-6	Series Coefficients for $b/a = 1$ and $c/a = .1$	177
A-7	Series Coefficients for $b/a = .5$ and $c/a = .25$	178
A-8	Series Coefficients for $b/a = .5$ and $c/a = .1$	179
A-9	Series Coefficients for $b/a = 1$ and $c/a = .25$	181

INTRODUCTION

One of the problems encountered in the study of EMP phenomena is the effect of a flux of gamma rays and X-rays impinging upon a satellite. To study this System Generated EMP it has been proposed to build a SGEMP simulator of the general configuration described by Baum⁽¹⁾. The simulator is to consist of a metal chamber in which a very high vacuum is to be maintained, a source of high energy photons (gamma rays and X-rays), and a method of coupling the beam of photons into the chamber (Figure 1). The device to be studied is placed in the vacuum chamber and the photons allowed to impinge on it. It is desirable that the chamber simulate the environment of free space as closely as possible. This requires the damping of electromagnetic resonances of the chamber, reduction of the capacitance between the device under study and the chamber to acceptable levels, absorption and/or trapping of particles striking the chamber walls, etc.

In his note describing a SGEMP simulator, Baum discusses some of the problems and design considerations which arise in the construction of such a simulator. This paper considers a possible solution to one of these problems, the production of Compton electrons at the wall of the chamber⁽²⁾. These electrons are produced by two different causes. When the incident photon beam enters the chamber, not all the photons will strike the device under test; some will strike the wall of the chamber and possibly produce Compton electrons. Similarly, photons striking the device will produce Compton electrons at the surface of the device. Some of these electrons will return to the device under the influence of electromagnetic fields, but others may proceed to the wall of the chamber and there produce secondary Compton electrons. Since electrons produced

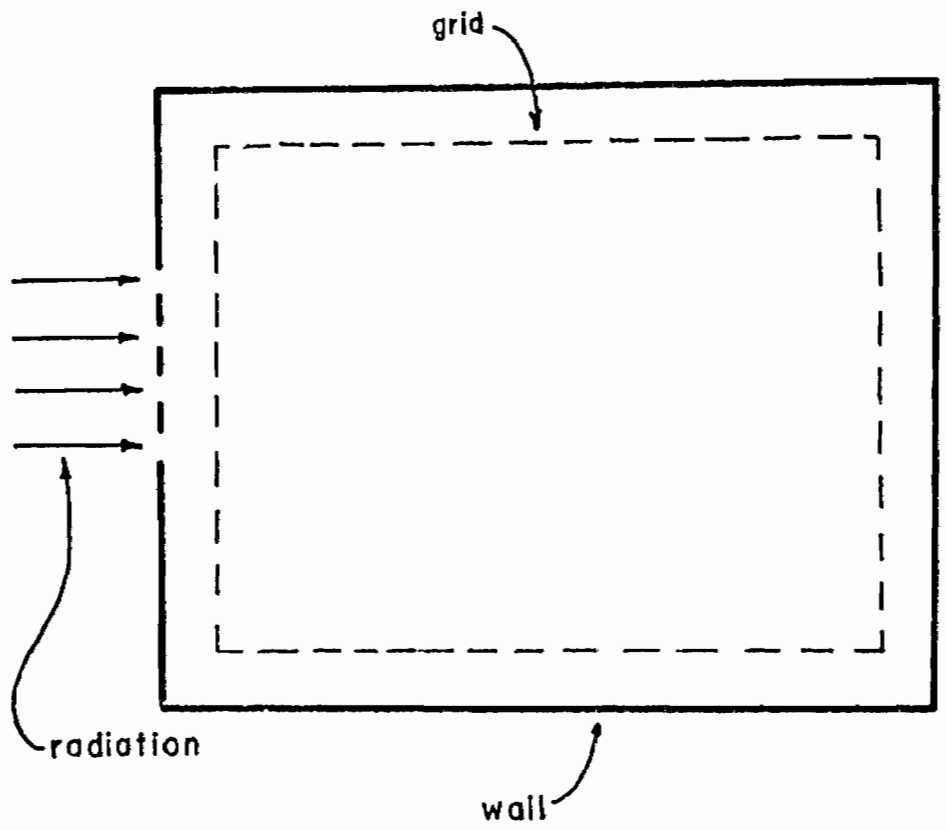


Figure 1. An SGEMP Simulator

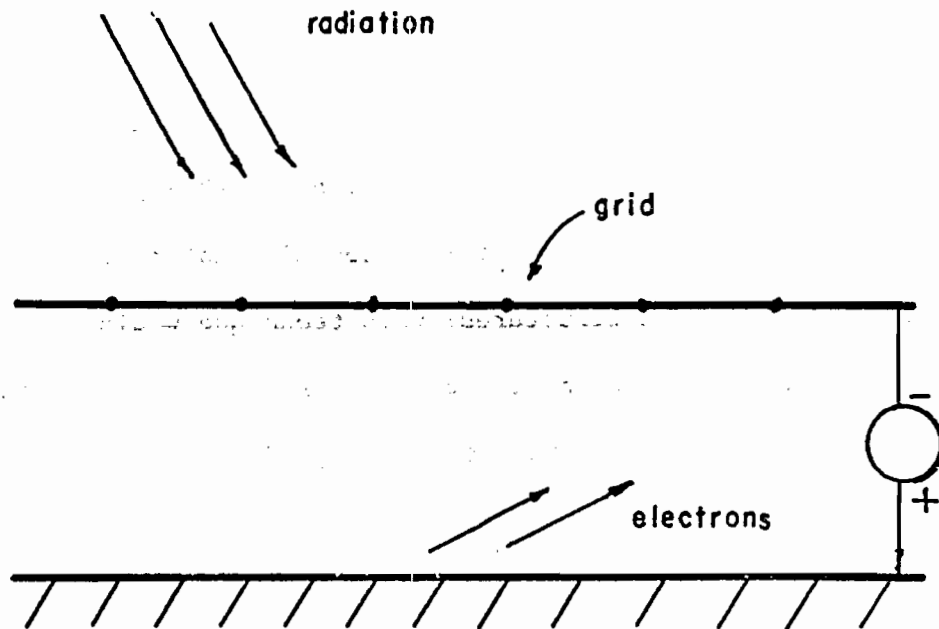


Figure 2. A Wire Grid Near a Ground Plane

grating of parallel rods near a ground plane in the study of an EMP parallel plate simulator⁽⁵⁾. For other studies where the line charge approximation may not be used or the finite extent of the conducting plane must be considered, other methods, such as the electrolyte tank, have been used to find the potential distribution^(6,7). The above methods are confined to two-dimensional geometries. The electrolyte tank as well as resistor networks have been used to find the potential distribution of electrostatic lenses and deflector systems of three-dimensional geometry but only those which have axial symmetry⁽⁷⁾. For more general geometries, the expansion of the potential in terms of spatial harmonics may be employed as was done in this paper. Another possible approach would be the use of an integral equation formulation as has been done with thin wire structures; this technique would be of interest if the charge densities on the conductors were of principal concern⁽⁸⁾.

To determine the effectiveness of the grids in containing electrons, it is necessary to determine the fraction of electrons escaping to the working volume of the chamber as a function of their initial kinetic energy. To do this, the trajectories of the electrons under the influence of the potential distribution produced by the grids must be determined. The effect of an electrostatic field on the paths of electrons has been studied in vacuum tubes and in electron microscopes and cathode ray tubes. Experimental techniques such as the direct measurement of the electron flux density in the devices have been used. The effect of the potential distribution may also be simulated by means of a stretched rubber sheet⁽⁹⁾. In this method the rubber sheet is deformed in such a way that the effect of the resulting gravitational potential on balls rolled on the sheet simulates the effect of the electrostatic

potential on electrons. An analytical technique has been developed by Hashimoto, et al., using conformal mapping and an axial ray theory to find the trajectories of electrons in an electrostatic field⁽¹⁰⁾. The disadvantage of many of these techniques is that they may only be used for two-dimensional field configurations. Furthermore, many of the techniques assume only small deflections of the electrons. The method employed in this paper of direct calculation of the electron trajectories by numerical techniques does not have these drawbacks and has become feasible with the use of high speed digital computers.

In this paper computer programs were developed which allowed the work done by Tesche to be extended to three dimensions. Single-layer and two-layer grids composed of wires of sufficiently small radii that they could be approximated by lines of charge were studied in this manner. Programs were then developed to study grids consisting of conductors of larger radii. These last programs employ a series solution to Laplace's equation and a least squared error fitting technique for the boundary conditions. In all cases the potential distribution was found and potential contour maps were drawn. The effectiveness of the grids was found as a function of the energy and position of the electrons and of the dimensions and potential of the grid by direct calculation of the trajectories of electrons leaving the ground plane. Plots of the function of electrons escaping as a function of energy and direction were made for a uniform distribution of electrons being emitted from the ground plane.

Many of the calculations performed in this paper required the use of a digital computer. The CDC 6600 located at Kirtland Air Force Base at Albuquerque, New Mexico was utilized to do these calculations. Some of the subroutines used in this paper, in particular BRUTE and DRAW4, were developed at The Dikewood Corporation of Albuquerque, New Mexico.

SECTION I

LINE CHARGE APPROXIMATION

1. Simplifying Assumptions

In this section we will obtain the potential distribution due to a grid of wires placed parallel to the wall of the simulator chamber. The chamber wall will be assumed to be perfectly conducting and to be locally flat. The potential of the wall will be assigned a value of zero. The problem then becomes, under these circumstances, that of finding the potential distribution of a wire mesh above and parallel to a perfectly conducting ground plane. A further assumption will be made that the mesh consists of parallel cylindrical conductors and that the diameter of the wires is small compared to both the distance from the wires to the ground plane and the distance between parallel wires. This last assumption allows the conductors to be replaced by lines of charge as will be shown in Section I-4.

2. Single Grid of Wires

The first geometry we will consider is that of a mesh of wires consisting of cylindrical conductors. The centerlines of all the conductors lie in a plane at a distance b above and parallel to the ground plane. The conductors intersect at right angles and form a square grid. Assuming the conductors have a small diameter, we replace them with line charges located at the centerlines of the conductors as shown in Figure I-1.

The configuration of Figure I-1 may be thought of as the superposition of two sets of parallel line charges, one set consisting of line charges extending in the x direction and the other set consisting of

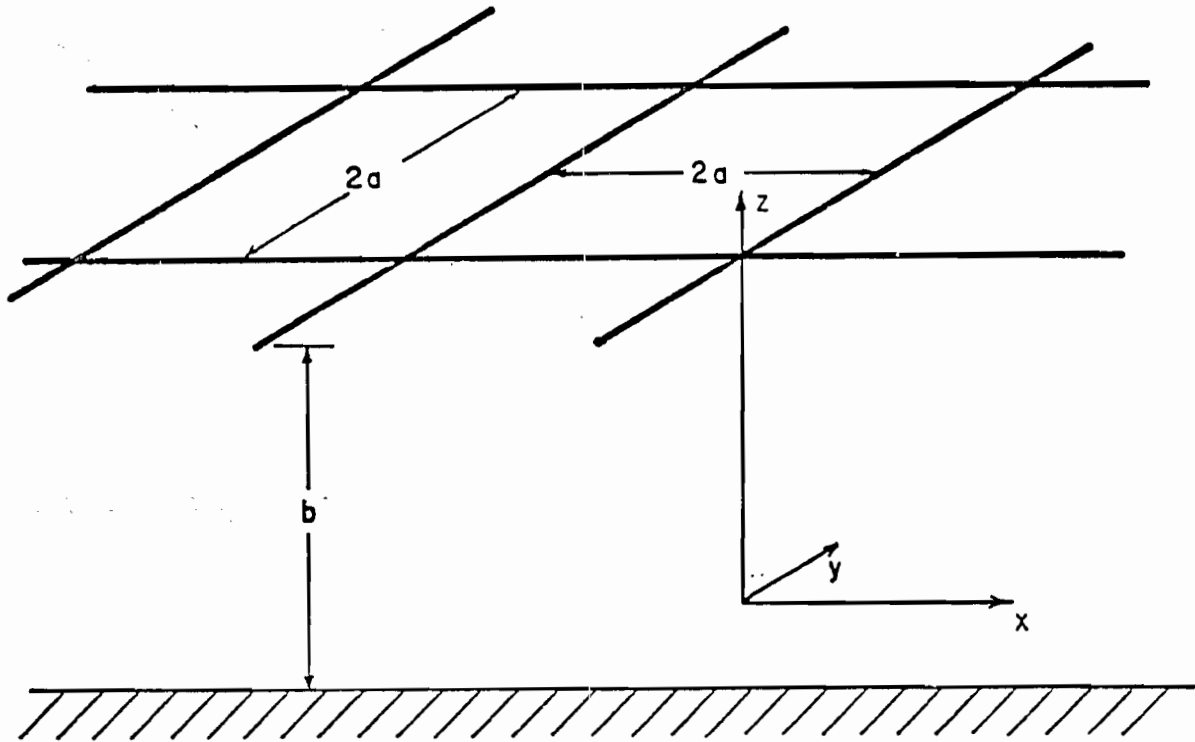


Figure I-1. A Single Grid of Line Charges

line charges extending in the y direction. In this case, superposition may be used since the wires have been replaced by fixed line charges. It now remains to find the potential distribution due to these sets of line charges so that they may be combined to yield the solution for the grid.

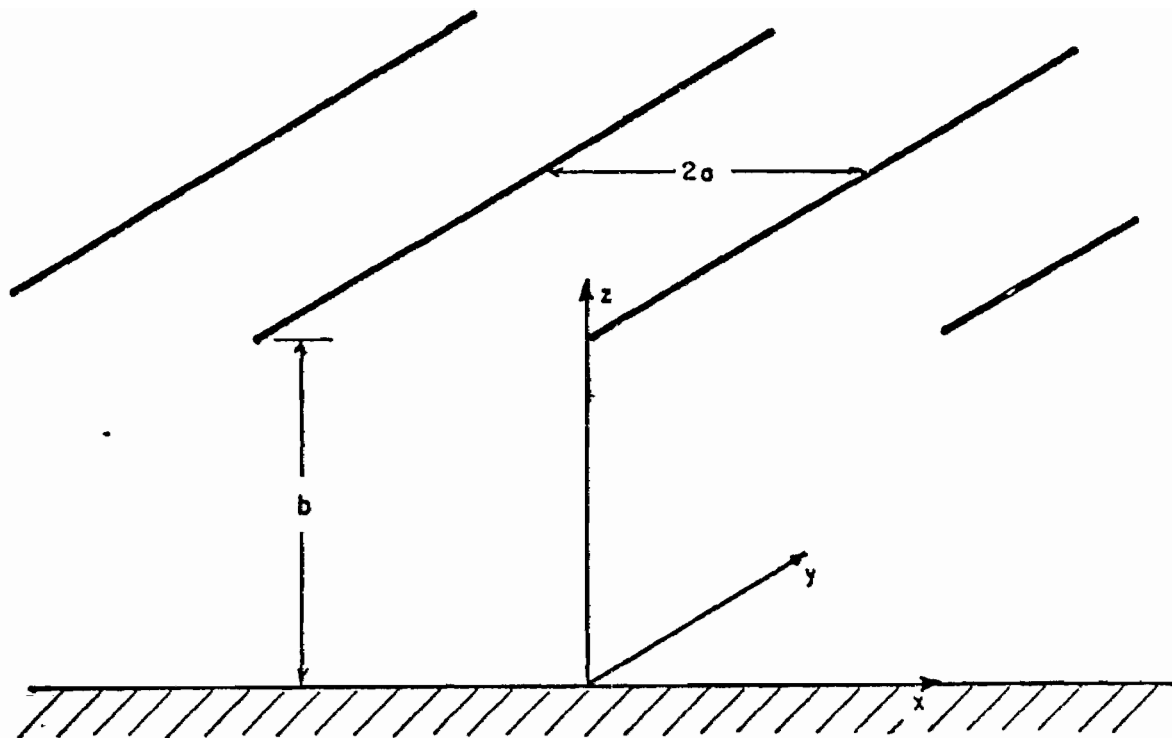


Figure I-2. A Set of Parallel Line Charges

Figure I-2 shows an infinite set of line charges at a distance b above a perfectly conducting ground plane. The line charges are parallel to each other and the ground plane. They extend to $\pm\infty$ in the y direction with a distance $2a$ between adjacent line charges. F. M. Tesche⁽⁴⁾ has shown that for this geometry the potential distribution can be found in closed form by conformal mapping techniques and is

$$\phi(x, z) = \frac{\rho_o}{4\pi\epsilon_o} \ln \left[\frac{\cosh(\pi(z+b)/a) - \cos(\pi x/a)}{\cosh(\pi(z-b)/a) - \cos(\pi x/a)} \right] \quad (1)$$

where $\phi(x, z)$ is the potential, ρ_o is the line charge density, ϵ_o is

the permittivity of free space, $2a$ is the spacing between line charges and b is the distance of the line charges from the ground plane.

From the above expression we see that in the limit as z becomes infinite the potential becomes

$$\frac{\rho_0}{2\epsilon_0} \left(\frac{b}{a}\right).$$

To obtain the potential distribution due to the grid of line charges shown in Figure I-1, we add the potential distributions for the two orthogonal sets of line charges. Let $\phi_0(x,y)$ be the potential distribution function given by Equation (1) but with ρ_0 equal to 1. The potential distribution for the geometry in Figure I-1 is then given by

$$\phi(x,y,z) = \rho_1 \phi_0(x,z) + \rho_2 \phi_0(y,z) \quad (2)$$

where ρ_1 and ρ_2 are the charge densities of the line charges extending in the y and x directions respectively. As z becomes infinite, the potential becomes

$$\phi(x,y,z) \Big|_{z \rightarrow \infty} = \frac{\rho_1}{2\epsilon_0} \left(\frac{b}{a}\right) + \frac{\rho_2}{2\epsilon_0} \left(\frac{b}{a}\right) \quad (3)$$

Confining our attention to the case where the charge densities of the two sets of line charges are identical, the potential distribution becomes

$$\phi(x,y,z) = \rho [\phi_0(x,z) + \phi_0(y,z)] \quad (4)$$

and the potential as z becomes infinite is

$$\phi(x,y,z) \Big|_{z \rightarrow \infty} = \frac{\rho b}{a\epsilon_0} \quad (5)$$

where ρ is the line charge density of both sets of line charges.

3. Double Grid of Wires

From the potential contour plots and electron trajectory plots shown in Section IV for the single grid case analyzed above, it was noted that the electrons had a tendency to escape through the center of the grid apertures. It was thought that placing another grid of wires above and parallel to the first grid and shifted so that the crossing points of the wires of the second grid would lie directly above the center of the apertures of the first grid (Figure I-3) would reduce the number of electrons escaping.

Again we approximate the wires by line charges located on the centerlines of the wires. We only treat the case of grids with square apertures and with the distance between the first and second grid being the same as the distance between the first grid and the ground plane. The principle of superposition is again employed to find the total potential distribution.

For the purposes of this analysis of the double grid case, let the potential distribution function for the single grid shown in Figure I-1 with charge density equal to 1.0 be represented by $\phi_{SG}(x,y,z,a,b)$ where $2a$ is the spacing between parallel line charges and b is the distance from the line charges to the ground plane. Here we have written the potential distribution as an explicit function of a and b as well as x , y , and z . The potential for the double grid configuration may then be written as

$$\begin{aligned}\phi_{DG}(x,y,z,a,b) &= \rho_1 \phi_{SG}(x,y,z,a,b) \\ &+ \rho_2 \phi_{SG}(x+a, y+a, z, a, 2b)\end{aligned}\quad (6)$$

where $\phi_{DG}(x,y,z,a,b)$ is the potential distribution for the double

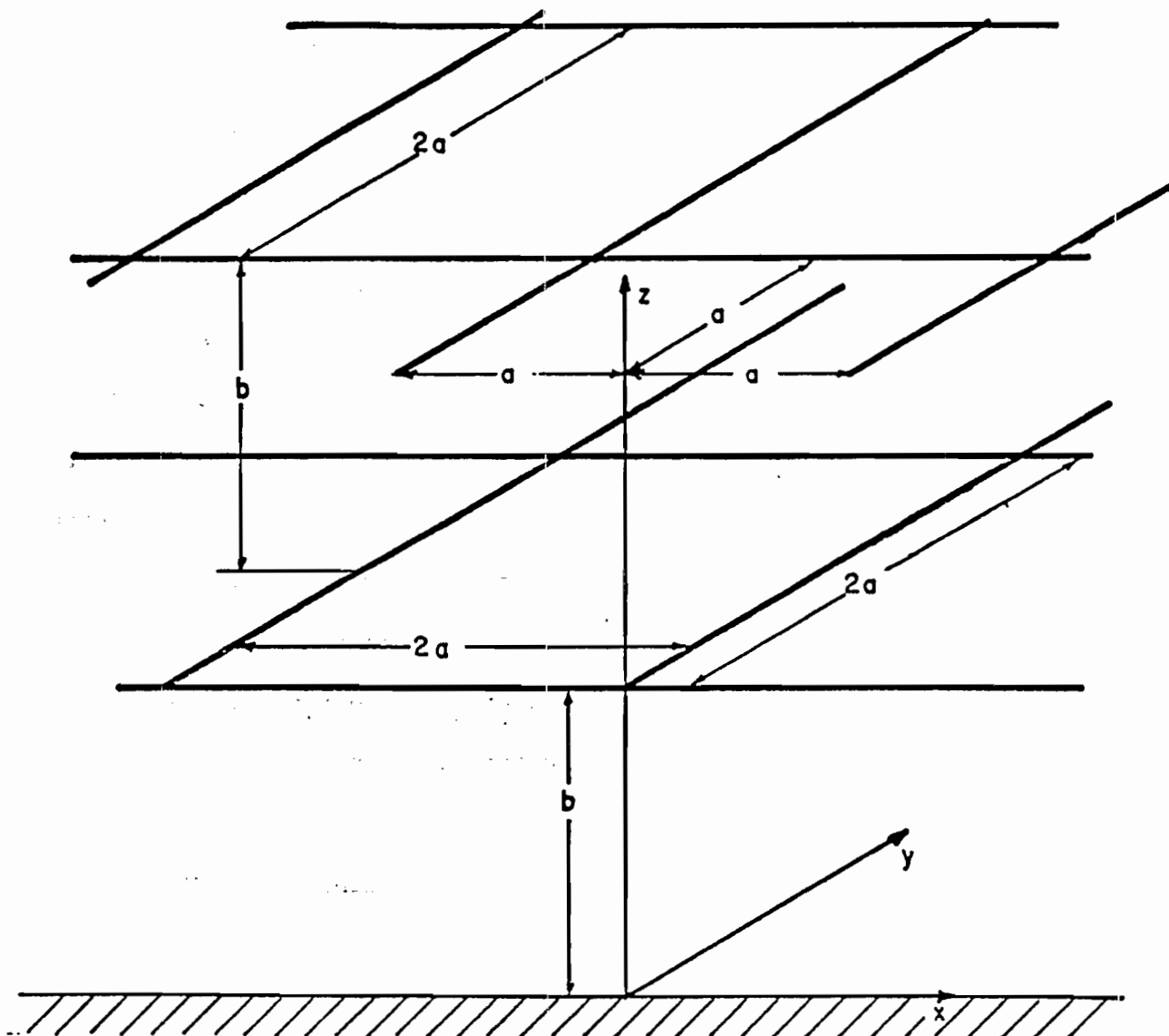


Figure I-3. A Double Grid of Line Charges

grid, ρ_1 is the line charge density on the lower grid, and ρ_2 is the line charge density on the upper grid. As z becomes infinite for this case the potential becomes

$$\phi_{DG}(x,y,z,a,b) \Big|_{z \rightarrow \infty} = \rho_1 \frac{b}{a\epsilon_0} + \rho_2 \frac{2b}{a\epsilon_0} \quad (7)$$

In this case, since we are considering two completely separate grids, we will not assume that the charge density on the two grids is the same.

4. Limits on Wire Size for Line Charge Approximation

In the single and double grid analysis, the wires were replaced by line charges. Intuitively, we know that for small distances from the line charge the potential distribution will be that of the logarithmic singularity of an isolated line charge and that a constant potential contour near the line charge would therefore be cylindrical. If this is indeed so, a cylindrical conductor placed so that its surface corresponds to such a contour and maintained at the same potential as the contour would produce the same field distribution outside of the conductor as the line charge. We will show that for a sufficiently small distance from the wire the contours are indeed cylindrical. We will also derive an approximate expression for the error encountered in using the line charge approximation.

To show that the contours near one of the line charges is cylindrical, consider Figure I-4. In this figure there is a set of parallel line charges spaced $2a$ apart and a distance b above the ground plane. The set of charges extends infinitely in the x direction and each line charge extends to $\pm \infty$ in the y direction.

The potential of a point lying on a circle of radius δ about the

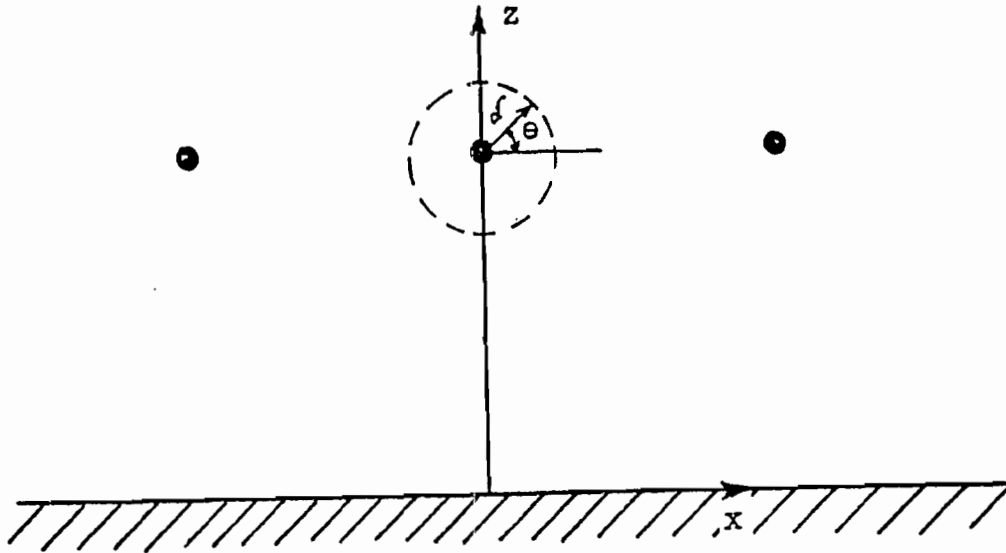


Figure I-4. A Set of Parallel Line Charges With a Point on a Circle of Radius δ

line charge on the z axis is

$$\phi(x,z) = \frac{\rho_0}{4\pi\epsilon_0} \ln \left[\frac{\cosh((2b+\delta\sin(\theta))\pi/a) - \cos(\delta\cos(\theta)\pi/a)}{\cosh((\delta\sin(\theta))\pi/a) - \cos(\delta\cos(\theta)\pi/a)} \right] \quad (8)$$

where x and z specify a point on the circle at an arbitrary angle θ .

If $\delta\pi/a$ is small compared to 1.0, we may use the approximation

$$\cos(\delta\cos(\theta)\pi/a) \approx 1.0 \quad (9)$$

If we further require that δ is small compared to $2b$, then

$$\cosh((2b+\delta\sin(\theta))\pi/a) \approx \cosh(2b\pi/a) \quad (10)$$

Using these approximations, the numerator of the term in brackets, which we will call N , becomes

$$N = \cosh(2b\pi/a) - 1 \quad (11)$$

To approximate the denominator of the term in brackets, the cosh and cos functions are expanded in a power series. The expansions for the functions are well known⁽¹¹⁾ and are

$$\cosh(X) = 1 + \frac{X^2}{2!} + \frac{X^4}{4!} + \dots \quad (12)$$

and

$$\cos(X) = 1 - \frac{X^2}{2!} + \frac{X^4}{4!} - \frac{X^6}{6!} + \dots \quad (13)$$

Using these expansions, the denominator, which we will call D, becomes

$$D = \left(\frac{T_1^2 + T_2^2}{2!} \right) + \left(\frac{T_1^4 - T_2^4}{4!} \right) + \dots \quad (14)$$

where

$$T_1 = \delta \sin(\theta) \pi/a \quad (15)$$

and

$$T_2 = \delta \cos(\theta) \pi/a. \quad (16)$$

Since we are assuming that $\delta\pi/a$ is much less than 1.0, both T_1 and T_2 are much less than 1.0. Ignoring terms of order four and higher, the denominator becomes

$$D \approx \frac{T_1^2 + T_2^2}{2!} = 1/2 \left[\delta \frac{\pi}{a} \right]^2 \quad (17)$$

The potential of Equation (8) is now

$$\phi(x, z) = \frac{\rho_o}{4\pi\epsilon_o} \ln \left[\frac{\cosh(2b\pi/a) - 1}{1/2 \left[\frac{\delta\pi}{a} \right]^2} \right] \quad (18)$$

Since this expression is not a function of θ , the potential is a constant on a circle of radius δ if δ is small compared to both $\frac{a}{\pi}$ and $2b$.

The above analysis has shown that the contours become cylindrical

as we approach the line charges. We will now derive an expression which will provide an estimate of how severely the actual contours deviate from being cylindrical for a given δ . We will calculate the difference in potential of two points, one at a distance δ and at an angle $\pi/2$ and the other at a distance δ and at an angle $-\pi/2$. The potentials at these two points are

$$\phi(x, z) \Big|_{\substack{x=0 \\ z=b+\delta}} \approx \frac{\rho_0}{4\pi\epsilon_0} \ln \left[\frac{\cosh((2b+\delta)\pi/a) - 1}{\cosh(\delta\pi/a) - 1} \right] \quad (19)$$

and

$$\phi(x, z) \Big|_{\substack{x=0 \\ z=b-\delta}} \approx \frac{\rho_0}{4\pi\epsilon_0} \ln \left[\frac{\cosh((2b-\delta)\pi/a) - 1}{\cosh(-\delta\pi/a) - 1} \right] \quad (20)$$

Subtracting these two expressions and using the fact that the cosh is an even function and the characteristics of logarithms, we find

$$\phi(x, z) \Big|_{\substack{x=0 \\ z=b+\delta}} - \phi(x, z) \Big|_{\substack{x=0 \\ z=b-\delta}} = \frac{\rho_0}{4\pi\epsilon_0} \ln \left[\frac{\cosh((2b+\delta)\pi/a) - 1}{\cosh((2b-\delta)\pi/a) - 1} \right] \quad (21)$$

We now write the cosh in terms of exponentials and factor the term $e^{\delta\pi/a}$ out of the numerator and the term $e^{-\delta\pi/a}$ out of the denominator.

Denoting the difference in potential as $\Delta\phi$, we write

$$\Delta\phi = \frac{\rho_0}{4\pi\epsilon_0} \ln \left[\frac{e^{\delta\pi/a} (1/2) ((e^{2b\pi/a} + e^{-2(b-\delta)\pi/a}) - e^{-\delta\pi/a})}{e^{-\delta\pi/a} (1/2) ((e^{2b\pi/a} + e^{-2(b+\delta)\pi/a}) - e^{\delta\pi/a})} \right] \quad (22)$$

If we require that δ be small compared to both b and a/π

$$e^{-(b-\delta)2\pi/a} \approx e^{-2b\pi/a} \quad (23)$$

and the difference in the potentials becomes

$$\Delta\phi = \frac{\rho_o}{4\pi\epsilon_o} \ln \left[\frac{e^{\delta\pi/a} (\cosh(2b\pi/a) - 1.0)}{e^{-\delta\pi/a} (\cosh(2b\pi/a) - 1.0)} \right] = \frac{\rho_o}{2\pi\epsilon_o} \left(\frac{\delta\pi}{a} \right) \quad (24)$$

Dividing this expression by the potential found in Equation (18) yields the fractional variation of potential between these two points. Denoting the potential of Equation (18) as ϕ_o , we find

$$\frac{\Delta\phi}{\phi_o} = \frac{2\delta\pi}{a} \ln \frac{\cosh(2b\pi/a) - 1}{\frac{1}{2} \left(\frac{\delta\pi}{a} \right)^2} \quad (25)$$

This expression provides an estimate of the accuracy obtained by substituting line charges for the actual conductors for various radii of the conductors. It is informative to calculate this fractional variation of potential for a few sample cases. The results of these calculations are shown in Table I-1.

δ/a	b/a	$\Delta\phi/\phi_o$
.003	1.0	.12%
.01	1.0	.48%
.03	1.0	1.7 %
.1	1.0	7.1 %
.003	.5	.15%
.01	.5	.68%
.03	.5	2.4 %
.1	.5	12.7 %

Table I-1 Fractional Variation of Potential

The analysis of this section was done using a set of parallel line charges. The results are applicable, however, to the grid of line

charges if the contributions to the potential of the other set or sets of line charges that make up the grid are small compared to that of the line charge representing the conductor. Since we are considering only small distances from the line charge, the potential due to this charge should be large compared to the other potential contributions if we avoid points near the intersections of the grid.

SECTION II

GRIDS OF LARGE RADII CONDUCTORS

1. Need for Series Solution

In Section I-4 an error expression was derived and the error calculated for several cases. As can be seen from Table I-1, the error increases rapidly with increasing radii of the conductors. In one case with a radius of .1 the error is greater than 10 percent. The error calculations were not carried out for larger values of conductor radii since larger radii would not satisfy the conditions which must be fulfilled to use the error equation.

The failure of the line charge approximation to give sufficiently accurate results for the larger values of conductor radii led to the use of a series approach to the potential problem. Two configurations of conductors were considered, that of a set of conductors parallel to each other and to a ground plane and that of a grid formed by the intersection of two sets of parallel conductors which are parallel to a ground plane.

2. Parallel Cylindrical Conductor Case

The geometry for this case is shown in Figure II-1. It consists of a set of cylindrical conductors which are parallel to each other and also parallel to a perfectly conducting ground plane. The set of conductors extends to infinity in both the positive and negative x direction and each conductor extends to $\pm\infty$ in the y direction. The conductors have radius c and are maintained at a potential V_0 .

To find the potential distribution for this configuration, Laplace's equation in two dimensions is solved in Cartesian coordinates by the

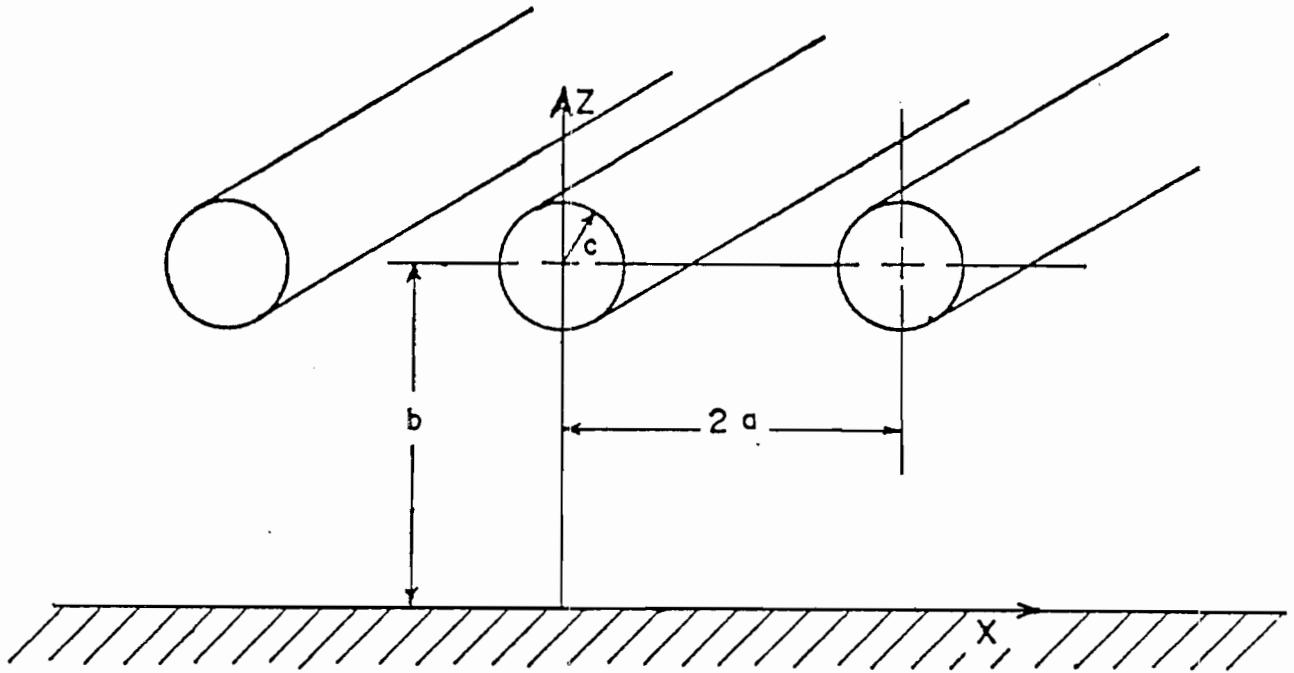


Figure II-1. A set of Parallel Cylindrical Conductors

method of separation of variables. ⁽¹²⁾ The solution is

$$\phi(x, z) = [C_1 \cosh(Kz) + C_2 \sinh(Kz)] [C_3 \cos(Kx) + C_4 \sin(Kx)] \quad (26)$$

where K , C_1 , C_2 , C_3 , and C_4 are constants which must be determined.

We must also consider the trivial solutions

$$\phi(x, z) = C_5 + C_6 x + C_7 z + C_8 xz \quad (27)$$

where C_5 , C_6 , C_7 , and C_8 are also constants which must be determined.

We next divide the region above the ground plane into two regions and determine the proper form of the solution to be used in each region. Region I is such that $0 \leq z \leq b$ and region II is such that $z \geq b$. In region I the solution must be an even periodic function of x of period $2a$. The potential must also satisfy the boundary condition on the ground plane and be equal to zero at $z = 0$. These requirements reduce the form of the solution to

$$\phi_I(x, z) = \sum_{n=1}^{\infty} A_n \sinh\left(\frac{n\pi}{a} z\right) \cos\left(\frac{n\pi}{a} x\right) + A_0 z \quad (28)$$

In region II the solution must also be an even periodic function of x of period $2a$. It must further satisfy the condition that the potential at infinity must remain finite. These conditions reduce the form of the solution in region II to

$$\phi_{II}(x, z) = \sum_{n=1}^{\infty} B_n e^{-n\pi z/a} \cos\left(\frac{n\pi x}{a}\right) + B_0 \quad (29)$$

where B_0 and B_n are constants and $\phi_{II}(x, z)$ is the potential in region II.

To find the coefficients A_0 , B_0 , A_n and B_n , it is necessary to satisfy the boundary conditions on the surface of the cylinders and at the boundary of the two regions lying between the cylinders. These conditions are:

$$\left. \begin{aligned} \phi_I(x, z) &= V_0 \\ \phi_{II}(x, z) &= V_0 \end{aligned} \right\} \begin{array}{l} \text{on the surface of} \\ \text{the conductors} \end{array} \quad (30)$$

$$\left. \begin{aligned} \phi_I(x, z) &= \phi_{II}(x, z) \\ \frac{d\phi_I(x, z)}{dz} &= \frac{d\phi_{II}(x, z)}{dz} \end{aligned} \right\} \begin{array}{l} \text{at } z = b \text{ between} \\ \text{the conductors} \end{array}$$

Since both $\phi_I(x,z)$ and $\phi_{II}(x,z)$ are even periodic functions of x with periods of $2a$, satisfying the boundary conditions on that part of the boundary for which $0 \leq x \leq a$ insures that the boundary conditions will be satisfied at all points on the boundaries. For this reason only those portions of the configuration for which $0 \leq x \leq a$ will be considered.

Since it is impossible to calculate an infinite number of coefficients, the series in Equation (28) and Equation (29) were truncated. If the contributions to the total potential of the terms removed by this truncation is small, this procedure will yield a solution very close to the actual solution. However, the boundary conditions cannot be satisfied exactly with the truncated series. To obtain the best possible fit to the boundary conditions the method of least squared error was employed.

To apply the method of least squares to this problem, the square of the error in satisfying the boundary conditions as a function of the coefficients must be determined. We first consider the error in satisfying the boundary condition on the conductors. In region I this squared error at a point on the conductors is given by

$$\text{ERROR}^2 = [V_0 - \phi_I(x,z)]^2 \quad (31)$$

where x and z specify a point on the surface of the conductor in region I. In region II this error is given by

$$\text{ERROR}^2 = [V_0 - \phi_{II}(x,z)]^2 \quad (32)$$

where x and z specify a point on the conductors in region II.

We next consider the squared error contributions due to the requirements on the potential at the boundary between the two regions between the conductors. The error here arises from two sources, the difference in potential between region I and region II and the difference in the normal derivative between the two regions. The two errors are

calculated separately, squared, and then added to find the total squared error for points on this boundary. The first squared error is given by

$$\text{ERROR}^2 = [\phi_1(x, z) - \phi_{II}(x, z)]^2 \quad (33)$$

and the second by

$$\text{ERROR}^2 = \left[a \frac{d\phi_I(x, z)}{dz} - a \frac{d\phi_{II}(x, z)}{dz} \right]^2 \quad (34)$$

where the expressions are evaluated at points where $z = b$ and

$$c \leq x \leq a.$$

Care must be taken in calculating the second squared error term above. When a function is represented by a series the derivative of the function cannot always be determined by a term-by-term differentiation of the series, as pointed out by Van Bladel.⁽¹³⁾ We know that this problem will occur, at least in the limiting case of very small radii conductors. To gain insight into how this problem occurs, we will look at the series solution of the set of parallel line charges problem in Figure I-2. Tesche⁽⁴⁾ has shown that this is

$$\phi'_I(x, z) = \frac{\rho_0}{a\epsilon_0} \left[\frac{z}{2} + \sum_{n=1}^{\infty} \frac{1}{\gamma_n} \cos(\gamma_n x) e^{-\gamma_n b} \sinh(\gamma_n z) \right] \quad (35)$$

in region I and

$$\phi'_{II}(x, z) = \frac{\rho_0}{a\epsilon_0} \left[\frac{b}{2} + \sum_{n=1}^{\infty} \frac{1}{\gamma_n} \cos(\gamma_n x) e^{-\gamma_n z} \sinh(\gamma_n b) \right] \quad (36)$$

in region II where region I and II are comprised of areas $0 \leq z \leq b$ and $b \geq z$ respectively, and $\gamma_n = n\pi/a$.

We will now differentiate these series term by term and evaluate the result at $x = a$ and $z = b$. In region I this results in the expression

$$\left. \frac{d\phi_I'(x,z)}{dz} \right|_{\substack{x=a \\ z=b}} = \frac{\rho_0}{2a\epsilon_0} \left[1 + \sum_{n=1}^{\infty} \cos(\gamma_n a) (1 + e^{-\gamma_n 2b}) \right] \quad (37)$$

which does not converge. However, at a point a small distance away from this point at $z = b - \delta$ and $x = a$, the expression becomes

$$\left. \frac{d\phi_I'(x,z)}{dz} \right|_{\substack{x=a \\ z=b-\delta}} = \frac{\rho_0}{2a\epsilon_0} \left[1 + \sum_{n=1}^{\infty} \cos(\gamma_n a) (e^{-\gamma_n \delta} + e^{-\gamma_n (2b-\delta)}) \right] \quad (38)$$

which does converge. This indicates that the series representing the potential could be differentiated using the term by term procedure at all points except those on the boundary. To avoid the difficulty at the boundary, the derivative was calculated numerically at the boundary using the following technique. The derivative in region I at the boundary is given approximately by

$$\left. \frac{d\phi_I(x,z)}{dz} \right|_{z=b} \approx \frac{\phi_I(x,b) - \phi_I(x,b-\delta)}{\delta} \quad (39)$$

and the derivative with respect to z in region II is given approximately by

$$\left. \frac{d\phi_{II}(x,z)}{dz} \right|_{z=b} = \frac{\phi_{II}(x,b+\delta) - \phi_{II}(x,b)}{\delta} \quad (40)$$

Since $\phi_I(x,z)$ and $\phi_{II}(x,z)$ converge for all points in their respective regions, the above expressions must converge and will provide a good approximation to the derivative for sufficiently small δ . This method of calculating the derivative was used for finding the derivative at $z = b$ of all series used.

Knowing the error at any point on the boundary, we now establish a set of points on the boundaries. The total squared error is found

by adding the squared error of each point. The resulting expression is differentiated with respect to each of the coefficients we wish to find and the result of each differentiation is set equal to zero. The resulting set of linear algebraic equations will have as their solution the values of the coefficients which will produce the minimum squared error. This was done for parallel conductor configuration and the equation was solved with the aid of a C.D.C. 6600 digital computer. The residual error was then determined by substitution of the coefficients into the equations for the potential and summing the squared error over the points (see Section II-5).

3. Crossed Cylindrical Conductor Case

The geometry for this case is shown in Figure II-2. It consists of two sets of parallel conducting cylinders like those of Figure II-1 but with one set orthogonal to the other. Both sets of cylinders are parallel to a perfectly conducting ground plane and the spacing between cylinders is the same for each set. This results in a grid with square apertures.

As in the preceding case, Laplace's equation was solved by the method of separation of variables. This time it is necessary to use Laplace's equation in three dimensions. The general solution in Cartesian coordinates is of the form

$$\phi(x,y,z) = [C_1 \cos(k_1x) + C_2 \sin(k_1x)] [C_3 \cos(k_2y) + C_4 \sin(k_2y)] [C_5 \cosh(\gamma z) + C_6 \sinh(\gamma z)] \quad (41)$$

where C_1, C_2, C_3, C_4, C_5 and C_6 are constants and $\gamma^2 = k_1^2 + k_2^2$. The trivial solutions which must also be considered are

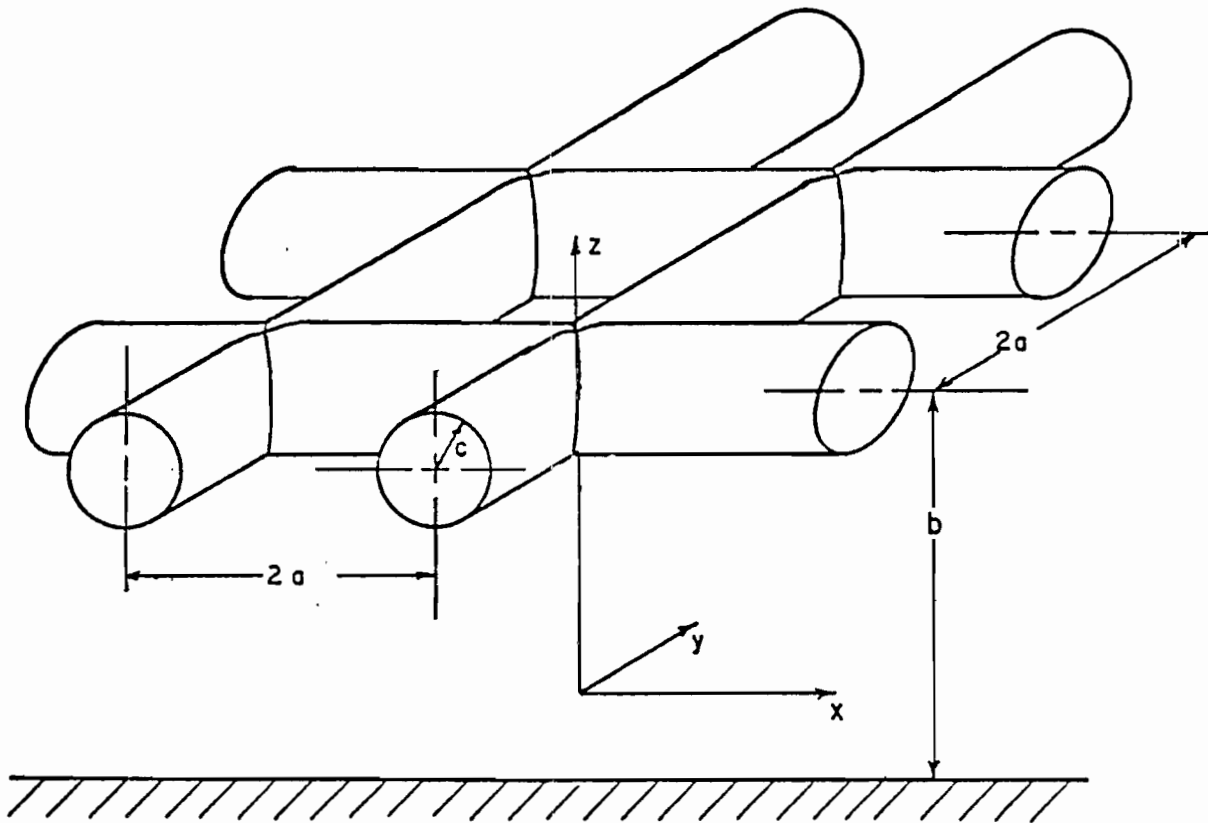


Figure II-2. A Set of Crossed Cylindrical Conductors

$$\begin{aligned} \phi(x, y, z) = & C_7 + C_8 x + C_9 y + C_{10} z + C_{11} xy + C_{12} xz + C_{13} yz \\ & + C_{14} xyz \end{aligned} \quad (42)$$

where $C_7, C_8, C_9, C_{10}, C_{11}, C_{12}, C_{13}$ and C_{14} are constants. As in the case of the parallel conducting cylinders, the space above the ground plane is divided into two regions. Regions I and II are those spaces such that $0 \leq z \leq b$ and $b \leq z$ respectively. In each of these regions the appropriate form of the solution is found.

In region I the solution must be an even periodic function of x with period $2a$. The solution must also satisfy the boundary condition at the ground plane which states that the potential is zero at $z = 0$. These restrictions reduce the form of the solution in region I to

$$\phi_I(x, y, z) = \sum_{n=0}^{\infty} \sum_{m=0}^{\infty} A_{n,m} \cos(n\pi x/a) \cos(m\pi y/a) \sinh(\gamma_{n,m} z) + A_{0,0} z \quad (43)$$

where the $A_{n,m}$ terms are constants and $\gamma_{n,m} = \frac{\pi}{a} \sqrt{n^2 + m^2}$.

In region II the potential must also be an even periodic function of x with period $2a$ and must satisfy the additional requirement that it remain finite as z goes to infinity. These requirements reduce the form of the solution in this region to

$$\phi_{II}(x, y, z) = \sum_{n=0}^{\infty} \sum_{m=0}^{\infty} B_{n,m} \cos(n\pi x/a) \cos(m\pi y/a) e^{-z\gamma_{n,m}} + B_{0,0} \quad (44)$$

where the $B_{n,m}$ terms are constants.

Since we have limited this discussion to grids having square apertures, additional simplifications result from the symmetry of the configuration. Consider the potential at two points in region I as shown in Figure II-3. The first point P is specified by the coordinates $x = \alpha$, $y = \beta$, and z . The second point P' is specified by the coordinates $x' = \beta$, $y' = \alpha$ and $z' = z$. These points are symmetrical about the line $l - l'$. Since the grid is also symmetrical about the line, the potentials at these two points are the same. Looking at the equations for the potential at these two points, we see that the potential at point P is given by

$$\phi_I(\alpha, \beta, z) = \sum_{n=0}^{\infty} \sum_{m=0}^{\infty} A_{n,m} \cos(n\pi\alpha/a) \cos(m\pi\beta/a) \sinh(\gamma_{n,m} z) + A_{0,0} z \quad (45)$$

and the potential at point P' is given by

$$\phi_I(\beta, \alpha, z) = \sum_{n=0}^{\infty} \sum_{m=0}^{\infty} A_{n,m} \cos(n\pi\beta/a) \cos(m\pi\alpha/a) \sinh(\gamma_{n,m}z) + A_{0,0}z \quad (46)$$

Subtracting these two expressions and interchanging the m and n indices in the summations of Equation (46) we

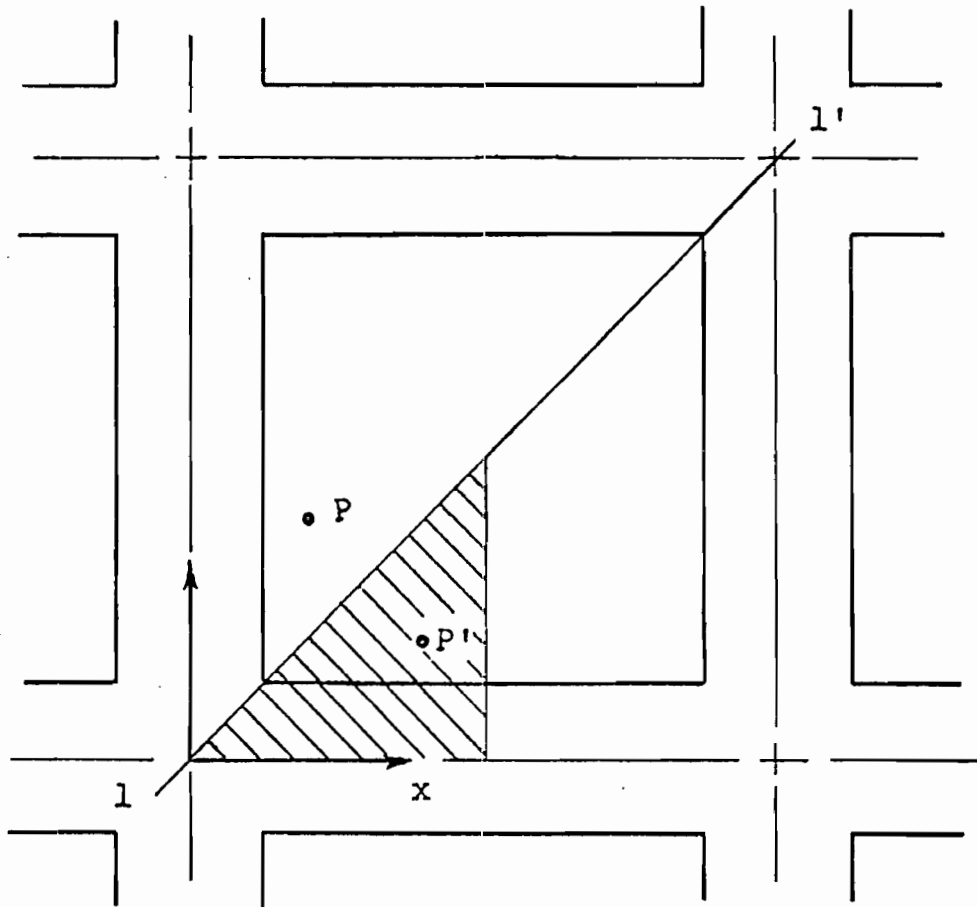


Figure II-3. Crossed Cylindrical Conductors - Top View

are then able to combine the two pair of summations into the expression

$$0 = \sum_{n=0}^{\infty} \sum_{m=0}^{\infty} \{ [A_{n,m} \cos(n\pi\alpha/a) \cos(m\pi\beta/a) \sinh(\gamma_{n,m} z)] - [A_{m,n} \cos(m\pi\beta/a) \cos(n\pi\alpha/a) \sinh(\gamma_{m,n} z)] \} \quad (47)$$

Since $\gamma_{n,m} = \gamma_{m,n}$ for all n and m , this equation may be rewritten as

$$0 = \sum_{n=0}^{\infty} \sum_{m=0}^{\infty} [A_{n,m} - A_{m,n}] \cos(n\pi\alpha/a) \cos(m\pi\beta/a) \sinh(\gamma_{n,m} z) \quad (48)$$

For this to be true for all α , β and z in region I, $A_{m,n}$ must equal $A_{n,m}$ for all n and m . Substituting this condition into Equation (48), the potential in region I now has the form

$$\phi_I(x, y, z) = \sum_{n=0}^{\infty} \sum_{m=n}^{\infty} A_{n,m} [\cos(n\pi x/a) \cos(m\pi y/a) + \cos(m\pi x/a) \cos(n\pi y/a)] \sinh(\gamma_{n,m} z) + A_{0,0} z^2 \quad (49)$$

A similar argument can be made for the potential solution in region II.

If this is done, the solution in region II is of the form

$$\phi_{II}(x, y, z) = \sum_{n=0}^{\infty} \sum_{m=n}^{\infty} B_{n,m} [\cos(n\pi x/a) \cos(m\pi y/a) + \cos(m\pi x/a) \cos(n\pi y/a)] e^{-z\gamma_{n,m}} + B_{0,0} \quad (50)$$

The simplification of the form of the potential solutions that was carried out above greatly reduces the number of coefficients which must be calculated. Also, since the solutions thus obtained are symmetrical about the line $l-l'$, satisfying the boundary conditions on one side of this line insures that the boundary conditions will be satisfied on both sides of the line. If we further note that the functions are even periodic functions of x and y , it can be seen that the boundary conditions need only be satisfied in the shaded area of Figure II-3 to insure that they are satisfied over all space.

The boundary conditions for this case, which are very similar to

those of the preceding case, are as follows:

$$\left. \begin{aligned} \phi_I(x,y,z) &= V_0 \\ \phi_{II}(x,y,z) &= V_0 \end{aligned} \right\} \text{on the conductor}$$

$$\left. \begin{aligned} \phi_I(x,y,z) &= \phi_{II}(x,y,z) \\ \frac{d\phi_I}{dz}(x,y,z) &= \frac{d\phi_{II}}{dz}(x,y,z) \end{aligned} \right\} \text{at } z = b \text{ between conductors}$$
(51)

For reasons previously mentioned, a truncated series of the solution was used to approximately satisfy the boundary conditions. A least squares fit was utilized to obtain the best possible approximation to the boundary conditions with the terms employed. The squared error was calculated only at points in the shaded area of Figure II-3. The residual mean squared error was also calculated for this case after the coefficients were determined (see Section II-5).

4. Application of the Line Charge Solutions to the Large Radii Cylindrical Conductor Cases

It was shown in Section I that for small radii cylindrical conductors a solution for the potential could be found by replacing the conductors with line charges and using conformal mapping techniques. For large radii conductors we found that the accuracy of this method decreases rapidly with increasing radii. However, it is still desirable to use this line charge model to give a first approximation which is then improved by the use of the series solution. To do this, we write the potential in the form

$$\phi_T = \phi_{LC} + \phi_S \tag{52}$$

where ϕ_T is the total potential, ϕ_{LC} is the potential from the line charge solution, and ϕ_S is the series solution.

The line charge solution term has a different form for each of the two configurations considered in this section. For the parallel cylinder case, this is merely the solution for the set of parallel line charges as found by Tesche⁽⁴⁾ and given in Equation (1). By adjusting the value of the charge density term of this solution, it may be made to match the potential of the conductor at one point on the conductor. We chose to have this point be the one at $z = b$ and $x = c$.

For the crossed conductor case, the line charge solution used is that of the single grid, i.e., Equation (4). Similarly for this case the charge density term may be adjusted so that the solution has the exact value of the potential of the conductor at $x = a$, $y = c$, and $z = b$.

Using the line charge solution to obtain a first approximation to the potential affects only the squared error term due to the matching of the potential at the conductor. The squared error terms due to the matching conditions at $z = b$ between the conductors are not affected. The squared error term at the conductor boundary may be easily modified to take account of the line charge solution as will be shown.

5. Least Squared Error Fitting

In this section we have stated that the boundary conditions will be approximately satisfied using a least squared error fitting procedure. The error terms for the various configurations and sections of the boundaries have been determined. These terms involve functions which are represented by series with unknown coefficients. We will now show how the coefficients of these series may be obtained to insure the best fit to the boundary conditions in the least squares sense.⁽¹⁴⁾ For the cases under consideration it is convenient to consider errors at a point P_i which can be represented by

$$\text{ERROR} = C(P_i) + \sum_{n=0}^N A_n \epsilon_n^1(P_i) + \sum_{n=0}^N B_n \epsilon_n^2(P_i) \quad (53)$$

where A_n and B_n are the coefficients to be determined and $C(P_i)$, $\epsilon_n^1(P_i)$ and $\epsilon_n^2(P_i)$ may be functions of position. The squared error is

$$[\text{ERROR}]^2 = \left[C(P_i) + \sum_{n=0}^N A_n \epsilon_n^1(P_i) + \sum_{n=0}^N B_n \epsilon_n^2(P_i) \right]^2 \quad (54)$$

Summing the error over a number of points, we have a total squared error of

$$[\text{TOTAL ERROR}]^2 = \sum_i \left[C(P_i) + \sum_{n=0}^N A_n \epsilon_n^1(P_i) + \sum_{n=0}^N B_n \epsilon_n^2(P_i) \right]^2 \quad (55)$$

where \sum_i is used to indicate the sum over the various points.

To minimize the total squared error, we differentiate this expression with respect to the coefficients and set the resulting expressions equal to zero. Differentiating with respect to A_m yields

$$0 = \sum_i 2 \left[C(P_i) + \sum_{n=0}^N A_n \epsilon_n^1(P_i) + \sum_{n=0}^N B_n \epsilon_n^2(P_i) \right] \epsilon_m^1(P_i) \quad (56)$$

$$m = 0, 1, 2 \dots N$$

Differentiating with respect to B_m yields

$$0 = \sum_i 2 \left[C(P_i) + \sum_{n=0}^N A_n \epsilon_n^1(P_i) + \sum_{n=0}^N B_n \epsilon_n^2(P_i) \right] \epsilon_m^2(P_i) \quad (57)$$

$$m = 0, 1, 2 \dots N$$

With simple algebraic manipulation, Equation (56) may be rewritten as

$$\sum_{n=0}^N A_n \sum_i \epsilon_n^1(P_i) \epsilon_m^1(P_i) + \sum_{n=0}^N B_n \sum_i \epsilon_n^2(P_i) \epsilon_m^1(P_i) = - \sum_i C(P_i) \epsilon_m^1(P_i) \quad (58)$$

$$m = 0, 1, 2 \dots N$$

Similarly, Equation (57) becomes

$$\sum_{n=0}^N A_n \sum_i \epsilon_n^1(P_i) \epsilon_m^2(P_i) + \sum_{n=0}^N B_n \sum_i \epsilon_n^2(P_i) \epsilon_m^2(P_i) = - \sum_i C(P_i) \epsilon_m^2(P_i) \quad (59)$$

$$m = 0, 1, 2 \dots N$$

Since m may take on values from zero to N , we see that we now have $2N + 2$ equations in $2N + 2$ unknowns, A_0 through A_N and B_0 through B_N . If all the parameters of these equations are known except for the coefficients, the coefficients may be found by solving this set of linear algebraic equations.

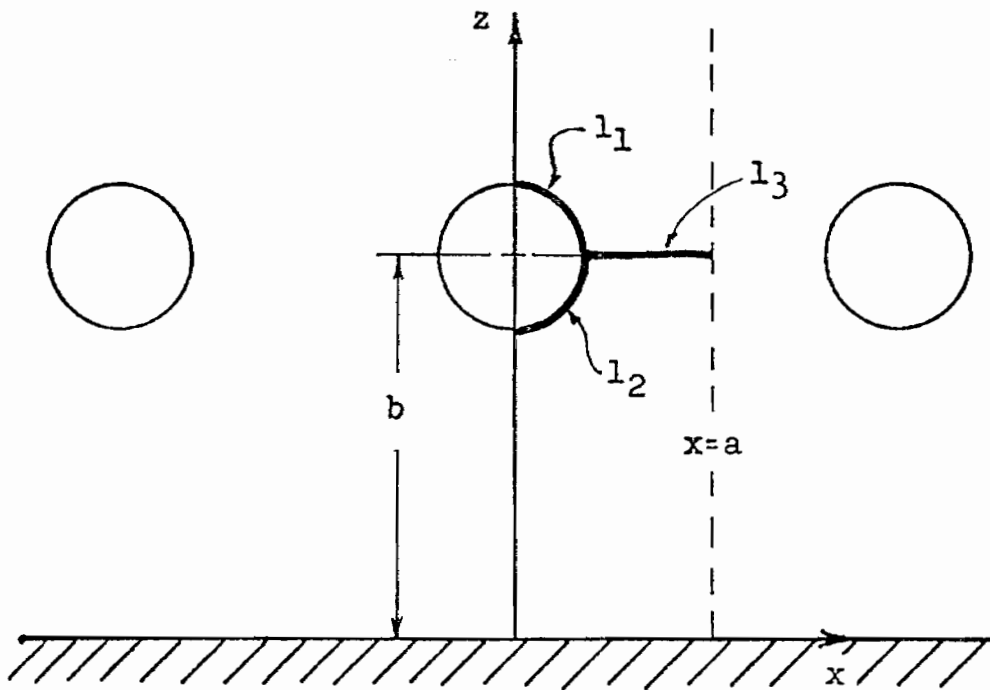


Figure II-4. A Set of Parallel Cylindrical Conductors

The preceding analysis may now be applied to the parallel conducting cylinders case. In Figure II-4 we see that there are three line segments where it is necessary to match the boundary conditions in the space such that $0 \leq x \leq a$. The segment l_1 is that part of the cylinder to the right of the z axis and for which $z \leq b$. The segment l_2 is that part of the cylinder to the right of the z axis for which $z \geq b$. Line segment l_3 is the boundary at $z = b$ outside of the cylinders.

For a point lying on the line segment l_1 , the error is of the form

$$\text{ERROR} = V_0 - \phi_I(x, z) = V_0 - \sum_{n=0}^N A_n \eta_n(x, z) \quad (60)$$

where

$$\eta_n = \cos(n\pi x/a) \sinh(n\pi z/a) \text{ for } n > 0 \quad (61)$$

$$\eta_0 = z$$

For points lying on the line segment l_2 the error is of the form

$$\text{ERROR} = V_0 - \phi_{II}(y, z) = V_0 - \sum_{n=0}^N B_n \xi_n(x, z) \quad (62)$$

where

$$\xi_n = \cos(n\pi x/a) e^{-n\pi z/a} \quad (63)$$

For points lying on the line segment l_3 the error resulting from discontinuity in the potential is of the form

$$\text{ERROR} = \left[\phi_I(x, z) - \phi_{II}(x, z) \right] = \sum_{n=0}^N \left[A_n \eta_n(x, z) - \sum_{n=0}^N B_n \xi_n(x, z) \right] \quad (64)$$

and the error resulting from discontinuity of the normal derivative of the potential is one of the form

$$\text{ERROR} = a \left[\frac{d\phi_{\text{I}}(x,z)}{dz} - \frac{d\phi_{\text{II}}(x,z)}{dz} \right] = \sum_{n=0}^N \left[A_n \eta_n'(x,z) - \sum_{n=0}^N B_n \xi_n'(x,z) \right] \quad (65)$$

where $\eta_n(x,z)$, and $\xi_n(x,z)$ are as defined previously and

$\eta_n'(x,z)$ = the derivative of $\eta_n(x,z)$ with respect to z found numerically as described in Section II-2 multiplied by a , and

$\xi_n'(x,z)$ = the derivative of $\xi_n(x,z)$ with respect to z found numerically as described in Section II-2, multiplied by a . (66)

Comparing these expressions with Equation (53), we see that on segment l_1

$$\begin{aligned} C(P_i) &= V_0 \\ \epsilon_n^1(P_i) &= -\eta_n(x,z) \\ \epsilon_n^2(P_i) &= 0 \end{aligned} \quad (67)$$

and on segment l_2

$$\begin{aligned} C(P_i) &= V_0 \\ \epsilon_n^1(P_i) &= 0 \\ \epsilon_n^2(P_i) &= -\xi_n(x,z) \end{aligned} \quad (68)$$

On segment l_3 the error due to the discontinuity of the potential results in

$$\begin{aligned} C(P_i) &= 0 \\ \epsilon_n^1(P_i) &= \eta_n(x,z) \\ \epsilon_n^2(P_i) &= -\xi_n(x,z) \end{aligned} \quad (69)$$

and the error due to the discontinuity of the normal derivative is

$$c(P_i) = 0$$

$$\epsilon_n^1(P_i) = \eta_n'(x, z) \quad (70)$$

$$\epsilon_n^2(P_i) = -\xi_n'(x, z)$$

Substituting these relationships into Equation (58) and summing over points on the three line segments, we obtain the following:

$$\begin{aligned} & \sum_{n=0}^N A_n \sum_{l_1} \eta_n(x, z) \eta_m(x, z) + \sum_{n=0}^N A_n \sum_{l_3} \eta_n(x, z) \eta_m(x, z) \\ & + \sum_{n=0}^N B_n \sum_{l_3} -\xi_n(x, z) \eta_m(x, z) + \sum_{n=0}^N A_n \sum_{l_3} \eta_n'(x, z) \eta_m'(x, z) \\ (71) \quad & + \sum_{n=0}^N B_n \sum_{l_3} -\xi_n'(x, z) \eta_m'(x, z) = \sum_{l_1} v_0 \eta_m(x, z) \\ & m = 0, 1, 2 \dots N \end{aligned}$$

Substituting into Equation (59), we obtain the following:

$$\begin{aligned} & \sum_{n=0}^N B_n \sum_{l_2} \xi_n(x, z) \xi_m(x, z) + \sum_{n=0}^N A_n \sum_{l_3} -\eta_n(x, z) \xi_m(x, z) \\ & + \sum_{n=0}^N B_n \sum_{l_3} \xi_n(x, z) \xi_m(x, z) + \sum_{n=0}^N A_n \sum_{l_3} -\eta_n'(x, z) \xi_m'(x, z) \\ (72) \quad & + \sum_{n=0}^N B_n \sum_{l_3} \xi_n'(x, z) \xi_m'(x, z) = \sum_{l_2} v_0 \xi_m(x, z) \\ & m = 0, 1, 2 \dots N \end{aligned}$$

Rearranging and gathering terms for the A_n and B_n coefficients, Equation (71) becomes

$$\begin{aligned}
& \sum_{n=0}^N \left[A_n \left\{ \sum_{1_1} \eta_n(x,z) \eta_m(x,z) + \sum_{1_3} \left[\eta_n(x,z) \eta_m(x,z) \right. \right. \right. \\
& \left. \left. \left. + \eta_n'(x,z) \eta_m'(x,z) \right] \right\} + B_n \left\{ \sum_{1_3} \left[-\xi_n(x,z) \eta_m(x,z) - \right. \right. \right. \\
& \left. \left. \left. - \xi_n'(x,z) \eta_m'(x,z) \right] \right\} \right] = \sum_{1_1} V_0 \eta_m(x,z) \quad (73)
\end{aligned}$$

$$m = 0, 1, 2, \dots, N$$

Rearranging the terms in Equation (72) yields

$$\begin{aligned}
& \sum_{n=0}^N \left[A_n \left\{ \sum_{1_3} \left[-\eta_n(x,z) \xi_m(x,z) - \eta_n'(x,z) \xi_m'(x,z) \right] \right\} \right. \\
& \left. + B_n \left\{ \sum_{1_2} \xi_n(x,z) \xi_m(x,z) + \sum_{1_3} \left[\xi_n(x,z) \xi_m(x,z) \right. \right. \right. \\
& \left. \left. \left. + \xi_n'(x,z) \xi_m'(x,z) \right] \right\} \right] = \sum_{1_2} V_0 \xi_m(x,z) \quad (74)
\end{aligned}$$

$$m = 0, 1, 2, \dots, N$$

If the line charge solutions are used to provide a first approximation to the potential as mentioned in Section II-4 the above equations are modified slightly. It may be seen that the effect of the line charge solution will be taken into account merely by replacing the term V_0 with the term $V_0 - \phi_{LC}(x,z)$ where $\phi_{LC}(x,z)$ is the line charge solution. This results in the right hand side of Equation (73) becoming

$$\sum_{1_1} [V_0 - \phi_{LC}(x,z)] \eta_m(x,z) \quad (75)$$

and the right hand side of Equation (74) becoming

$$\sum_{1_2} [V_0 - \phi_{LC}(x,z)] \xi_m(x,z) \quad (76)$$

We will now apply the least squares error fitting scheme to the grid of crossed cylindrical conductors. Referring to Figure II-5, which shows the crossed cylindrical conductor configuration, we see that there are three surfaces over which the boundary conditions must be satisfied in the space where $0 \leq x \leq a$ and $0 \leq y \leq a$. The surface S_1 is that part of the conductor such that $z \leq b$, and is to one side of a diagonal of the aperture. The surface S_2 is specified the same way as S_1 but such that $z \geq b$. The surface S_3 is the area at $z = b$ to one side of a diagonal of the aperture and not on the conductor. For points lying on the surface S_1 the error is of the form

$$\text{ERROR} = V_0 - \phi_{\text{I}}(x, y, z) = V_0 - \sum_{n=0}^N \sum_{m=n}^N A_{n,m} \eta_{n,m}(x, y, z) \quad (77)$$

where

$$\eta_{n,m}(x, y, z) = [\cos(n\pi x/a) \cos(m\pi y/a) + \cos(m\pi x/a) \cos(n\pi y/a)] \sinh(\gamma_{n,m} z)$$

$$\text{and } \gamma_{n,m} = \frac{\pi}{a} \sqrt{n^2 + m^2}. \quad (79)$$

For points lying on the surface S_2 the error is of the form

$$\text{ERROR} = V_0 - \phi_{\text{II}}(x, y, z) = V_0 - \sum_{n=0}^N \sum_{m=n}^N B_{n,m} \xi_{n,m}(x, y, z) \quad (79)$$

where

$$\xi_{n,m} = [\cos(n\pi x/a) \cos(m\pi y/a) + \cos(m\pi x/a) \cos(n\pi y/a)] e^{-z\gamma_{n,m}} \quad (80)$$

For points on the surface S_3 the error due to the discontinuity of the potential is

$$\text{ERROR} = [\phi_I(x,y,z) - \phi_{II}(x,y,z)] = \sum_{n=0}^N \sum_{m=n}^N [A_{n,m} \eta_{n,m}(x,y,z) - B_{n,m} \xi_{n,m}(x,y,z)] \quad (81)$$

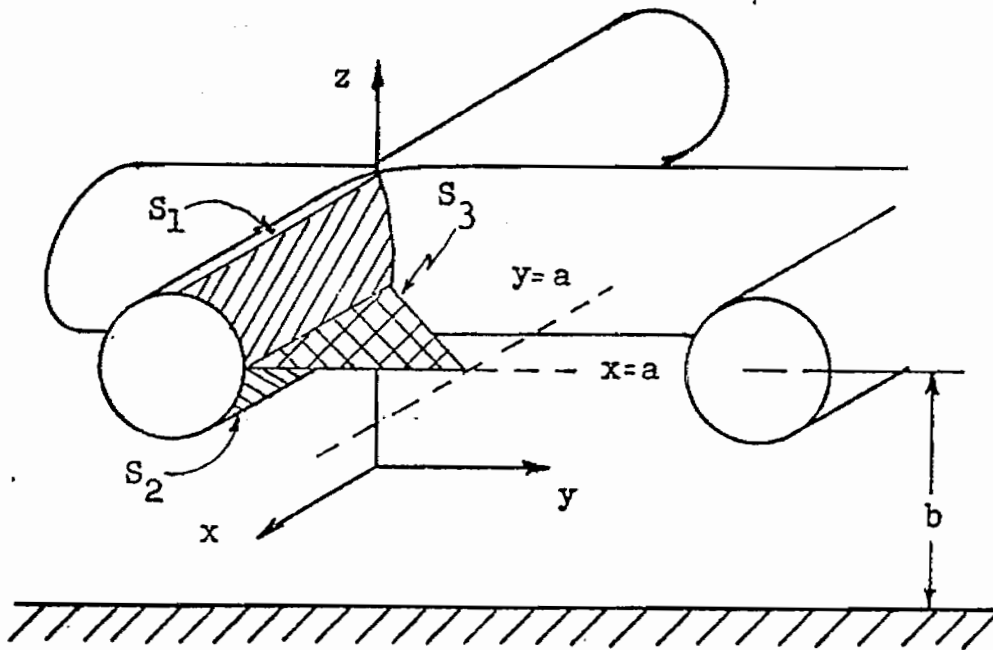


Figure II-5. A Set of Crossed Cylindrical Conductors

and the error due to the discontinuity of the normal derivative of the potential is

$$\text{ERROR} = a \left[\frac{d\phi_{\text{I}}(x,y,z)}{dz} - \frac{d\phi_{\text{II}}(x,y,z)}{dz} \right] = \sum_{n=0}^N \sum_{m=n}^N [A_{n,m} \eta'_{n,m}(x,y,z) - B_{n,m} \xi'_{n,m}(x,y,z)] \quad (82)$$

where $\eta_{n,m}(x,y,z)$ and $\xi_{n,m}(x,y,z)$ are as defined previously and

$$\begin{aligned} \eta'_{n,m}(x,y,z) &= \text{the derivative of } \eta_{n,m}(x,y,z) \text{ with respect to } z \\ &\text{calculated numerically as shown in Section II-2} \\ &\text{multiplied by } a, \\ \xi'_{n,m}(x,y,z) &= \text{the derivative of } \xi_{n,m}(x,y,z) \text{ with respect to } z \\ &\text{calculated numerically as shown in Section II-2} \\ &\text{multiplied by } a. \end{aligned} \quad (83)$$

Since the two summations in the equations are finite, they may be regarded as merely a more convenient method of writing a single sum. Thus, the identification of terms to be substituted into Equations (58) and (59) may be carried out much as was done in the parallel conducting cylinders case. The error terms for this case are seen to be very similar to those of the parallel conducting cylinders case. Therefore we may write by inspection the following equations:

$$\begin{aligned} \sum_{n=0}^N \sum_{m=n}^N A_{n,m} \left[\sum_{S_1} \eta_{n,m}(x,y,z) \eta_{\ell,p}(x,y,z) + \sum_{S_3} \eta_{n,m}(x,y,z) \eta_{\ell,p}(x,y,z) \right. \\ \left. + \eta'_{n,m}(x,y,z) \eta'_{\ell,p}(x,y,z) \right] + B_{n,m} \left[\sum_{S_3} - \xi_{n,m}(x,y,z) \eta_{\ell,p}(x,y,z) \right. \\ \left. - \xi'_{n,m}(x,y,z) \eta'_{\ell,p}(x,y,z) \right] = \sum_{S_1} V_0 \eta_{\ell,p}(x,y,z) \end{aligned}$$

$$\ell = 0, 1, 2, \dots, N \quad (84)$$

$$P = 0, 1, 2, \dots, N$$

$$P \geq \ell$$

and

$$\begin{aligned} & \sum_{n=0}^N \sum_{m=n}^N \left[A_{n,m} \sum_{S_3} -\eta_{n,m}(x,y,z) \xi_{\ell,p}(x,y,z) - \eta'_{n,m}(x,y,z) \xi'_{\ell,p}(x,y,z) \right] \\ & + B_{n,m} \left[\sum_{S_2} \xi_{n,m}(x,y,z) \xi_{\ell,p}(x,y,z) + \sum_{S_3} \xi_{n,m}(x,y,z) \xi_{\ell,p}(x,y,z) \right] \\ & + \xi'_{n,m}(x,y,z) \xi'_{\ell,p}(x,y,z) \Big] = \sum_{S_2} v_0 \xi_{\ell,p}(x,y,z) \end{aligned}$$

$$\ell = 0, 1, 2, \dots, N \quad (85)$$

$$P = 0, 1, 2, \dots, N$$

$$P \geq \ell$$

As in the parallel conducting cylinders case, the effect of using the line charge solution to obtain a first approximation to the potential is merely to modify the right hand term in Equations (84) and (85).

The right hand term of Equation (84) becomes

$$\sum_{S_1} \left(v_0 - \phi_{LC}(x,y,z) \right) \eta_{\ell,p}(x,y,z) \quad (86)$$

and the right hand term of Equation (85) becomes

$$\sum_{S_2} \left(v_0 - \phi_{LC}(x,y,z) \right) \xi_{\ell,p}(x,y,z) \quad (87)$$

where $\phi_{LC}(x,y,z)$ is the appropriate line charge solution.

Thus we see that the equations for the two configurations are very similar. The complexity of the grid of crossed cylindrical conductors case is much greater, however, due to the double summations,

the more complicated regions over which the error must be calculated, and the larger number of points which must be used for a reasonable least squares fit. In both cases we have found a set of linear simultaneous algebraic equations which may be solved on a digital computer using any standard method such as Gaussian elimination. It should be noted that the number of error terms used must be larger than the total number of coefficients, and preferably should be much larger than the number of coefficients.

SECTION III

ELECTRON TRAJECTORIES

1. Need for Electron Trajectories

In the preceding sections the potential distribution for a number of configurations has been calculated. This information does not tell us the effectiveness of the various grids in preventing electrons which leave the ground plane with an initial velocity from reaching the interior of the chamber. To evaluate this fully, the actual trajectories of the electrons leaving the ground plane must be determined. The procedure used to find the trajectories of the electrons is discussed in this section. However, some limits for the behavior of the electrons can be deduced from the potential distribution. These are discussed in the third part of this section.

2. Calculation of Electron Trajectories

In this part we are concerned with the actual path of the electrons as they leave the ground plane. We assume a high vacuum and small electron flux density so that the electrons do not interact with other particles or among themselves. If the initial velocity of an electron is \vec{v} and the initial position of the electron is \vec{x} , we may calculate a new position and velocity at a small increment of time later by assuming that the increment of time is sufficiently small so that the electric field over the distance of travel of the electron is essentially constant. To do this, we must first find the equation of motion of the electron.

The electric field at a point is given by the negative gradient of the potential, and the force exerted on the electron by the electric

field is therefore given by

$$\bar{F} = - e\nabla\phi \quad (88)$$

where ϕ is the potential and e is the charge of the electron. From Newton's first law of motion, the acceleration produced by this force is

$$\bar{a} = - \frac{e\nabla\phi}{m} \quad (89)$$

where m is the mass of electron. Integrating twice with respect to time and supplying the proper constants of integration, and assuming a small increment of time Δt , the new position of the electron may be well approximated by

$$\bar{x}' = - \frac{e}{2m} \nabla\phi(\Delta t)^2 + \bar{v}(\Delta t) + \bar{x} \quad (90)$$

Similarly, the velocity of the electron after an amount of time Δt is given by

$$\bar{v}' = - \frac{e}{2m} \nabla\phi(\Delta t) + \bar{v} \quad (91)$$

These equations in their normalized form were used to obtain the trajectories of the electrons. This was done by starting with the electron at the ground plane and from the initial velocity and position calculating the new velocity and position at a time Δt later. We then repeat the procedure until the entire trajectory is determined. The equations in their present form are not convenient, however, for this purpose. We desire to write them in a form normalized with respect to the potential as $z \rightarrow \infty$ and in terms of the initial energy.

If the initial kinetic energy of the electron is τ , then the magnitude of the initial velocity is

$$|v| = \sqrt{\frac{2\tau}{m}} \quad (92)$$

where m is the mass of the electron. The minimum kinetic energy that an electron may have and still escape is the potential energy of an electron at z equals infinity. This corresponds to a minimum escape velocity magnitude of

$$|v_e| = \sqrt{\frac{2e\phi_\infty}{m}} \quad (93)$$

where ϕ_∞ is the potential as $z \rightarrow \infty$.

We now rewrite equation (90) in terms of $\nabla\phi/\phi_\infty$ and $|v|/|v_e|$.

$$\bar{x}' = -\frac{e\phi_\infty}{2m} \frac{\nabla\phi}{\phi_\infty} (\nabla t)^2 + \frac{\bar{v}}{|v_e|} |v_e| (\Delta t) + \bar{x} \quad (94)$$

But

$$\frac{e\phi_\infty}{m} = \frac{1}{2} |v_e|^2 \quad (95)$$

Therefore, Equation (94) becomes

$$\bar{x}' = -\frac{1}{2} \left(\frac{|v_e|}{\sqrt{2}} \Delta t \right)^2 \frac{\nabla\phi}{\phi_\infty} + \frac{\bar{v}}{|v_e|} (\Delta t) |v_e| + \bar{x} \quad (96)$$

Letting

$$T = \frac{|v_e| \Delta t}{\sqrt{2}} \quad (97)$$

Equation (96) becomes

$$\bar{x}' = -\frac{1}{2} \frac{\nabla\phi}{\phi_\infty} \Delta T + \sqrt{2} \frac{\bar{v}}{|v_e|} \Delta T + \bar{x} \quad (98)$$

Writing Equation (91) in terms of $\nabla\phi/\phi_\infty$ and $v/|v_e|$ and dividing by v_e ,

we have

$$\frac{\bar{v}'}{|v_e|} = \frac{e\phi_\infty}{m|v_e|} \left(\frac{\Delta\phi}{\phi_\infty} \right) \Delta t + \frac{\bar{v}}{|v_e|} \quad (99)$$

Since

$$\frac{e\phi_{\infty}}{m} = \frac{1}{2} |v_e|^2 \quad (100)$$

Equation (99) becomes

$$\frac{\bar{v}'}{|v_e|} = \frac{1}{2} \left(\frac{\Delta\phi}{\phi_{\infty}} \right) |v_e| \Delta t + \frac{\bar{v}}{|v_e|} \quad (101)$$

Substituting $\Delta T = \frac{|v_e| \Delta t}{2}$, this equation is now

$$\frac{\bar{v}'}{|v_e|} = \frac{1}{\sqrt{2}} \frac{\nabla\phi}{\phi_{\infty}} \Delta T + \frac{\bar{v}}{|v_e|}$$

We now have the equations in the normalized form that was utilized in calculating the actual electron trajectories. The trajectories were calculated for various positions on the ground plane and for various energies and angles of departure. The fraction of electrons escaping for each set of parameters was recorded in order to evaluate the effectiveness of the grids.

3. Some Approximations for Determining Whether an Electron Will Escape

Although the trajectory of an electron must be followed in most cases to see if an electron will escape, in some cases it is possible to determine this fact from the potential distribution data. The first case to be considered is that of a lower limit on the kinetic energy which must be possessed by the electron in order to escape. As stated in the preceding part, this energy corresponds to the potential energy that an electron would have at z equals infinity and is given by $-e\phi_{\infty}$.

It was found that the following approximation has significance for higher energy electrons in the line charge cases. If we approximate the field distribution of the grid by assuming the potential increases linearly in the z direction and is constant in the x and y direction, the only effect of the electric field is to exert a force on the electron

in the negative z direction. Since this is true, the electron will escape if and only if its initial velocity in the z direction is greater than or equal to the escape velocity. Therefore, the electron will escape if the following equation is satisfied:

$$\sqrt{\frac{2\tau}{m}} \cos\theta \geq |v_e| \quad (103)$$

where θ is the angle between the z axis and the velocity vector of the electron.

SECTION IV

COMPUTER SOLUTIONS

1. Preliminaries

In the preceding sections, methods have been described for calculating the potential distribution for the various conductor configurations considered in this paper. A scheme has also been presented to find the trajectories of electrons under the influence of an electrostatic potential. Utilizing this information and a digital computer, we evaluate the effectiveness of the various grids in containing Compton electron produced on the ground plane.

Potential contour plots as well as information on the trajectories of the electrons are shown for each configuration. For cases involving a series solution for the potential, comparisons are made between the error obtained using a line charge approximation and the error obtained using the series and line charge solution together. Due to limitations of time and resources, an exhaustive examination of all cases was not attempted. The programs which have been written allow such a study to be made and suggestions in the future work section would hopefully reduce the time needed to do this.

Before proceeding with the results of the computer study, we present the drawing below to clarify the labeling used in this section. The ground plane corresponds at all times to the x-y plane. The angles θ and β are used in the following parts of this section in specifying the direction of the electrons leaving the ground plane. The values of the angle θ are given in degrees and those of the angle β are given in radians.

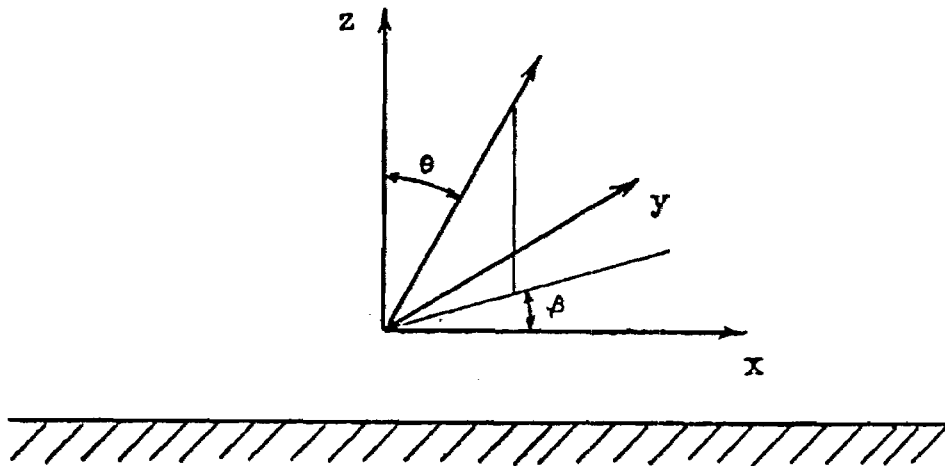


Figure IV-1. Coordinate System and Angles

2. Single Grid of Small Radii Conductors

We first consider the case of Section I in which the conductors have a diameter which is sufficiently small so that they may be approximated by line charges. We present potential contour maps for four spacings of conductors. Since the geometry is three dimensional, the potential is plotted in several sections normal to the grid. Five planes were used, the first plane being the x-z plane. The other four planes were parallel to this plane and are located at $y = a/4$, $y = a/2$, $y = 3a/4$, and $y = a$. Since the potential is periodic, the plot of the potential in a plane located at $y = 5a/4$ is the same as that in the plane at $y = 3a/4$, etc. The potentials in these plots have been normalized so that the potential at $z = \infty$ is 1.0

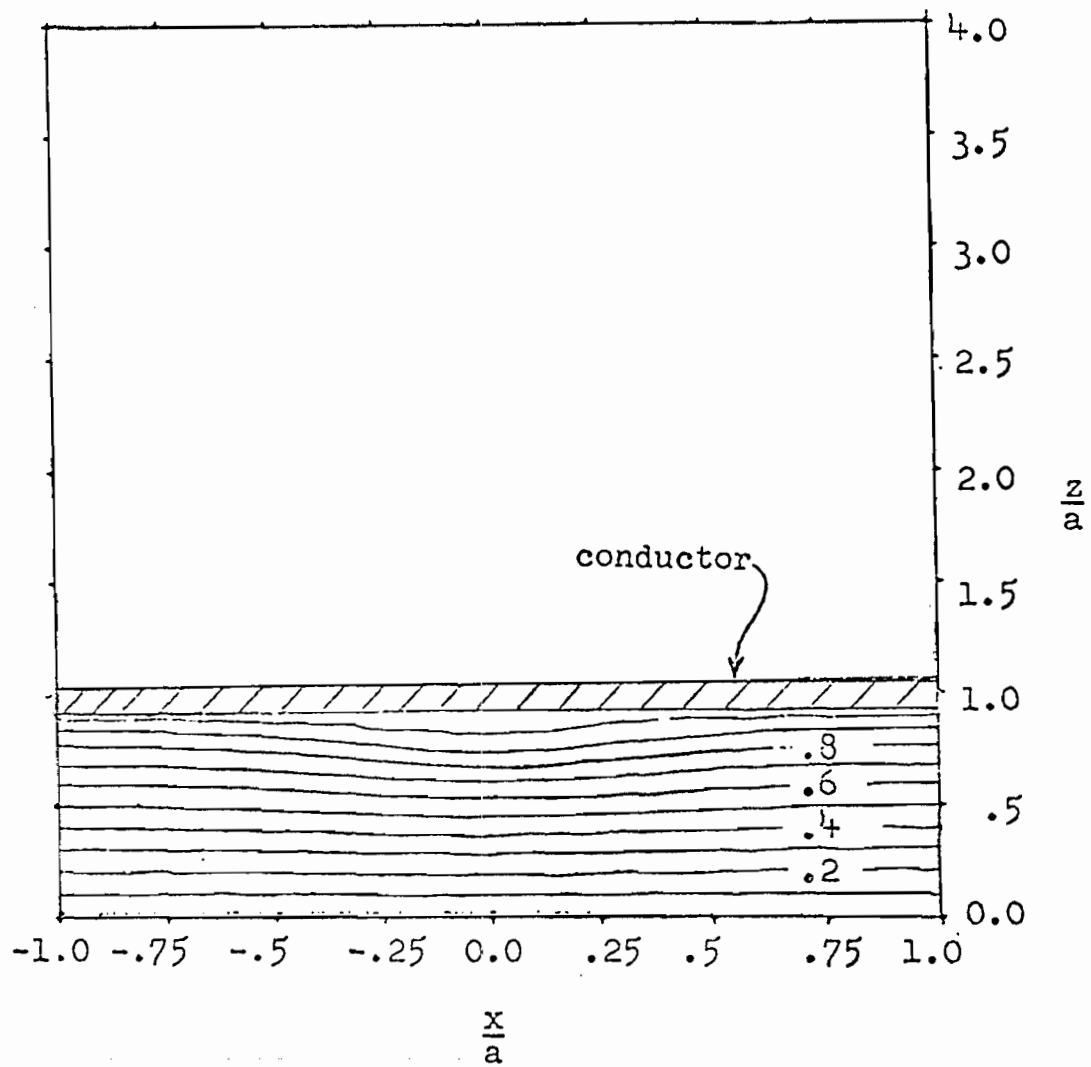


Figure IV-2a. Normalized Potential Contour Plot for $b/a = 1.0$ and $z = 0$

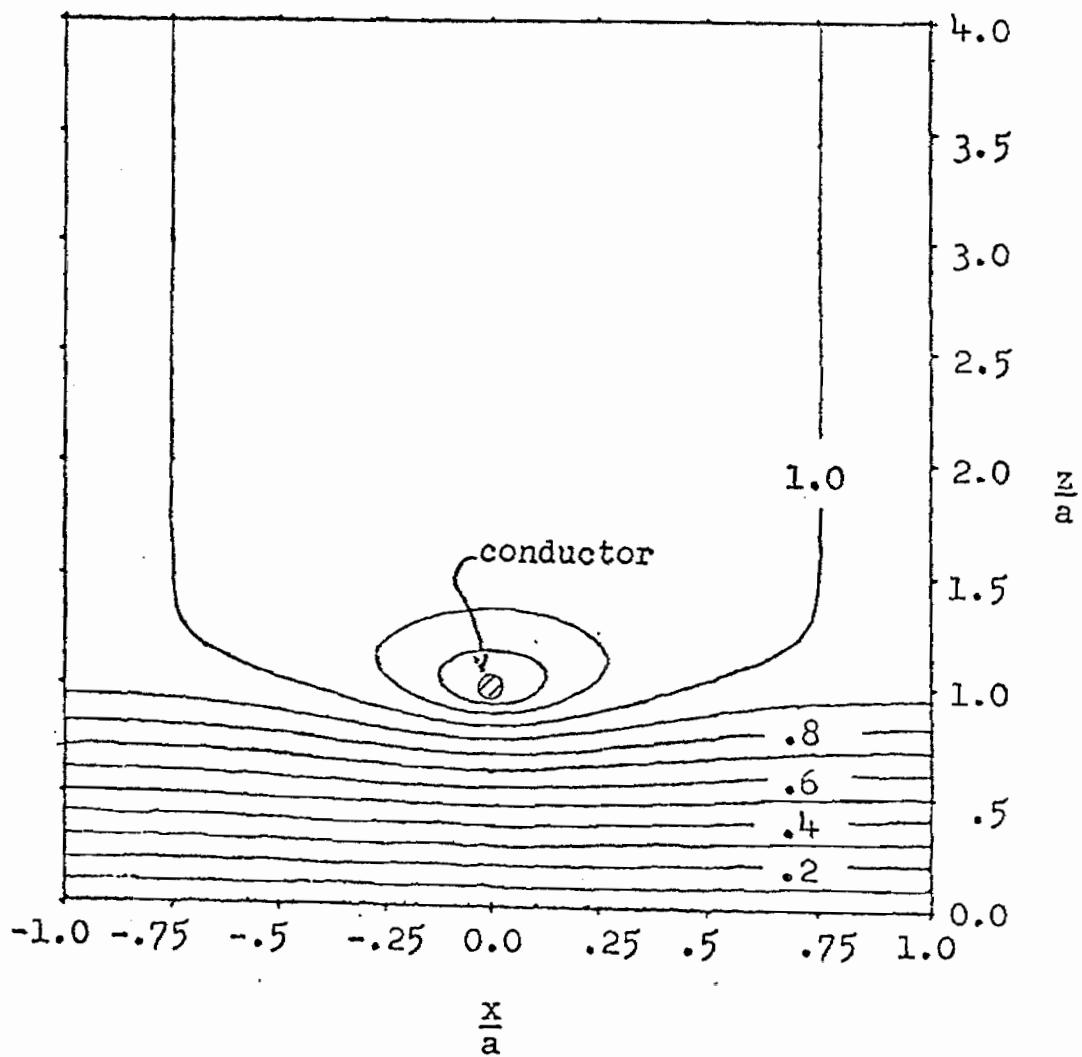


Figure IV-2b. Normalized Potential Contour Plot for $b/a = 1.0$ and $z = a/4$

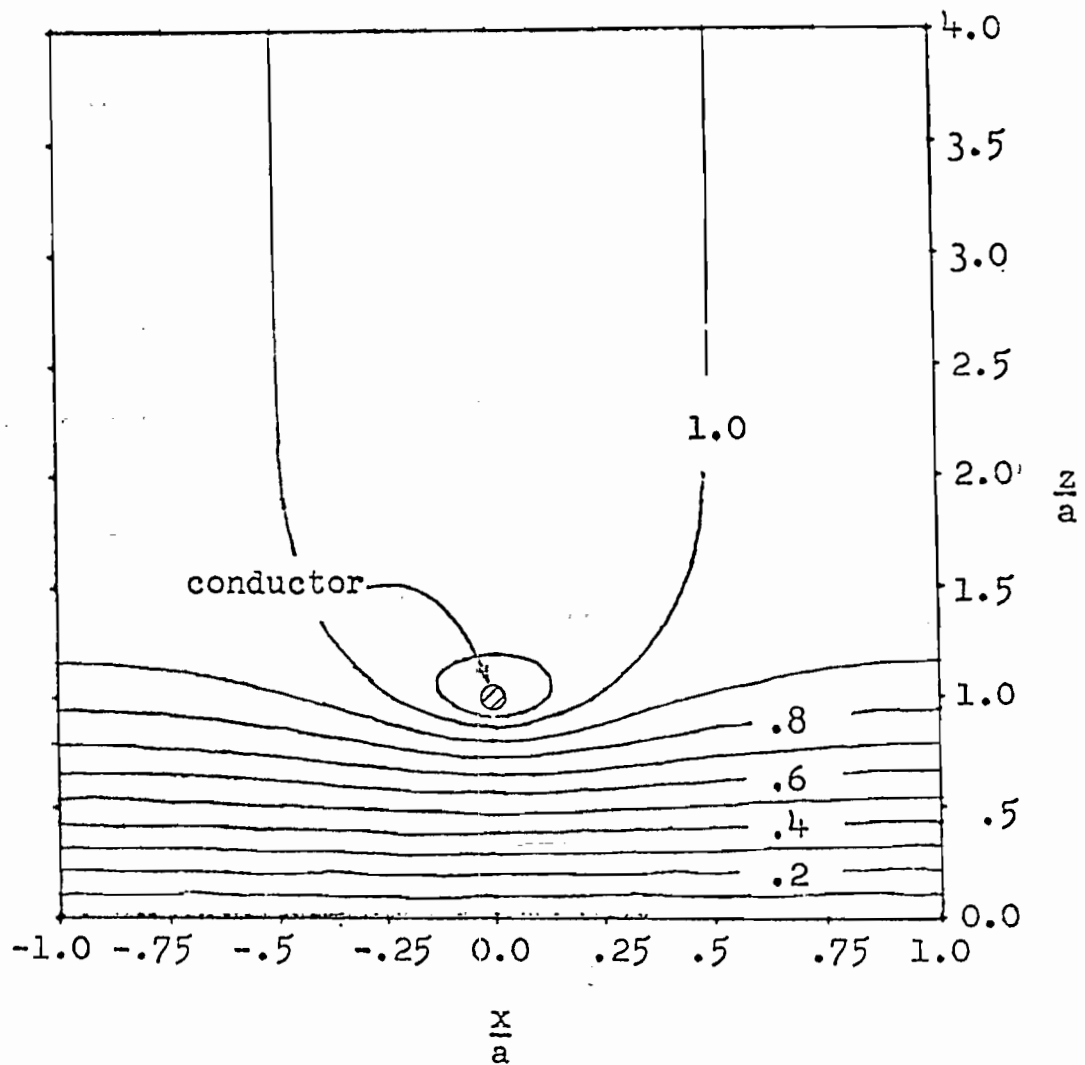


Figure IV-2c. Normalized Potential Contour Plot for $b/a = 1.0$ and $z = a/2$

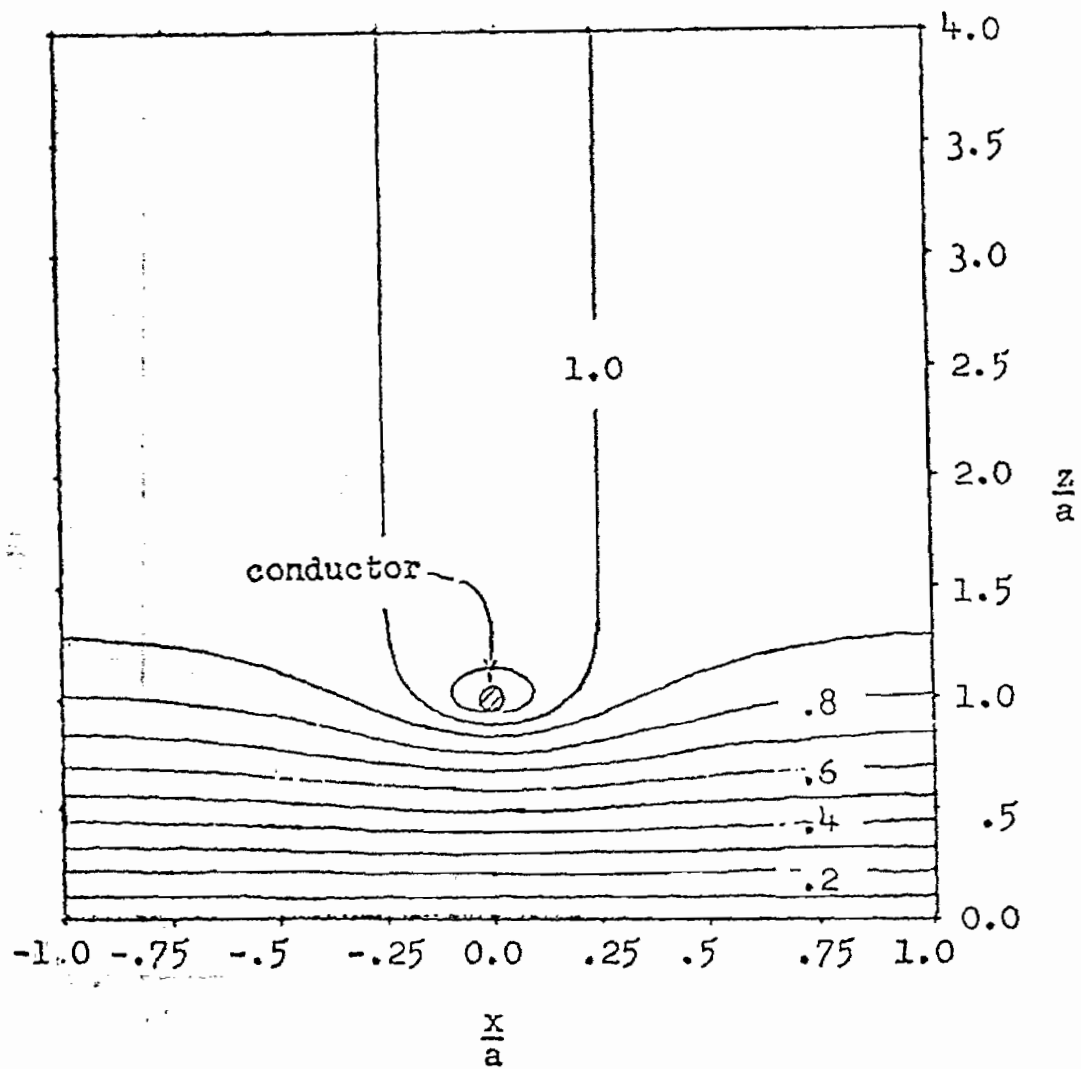


Figure IV-2d. Normalized Potential Contour Plot for $b/a = 1.0$ and $z = 3a/4$

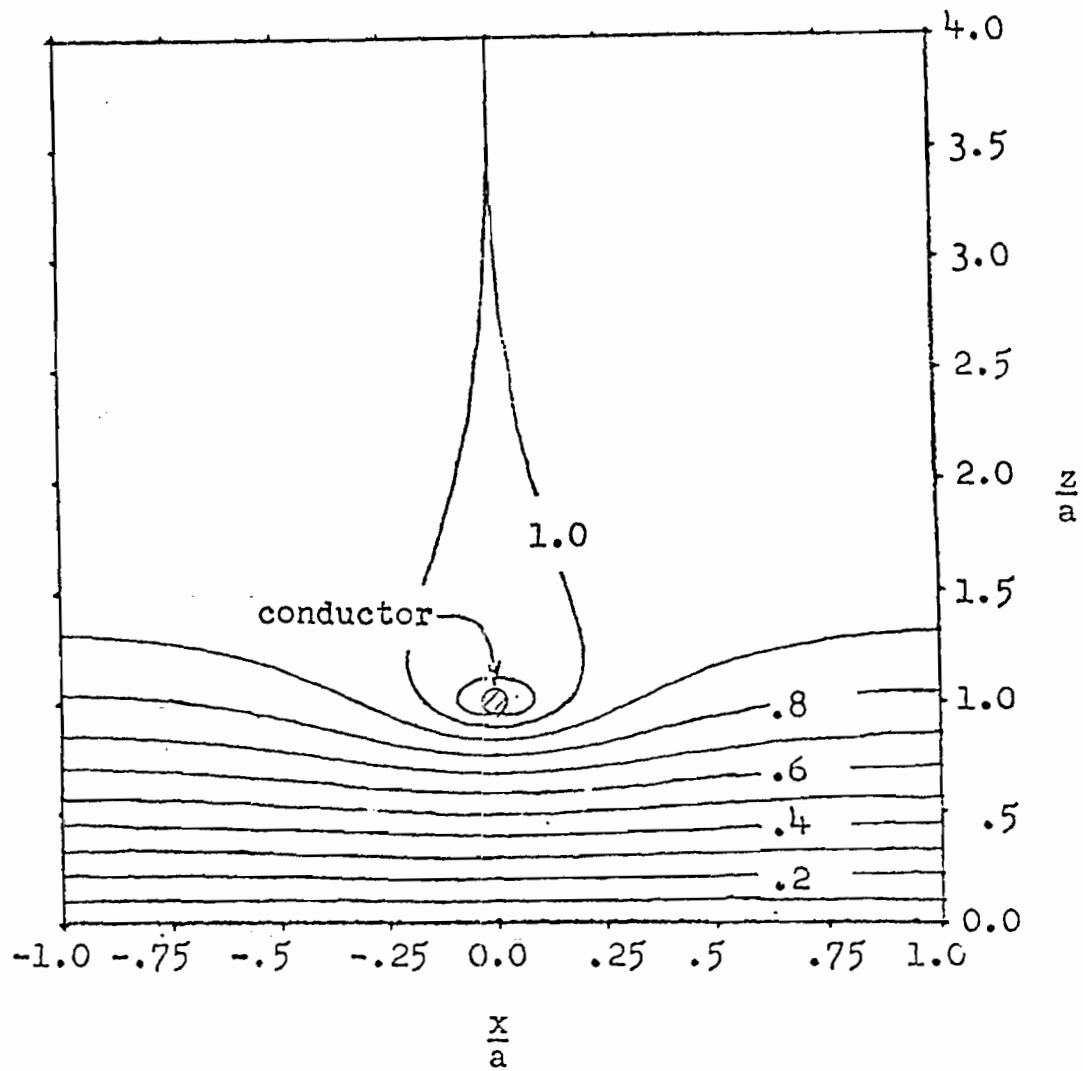


Figure IV-2e. Normalized Potential Contour Plot for $b/a = 1.0$ and $z = a$

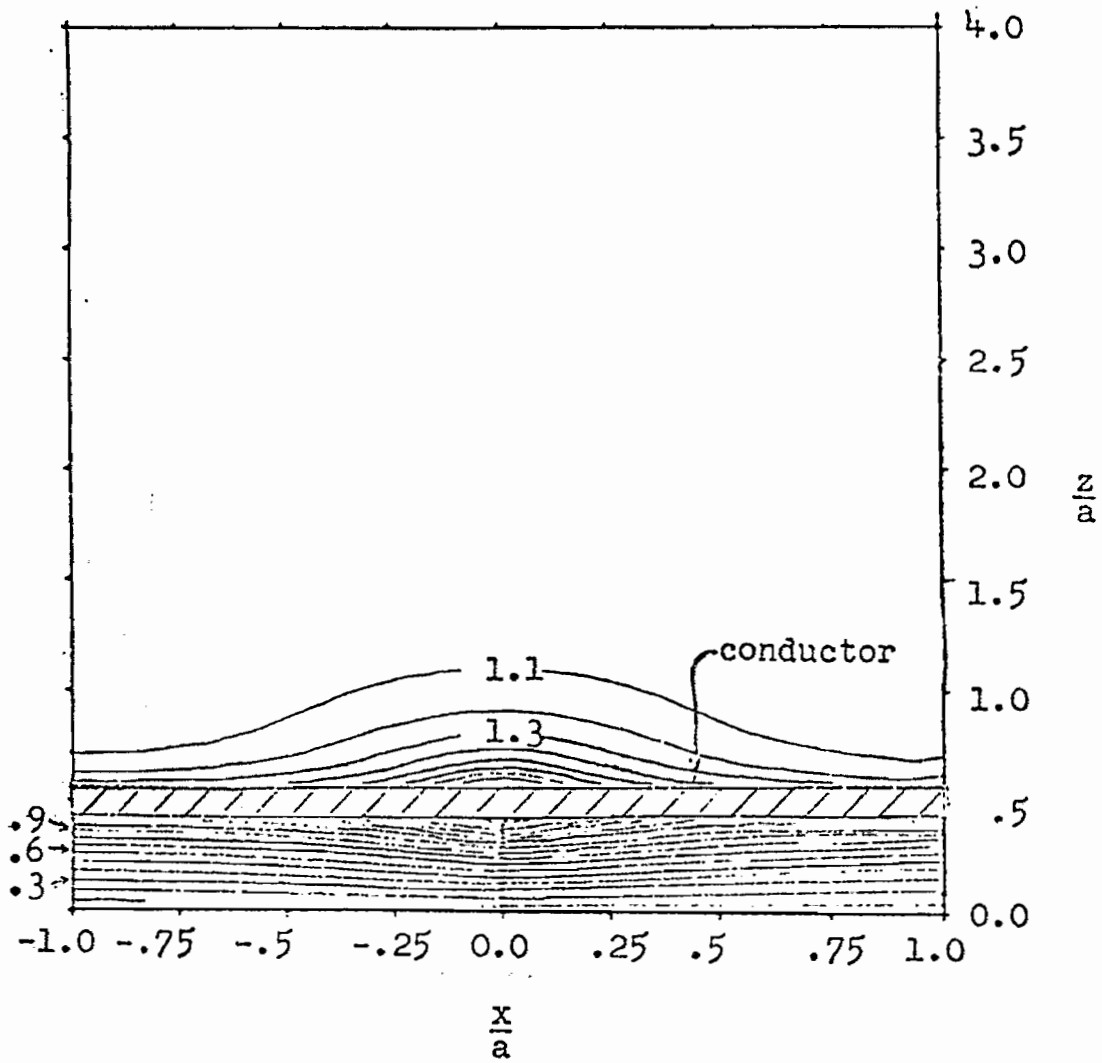


Figure IV-3a. Normalized Potential Contour Plot for $b/a = .5$ and $z = 0$

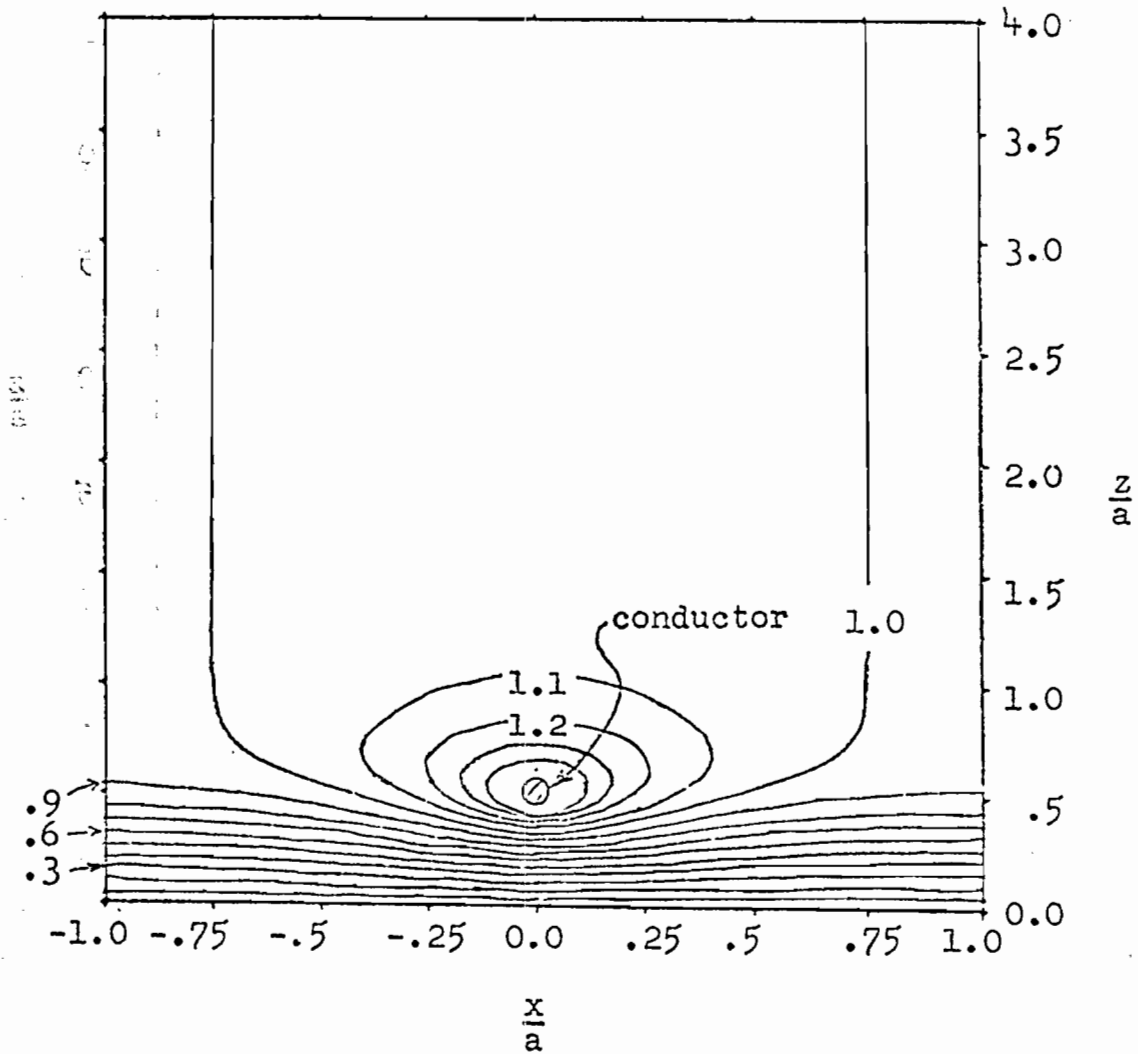


Figure IV-3b. Normalized Potential Contour Plot for $b/a = .5$ and $z = a/4$

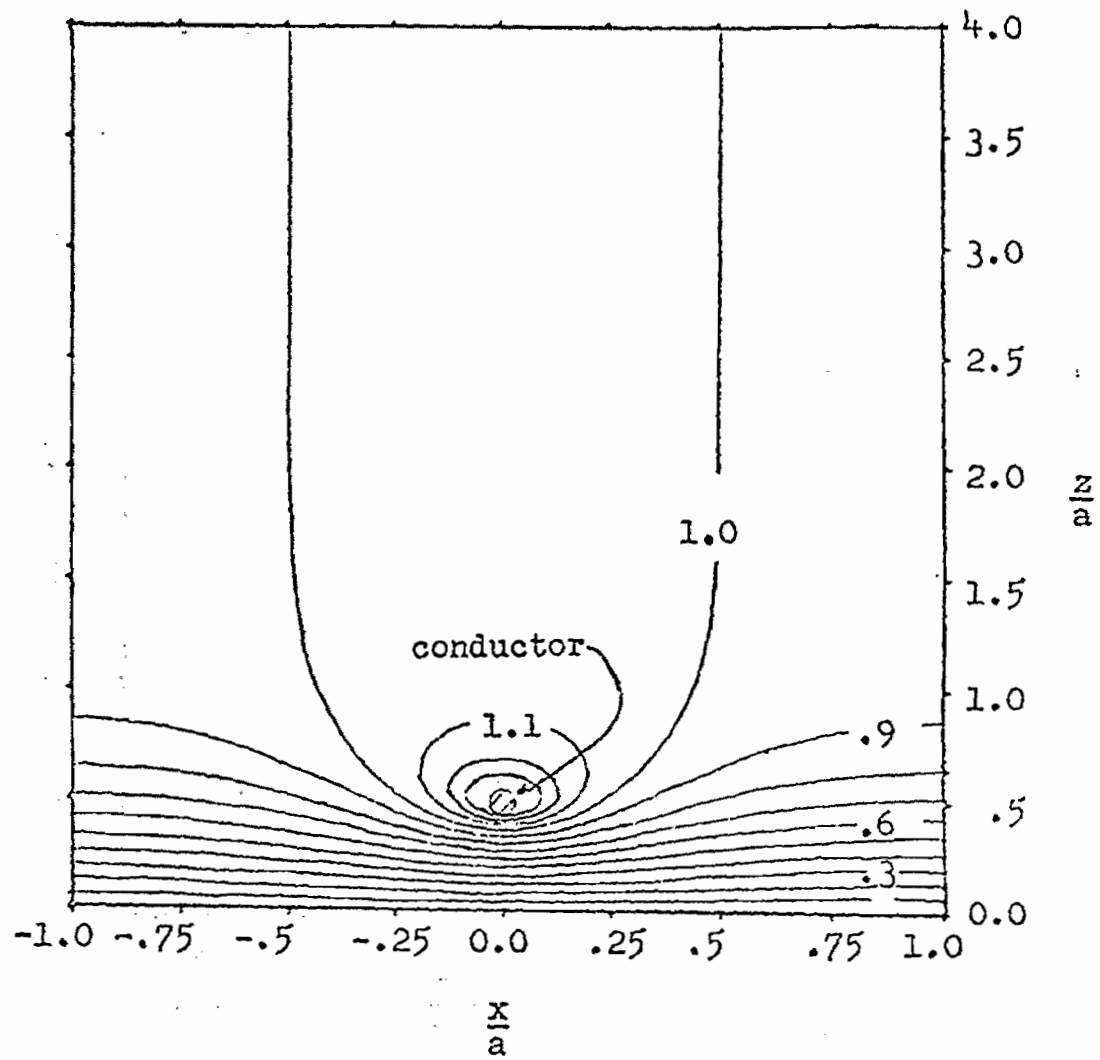


Figure IV-3c. Normalized Potential Contour Plot for $b/a = .5$ and $z = a/2$

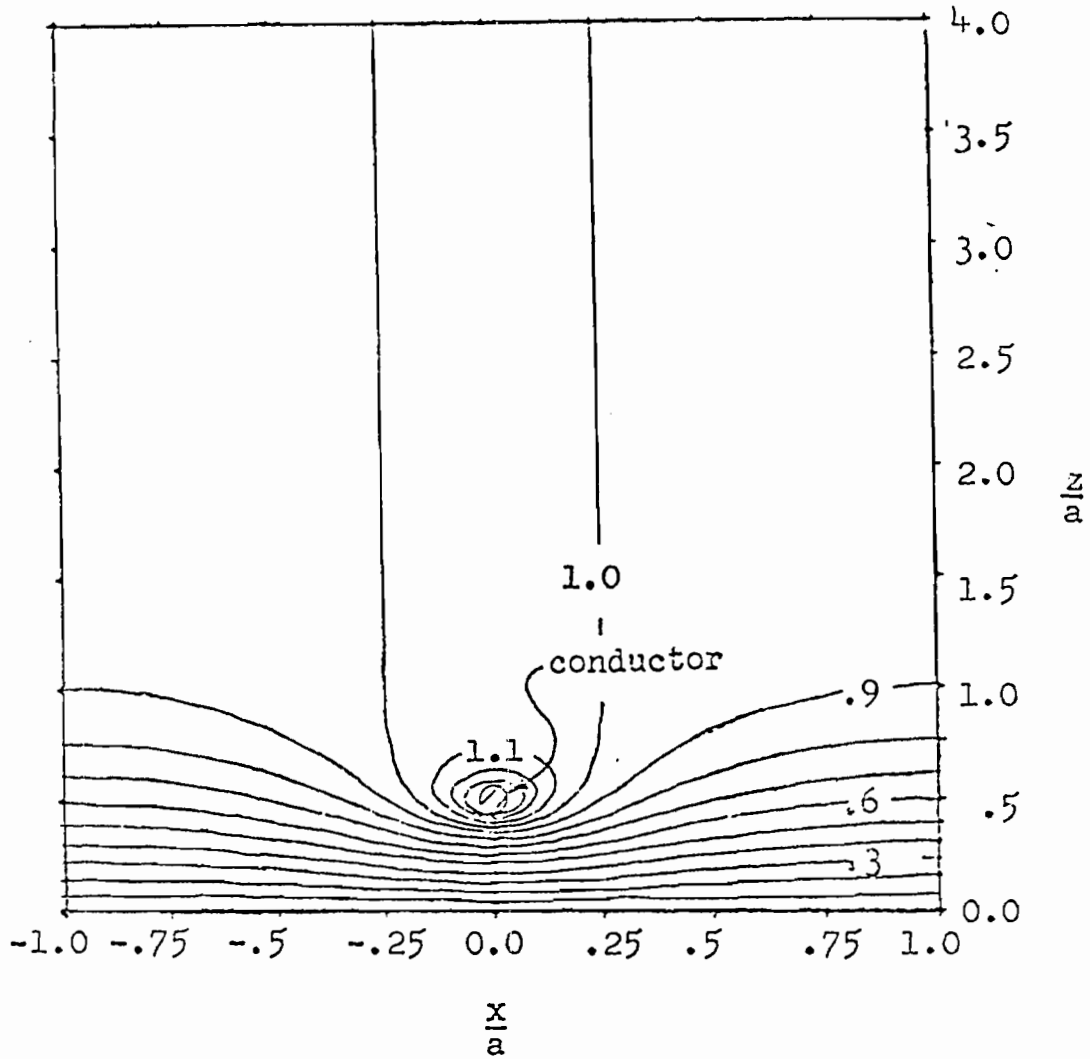


Figure IV-3d. Normalized Potential Contour Plot for $b/a = .5$
and $z = 3a/4$

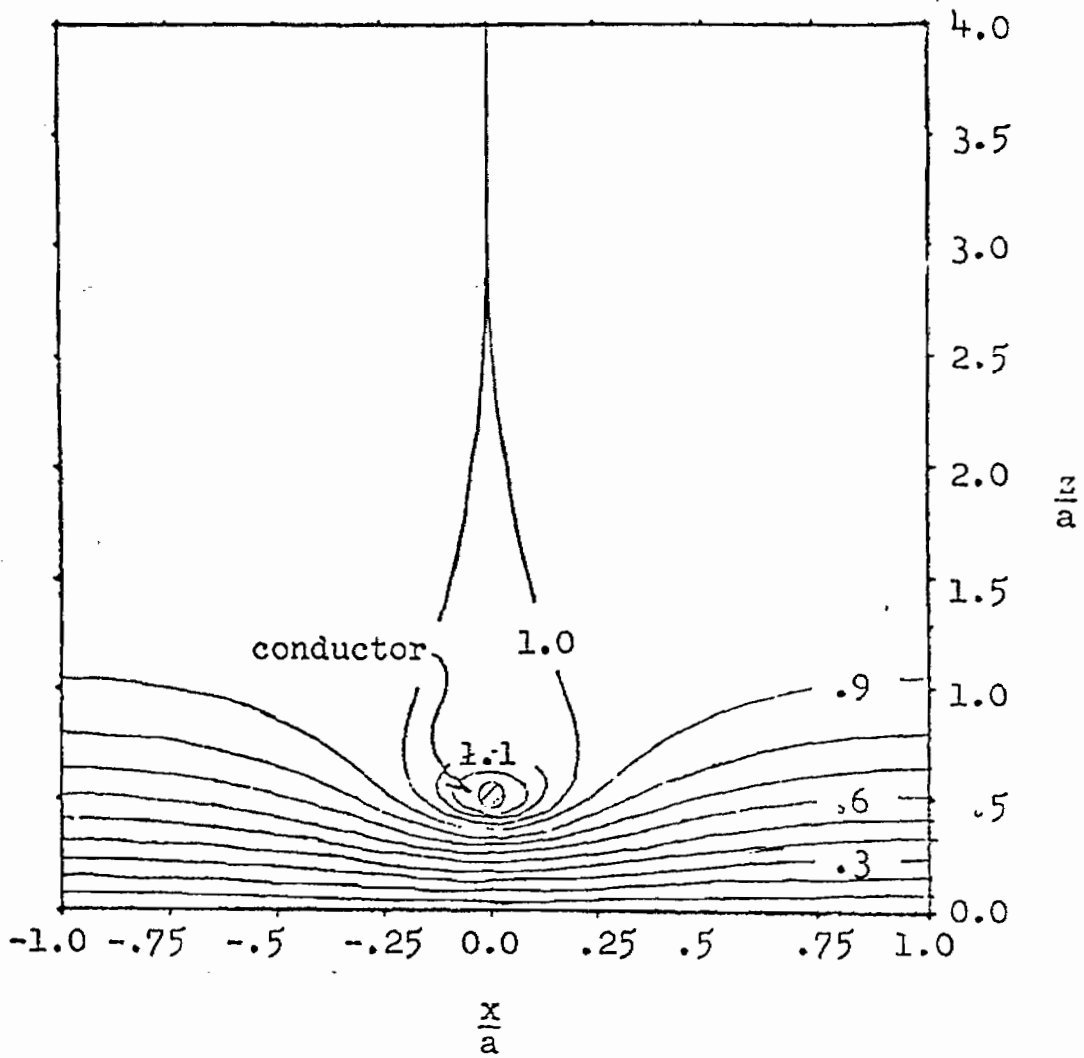


Figure IV-3e. Normalized Potential Contour Plot for $b/a = .5$ and $z = a$

The preceding plots were informative as to the potential distribution, but it is not readily apparent whether an electron leaving the ground plane will escape. In order to determine this, plots of the electron trajectories were made using the scheme described in Section III. The grid and the trajectories are shown in isometric projection. All of the electrons in one plot have the same energy and angles of departure. The initial positions of the electrons are evenly distributed on the ground plane beneath one aperture of the grid. Due to the periodicity of the potential, no other initial positions of the electrons and only those values of β between 0 and $\pi/4$ radians need be considered. The electron trajectories were calculated until the electron either returned to the ground plane or the z component of its position was equal to 2, at which time it was deemed to have escaped. For clarity, only one aperture of the grid is shown in the plots.

In the interest of brevity, a complete set of trajectories for normalized energies of 1.1, 1.3, and 2.0 with value of θ of 0° , 10° , 20° and 30° with values of β of 0, $\pi/8$, and $\pi/4$ radians are given only for the spacing $b/a = 1.0$. For the spacing of $b/a = .5$, only the trajectories for a normalized energy of 1.1 are presented for comparison.

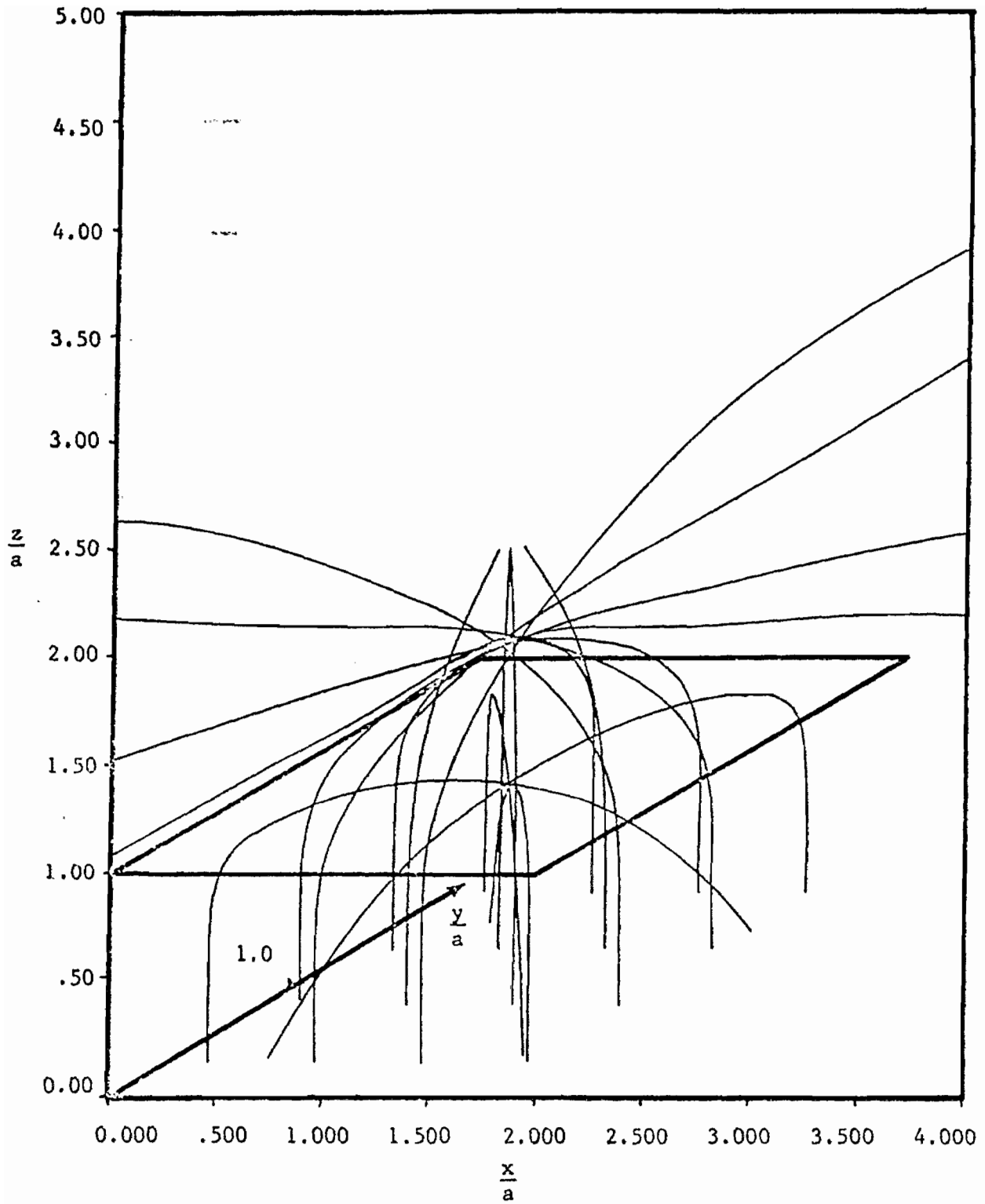


Figure IV-4a. Electron Trajectories for $b/a = 1.0$, Normalized Energy of 1.1, $B = 0$ radian, and $\theta = 0^\circ$

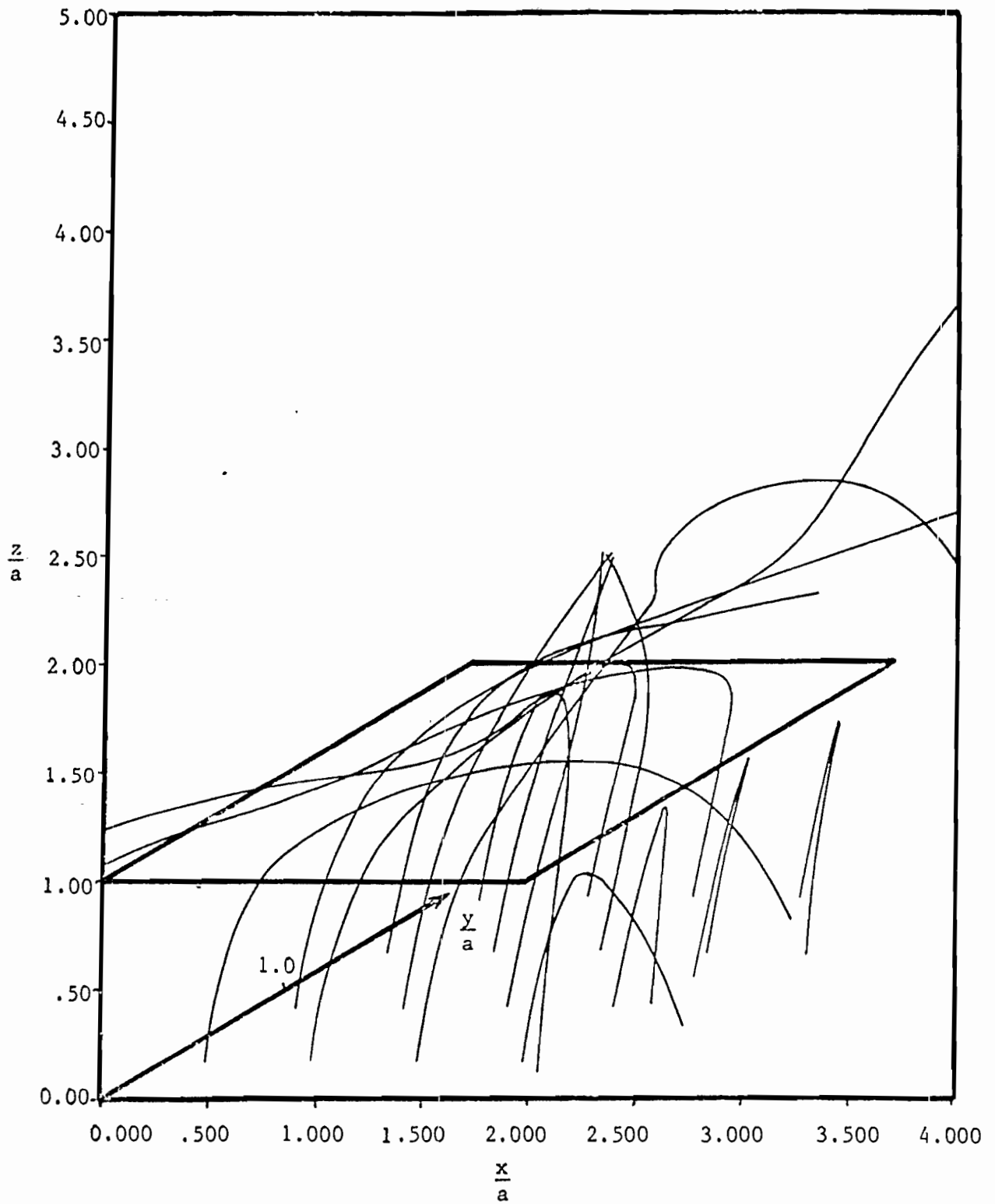


Figure IV-4b. Electron Trajectories for $b/a = 1.0$, Normalized Energy of 1.1, $B = 0$ radian, and $\theta = 10^\circ$

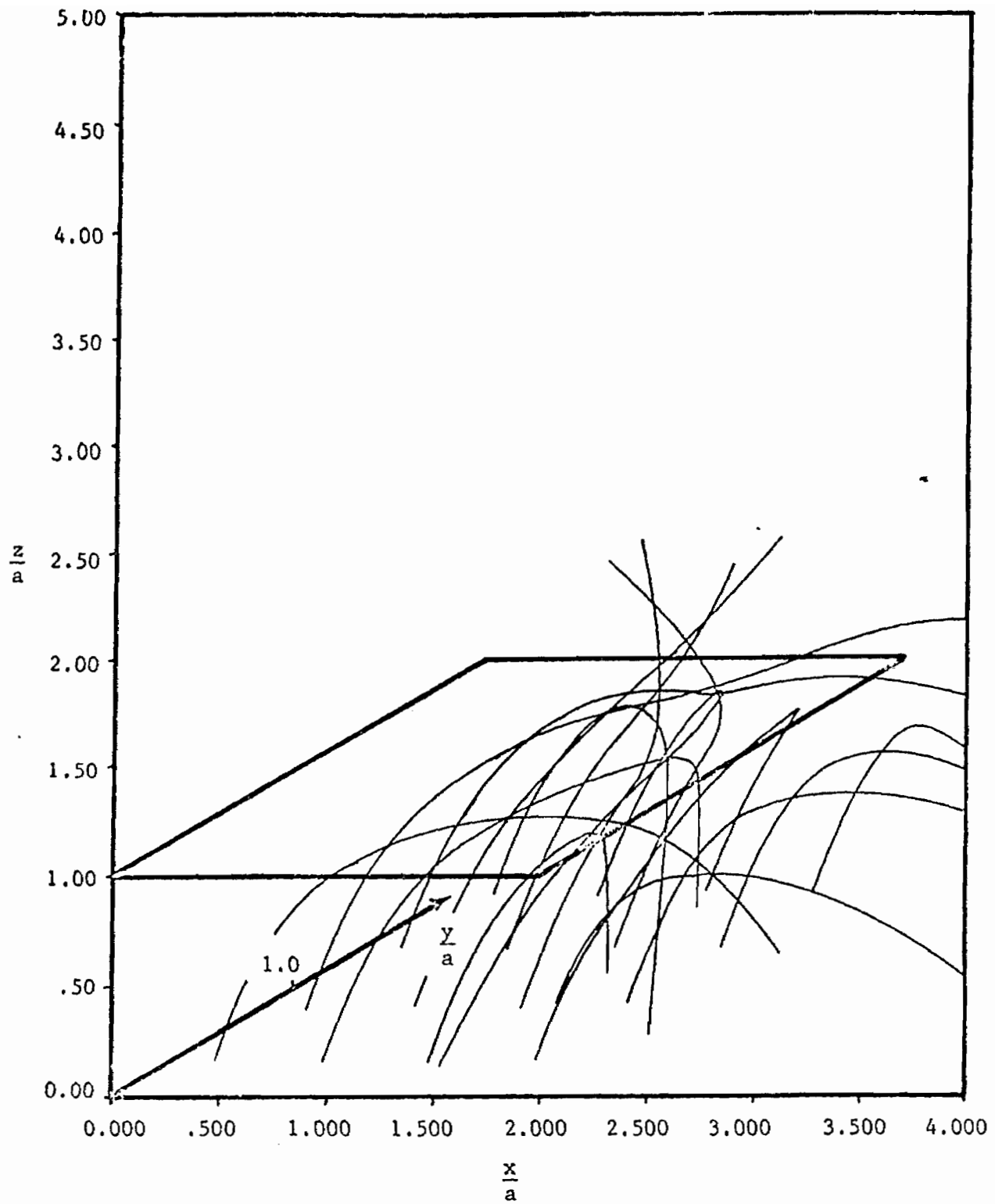


Figure IV-4c. Electron Trajectories for $b/a = 1.0$,
 Normalized Energy of 1.1, $B = 0$ radian, and $\theta = 20^\circ$

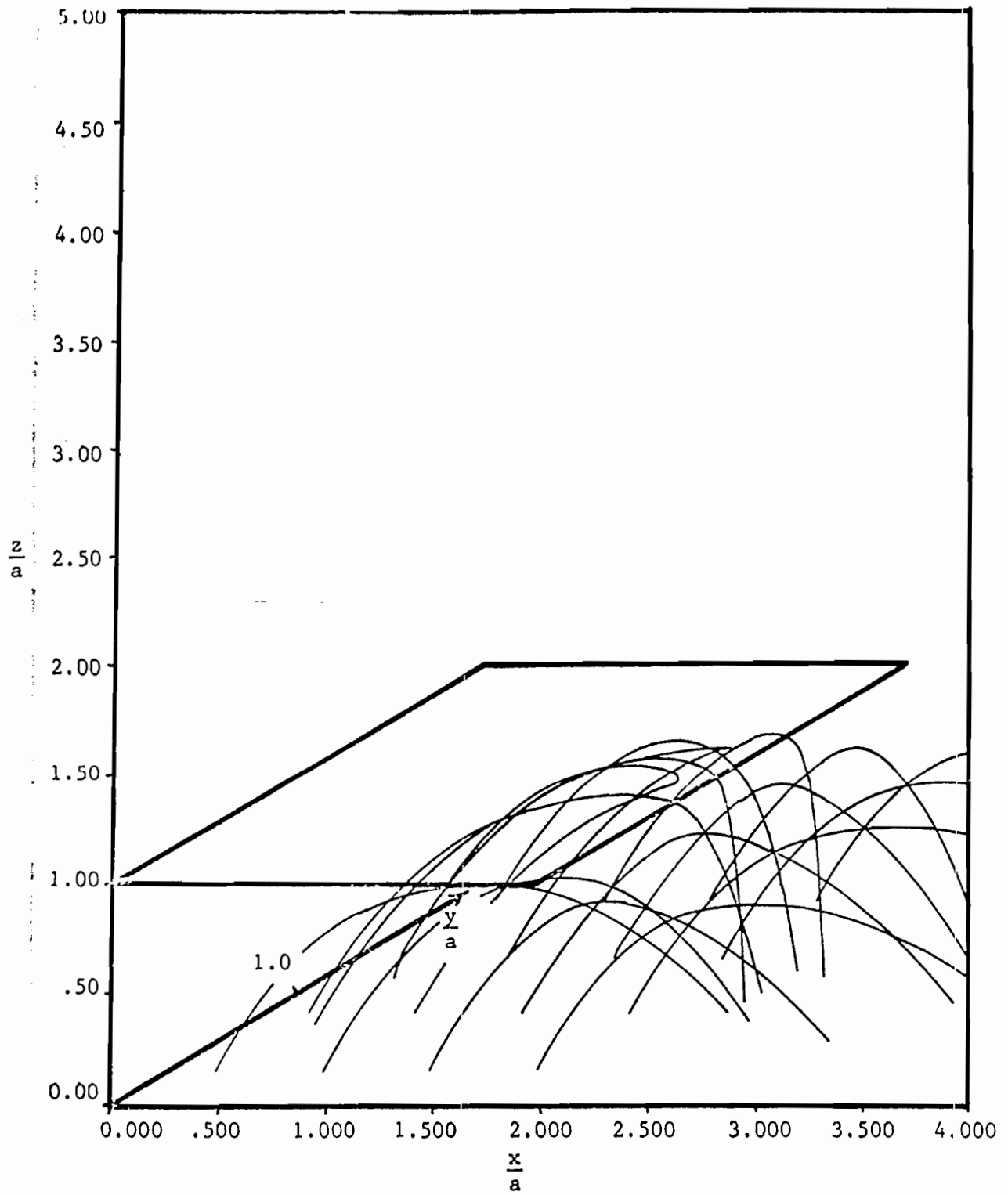


Figure IV-4d. Electron Trajectories for $b/a = 1.0$,
 Normalized Energy of 1.1, $B = 0$ radian, and $\theta = 30^\circ$

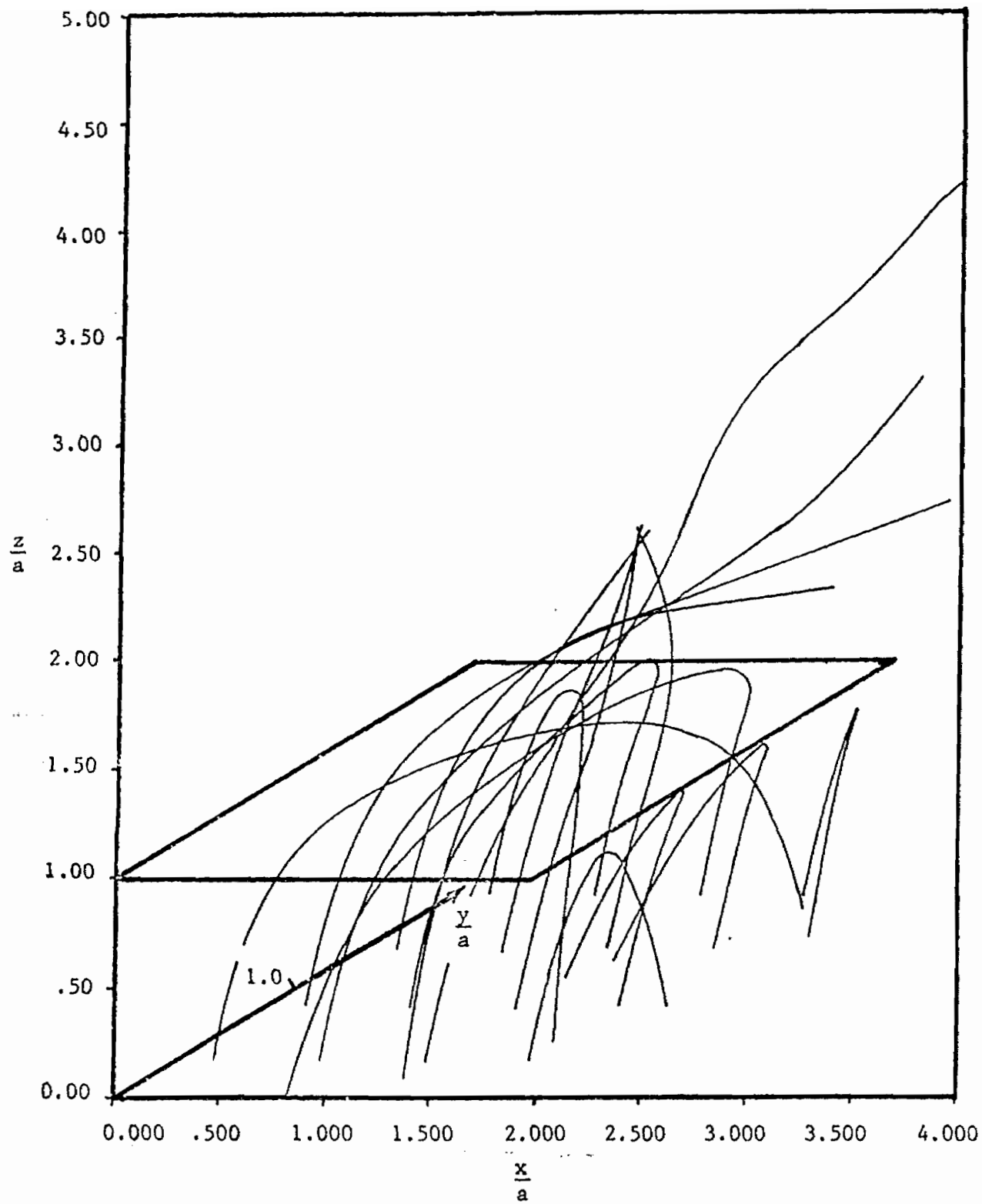


Figure IV-4e. Electron Trajectories for $b/a = 1.0$, Normalized Energy of 1.1, $B = \pi/8$ radians, and $\theta = 10^\circ$

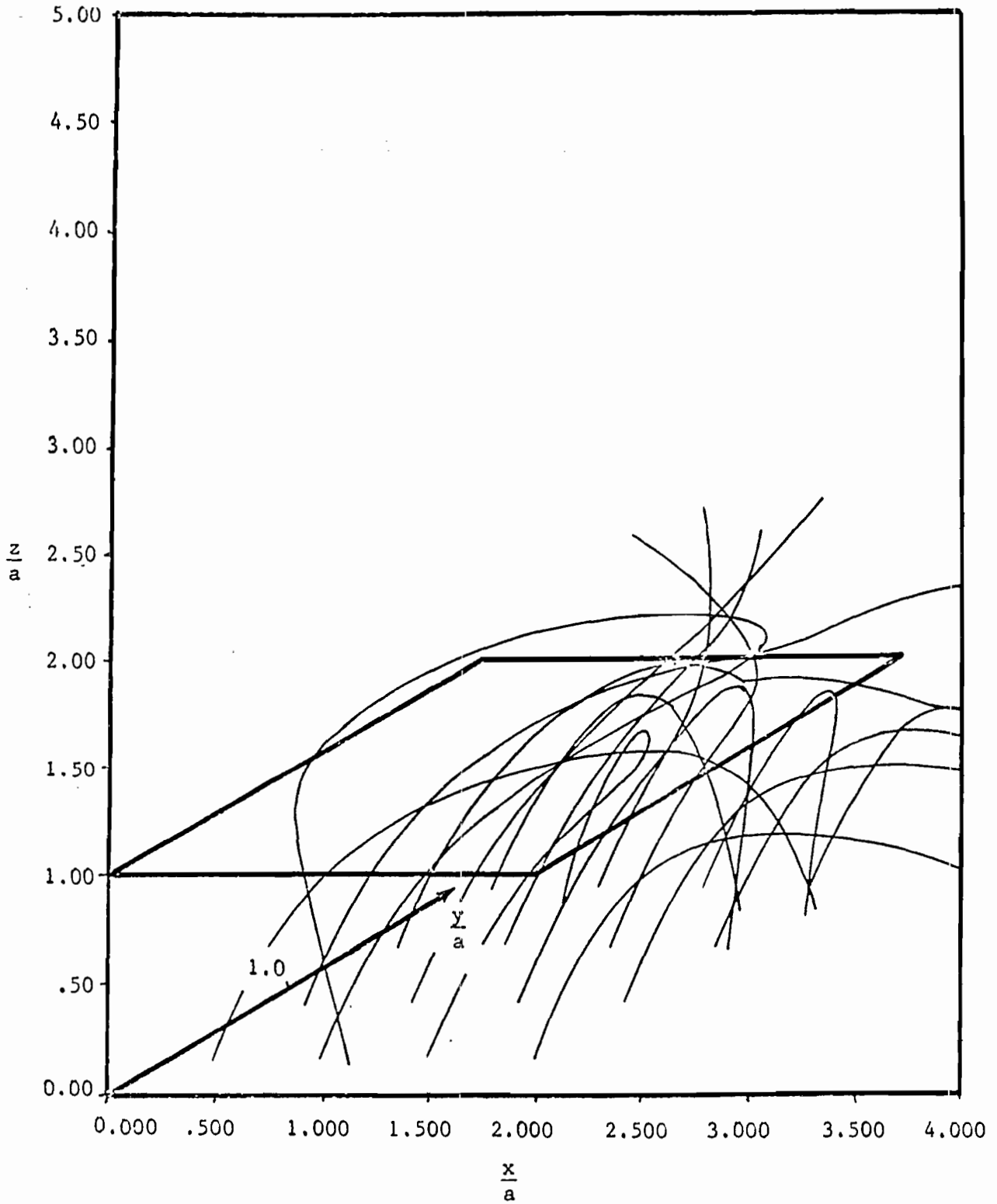


Figure IV-4f. Electron Trajectories for $b/a = 1.0$,
 Normalized Energy of 1.1, $B = \pi/8$ radians, and $\theta = 20^\circ$

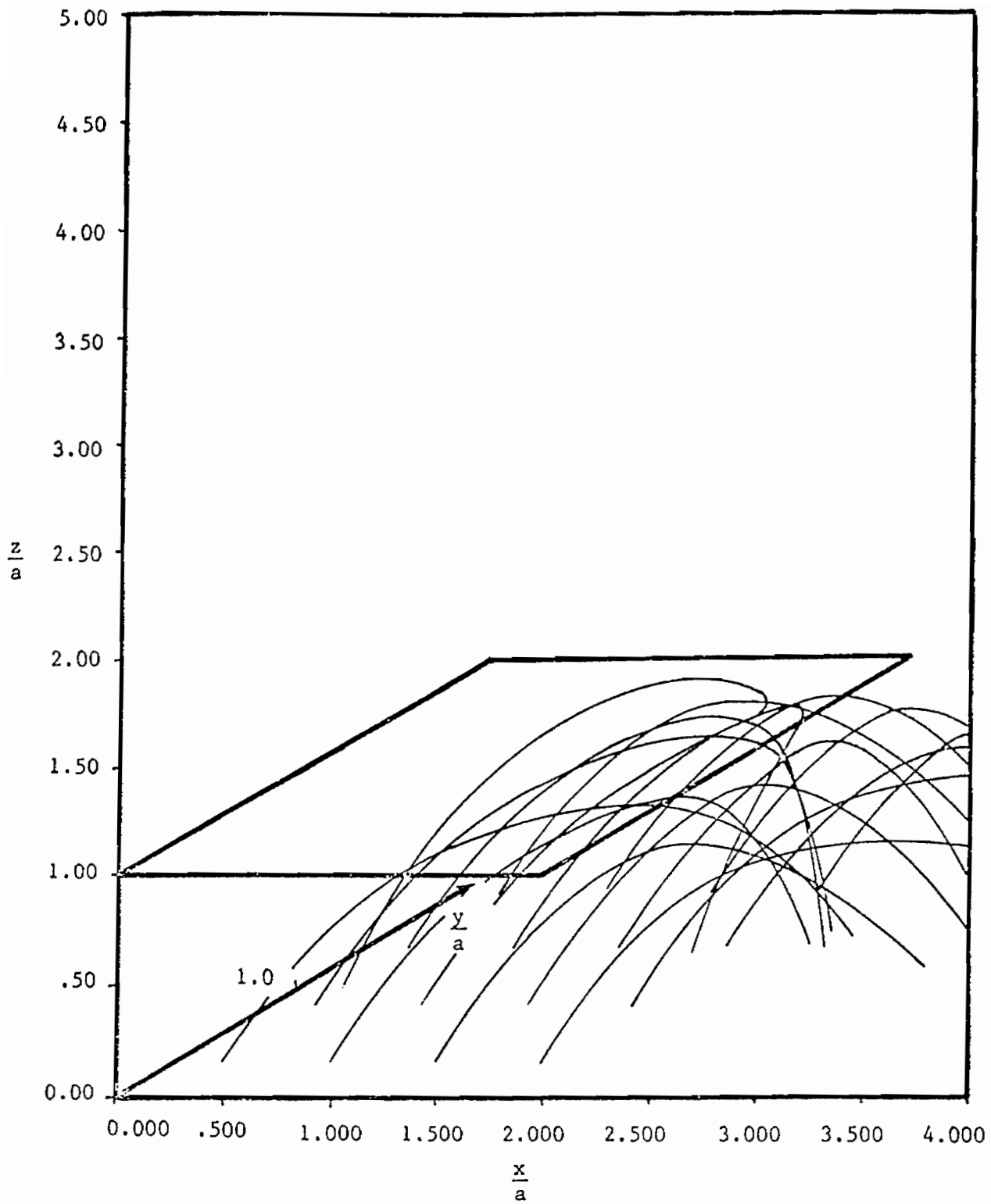


Figure IV-4g. Electron Trajectories for $b/a = 1.0$,
 Normalized Energy of 1.1, $B = \pi/8$ radians, and $\theta = 30^\circ$

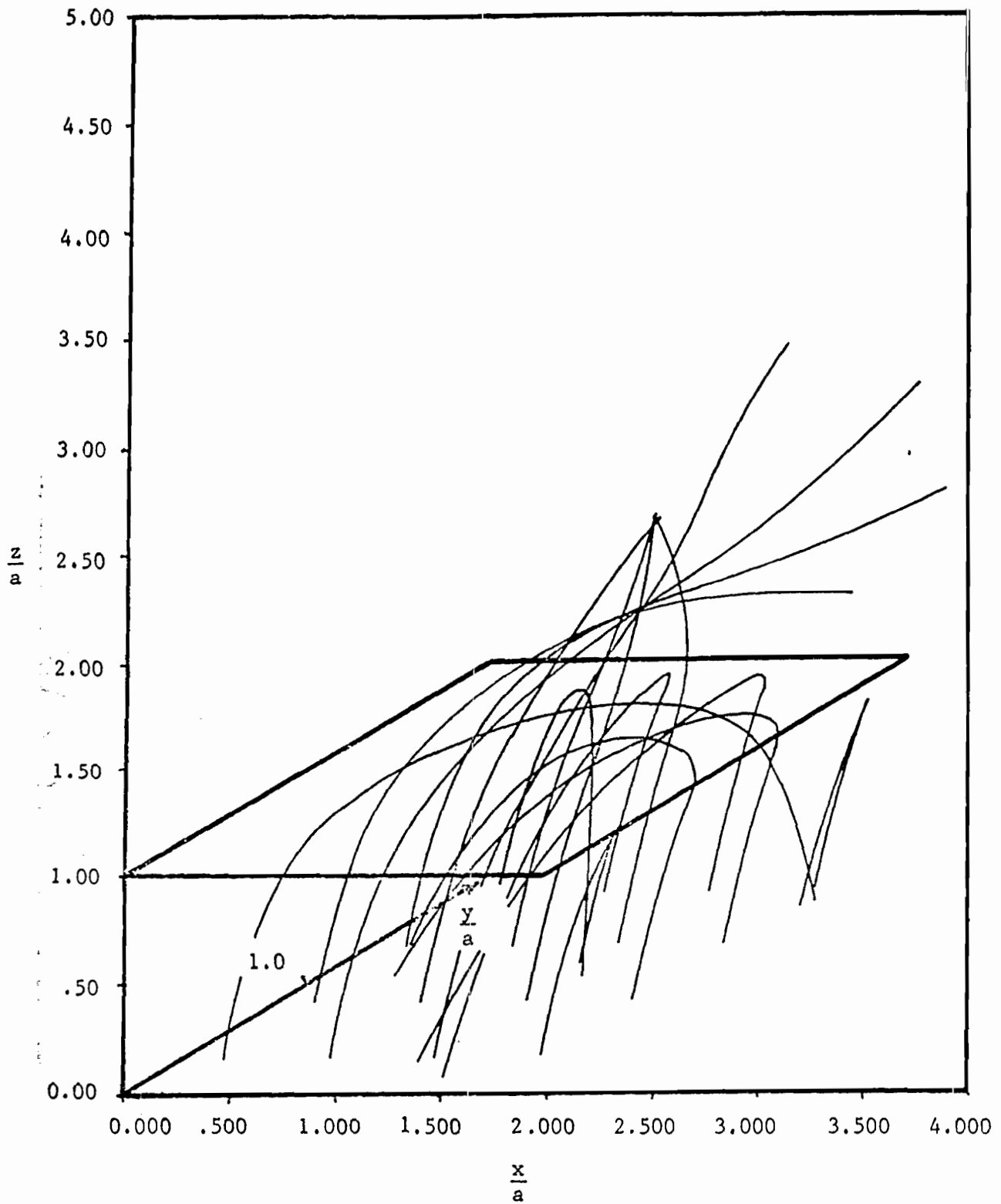


Figure IV-4h. Electron Trajectories for $b/a = 1.0$,
 Normalized Energy of 1.1, $B = \pi/4$ radian, and $\theta = 10^\circ$

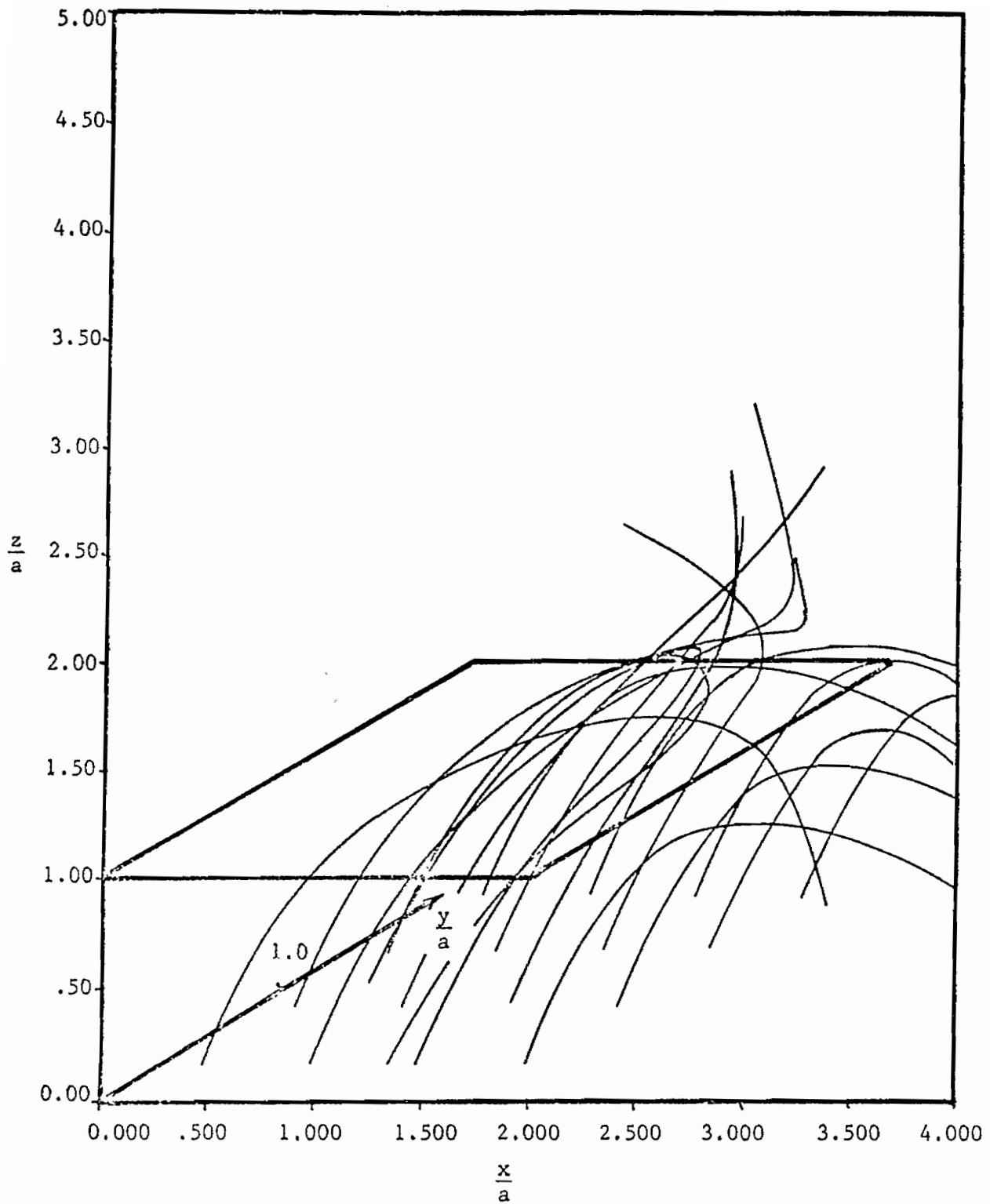


Figure IV-4i. Electron Trajectories for $b/a = 1.0$,
 Normalized Energy of 1.1, $B = \pi/4$ radians, and $\theta = 20^\circ$

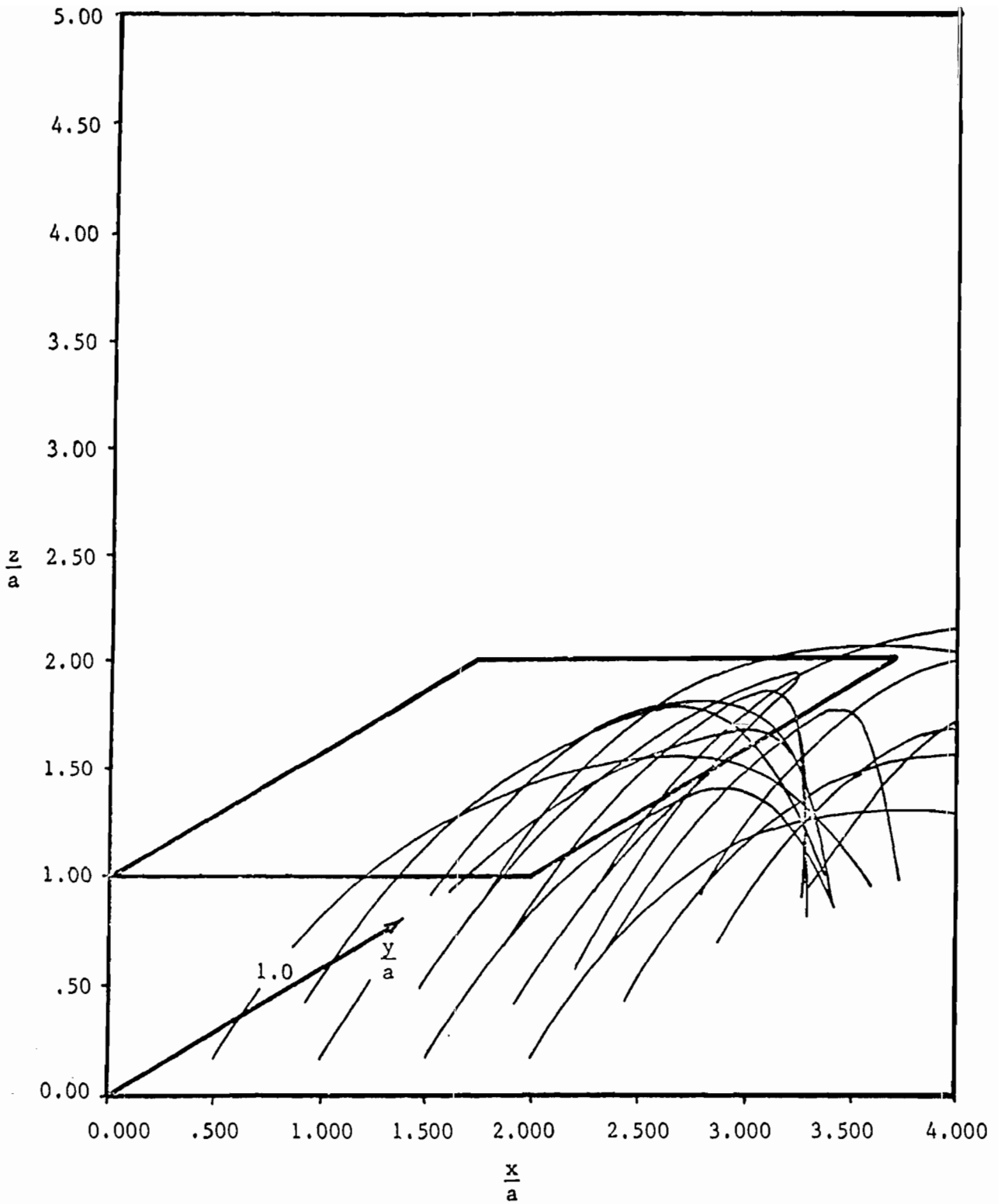


Figure IV-4j. Electron Trajectories for $b/a = 1.0$,
 Normalized Energy of 1.1, $B = \pi/4$ radians, and $\theta = 30^\circ$

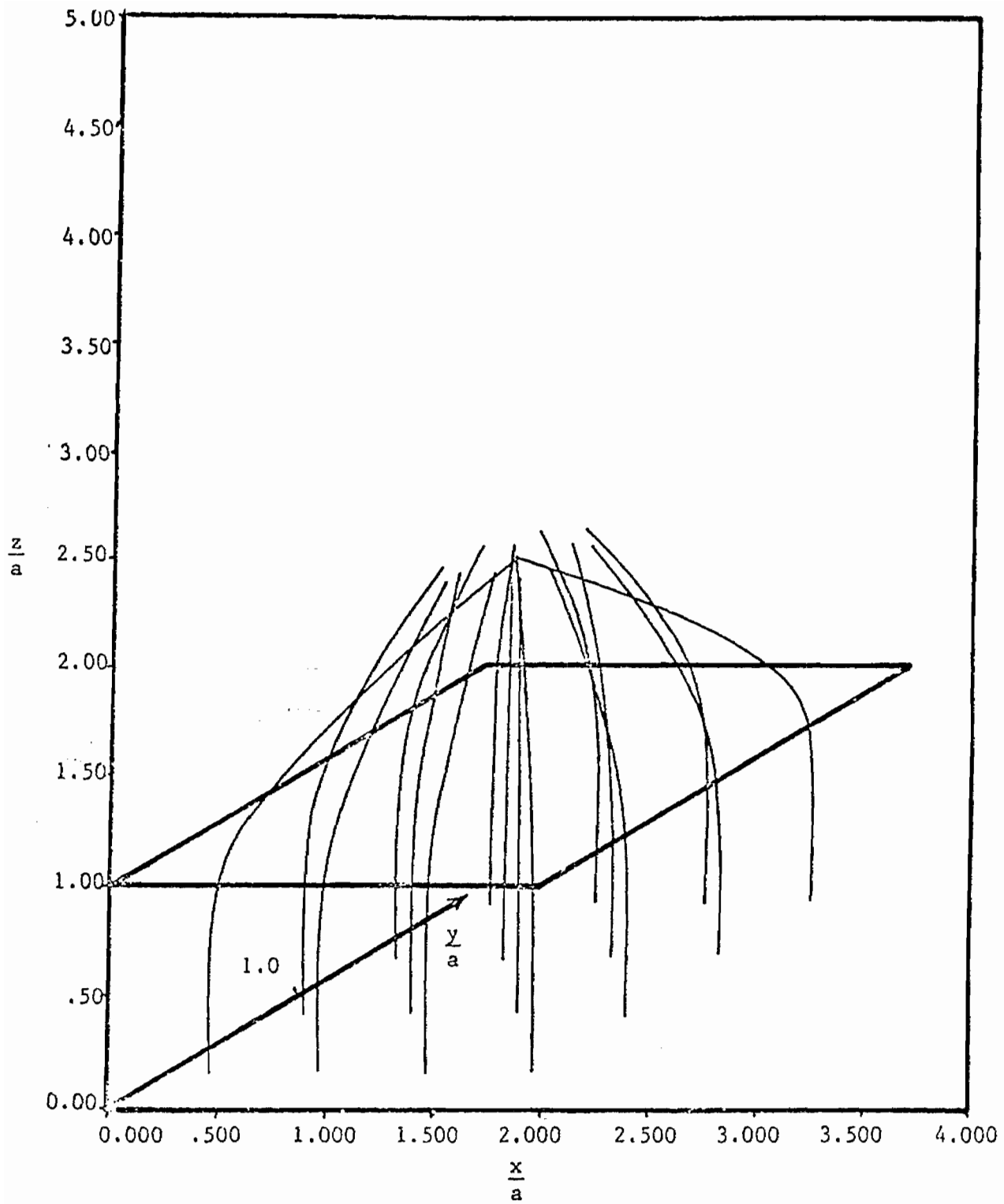


Figure IV-5a. Electron Trajectories for $b/a = 1.0$, Normalized Energy of 1.3, $B = 0$ radian, and $\theta = 0^\circ$

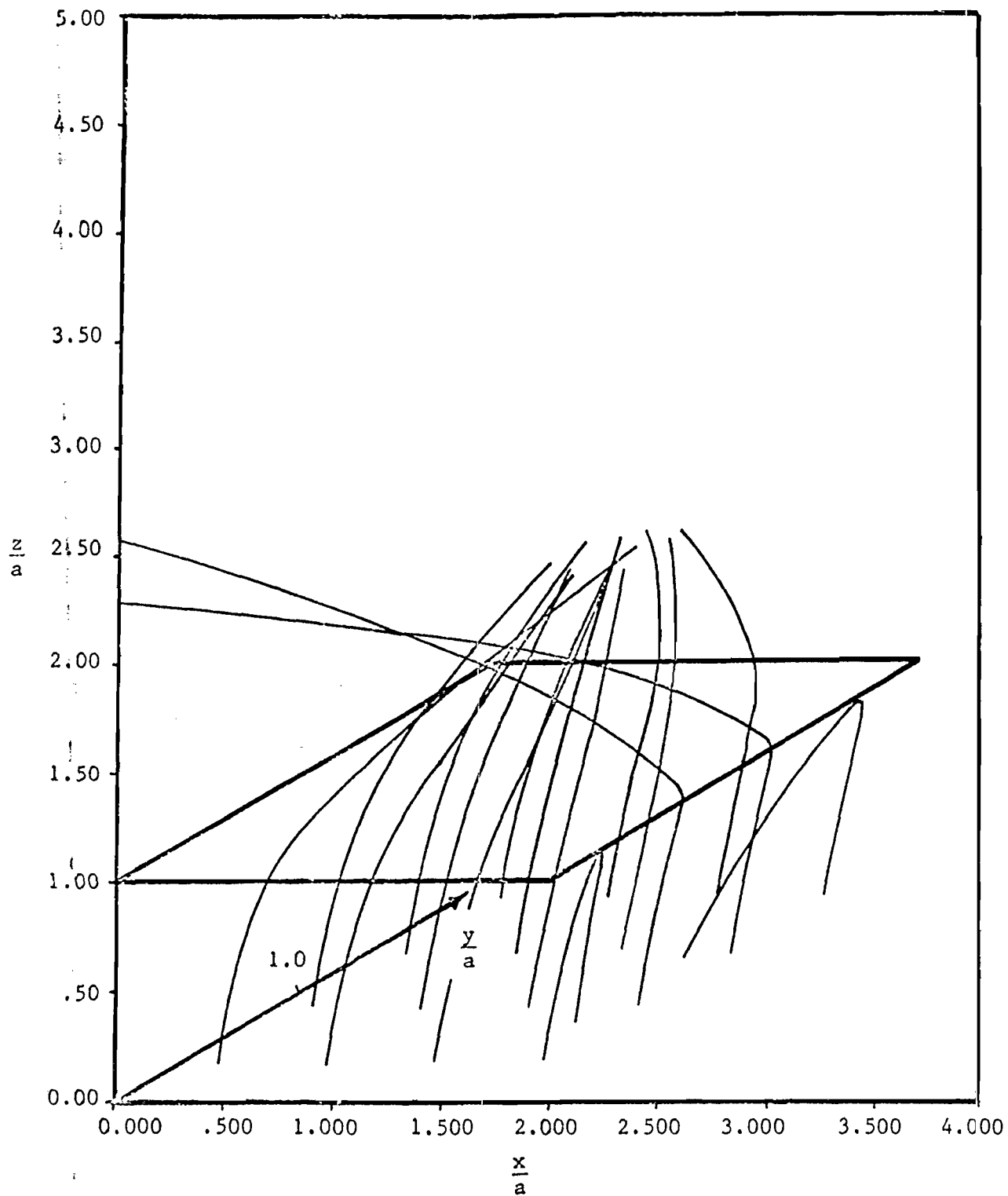


Figure IV-5b. Electron Trajectories for $b/a = 1.0$,
 Normalized Energy of 1.3, $B = 0$ radian, and $\theta = 10^\circ$

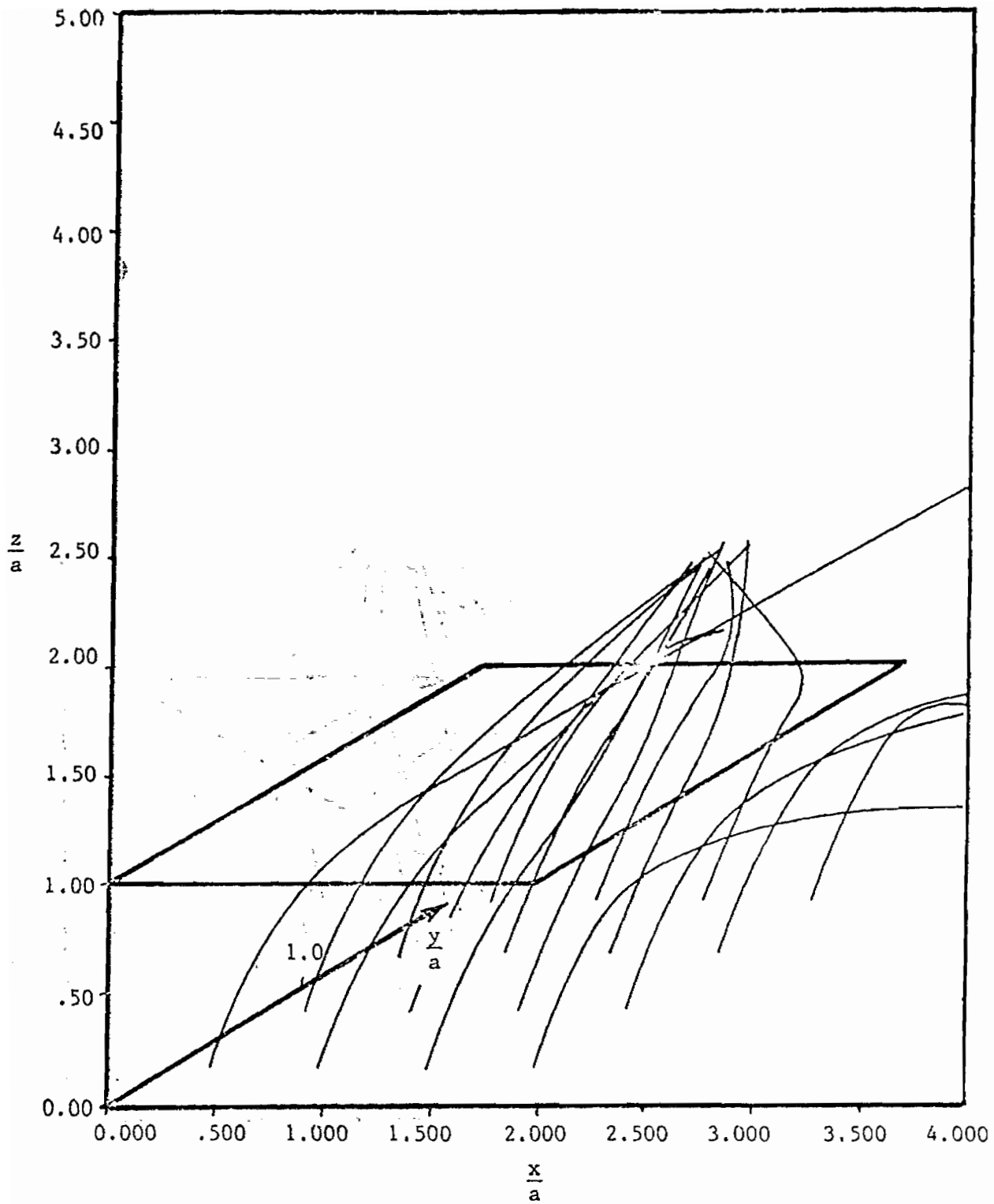


Figure IV-5c. Electron Trajectories for $b/a = 1.0$,
 Normalized Energy of 1.3, $B = 0$ radian, and $\theta = 20^\circ$

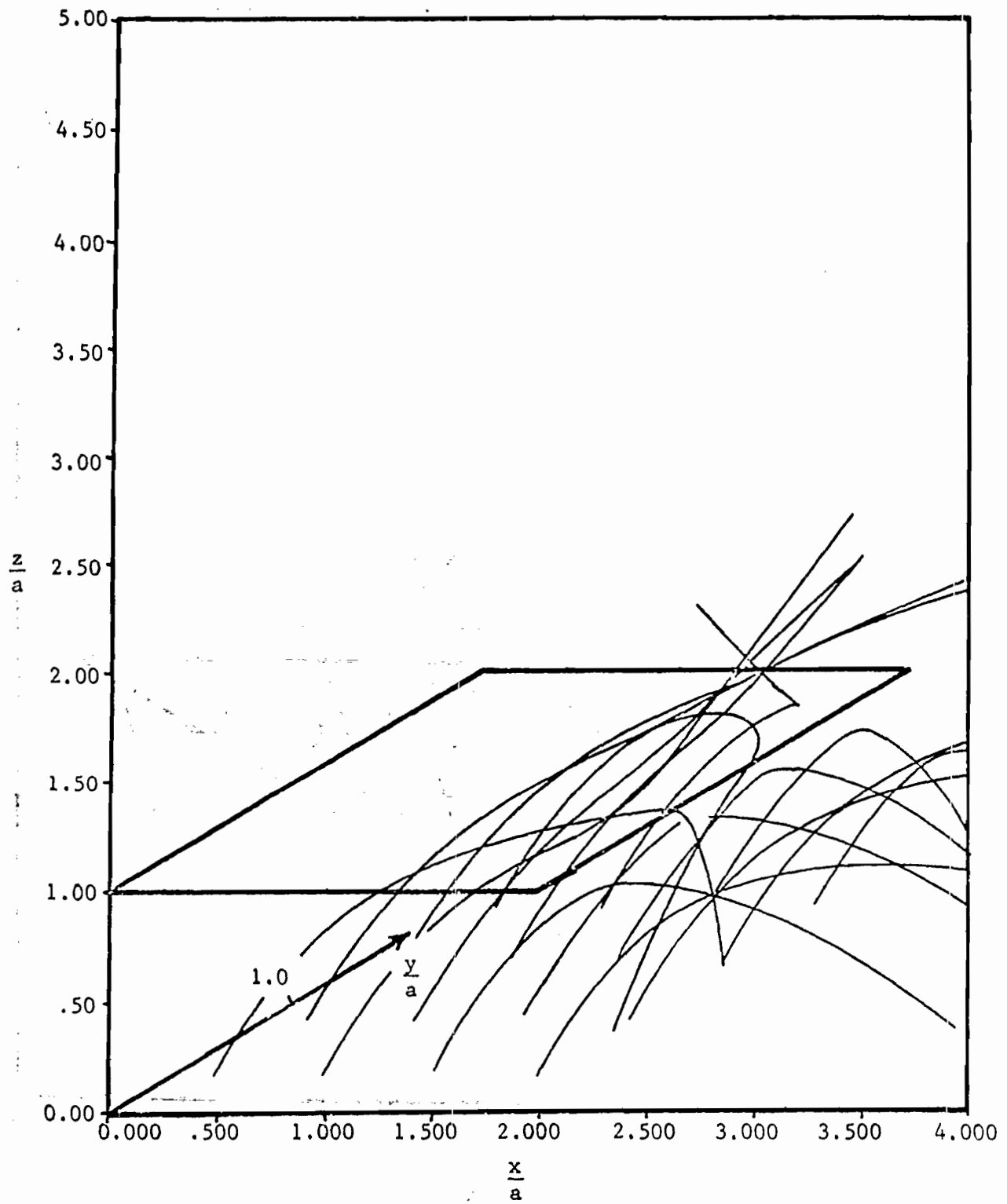


Figure IV-5d. Electron Trajectories for $b/a = 1.0$,
 Normalized Energy of 1.3, $B = 0$ radian, and $\theta = 30^\circ$

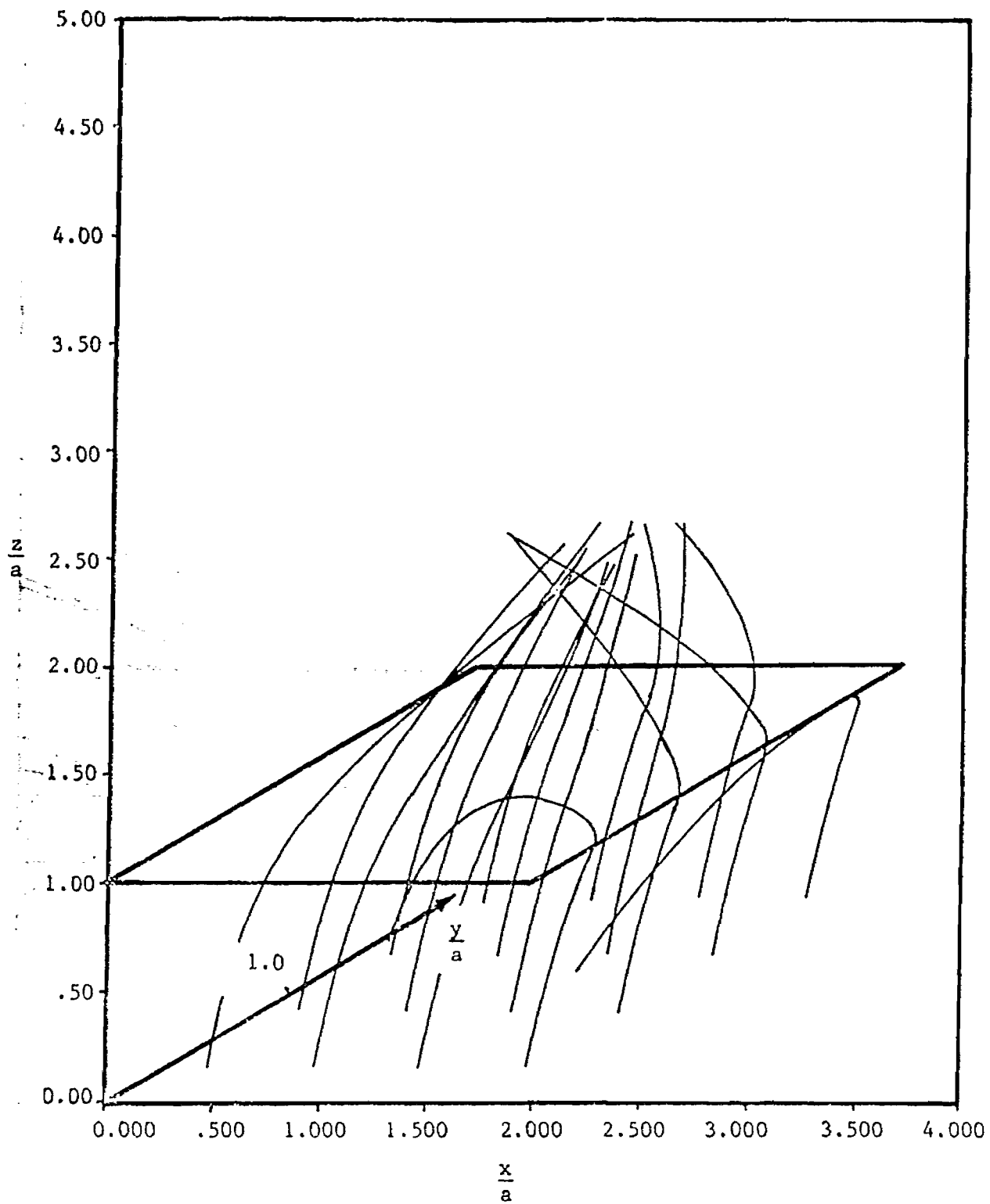


Figure IV-5e. Electron Trajectories for $b/a = 1.0$,
 Normalized Energy of 1.3, $B = \pi/8$ radians, and $\theta = 10^\circ$

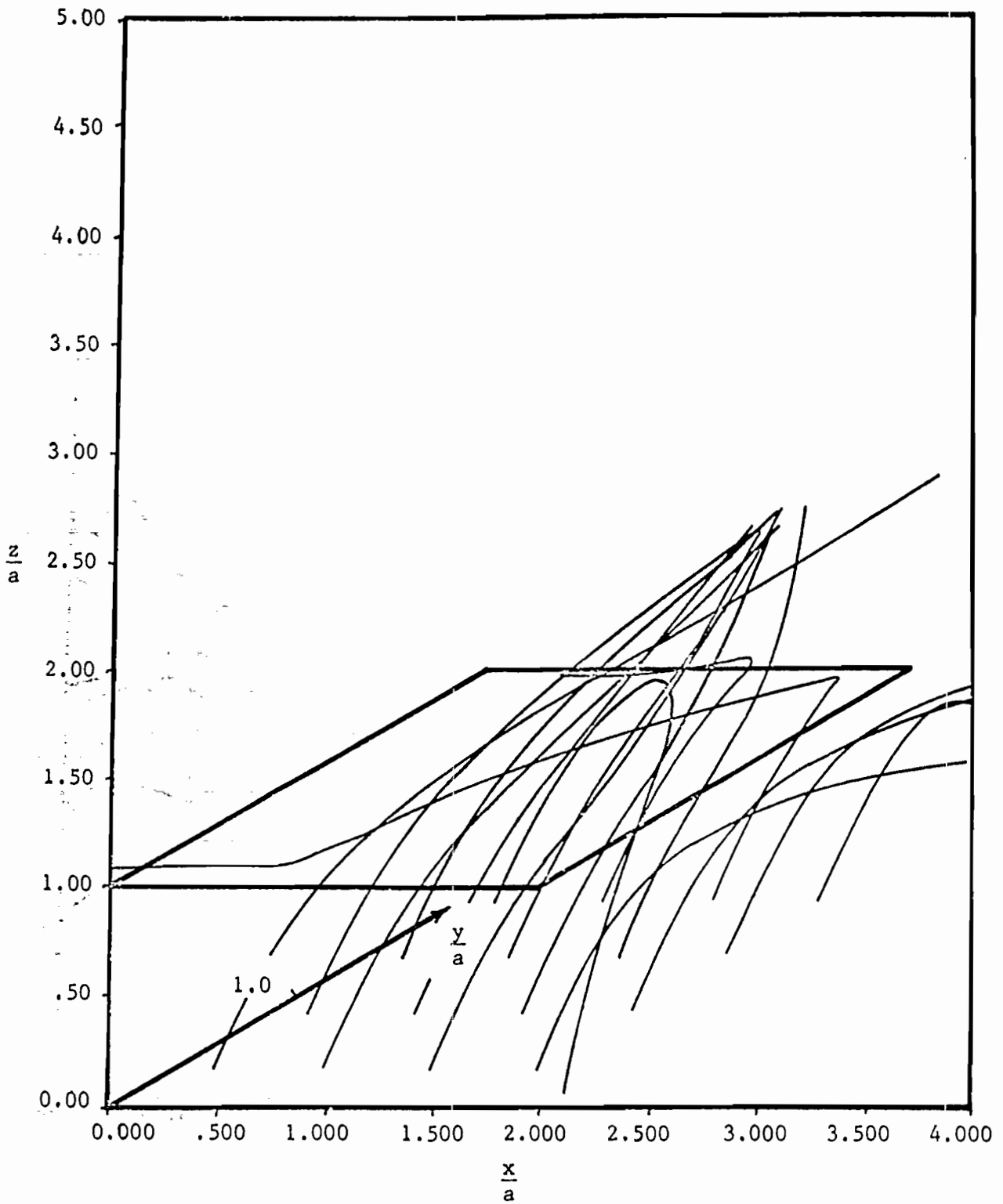


Figure IV-5f. Electron Trajectories for $b/a = 1.0$,
 Normalized Energy of 1.3, $B = \pi/8$ radians, and $\theta = 20^\circ$

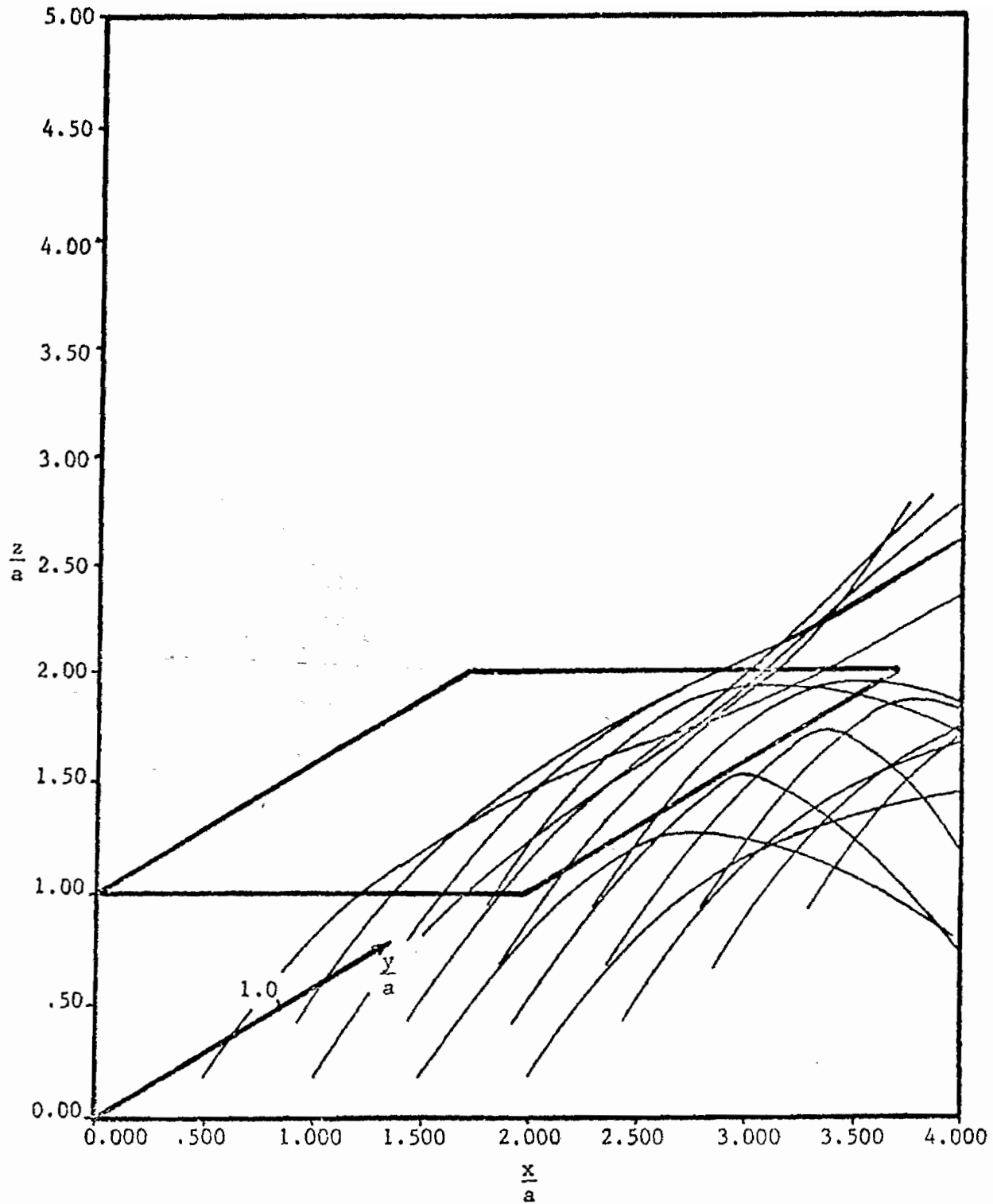


Figure IV-5g. Electron Trajectories for $b/a = 1.0$,
 Normalized Energy of 1.3, $B = \pi/8$ radians, and $\theta = 30^\circ$

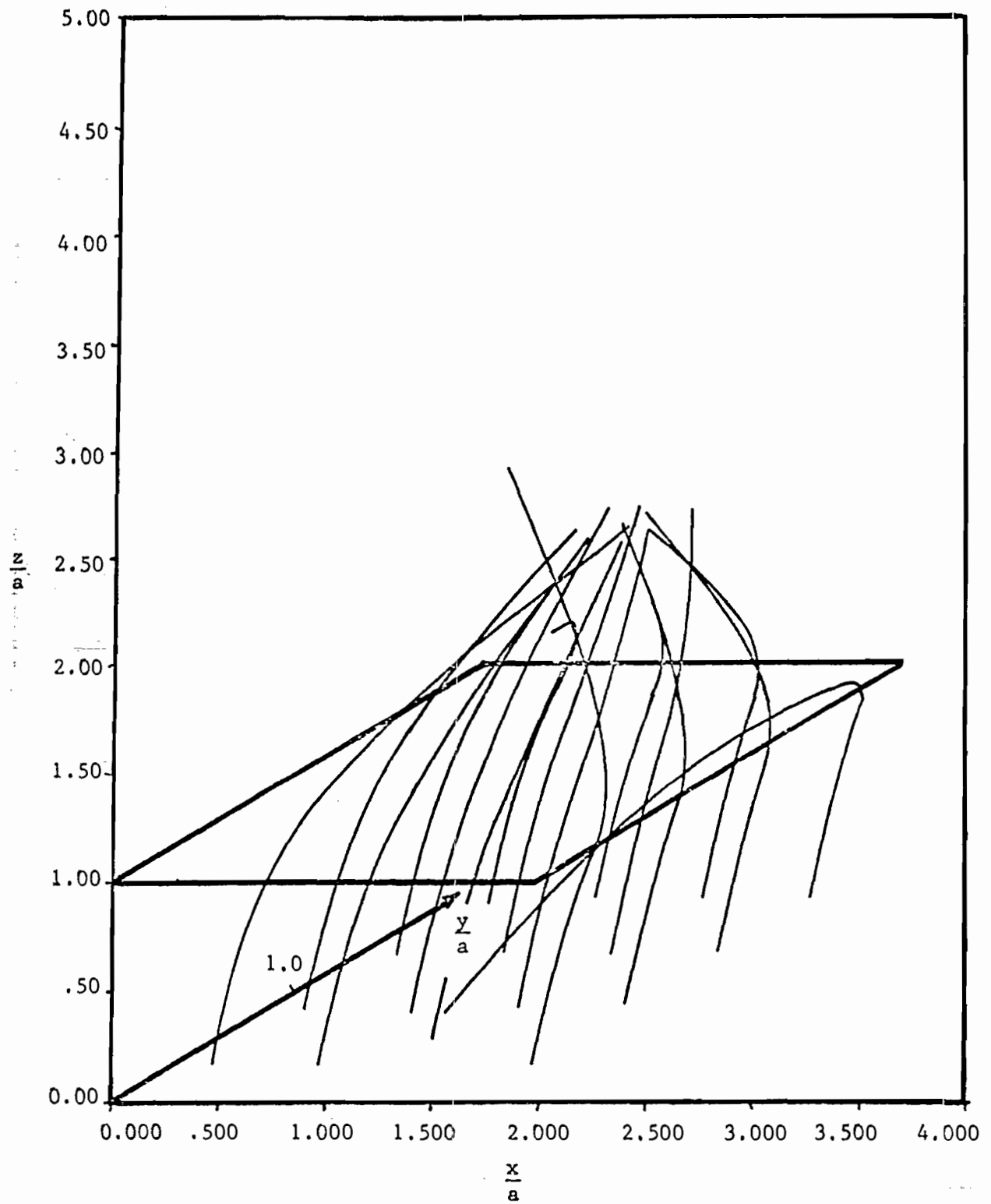


Figure IV-5h. Electron Trajectories for $b/a = 1.0$,
 Normalized Energy of 1.3, $B = \pi/4$, and $\theta = 10^\circ$

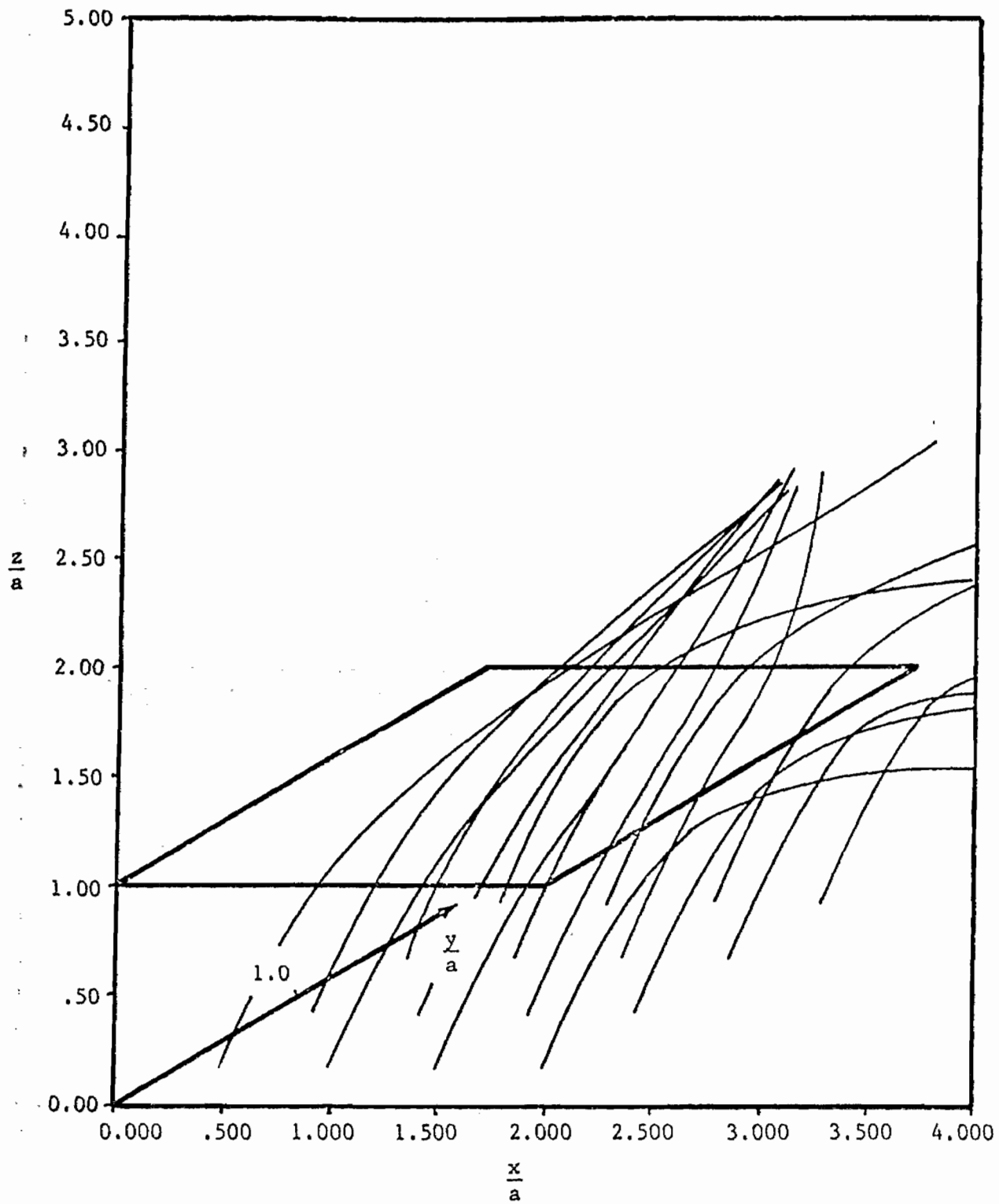


Figure IV-5i. Electron Trajectories for $b/a = 1.0$,
 Normalized Energy of 1.3, $B = \pi/4$, and $\theta = 20^\circ$

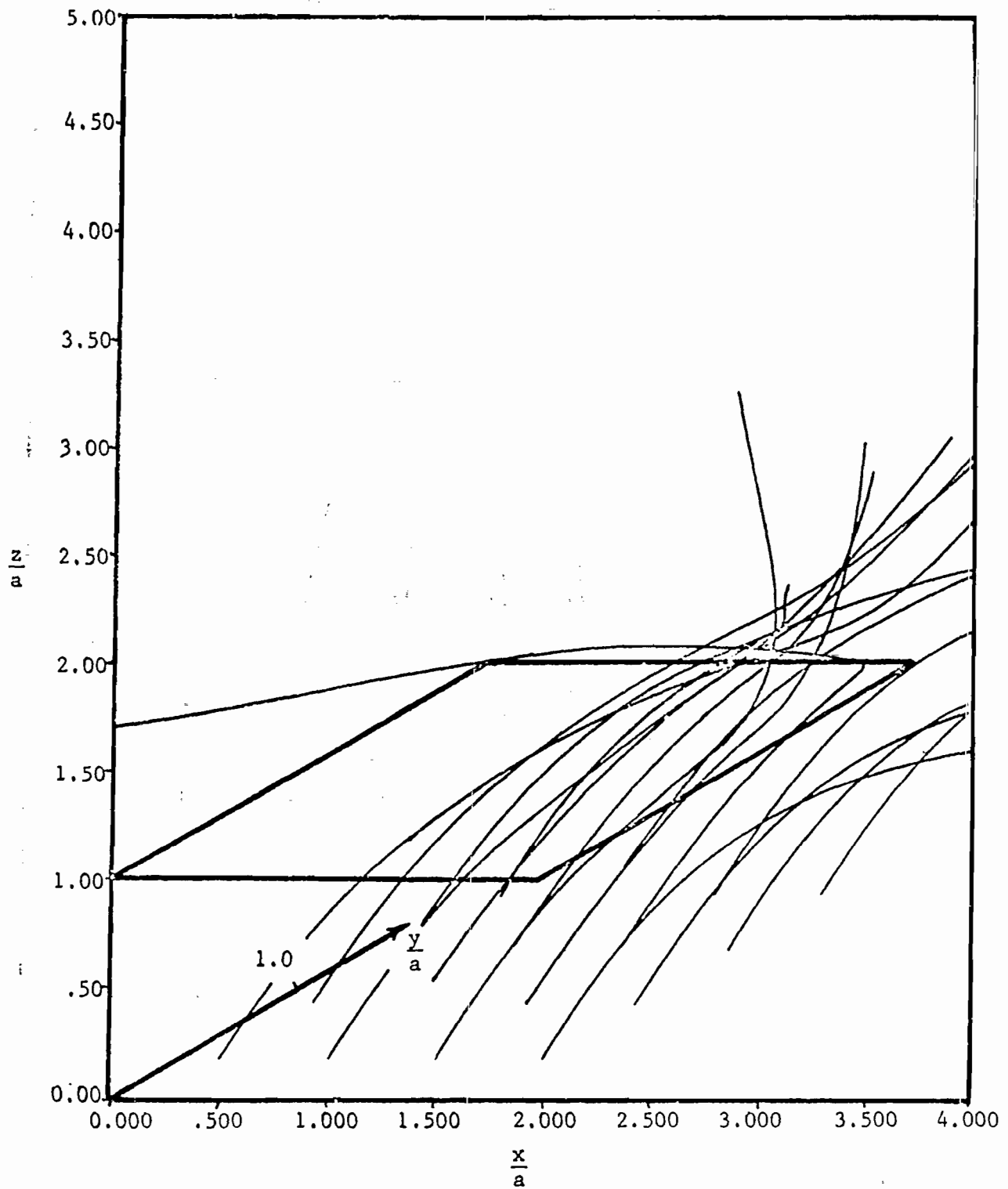


Figure IV-5j. Electron Trajectories for $b/a = 1.0$,
 Normalized Energy of 1.3, $B = \pi/4$, and $\theta = 30^\circ$

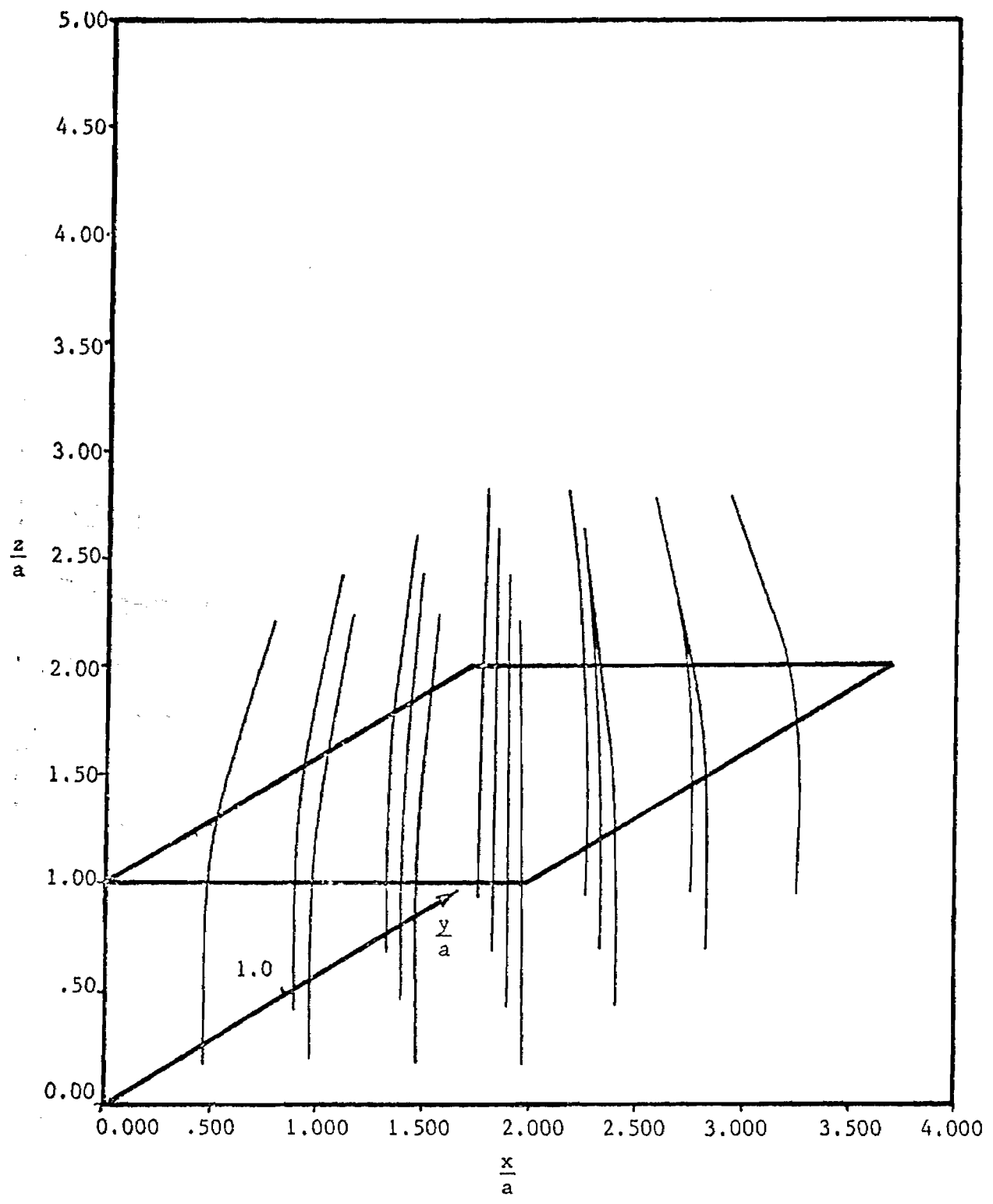


Figure IV-6a. Electron Trajectories for $b/a = 1.0$, Normalized Energy of 2.0, $B = 0$ radian, and $\theta = 10^\circ$

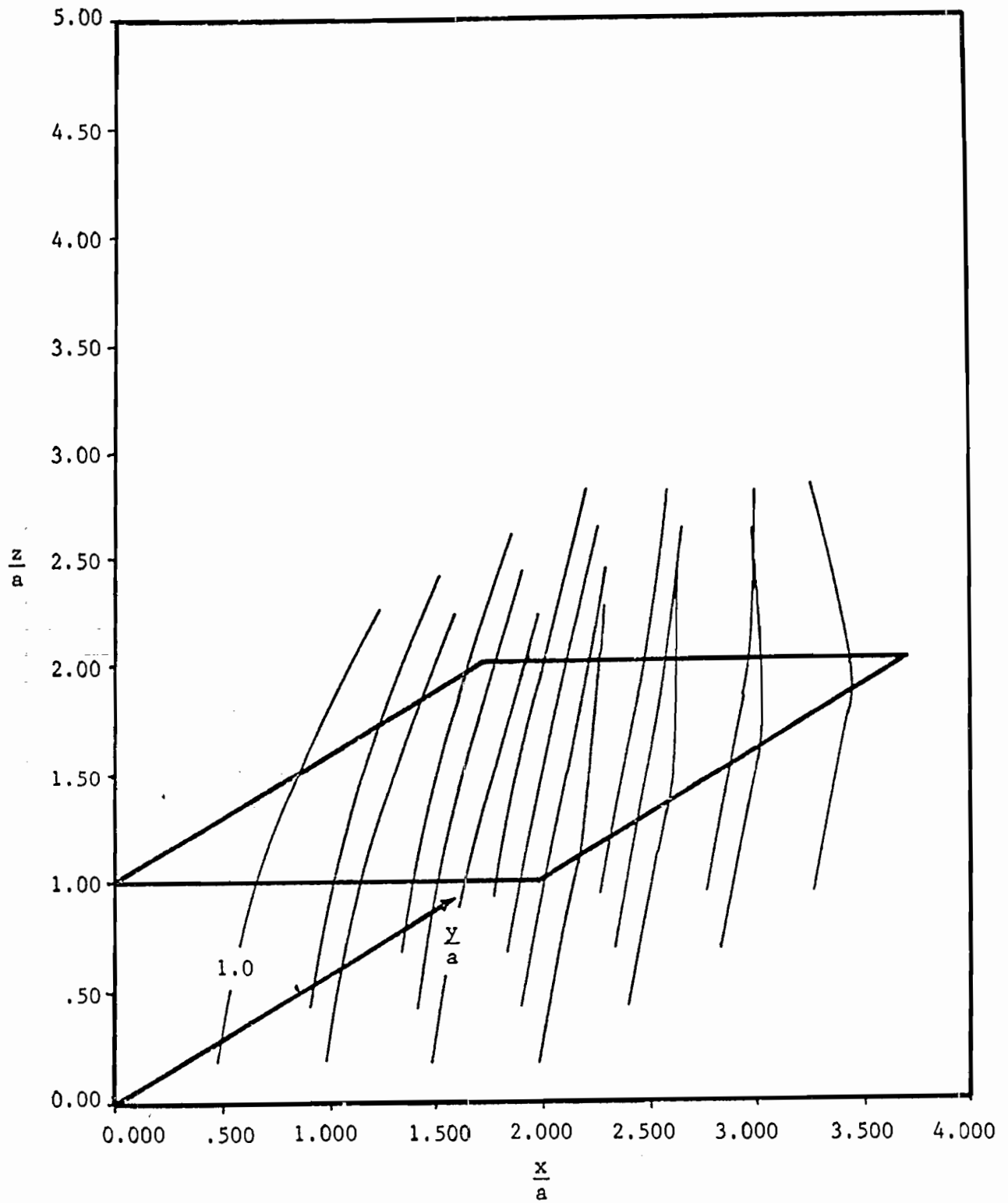


Figure IV-6b. Electron Trajectories for $b/a = 1.0$,
 Normalized Energy of 2.0, $B = 0$ radian, and $\theta = 10^\circ$

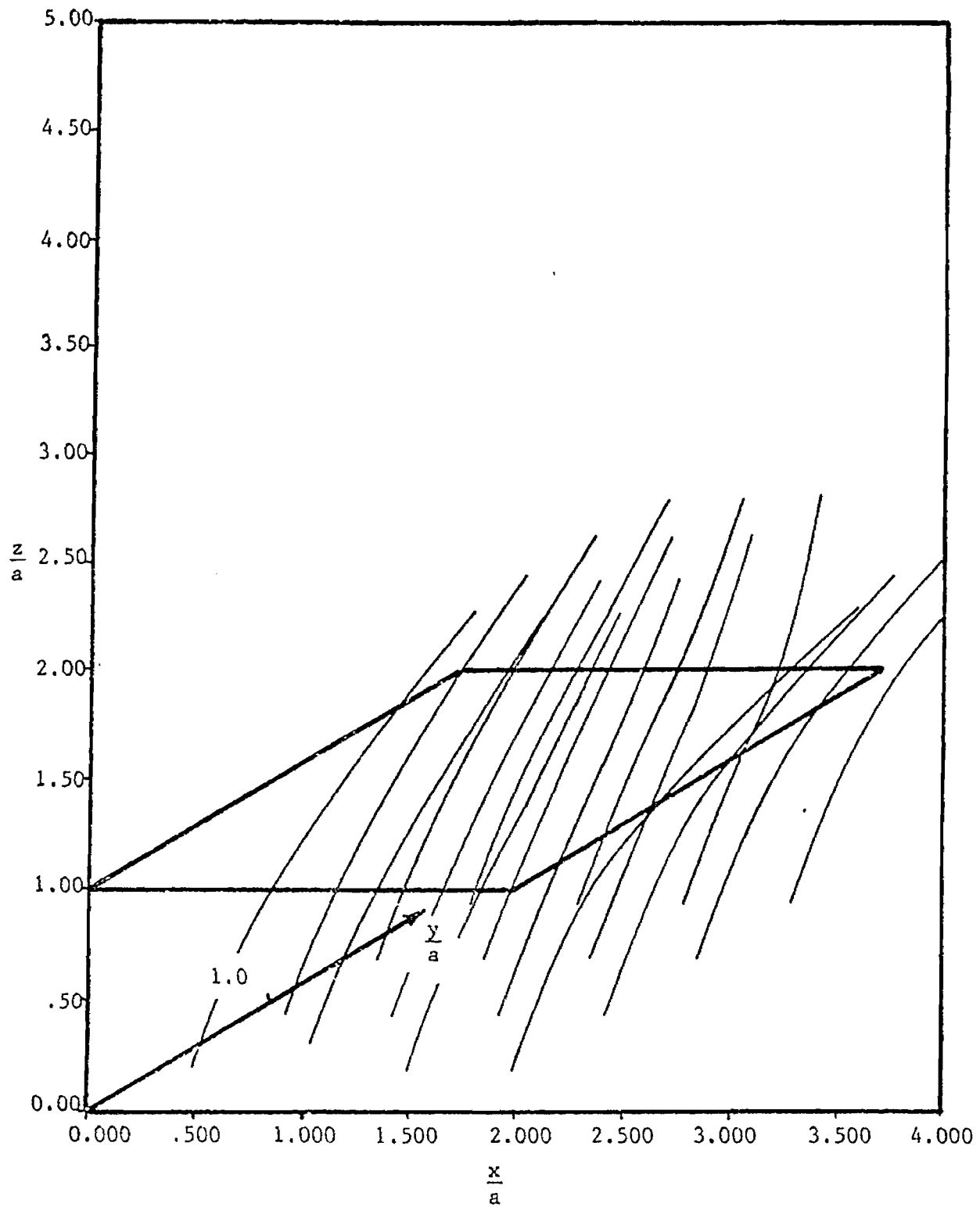


Figure IV-6c. Electron Trajectories for $b/a = 1.0$, Normalized Energy of 2.0, $B = 0$ radian, and $\theta = 20^\circ$

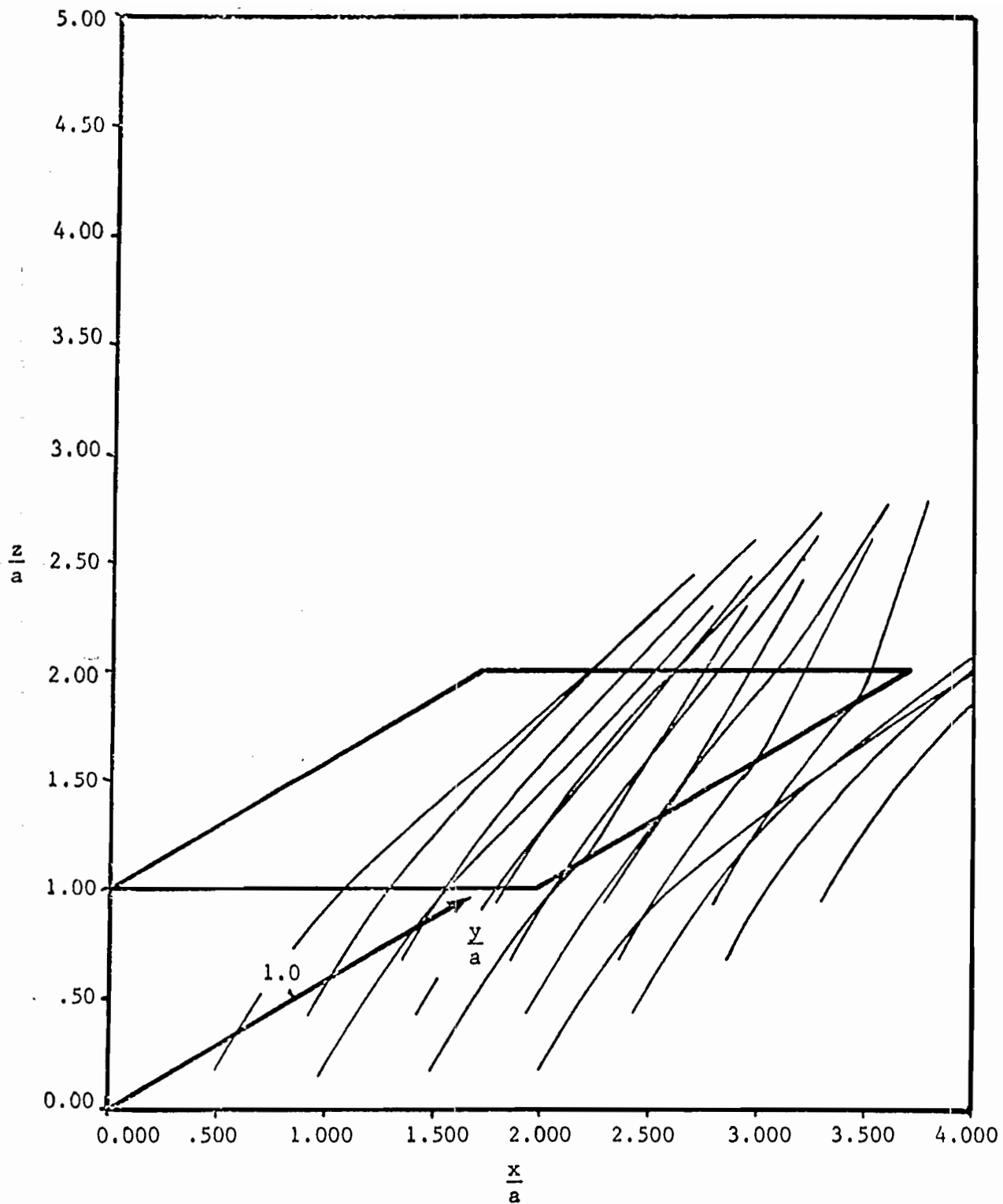


Figure IV-6d. Electron Trajectories for $b/a = 1.0$,
 Normalized Energy of 2.0, $B = 0$ radian, and $\theta = 30^\circ$

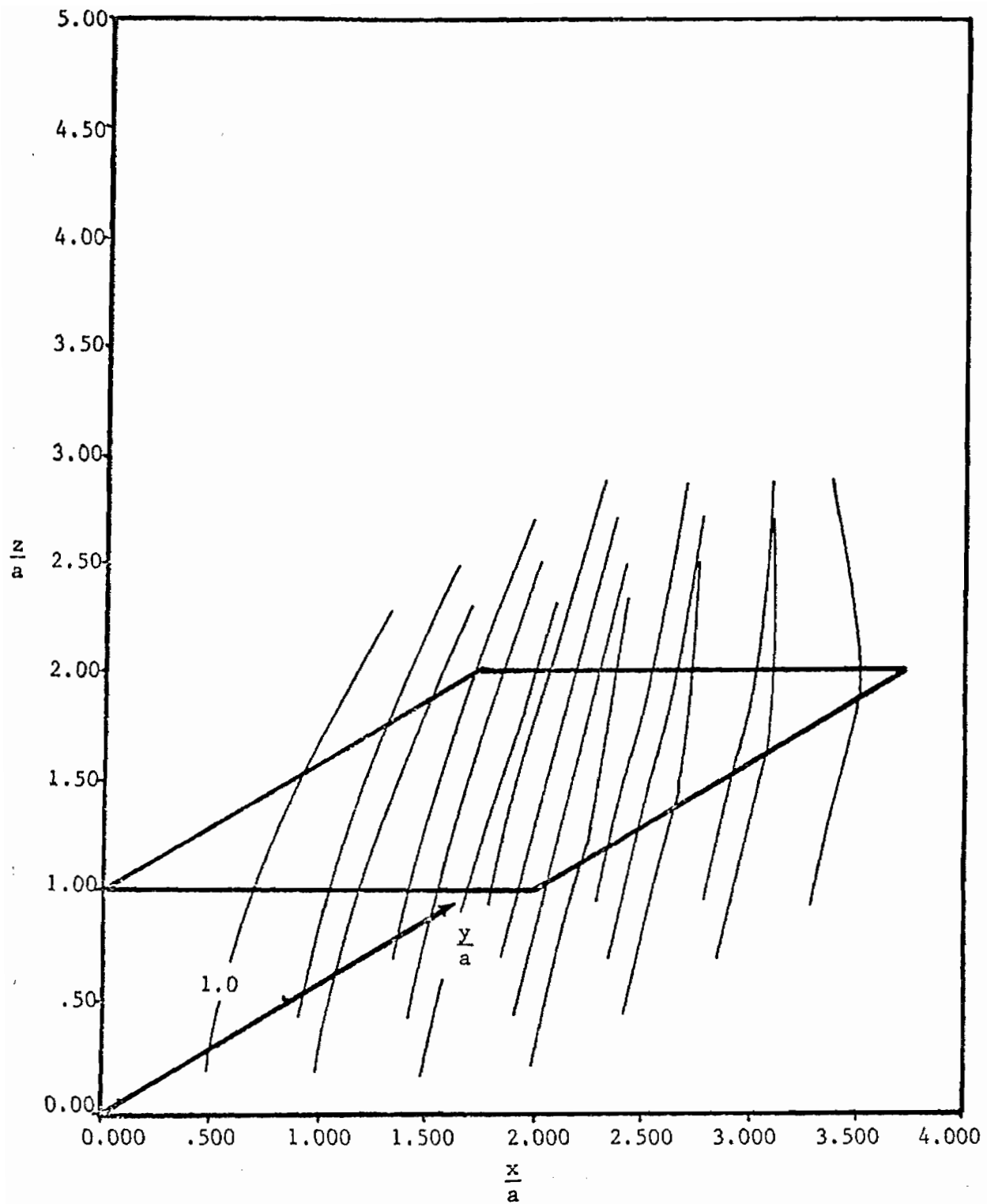


Figure IV-6c. Electron Trajectories for $b/a = 1.0$, Normalized Energy of 2.0, $B = \pi/8$ radians, and $\theta = 10^\circ$

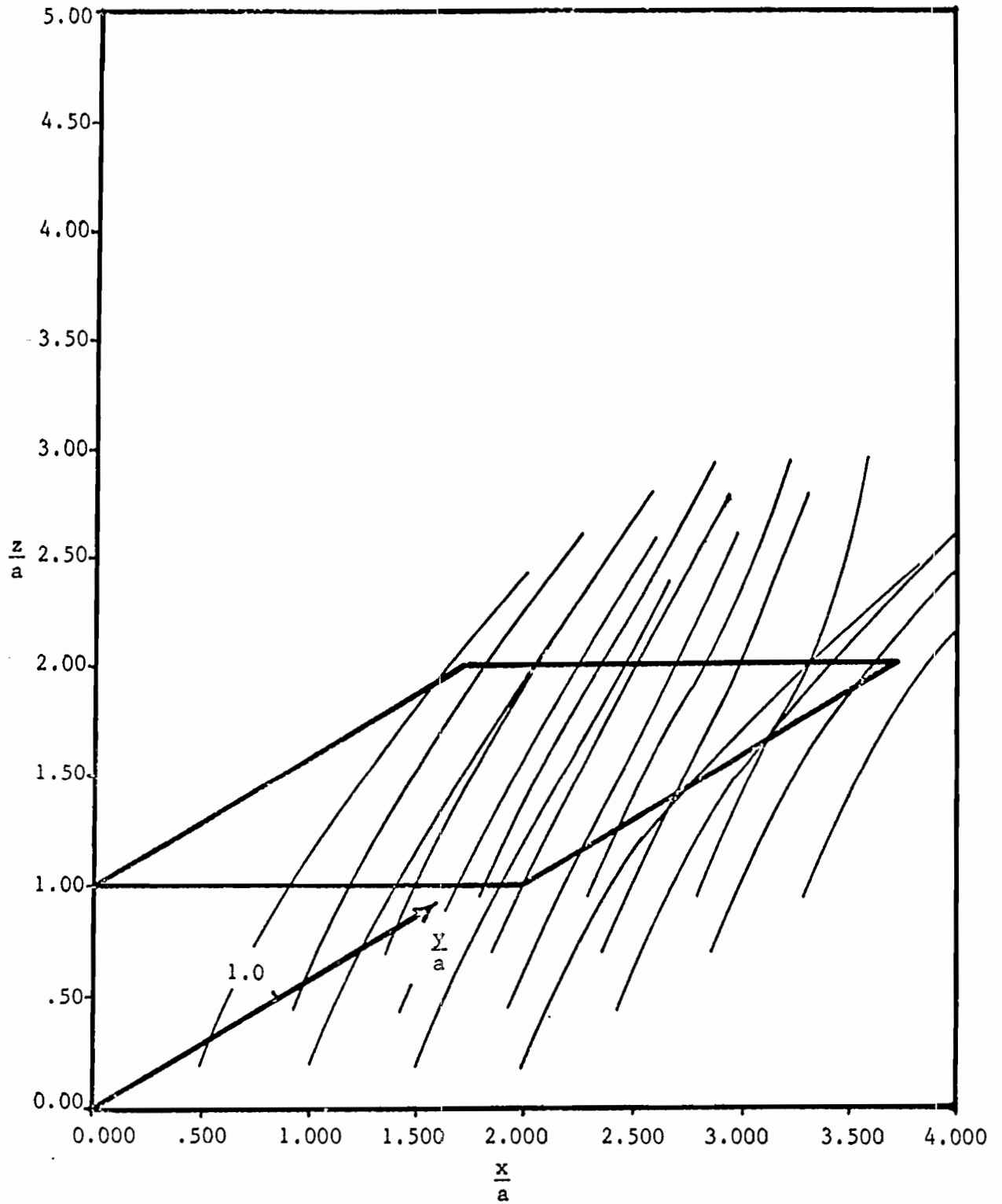


Figure IV-6f. Electron Trajectories for $b/a = 1.0$, Normalized Energy of 2.0, $B = \pi/8$ radians, and $\theta = 20^\circ$

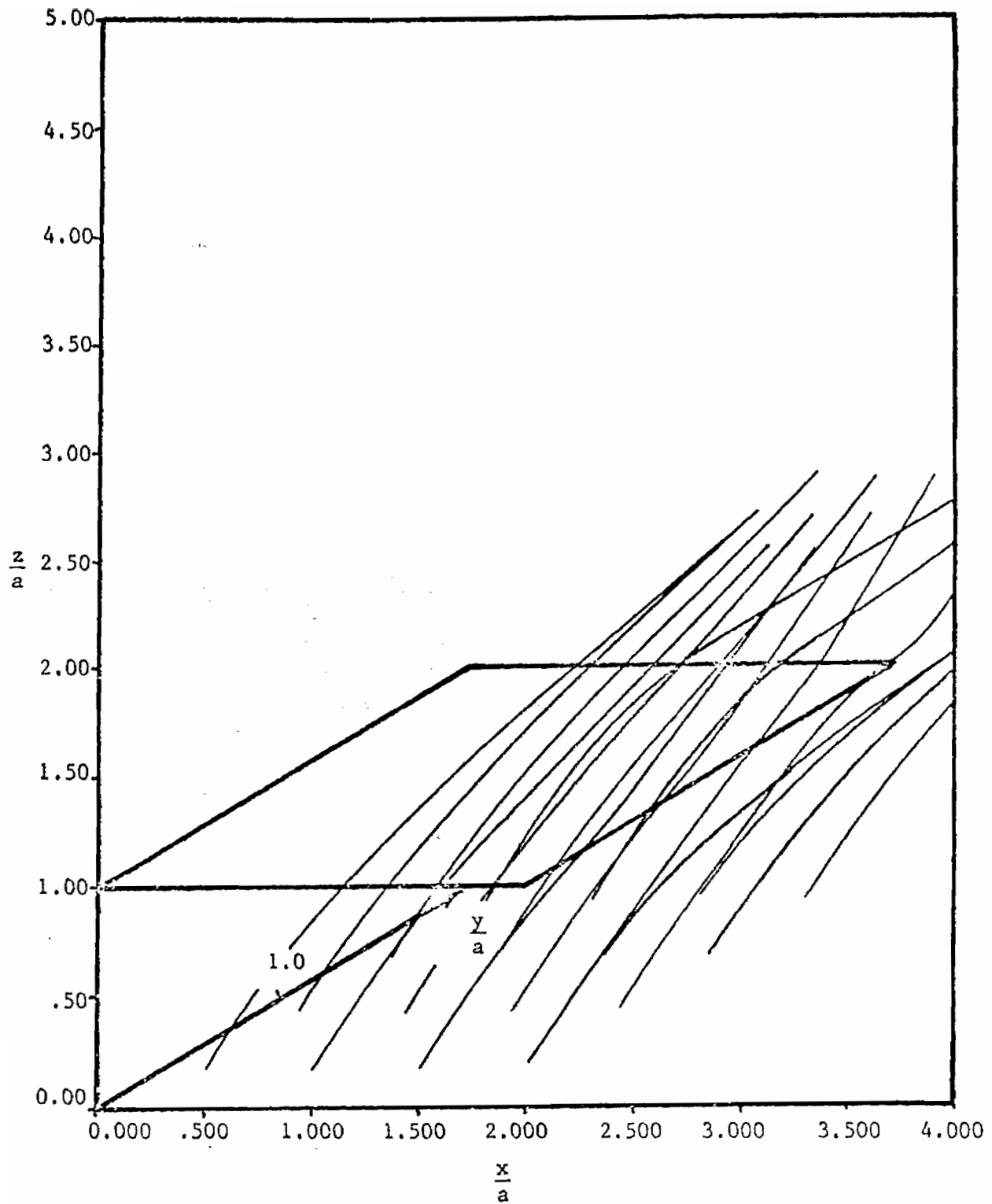


Figure IV-6g. Electron Trajectories for $b/a = 1.0$, Normalized Energy of 2.0, $B = \pi/8$ radians, and $\theta = 30^\circ$

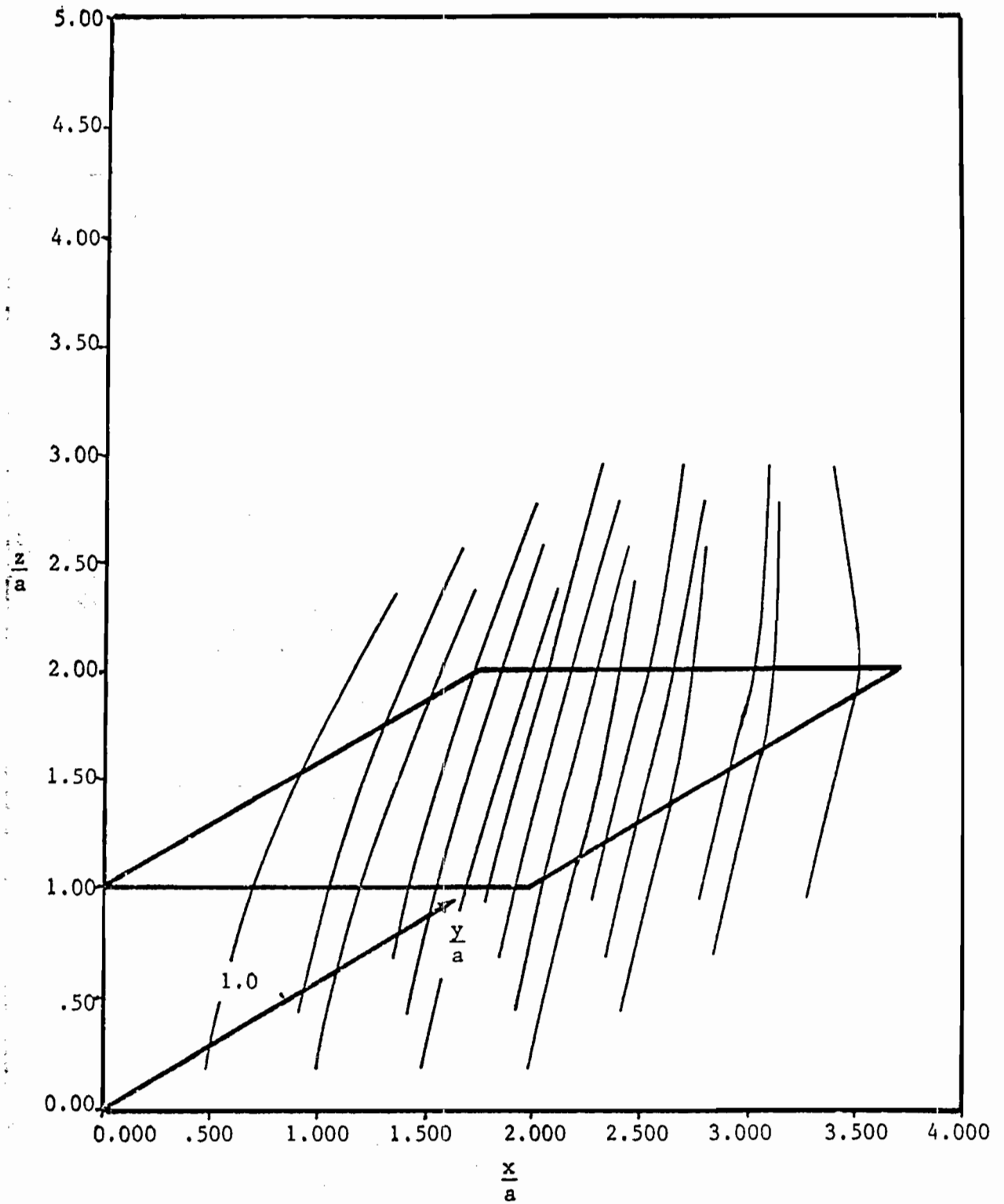


Figure IV-6h. Electron Trajectories for $b/a = 1.0$, Normalized Energy of 2.0, $B = \pi/4$ radians, and $\theta = 10^\circ$

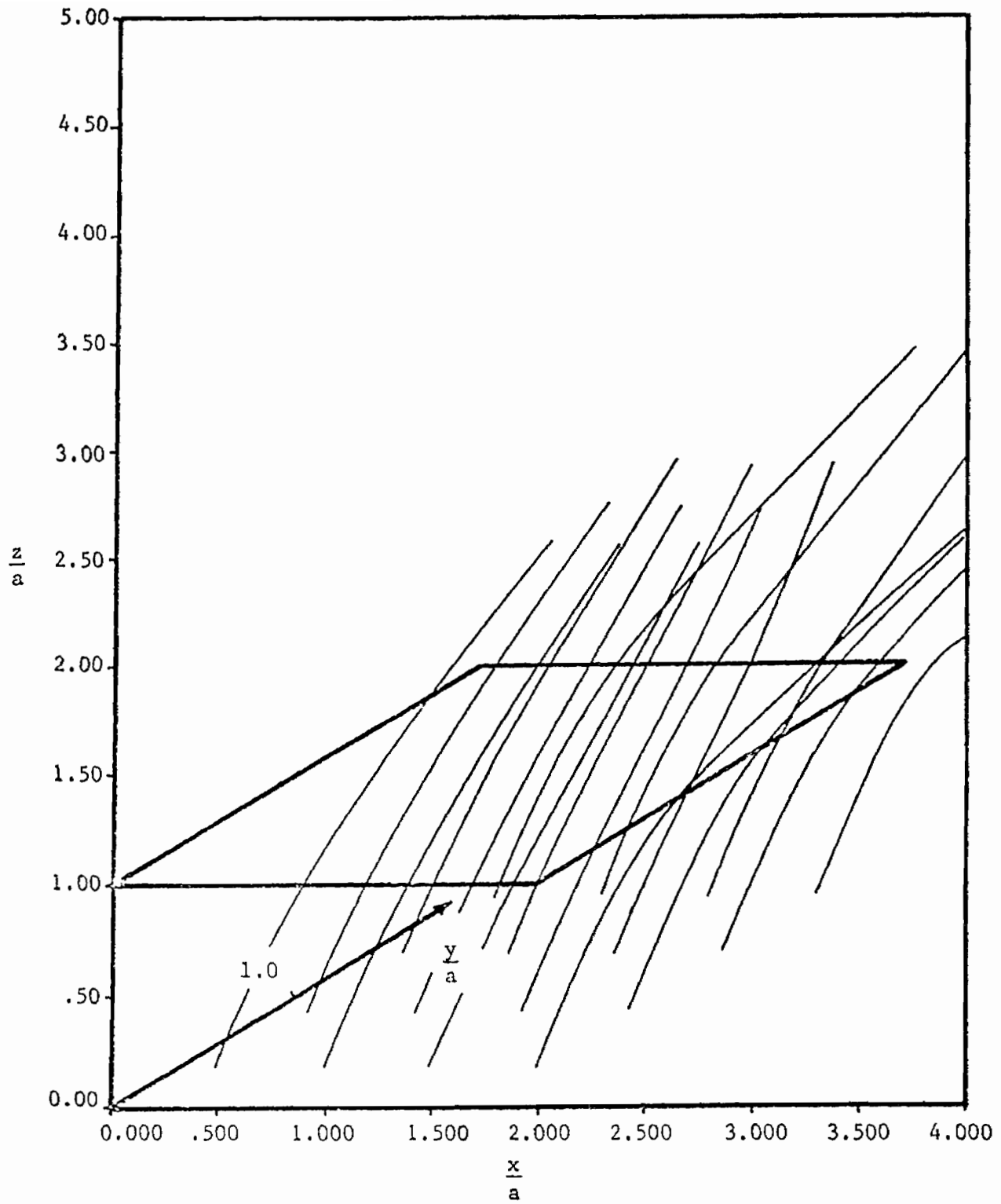


Figure IV-6i. Electron Trajectories for $b/a = 1.0$,
 Normalized Energy of 2.0, $B = \pi/4$ radians, and $\theta = 20^\circ$

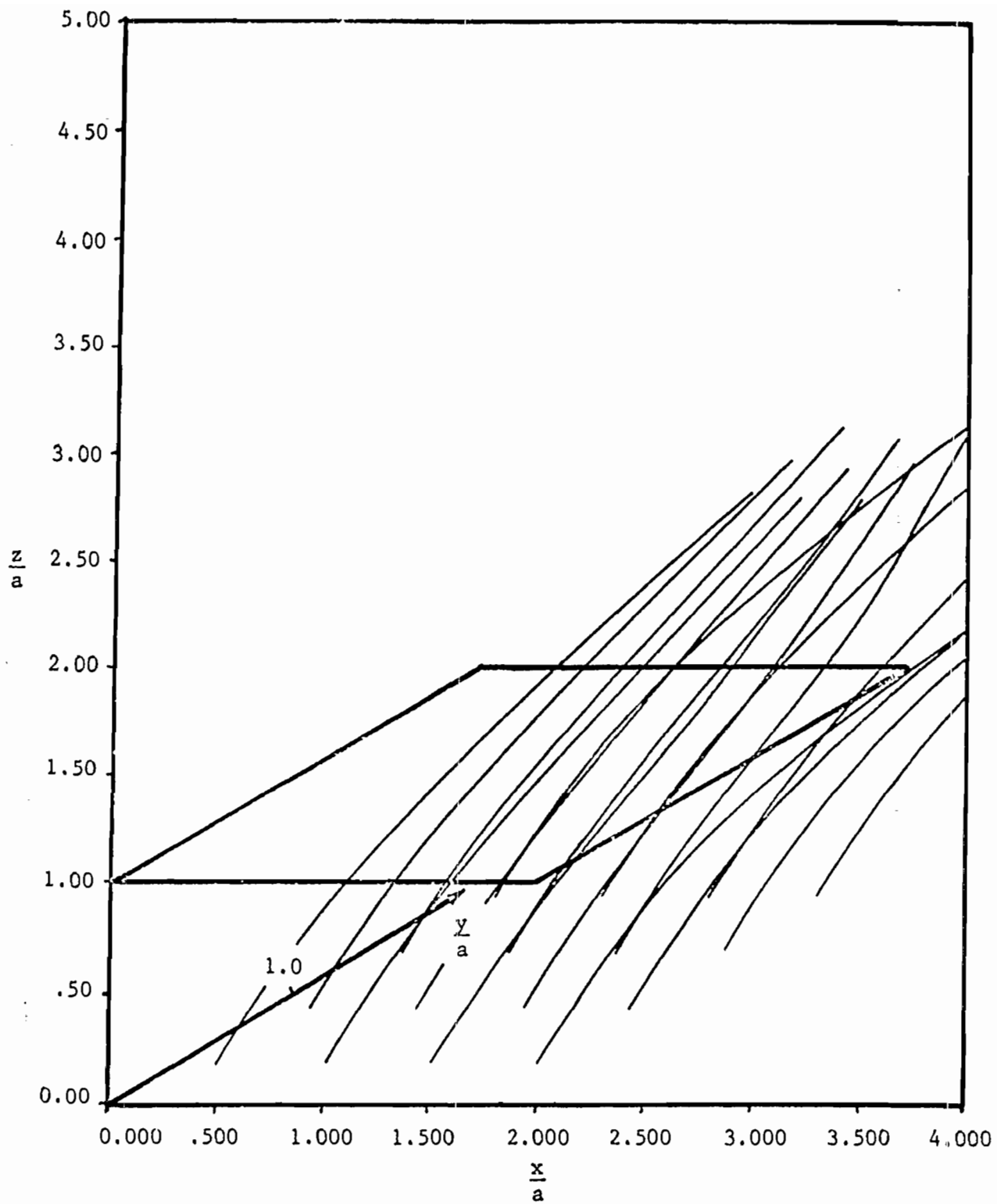


Figure IV-6j. Electron Trajectories for $b/a = 1.0$,
 Normalized Energy of 2.0, $B = \pi/4$ radians, and $\theta = 30^\circ$

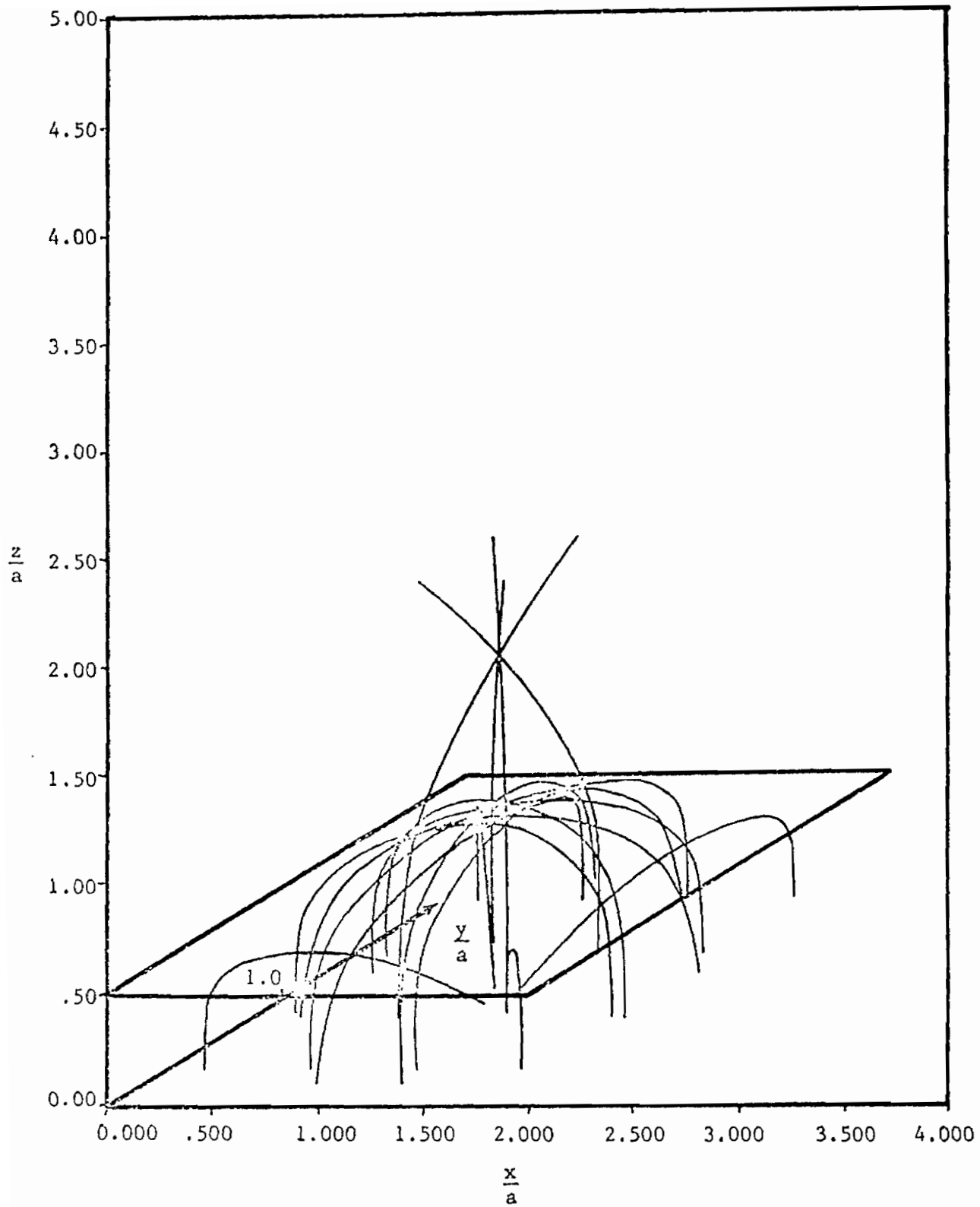


Figure IV-7a. Electron Trajectories for $b/a = .5$, Normalized Energy of 1.1, $B = 0$ radian, and $\theta = 0^\circ$

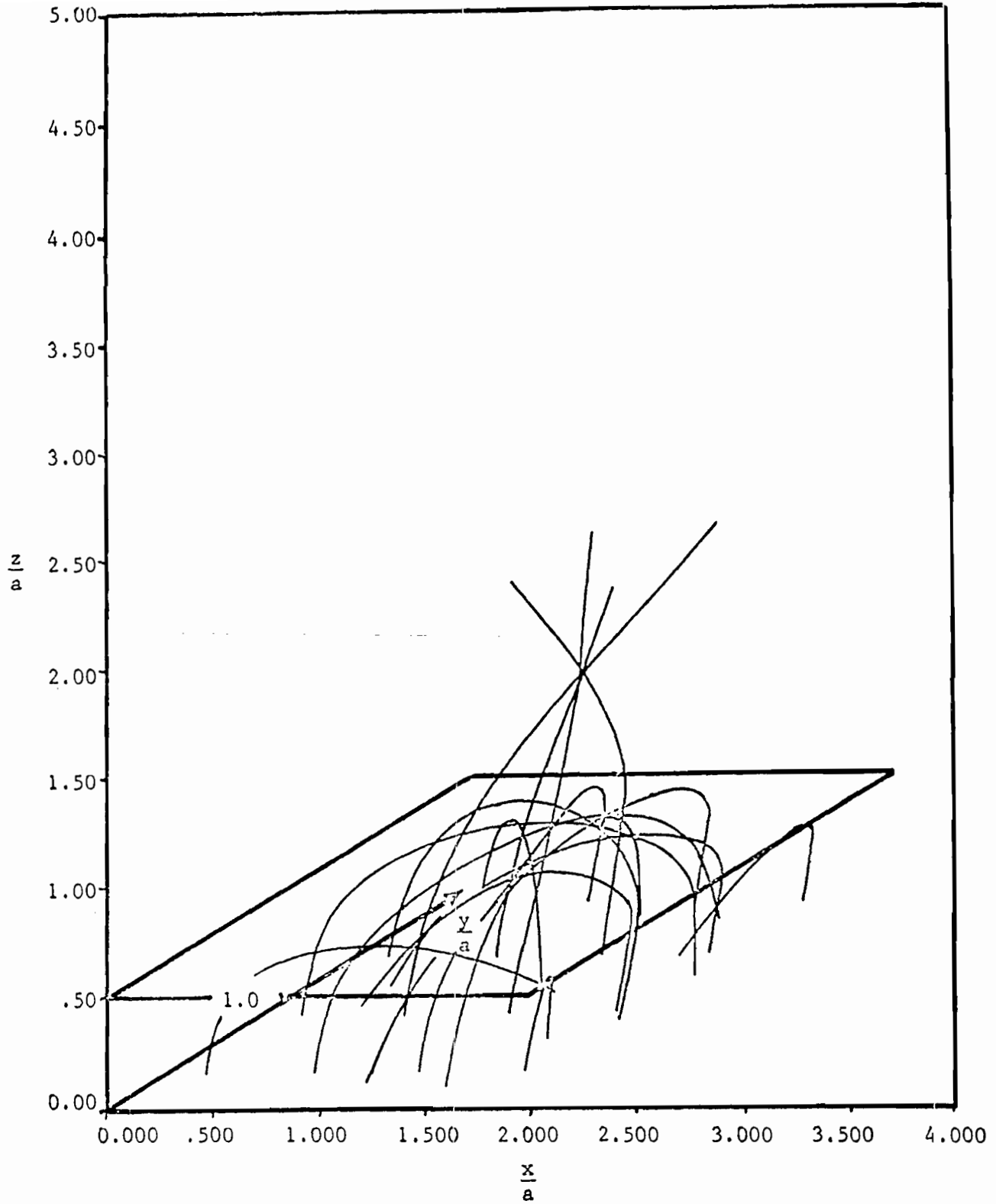


Figure IV-7b. Electron Trajectories for $b/a = .5$,
 Normalized Energy of 1.1, $B = 0$ radian, and $\theta = 10^\circ$

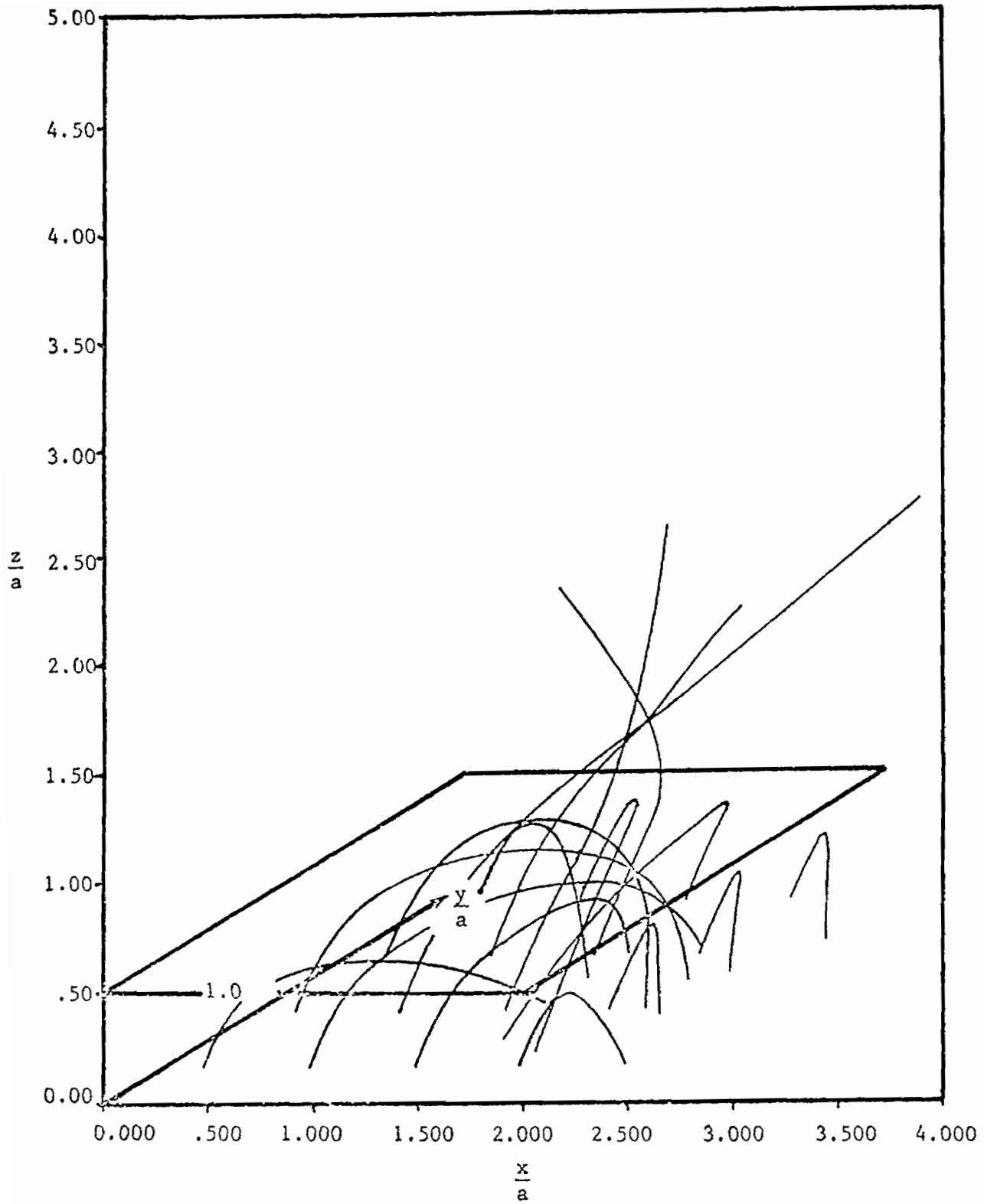


Figure IV-7c. Electron Trajectories for $b/a = .5$,
 Normalized Energy of 1.1, $B = 0$ radian, and $\theta = 20^\circ$

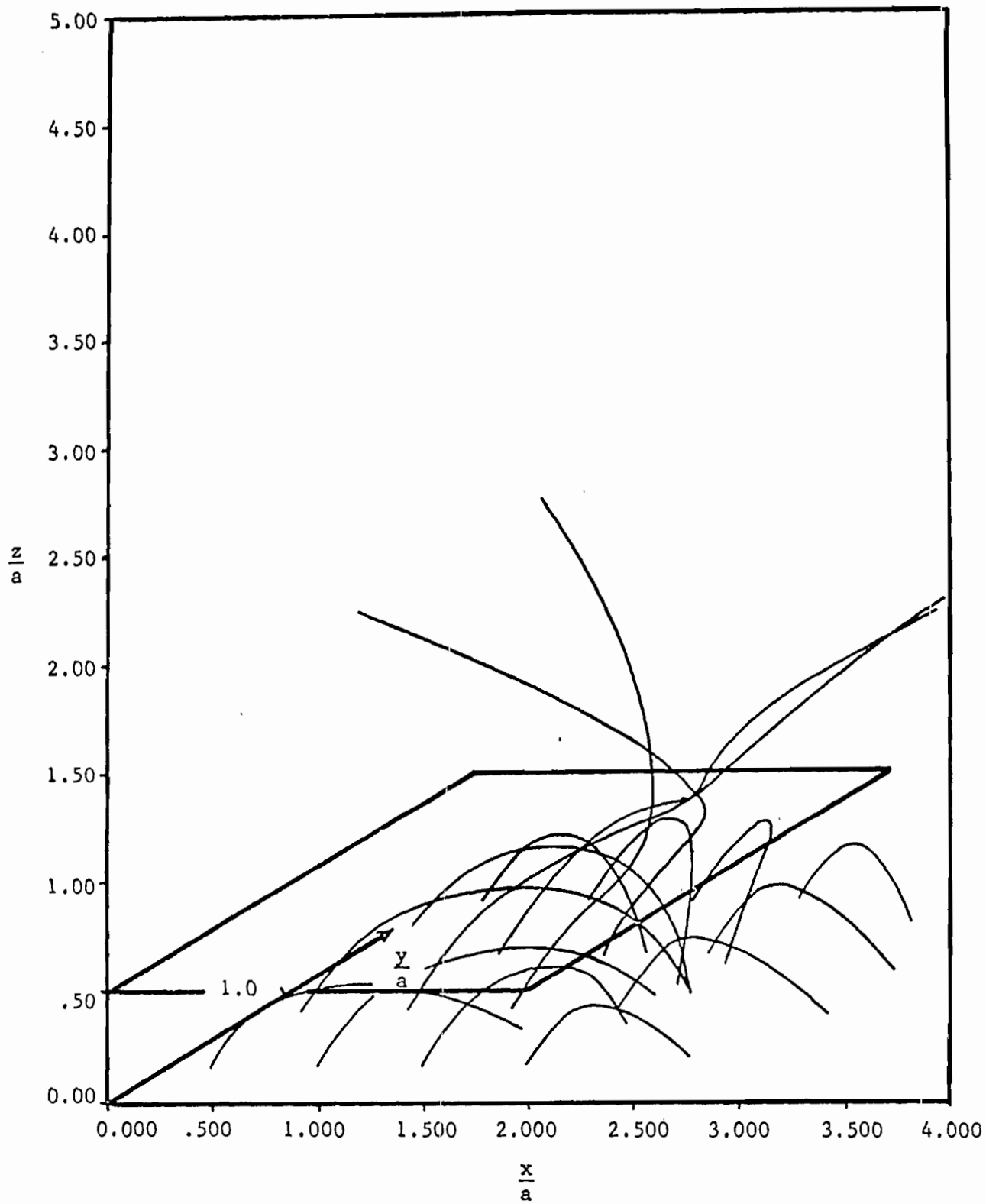


Figure IV-7d. Electron Trajectories for $b/a = .5$,
 Normalized Energy of 1.1, $B = 0$ radian, and $\theta = 30^\circ$

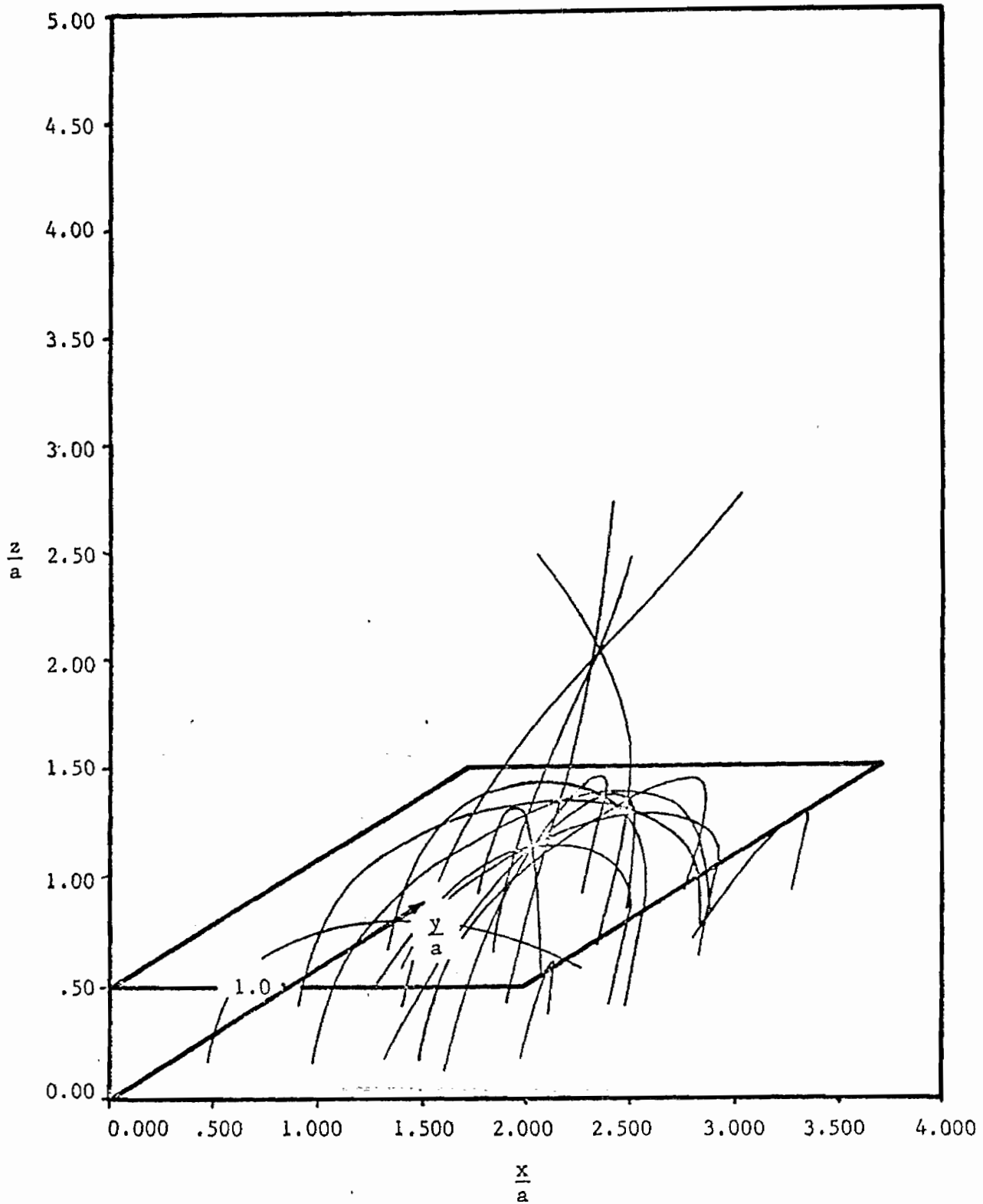


Figure IV-7e. Electron Trajectories for $b/a = .5$,
 Normalized Energy of 1.1, $B = \pi/8$ radians, and $\theta = 10^\circ$

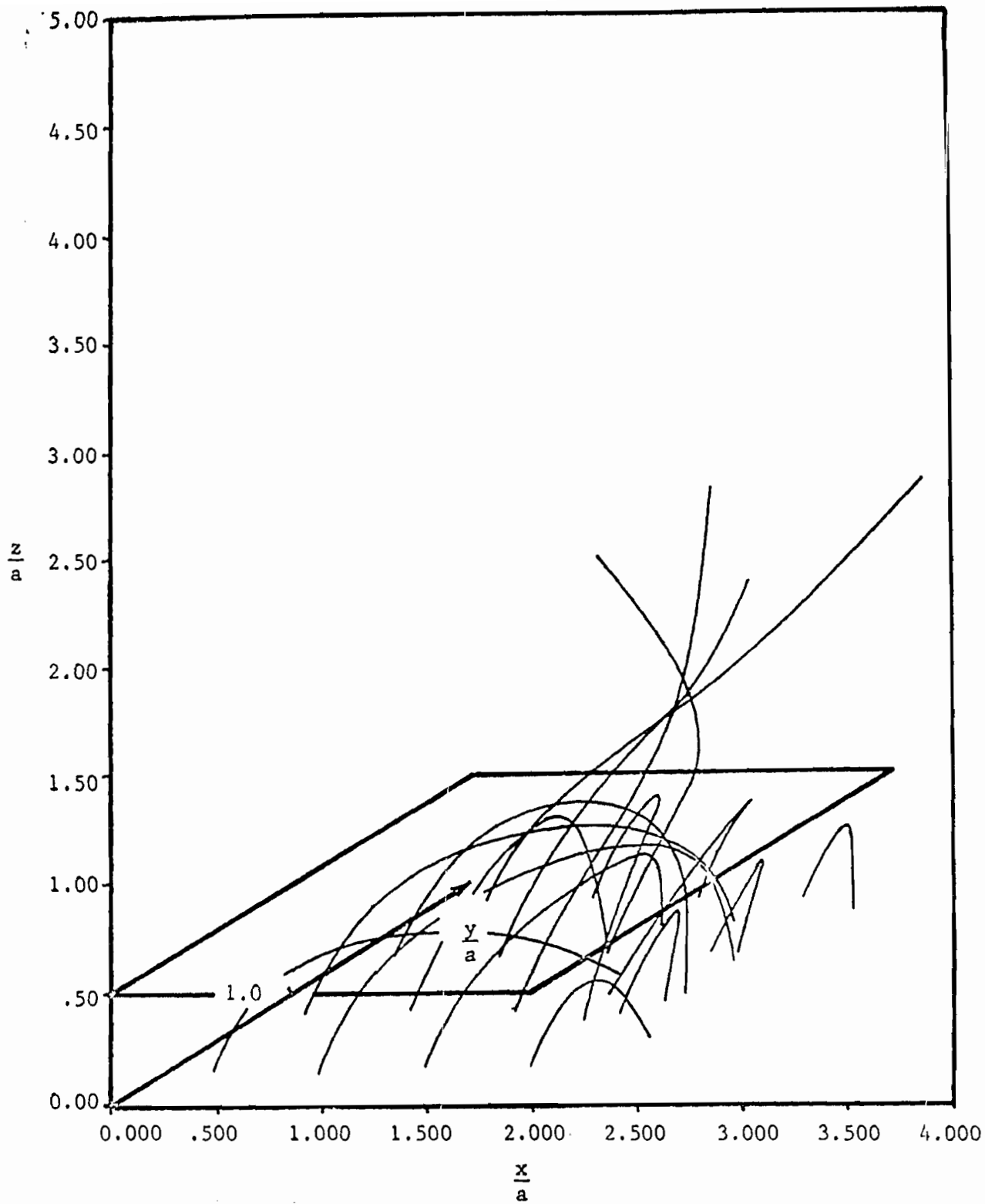


Figure IV-7f. Electron Trajectories for $b/a = .5$,
 Normalized Energy of 1.1, $B = \pi/8$ radians, and $\theta = 20^\circ$

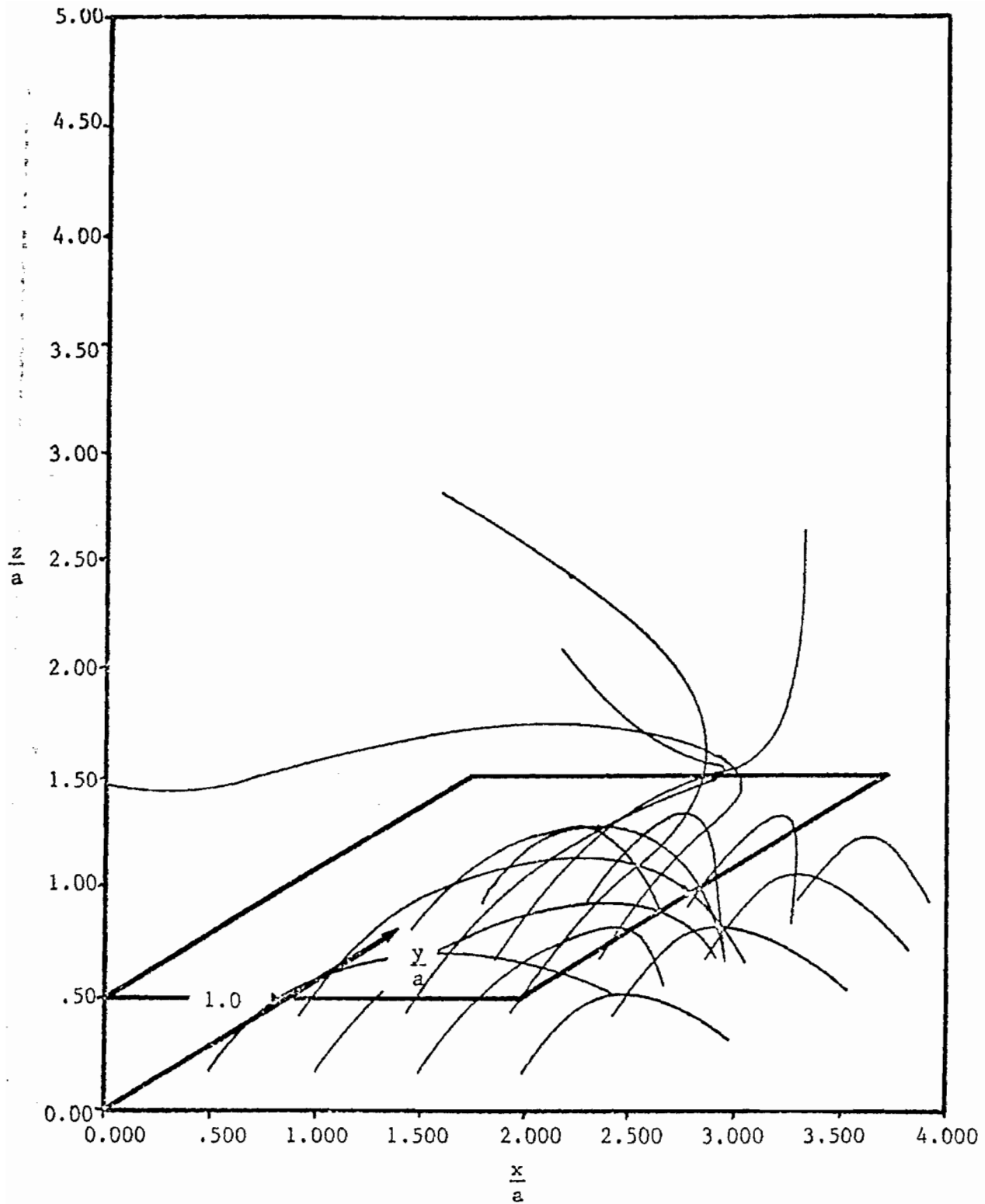


Figure IV-7g. Electron Trajectories for $b/a = .5$,
 Normalized Energy of 1.1, $B = \pi/8$ radians, and $\theta = 30^\circ$

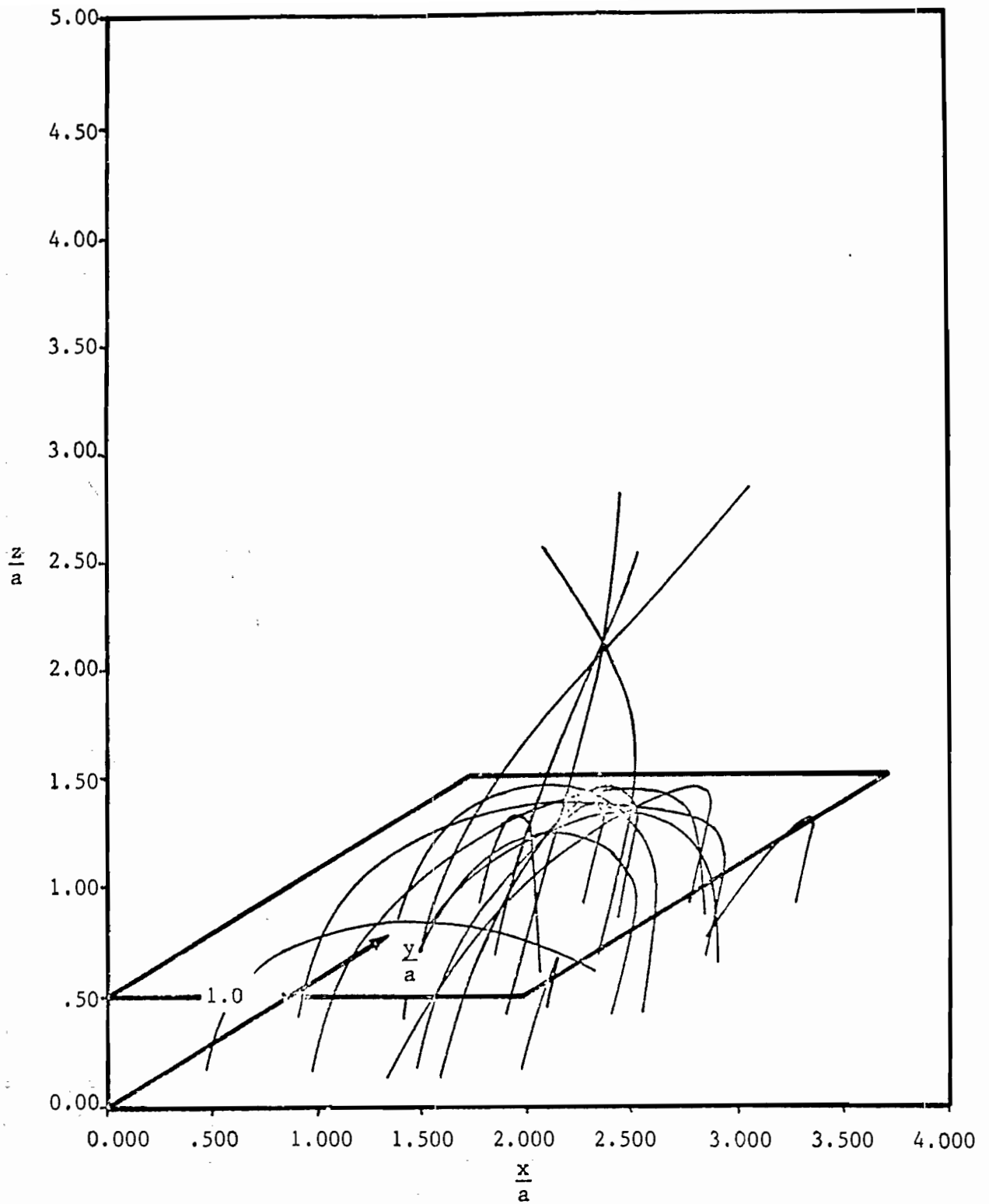


Figure IV-7h. Electron Trajectories for $b/a = .5$,
 Normalized Energy of 1.1, $B = \pi/4$ radians, and $\theta = 10^\circ$

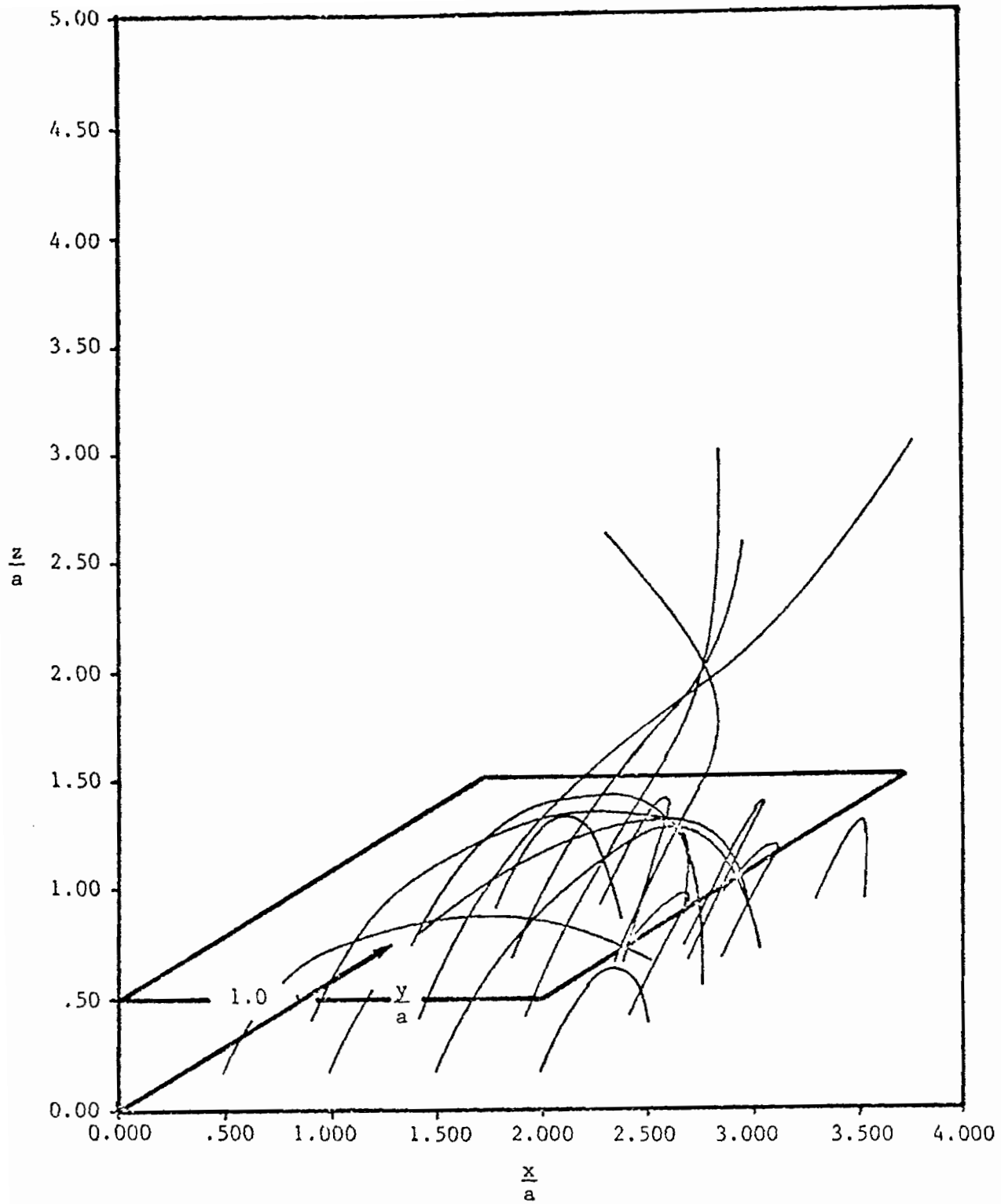


Figure IV-7i. Electron Trajectories for $b/a = .5$,
 Normalized Energy of 1.1, $B = \pi/4$ radians, and $\theta = 20^\circ$

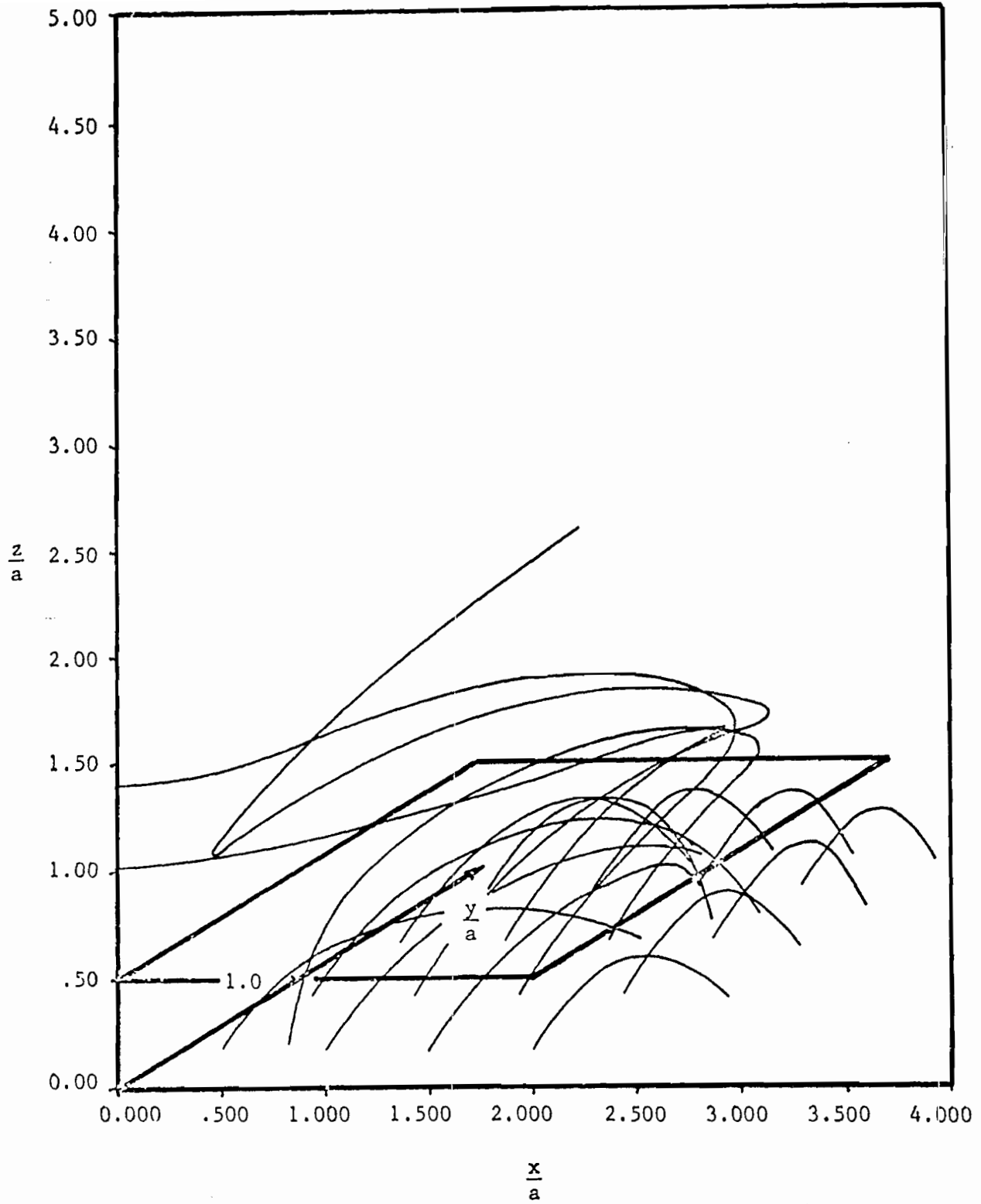


Figure IV-7j. Electron Trajectories for $b/a = .5$,
 Normalized Energy of 1.1, $B = \pi/4$ radians, and $\theta = 30^\circ$

The preceding plots provided information as to the trajectories followed by the electrons. It was noticed that particularly for the $\theta = 0$ case the electrons tended to be forced to the center of the apertures. This led to the consideration of the double grid configuration. Otherwise, the results were much as anticipated and little new information was obtained from the detailed information about the trajectories. To obtain a quantitative measure of the effectiveness of the grids, the trajectory program was run using 100 initial positions for the electrons and recording the fraction escaping and the fraction contained. Actual electron trajectory plots were not produced in these runs. The results of the runs are summarized in graphical form on the following pages.

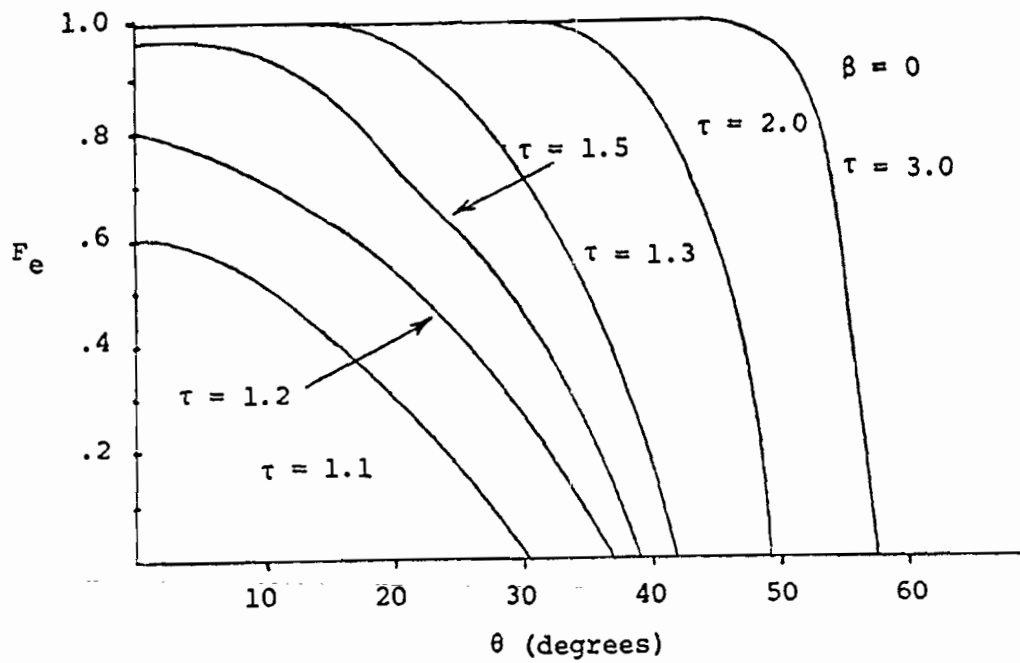


Figure IV-8a. Fraction of Electrons Escaping (F_e) for $b/a = 1.0$

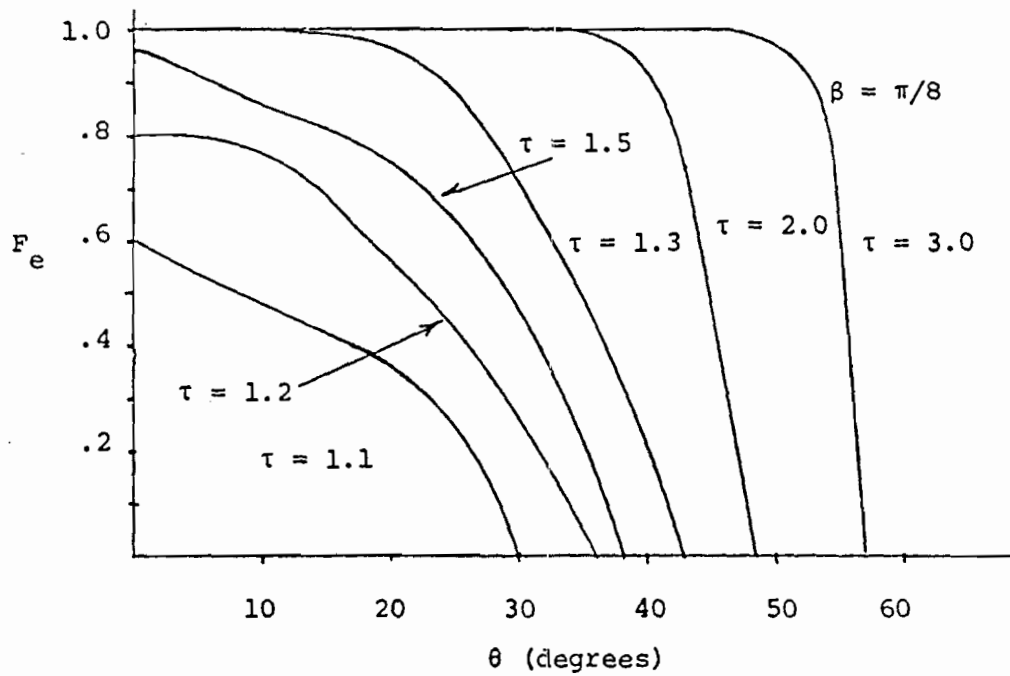


Figure IV-8b. Fraction of Electrons Escaping (F_e) for $b/a = 1.0$

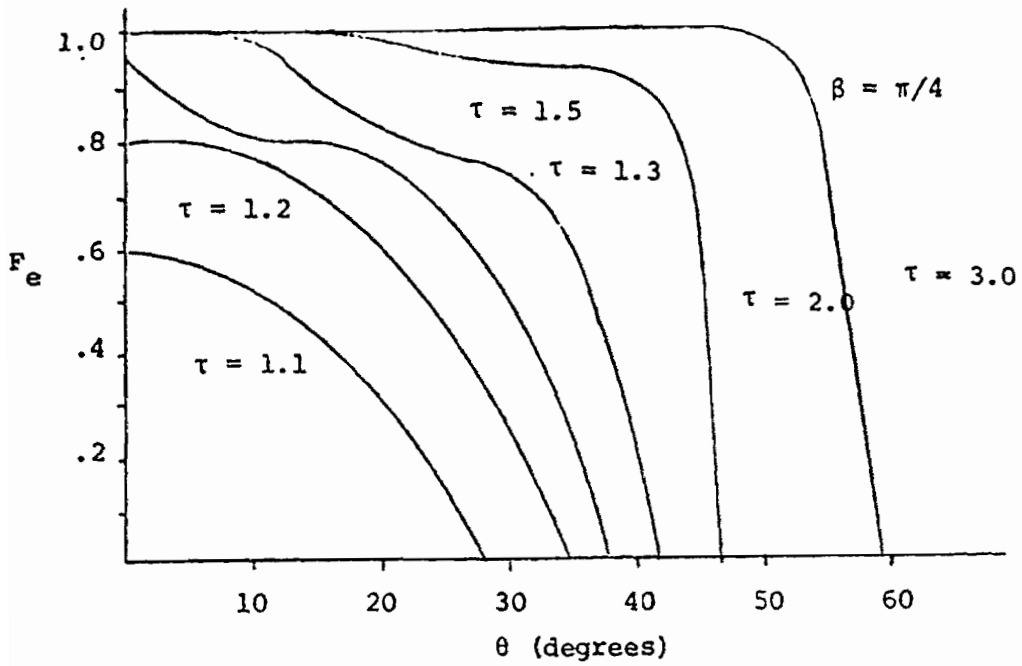


Figure IV-8c. Fraction of Electrons Escaping (F_e) for $b/a = 1.0$

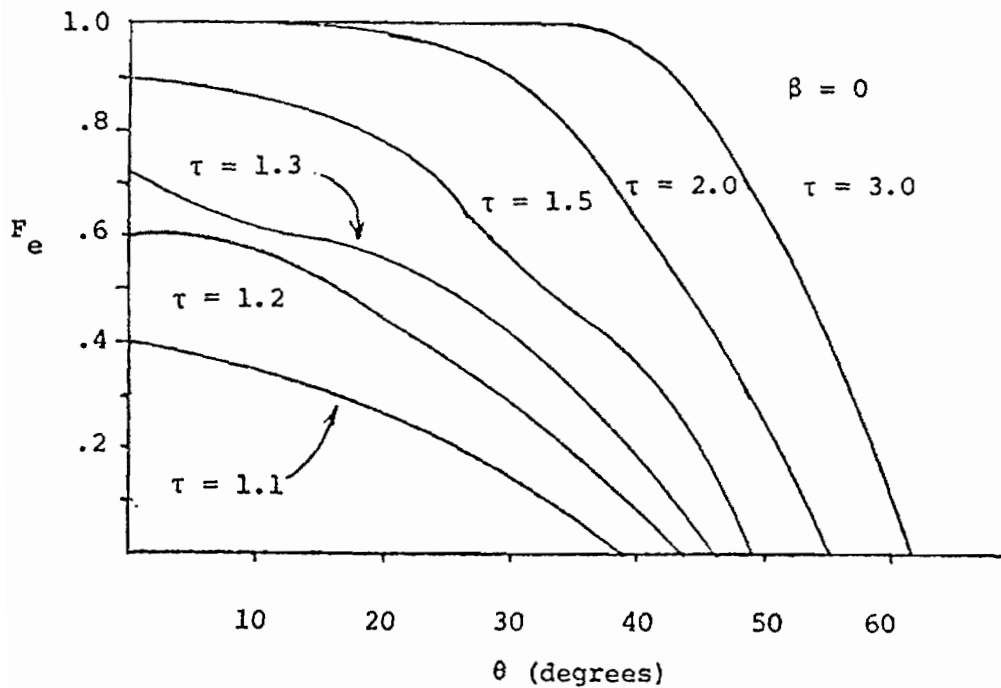


Figure IV-9a. Fraction of Electrons Escaping for $b/a = .5$

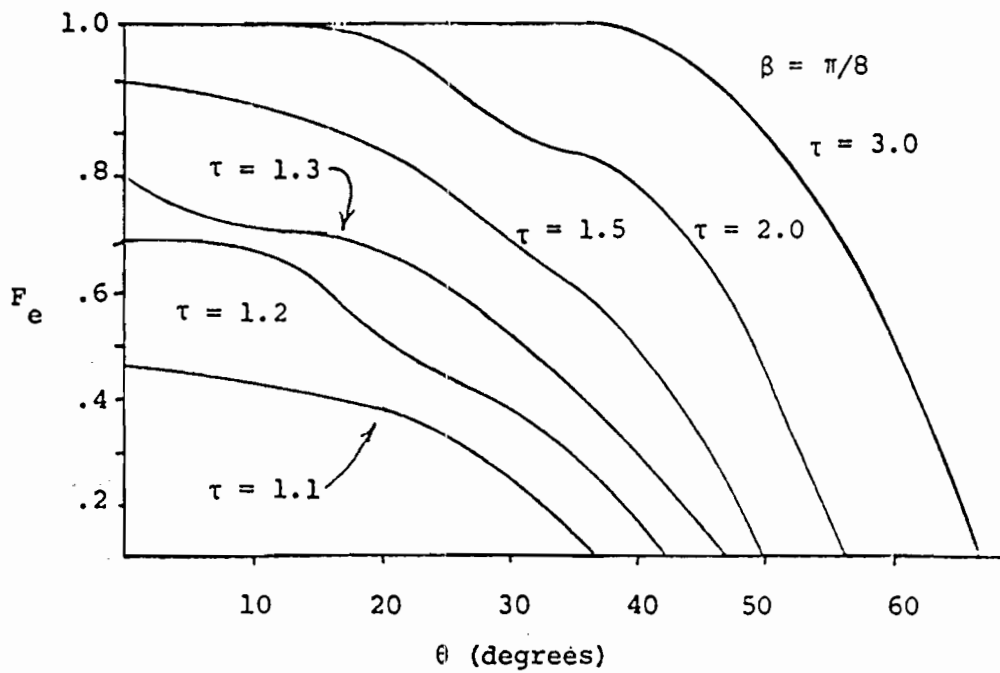


Figure IV-9b. Fraction of Electrons Escaping for $b/a = .5$

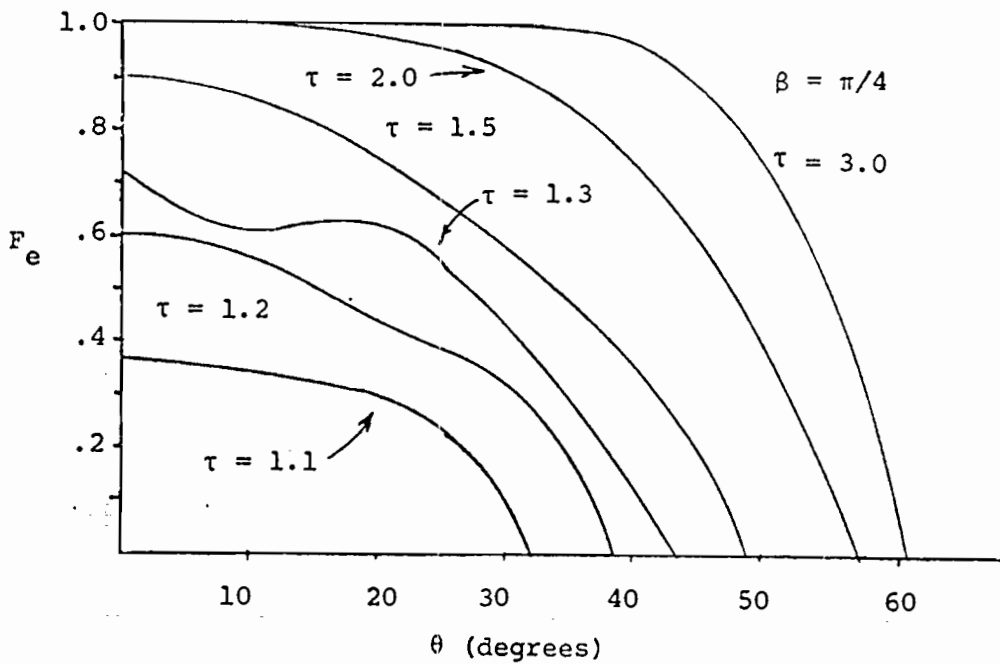


Figure IV-9c. Fraction of Electrons Escaping for $b/a = .5$

3. Double Grid of Small Radii Conductors

The double grid of small radii conductors was considered in an effort to reduce the number of electrons that escape through the center of the aperture of the single grid. The potential for this configuration is given by Equation (6). In this equation there are different charge densities for each of the two grids. For the purposes of analysis in this paper, the charge density on the upper grid was set to a value of 1/2 of that of the lower grid. This causes the contribution to the potential at $z = \infty$ to be the same for each grid. This somewhat arbitrary choice was made since the relationship between the ratio of the charge densities and the voltage on the wire approximated by the line charges is not a simple one. For example, let the grids be specified by the dimensions $a = 1$ and $b = 1$. For the same charge density on the two grids we will now look at the ratio of the voltages on wires of varying radii which would be approximated by the line charges. If Δ is the ratio of the voltage required on the wire of the lower grid to that of the upper grid, we obtain the following table by the use of Equation (18).

radius of conductor	Δ
.1	.581
.01	.633
.001	.741

Table IV-1. Ratio of Voltages Required on Conductors to be Approximated by Equal Charge Densities.

If the possibility exists of different radii wires being employed for the upper grid than are used for the lower grid, the problem becomes even greater.

Using the two to one charge density ratio mentioned above, contour plots were made for the double grid configuration as was done for the single grid. It is interesting to note that the potential contours for this configuration tend to be parallel to the ground plane indicating a potential distribution that tends to increase linearly in the z direction. The effect of this on the electron trajectories will be discussed later.

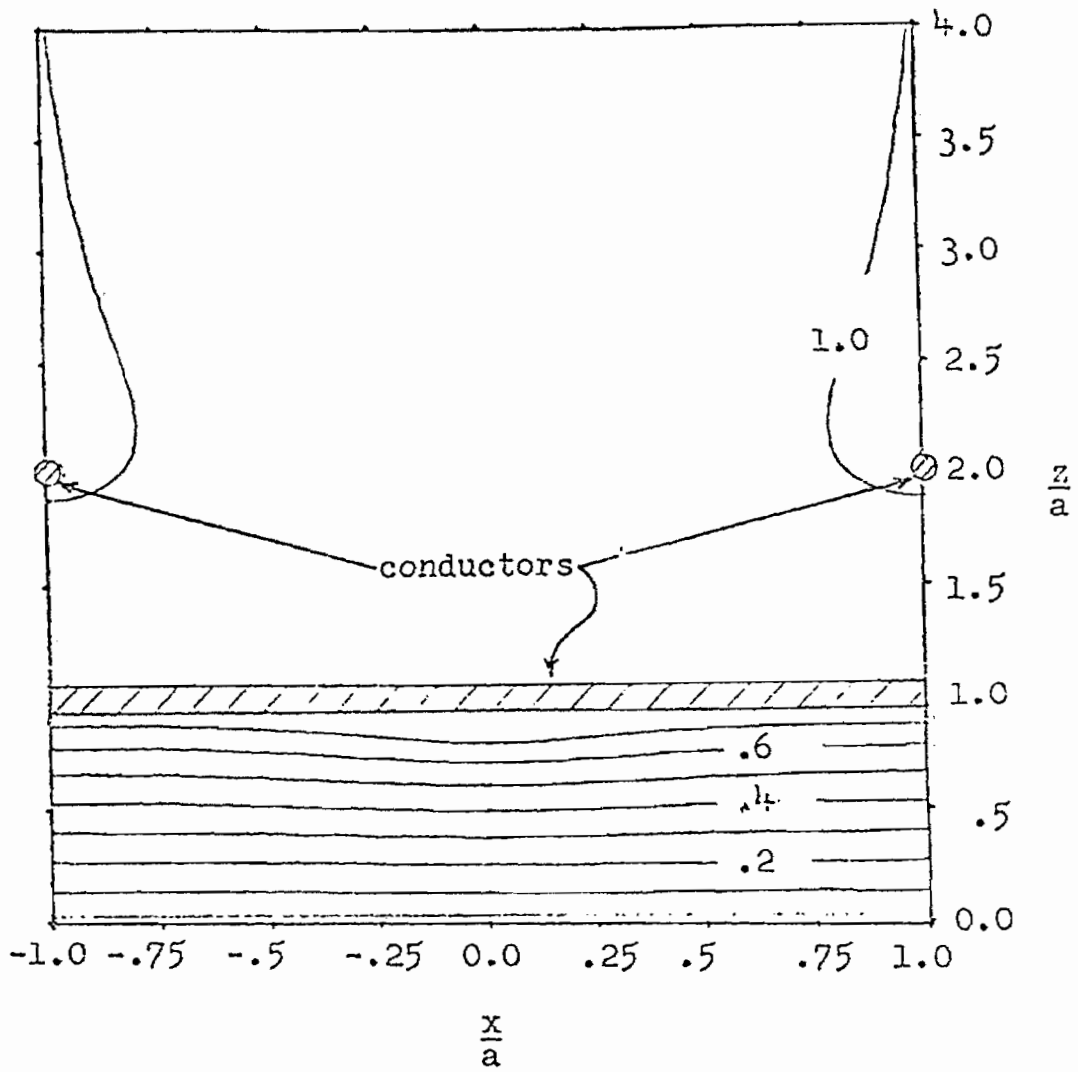


Figure IV-10a. Normalized Potential Contour Plots for $b/a = 1.0$ and $z = 0$

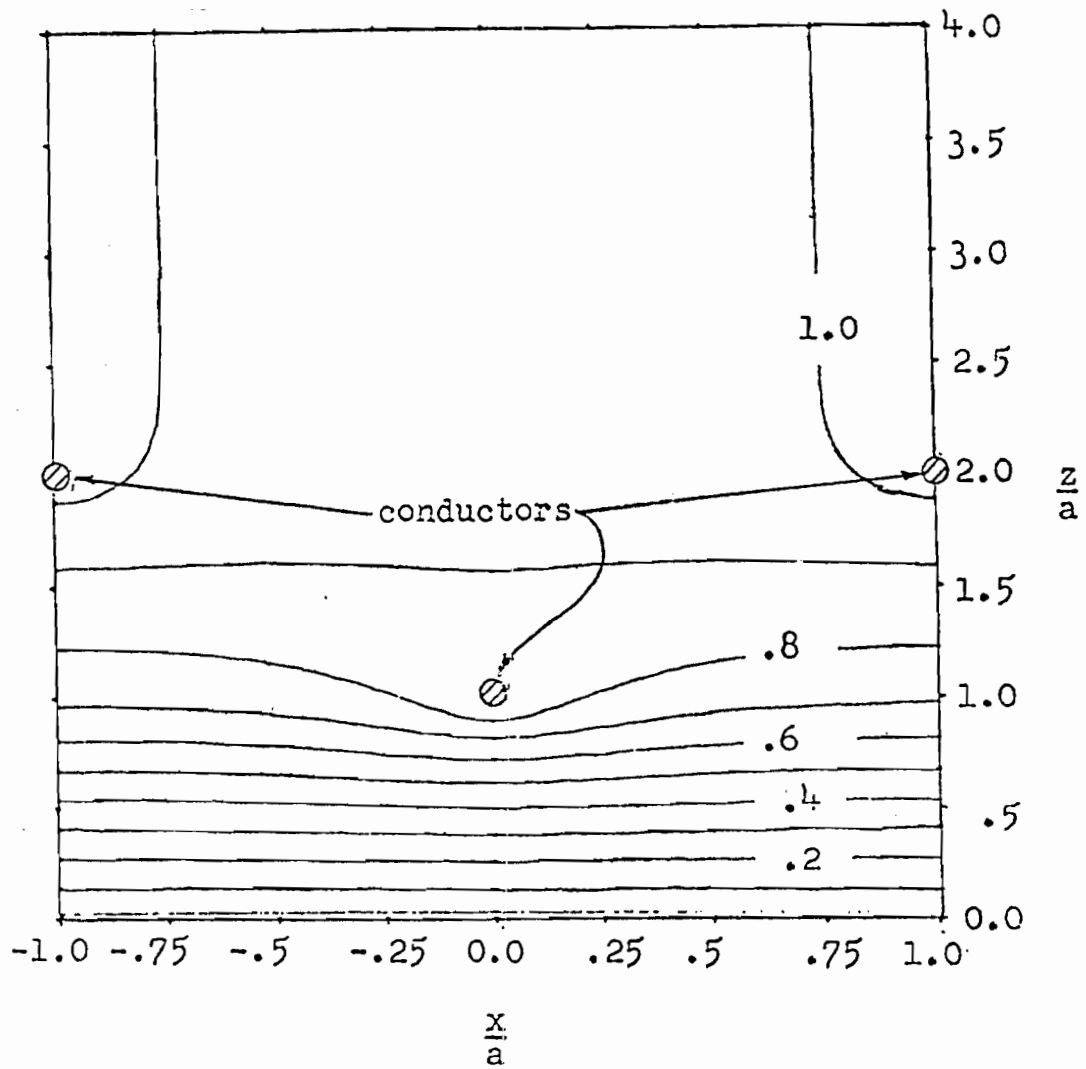


Figure IV-10b. Normalized Potential Contour Plots for $b/a = 1.0$ and $z = a/4$

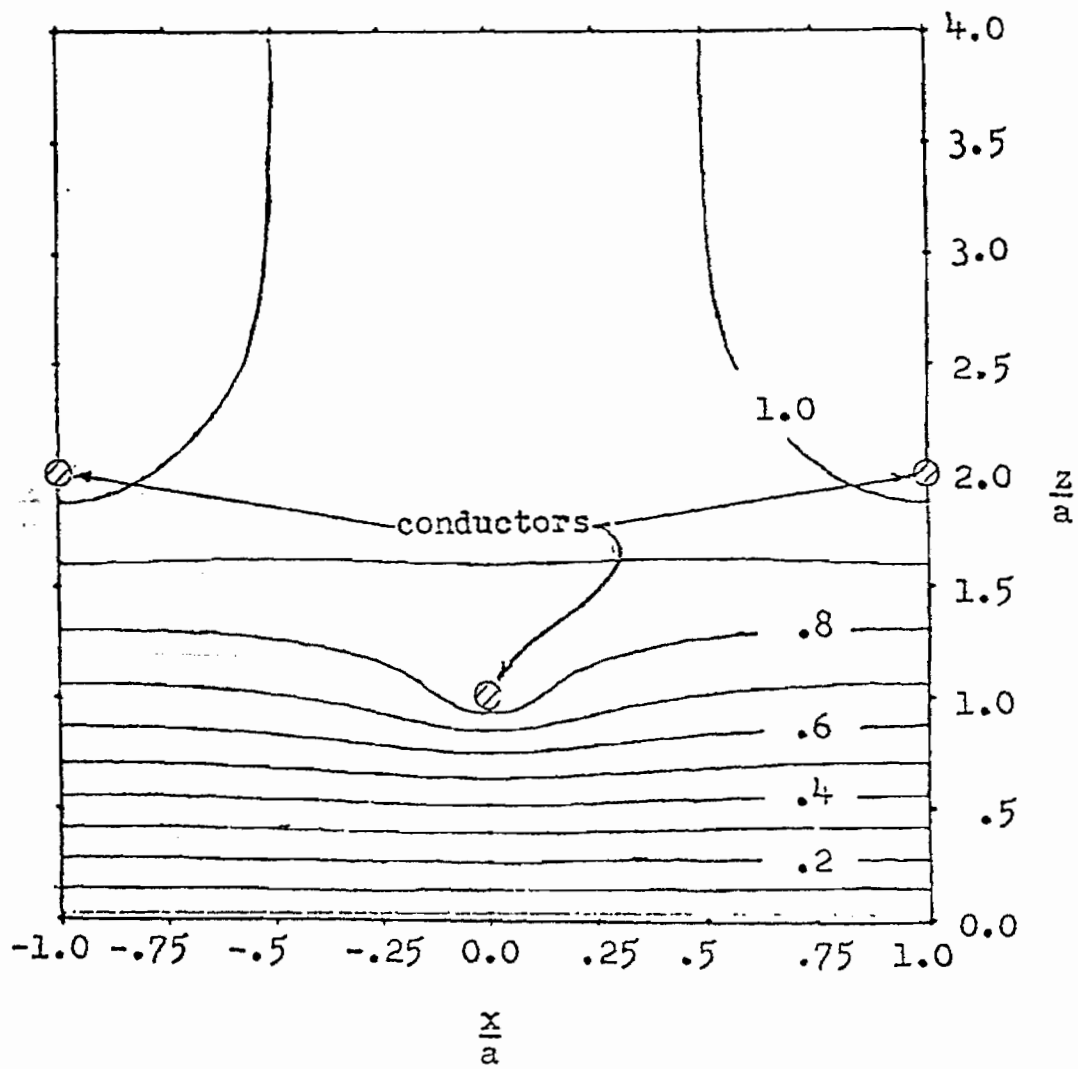


Figure IV-10c. Normalized Potential Contour Plots for $b/a = 1.0$ and $z = a/2$

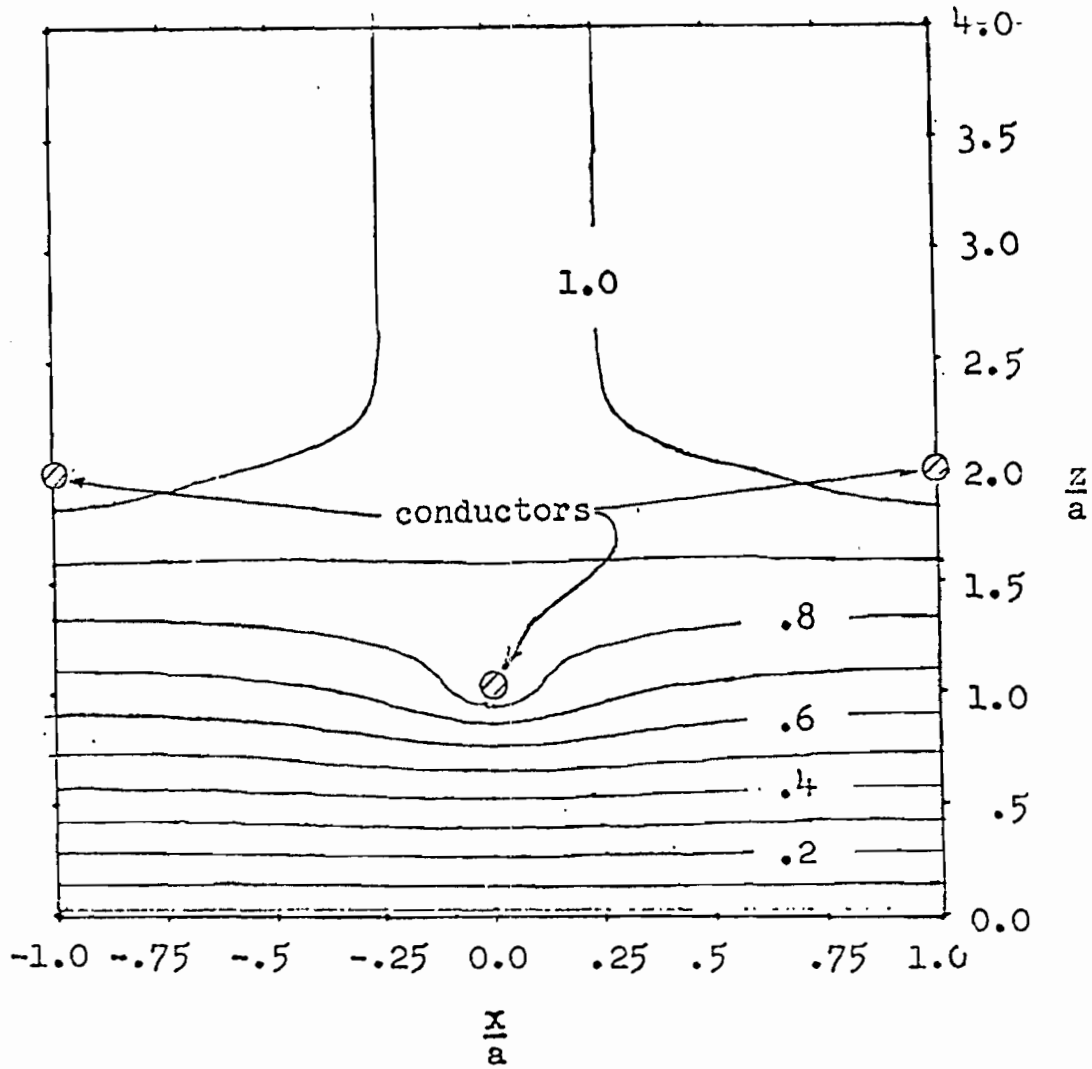


Figure IV-10d, Normalized Potential Contour Plots for $b/a = 1.0$ and $z = 3a/4$

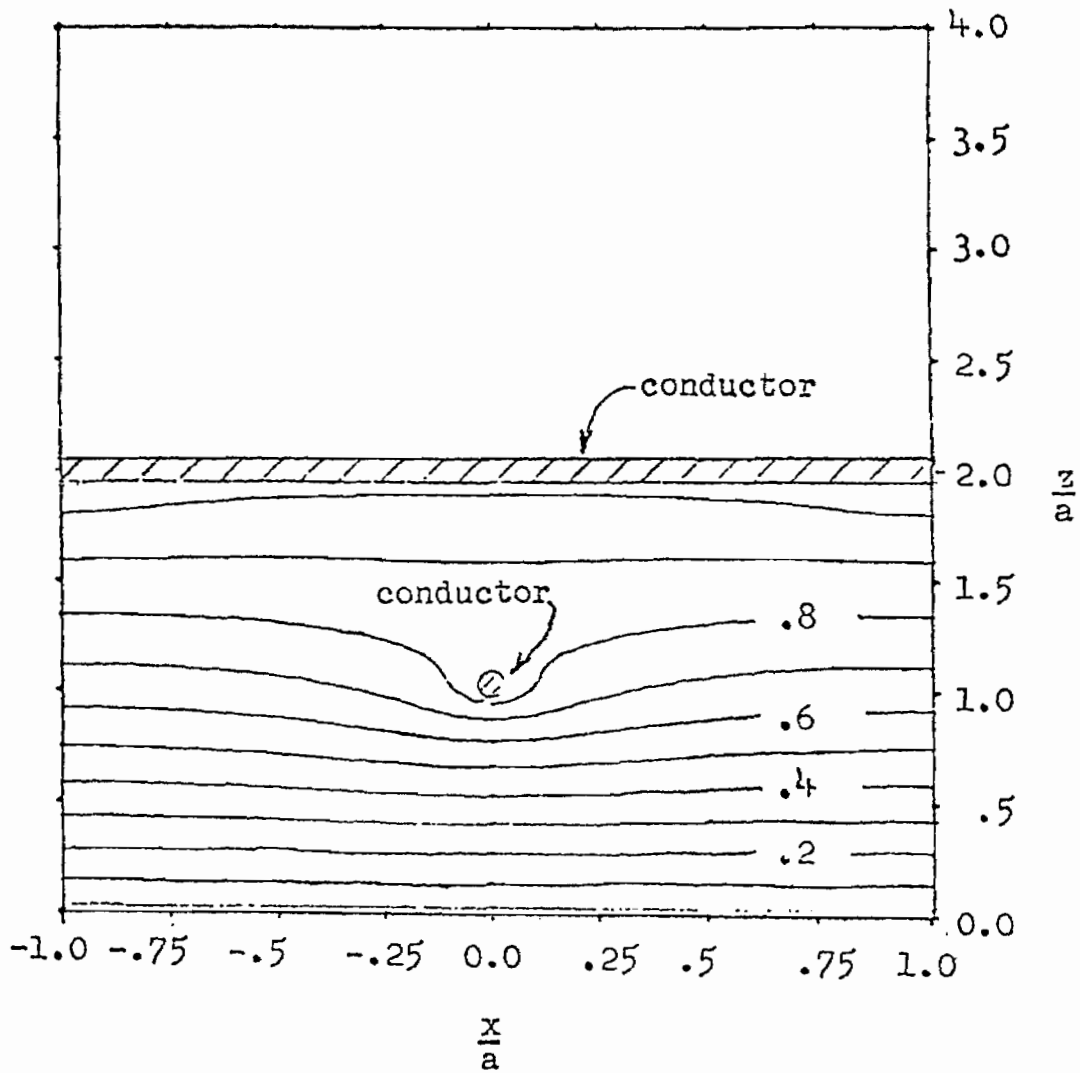


Figure IV-10e, Normalized Potential Contour Plots for $b/a = 1.0$ and $z = a$

Electron trajectory plots were made for this case as for the single grid case. In general, the actual trajectory plots will not be presented for this and the following cases, but one final plot follows. This plot is for electrons of a normalized energy of 1.1 and with the electrons rising vertically out of the ground plane. It illustrates the tendency of the second grid, particularly for the $\theta = 0$ case, to "straighten out" the trajectories of the electrons. In the single grid case, some of the electrons with an energy of 1.1 and $\theta = 0$ were returned to the ground plane primarily due to a change in direction. The straightening effect of the second grid makes this behavior much more unlikely.



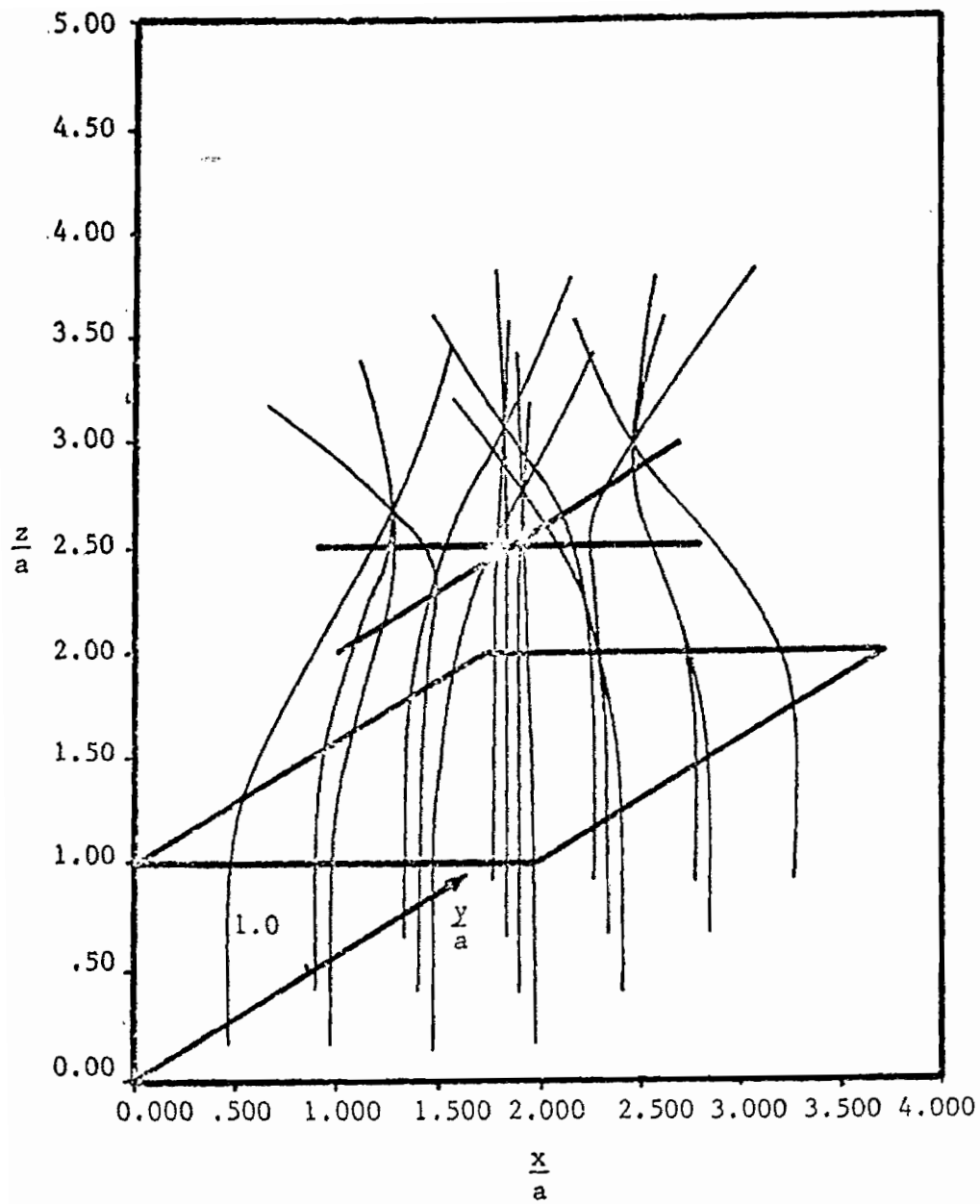


Figure IV-11. Electron Trajectories for $b/a = 1.0$, Normalized Energy of 1.1, $B = 0$ radian, and $\theta = 0^\circ$

The following are plots of the fraction of electrons escaping as a function of energy and direction. As in the single grid case, 100 initial positions were used for the electrons at each energy and direction. In considering the results for the double grid case, one should keep in mind that the potential has been normalized to be 1.0 at $z = \infty$. It is not, therefore, equivalent to the single grid case which produces a potential of 1.0 at $z = \infty$ with the addition of another grid which also produces a potential of 1.0 at $z = \infty$. Even so, the double grid configuration does not seem to have sufficiently better characteristics to warrant a detailed study. Therefore, only the results of one spacing of the grids is presented.

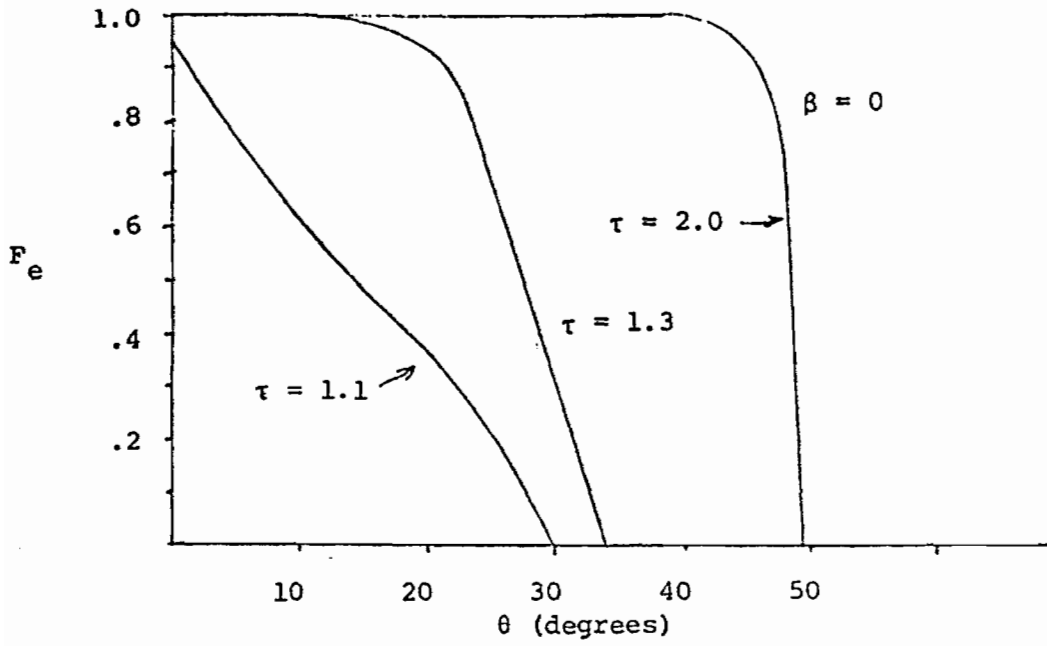


Figure IV-12a. Fraction of Electrons Escaping (F_e) for $b/a = 1.0$

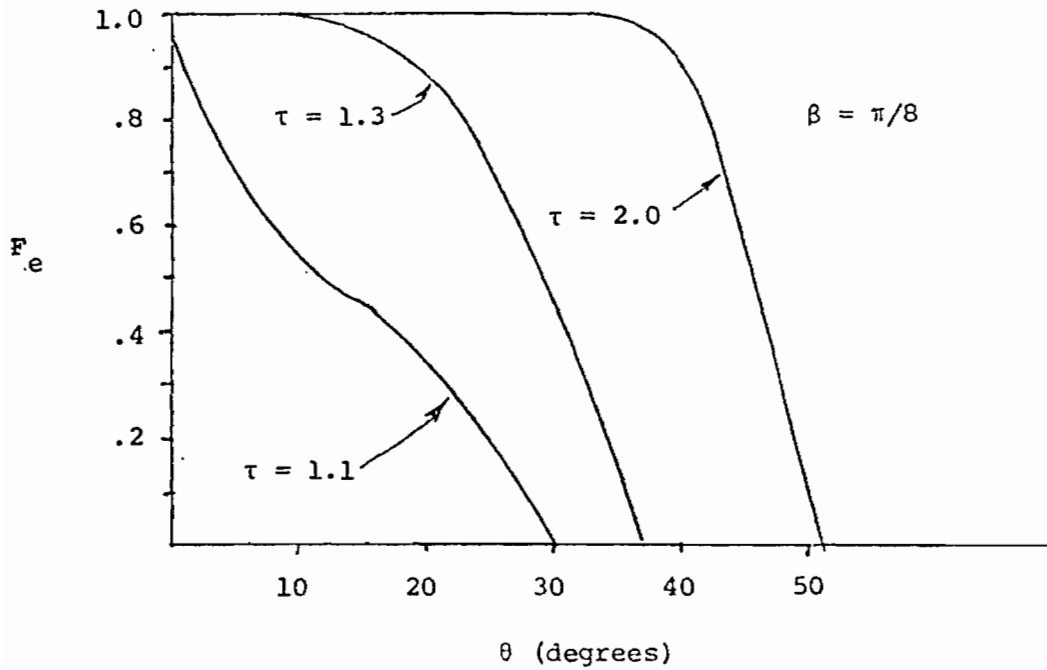


Figure IV-12b. Fraction of Electrons Escaping (F_e) for $b/a = 1.0$

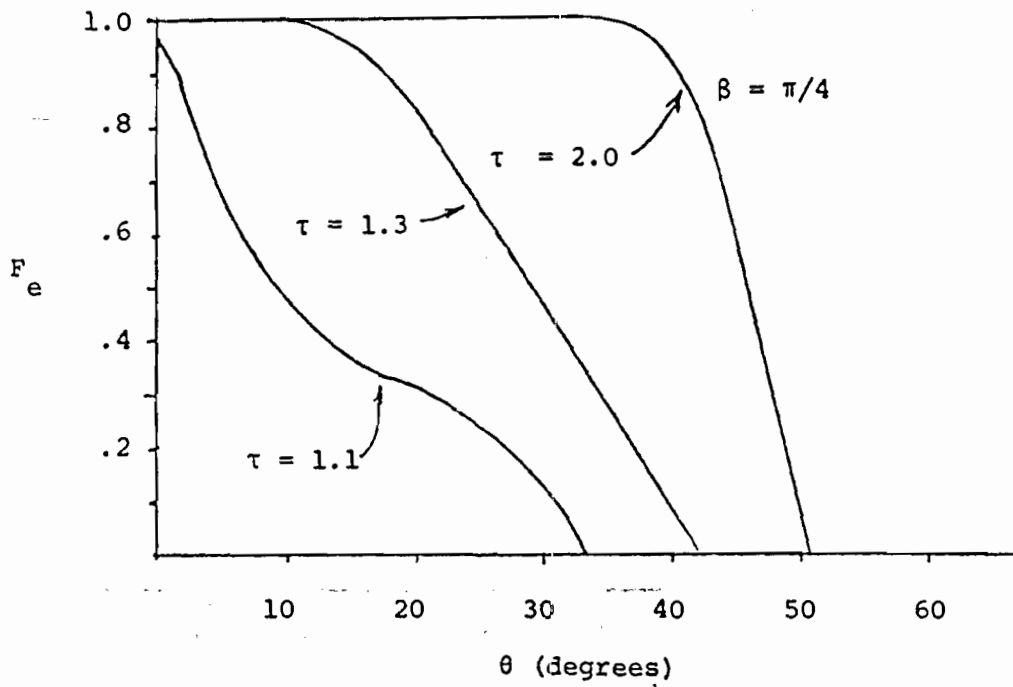


Figure IV-12c. Fraction of Electrons Escaping (F_e) for $b/a = 1.0$

4. Parallel Cylindrical Conductors Case

The potential distribution for a series of cylindrical conductors set parallel to a ground plane was found using the approach of Section II-2 and the least squares fitting of Section II-5. The coefficients for the series for the potential are given in Appendix A. The line charge solution was used as described in Section II-4 to give a first approximation to the potentials used in the analysis of this configuration. For the purposes of comparison the mean squared error was calculated in the same manner for three different solutions. The solutions used for the comparison are the line charge solution only, the series solution only, and the series and line charge solution together. The results of the error calculation for these three different solutions are shown below.

Dimensions		Mean squared error (volts) ²		
b/a	c/a	Line charge approximation	Series solution	Series and line charge solution
1.0	.25	4.69×10^{-3}	1.91×10^{-6}	1.07×10^{-6}
1.0	.1	4.54×10^{-4}	1.44×10^{-3}	7.48×10^{-6}
.5	.25	2.00×10^{-2}	2.35×10^{-5}	1.56×10^{-5}
.5	.1	1.41×10^{-3}	3.82×10^{-3}	2.47×10^{-5}

Table IV-2. Mean Squared Error for Various Solutions

All the series calculations were made using fifteen terms of the series in each region and with potential of the conductor set to 1.0.

The first thing we note from the table is that the line charge approximation becomes better as the radii of the conductor approximated becomes smaller and as the spacing between the conductor and the ground plane becomes larger. The series solution also becomes better as the distance from the conductors to the ground plane increases, but the error increases with decreasing radii. In both cases where the ratio c/a is .1, the error of the line charge solution alone is comparable to that of the series solution alone. It would appear that this ratio is the approximate value at which the use of the series solution results in significant improvement, at least for the number of terms of the series calculated here. As Table IV-2 shows the combination of the series and line charge solution results in appreciable improvement over the use of either one separately.

On the following pages are presented potential contour plots for the four cases presented in Table IV-2. To reiterate, 15 terms were used in each solution region and the potential of the conductor was normalized to 1.0. The solution used to obtain these plots is the combination of the line charge and series solution.

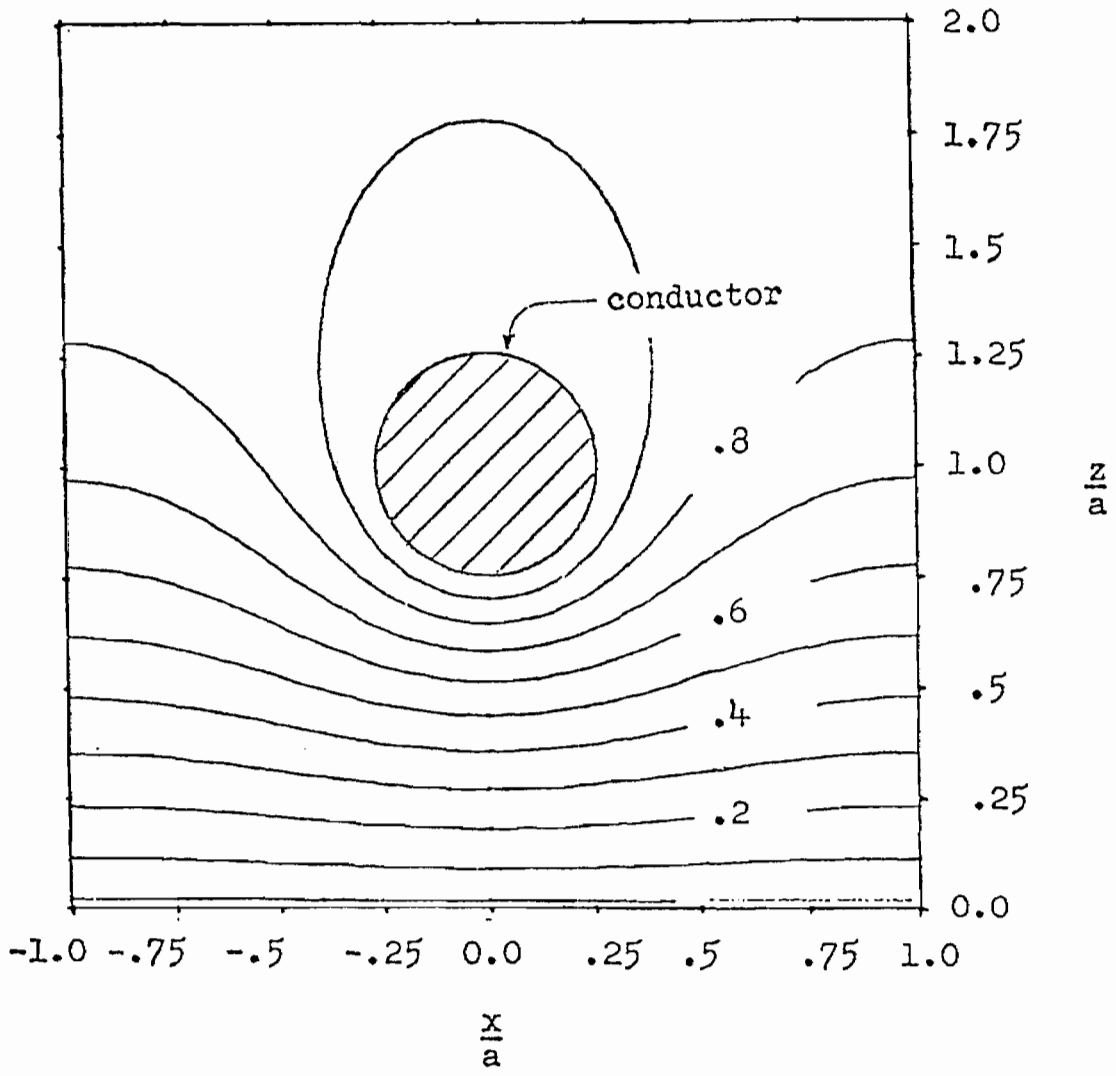


Figure IV-13. Normalized Potential Contour Plot for $b/a = 1.0$ and $c/a = .25$

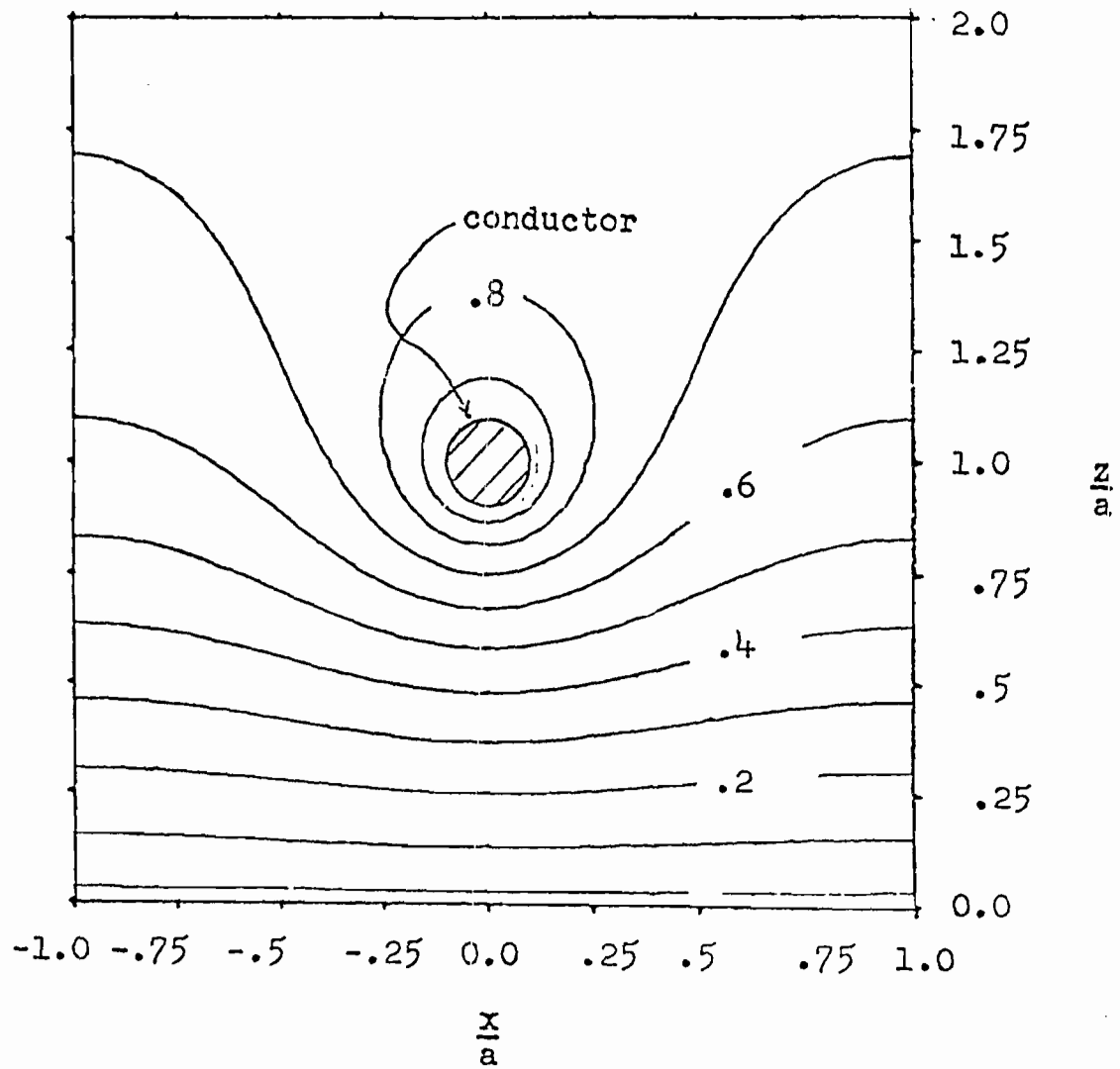


Figure IV-14. Normalized Potential Contour Plot for $b/a = 1.0$ and $c/a = .1$

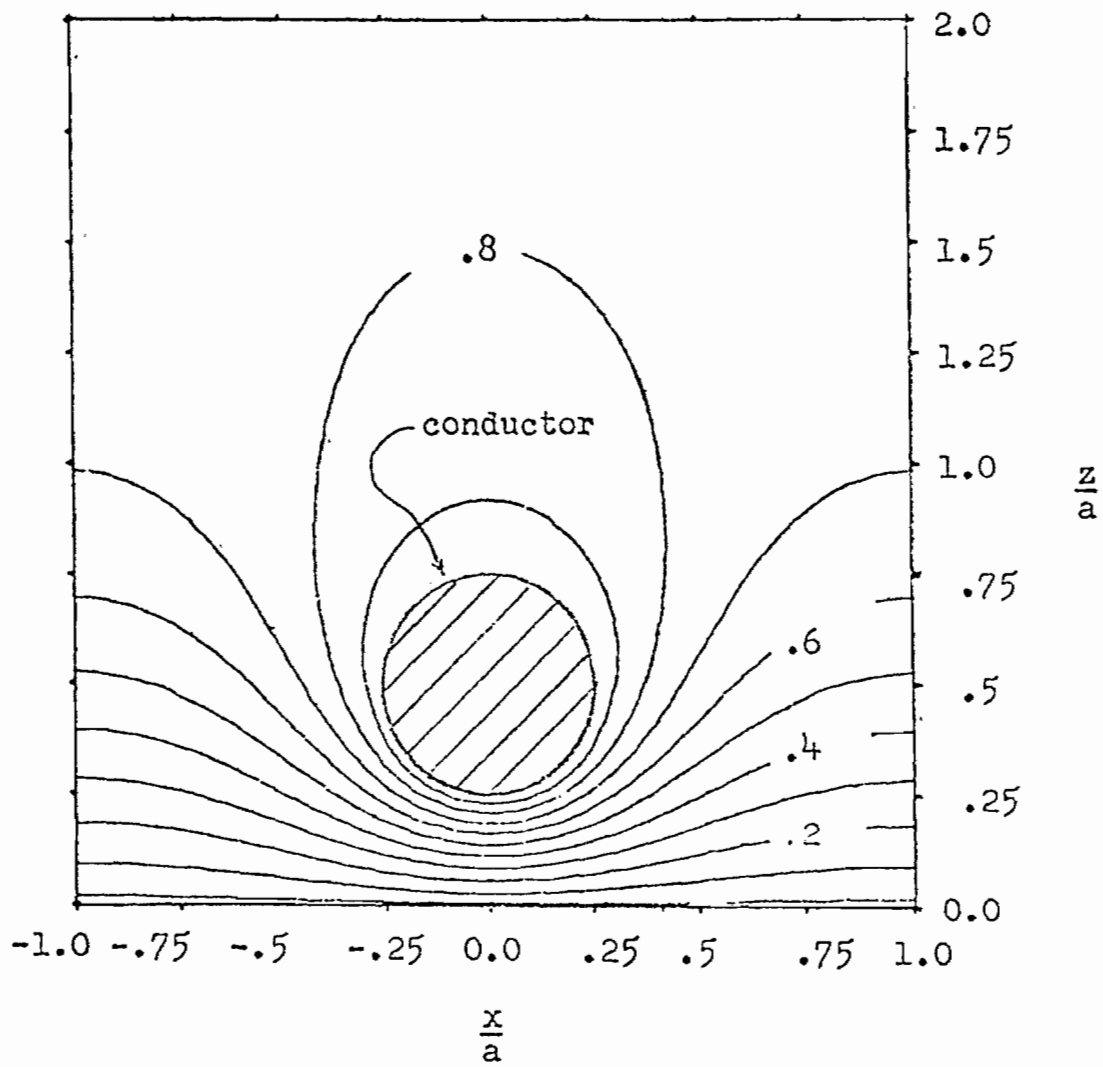


Figure IV-15. Normalized Potential Contour Plot for $b/a = .5$ and $c/a = .25$

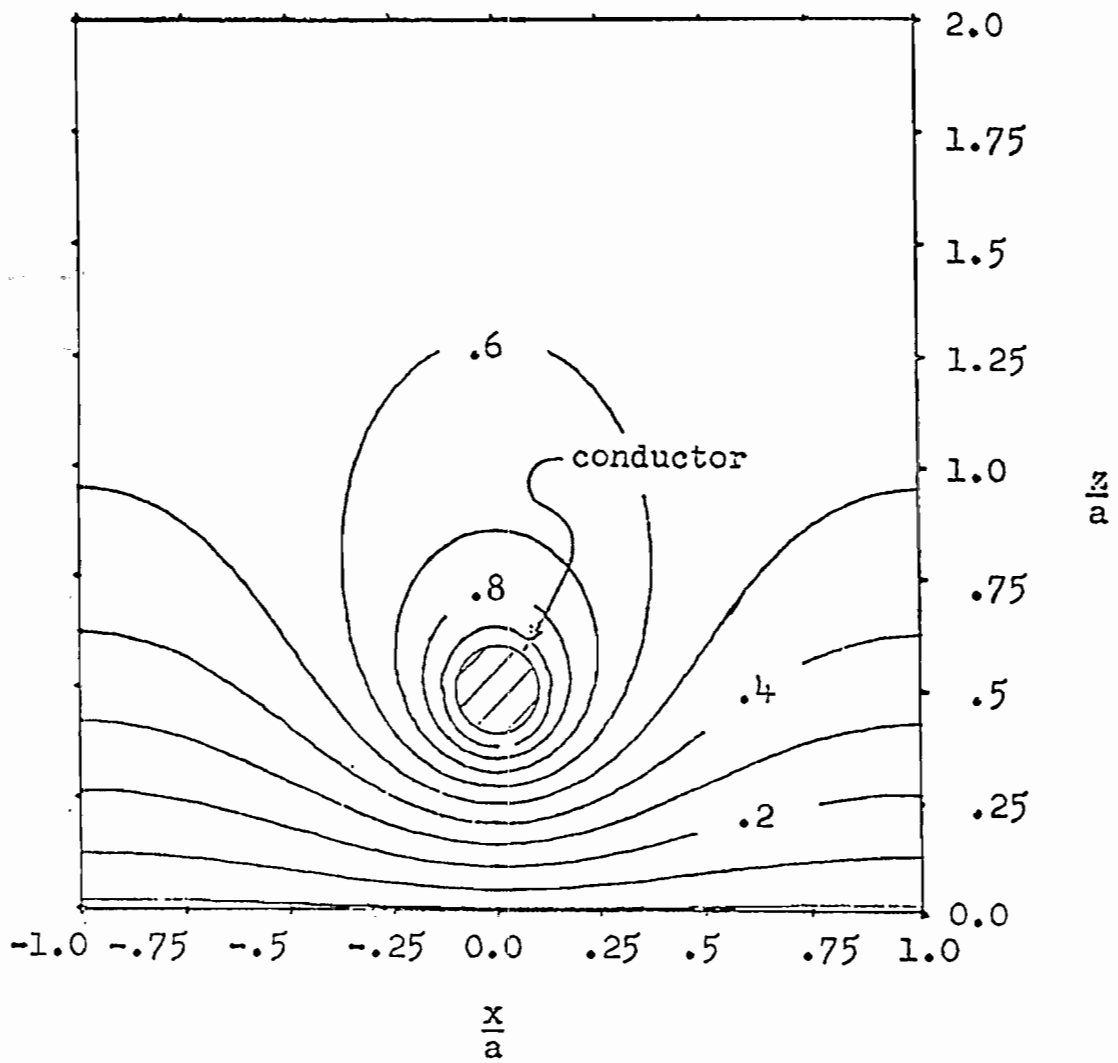


Figure IV-16. Normalized Potential Contour Plot for $b/a = .5$ and $c/a = .1$

Electron trajectories were found for this case in the same manner as was done previously except that only the $\theta = 0$ angle needed to be considered. The data obtained from these trajectories are shown in graphical form on the following pages. Since we are now using conductors of finite radii, the possibility of the electrons striking the conductors must be considered. Since we do not know the type of collision to expect between the electrons and the conductors, the percentage of the electrons striking the conductor is merely listed. If the collision is elastic, the program may be easily modified to continue the trajectories after the collision. If the electrons are absorbed by the conductors, the fraction of electrons striking the conductors should be added to the fraction of electrons contained. If secondary Compton electrons are produced from these electrons, and data is available concerning the initial velocity distribution of the secondary electrons, the program may be modified to account for this phenomenon.

Another consideration that arises due to the finite size of the conductors is that Compton electrons could be produced on the conductors themselves by the incoming radiation.⁽¹⁵⁾ Closely related to this is the fact that the conductor would shield a portion of the ground plane from the incoming radiation.⁽¹⁵⁾ Both of these phenomena are dependent on the direction of the incoming radiation. These effects were ignored in the present analysis, but could be accounted for if more detailed information concerning them were available.

It is useful to calculate the ratio V_0/V_∞ for the various spacings of conductors used for this figuration where V_0 is the potential of the conductor and V_∞ is the potential at $z = \infty$. If the energy of the electron, normalized to the potential energy of an electron at $z = \infty$, is

less than this value of V_0/V_∞ , it is impossible for the electron to strike the conductor.

b/a	c/a	V_0/V_∞
1.0	.25	1.135
1.0	.1	1.38
.5	.25	1.28
.5	.1	1.74

Table IV-3. V_0/V_∞ for Various Spacings of Conductors

The data for the plots presented on the following pages were obtained using 30 initial positions for the electrons on the ground plane. Due to the increase in computer time needed to calculate each trajectory the number of trajectories had to be reduced from the 100 used in the line charge case. For similar reasons, normalized energies of 1.1, 1.3, and 2.0 were used for the $a/b = 1.0$ and $c/a = .25$ spacing only and the normalized energy of 1.1 was used for the other spacings of $b/a = 1.0$ and $c/a = .1$, $b/a = .5$ and $c/a = .25$, and $b/a = .5$ and $c/a = .1$.

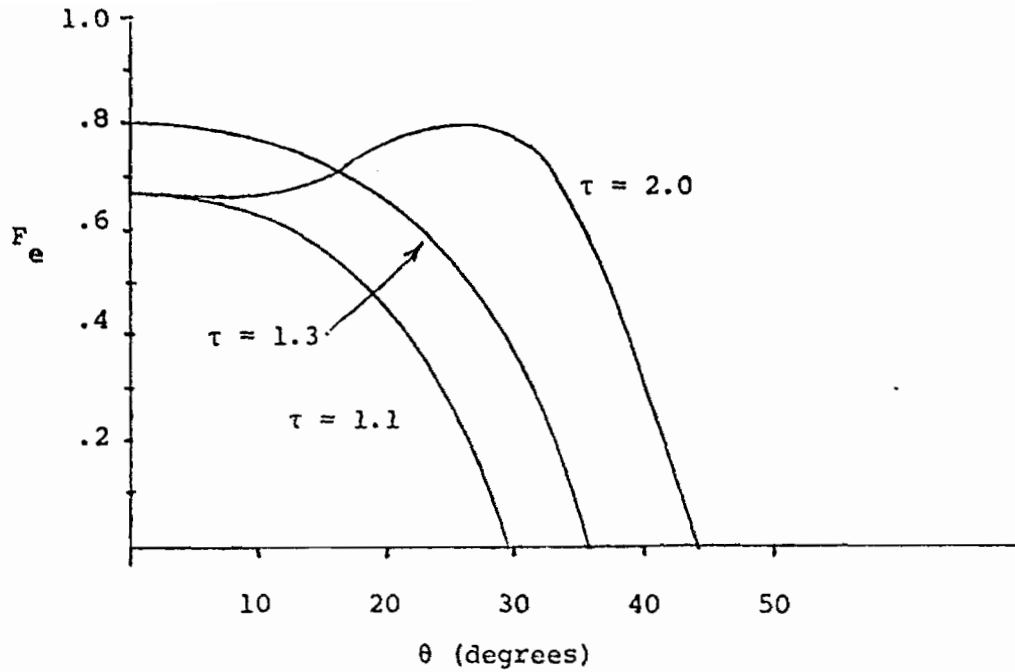


Figure IV-17. Fraction of Electrons Escaping (F_e) for $b/a = 1.0$ and $c/a = .25$

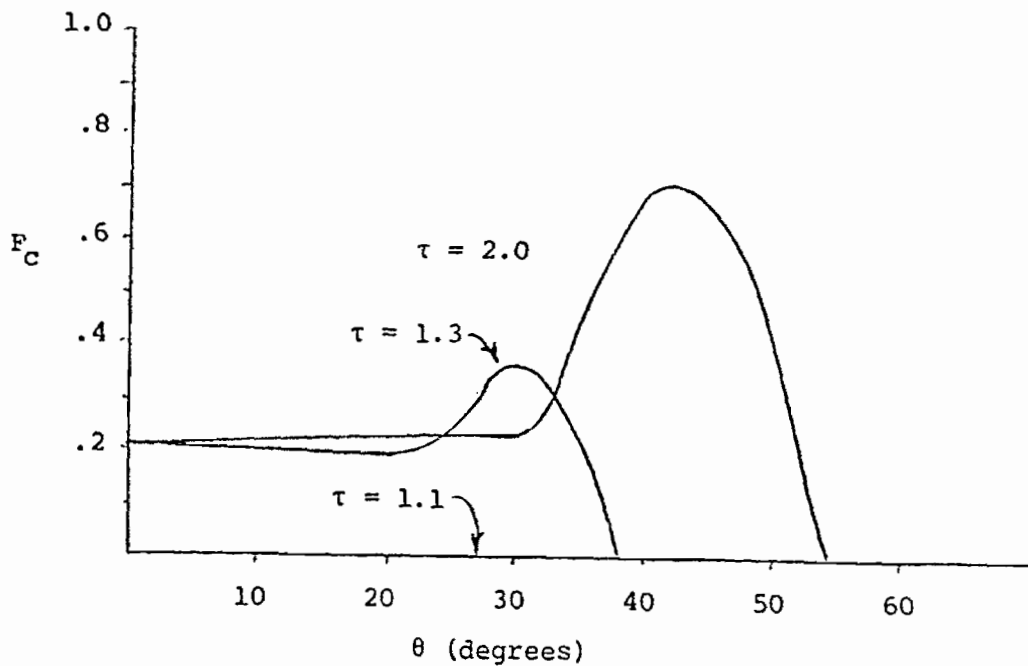


Figure IV-18. Fraction of Electrons Striking Conductor (F_c) for $b/a = 1.0$ and $c/a = .25$

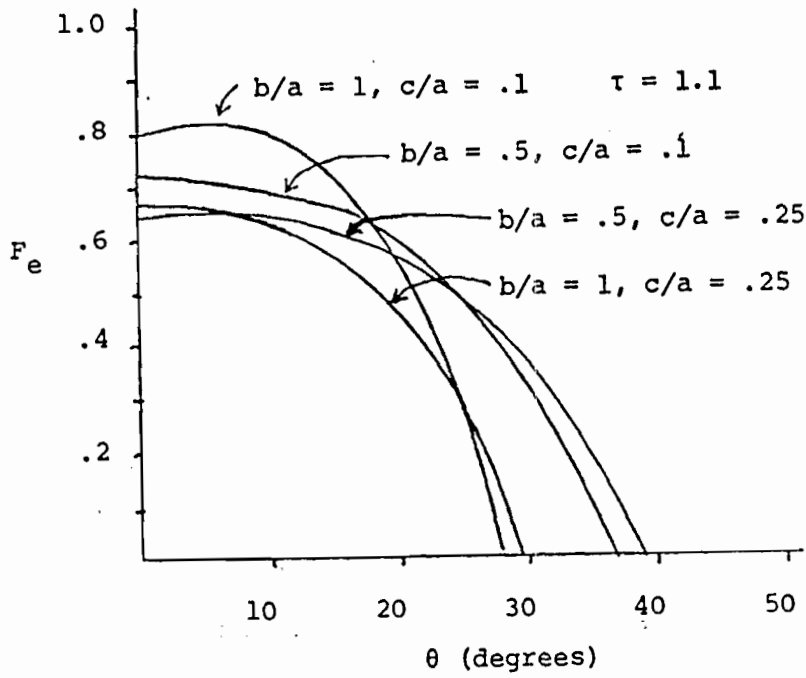


Figure IV-19. Fraction of Electrons Escaping (F_e) for a Normalized Energy of 1.1

5.0 Crossed Cylindrical Conductors Case

The potential distribution for the grid of crossed cylindrical conductors was found using the approach of Section II-3 and the least squares fitting of Section II-5. The actual coefficients for the series for the cases studied are given in Appendix A. For the purpose of comparison, the error was calculated using the line charge portion of the solution along and for the line charge and series solution combined. Due to the longer time necessary for calculation, the solution obtained by using only the series form was not calculated. Table IV-4 shows the error obtained for these solutions.

Dimensions		Mean Squared Error (volts) ²	
b/a	c/a	Line charge Approximation	Series and line charge solution
1.0	.25	3.93×10^{-2}	6.28×10^{-4}
1.0	.1	7.60×10^{-3}	2.54×10^{-3}
.5	.25	.172	4.09×10^{-3}
.5	.1	.243	9.18×10^{-3}

Table IV-4. Mean Squared Error for Two Solutions

On the following pages, potential contour plots are shown for the spacings shown in Table IV-4. The potentials are those found using the line charge and series solutions together. The potential of the conductors was normalized to 1.0 and 15 terms of the series solution were used in each region.

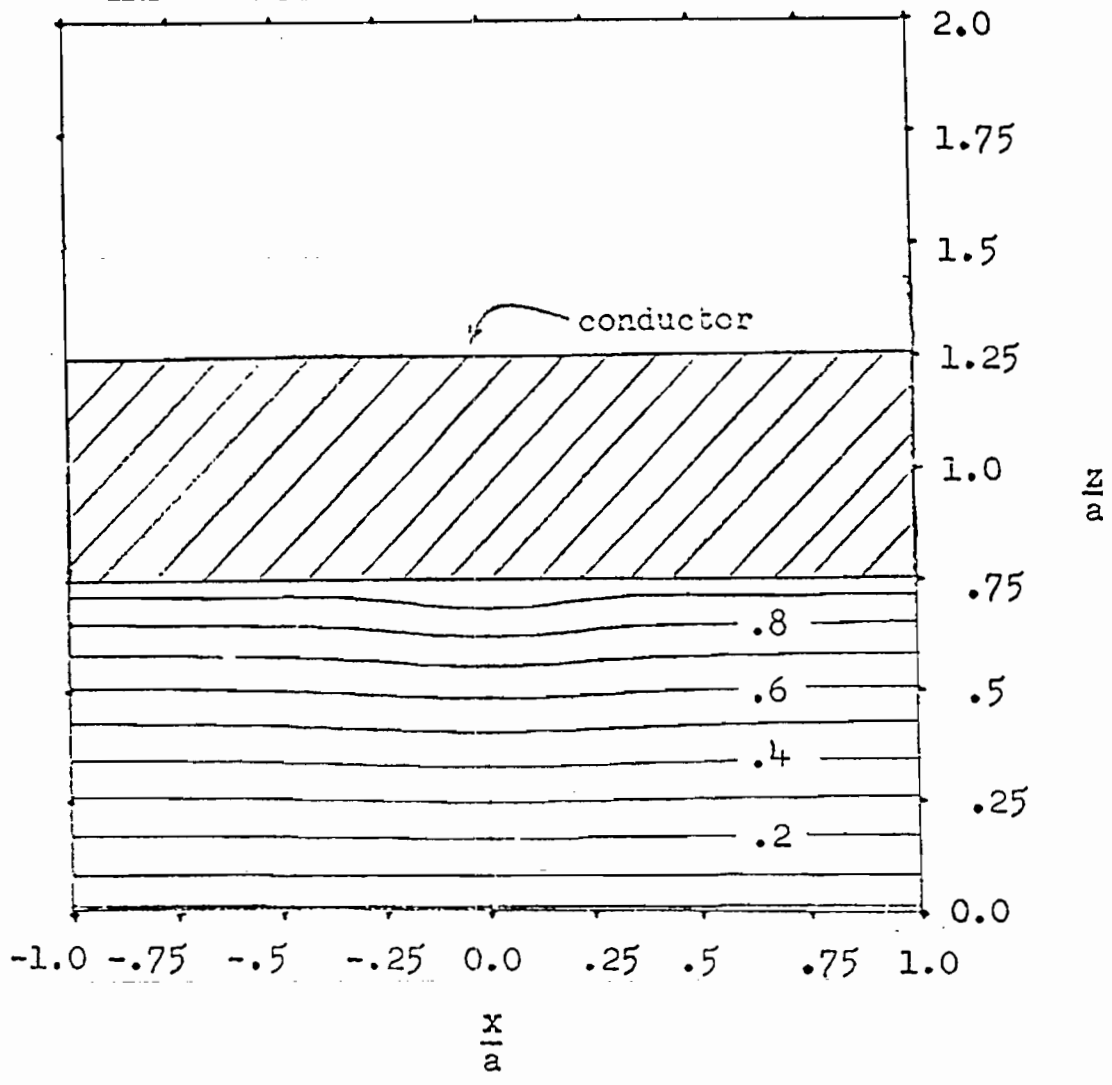


Figure IV-20a. Normalized Potential Contour Plot for $b/a = 1.0$, $c/a = .25$ and $z = 0$

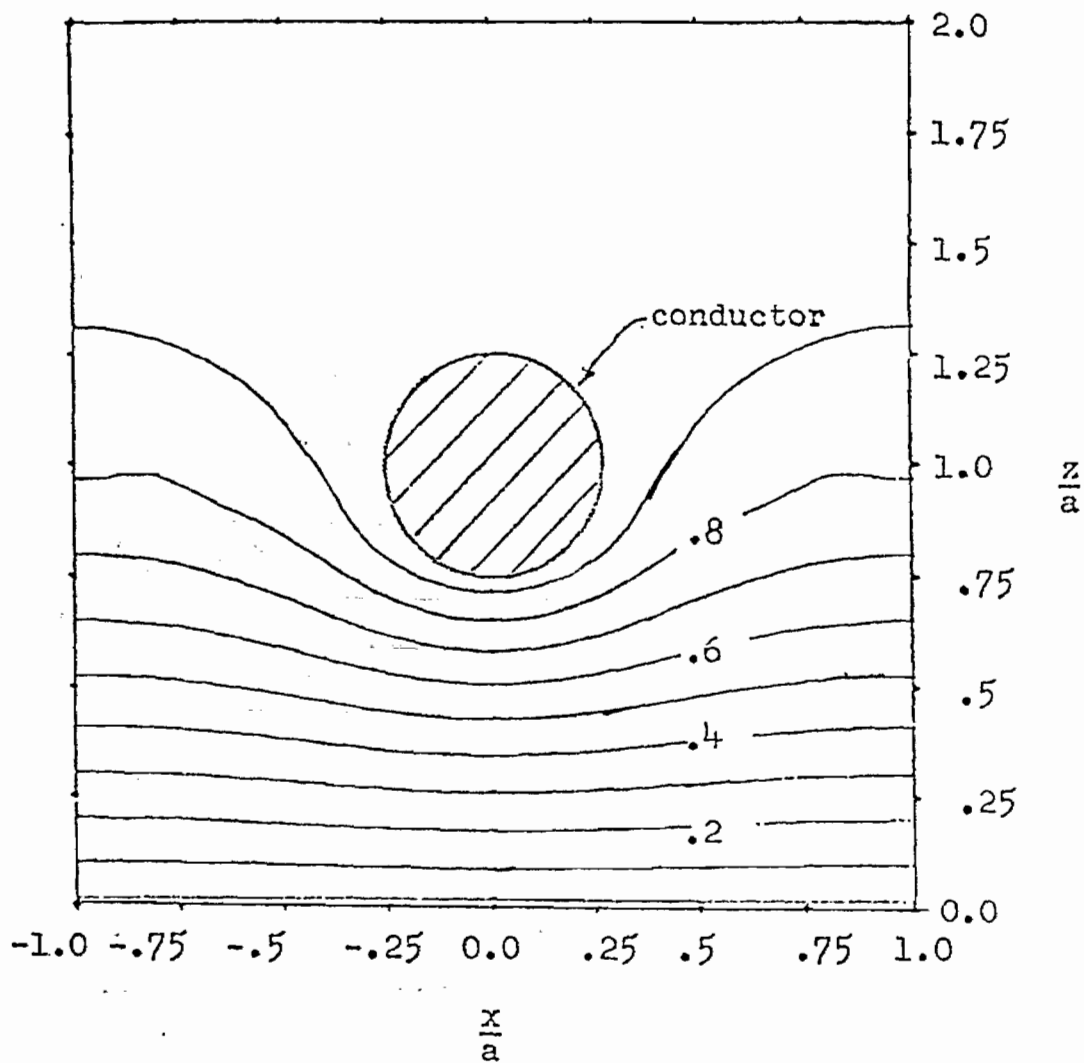


Figure IV-20b. Normalized Potential Contour Plot for $b/a = 1.0$, $c/a = .25$ and $z = a/4$

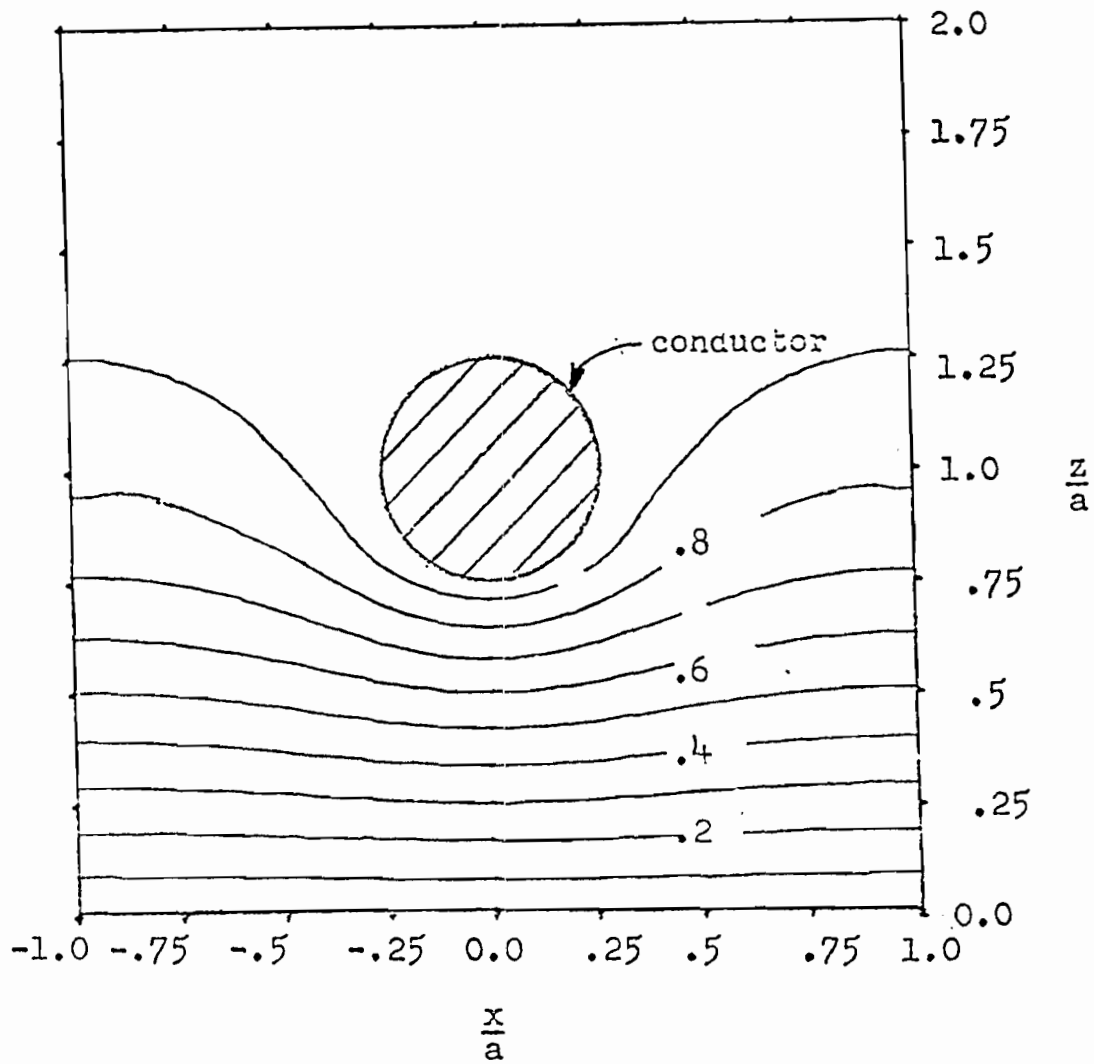


Figure IV-20c. Normalized Potential Contour Plot for $b/a = 1.0$, $c/a = .25$ and $z = a/2$

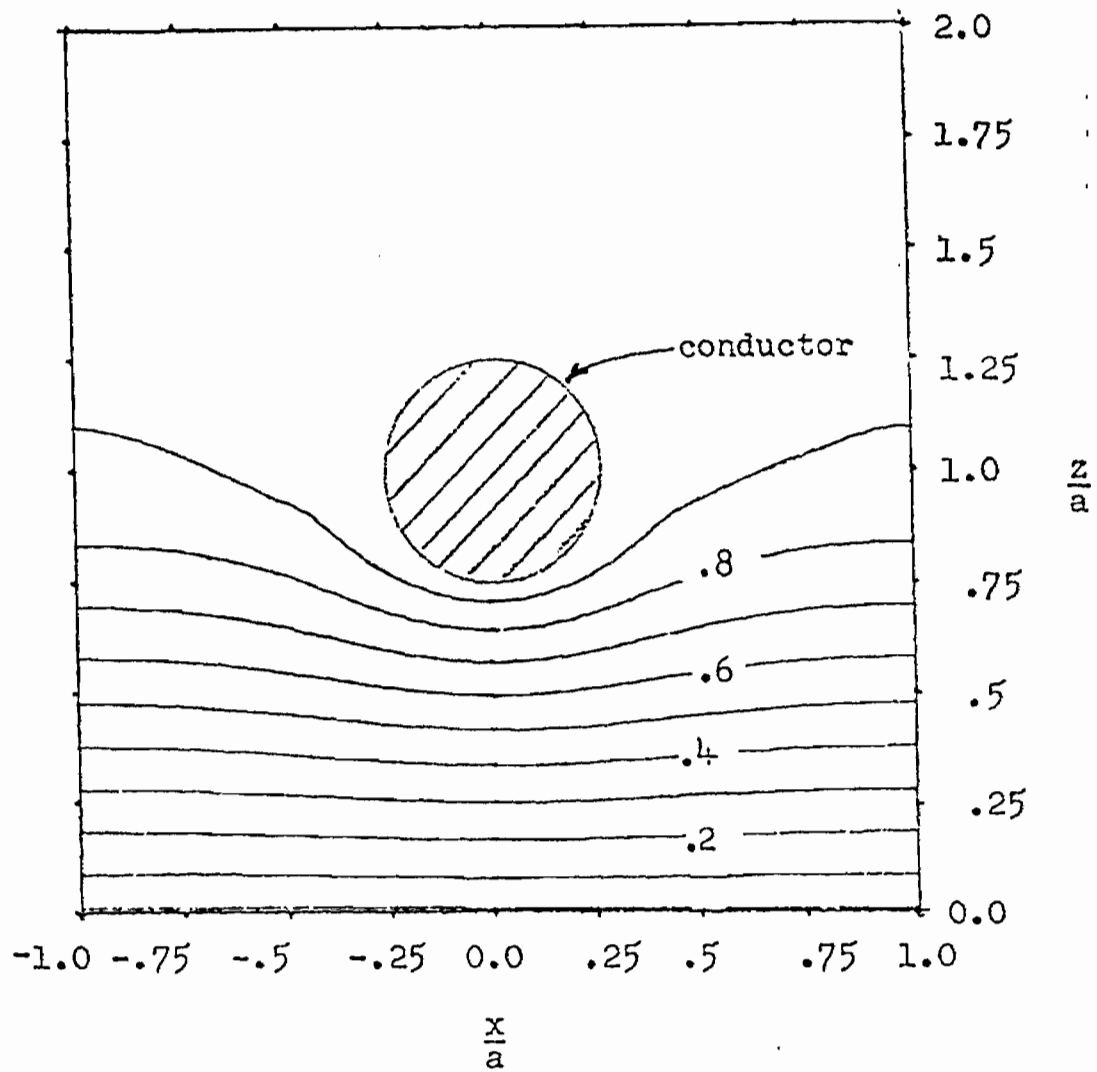


Figure IV-20d. Normalized Potential Contour Plot for $b/a = 1.0$, $c/a = .25$ and $z = 3a/4$

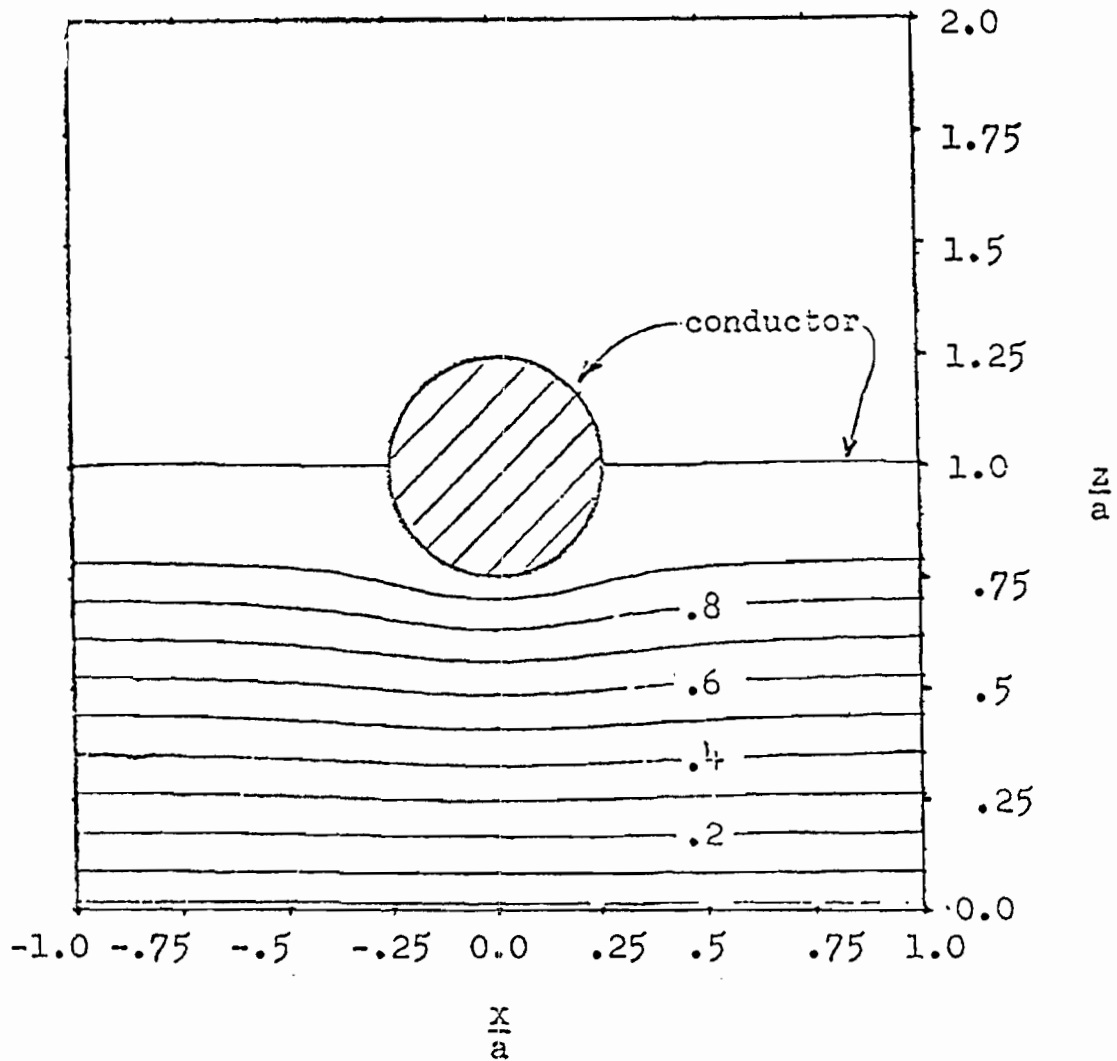


Figure IV-20e. Normalized Potential Contour Plot for $b/a = 1.0$, $c/a = .25$ and $z = a$

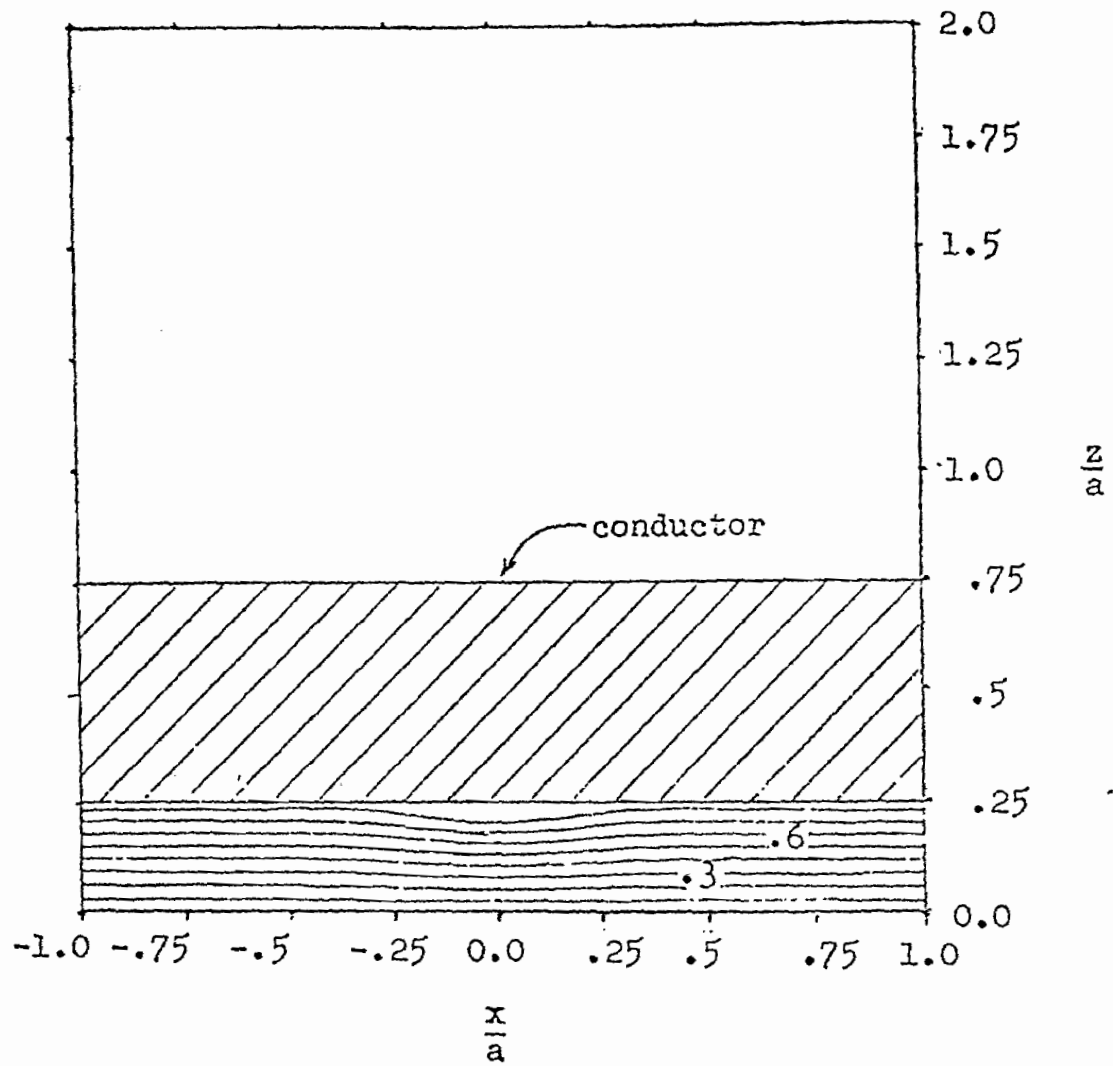


Figure IV-21a. Normalized Potential Contour Plot for $b/a = .5$, $c/a = .25$ and $z = 0$

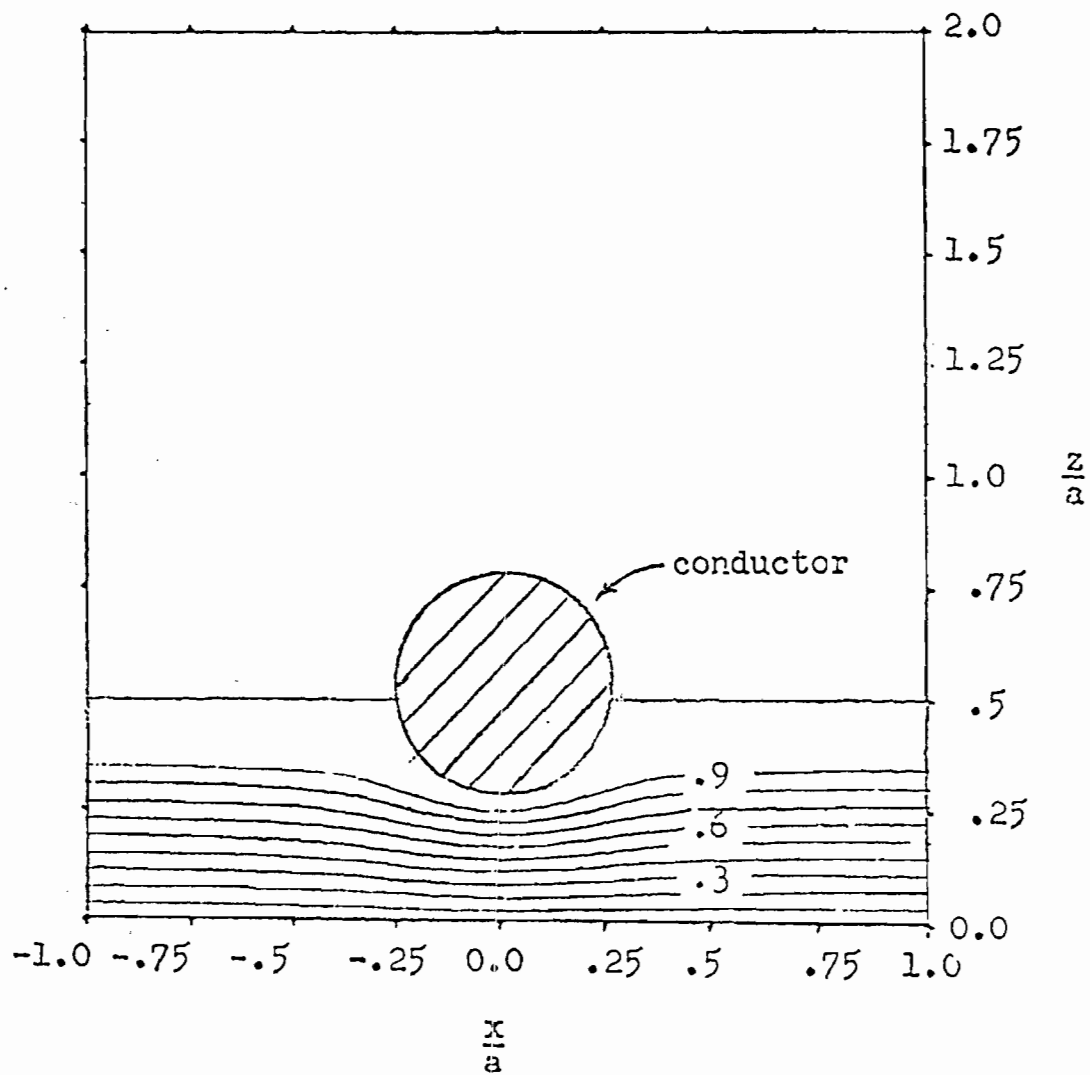


Figure IV-21b. Normalized Potential Contour Plot for $b/a = .5$, $c/a = .25$ and $z = a/4$

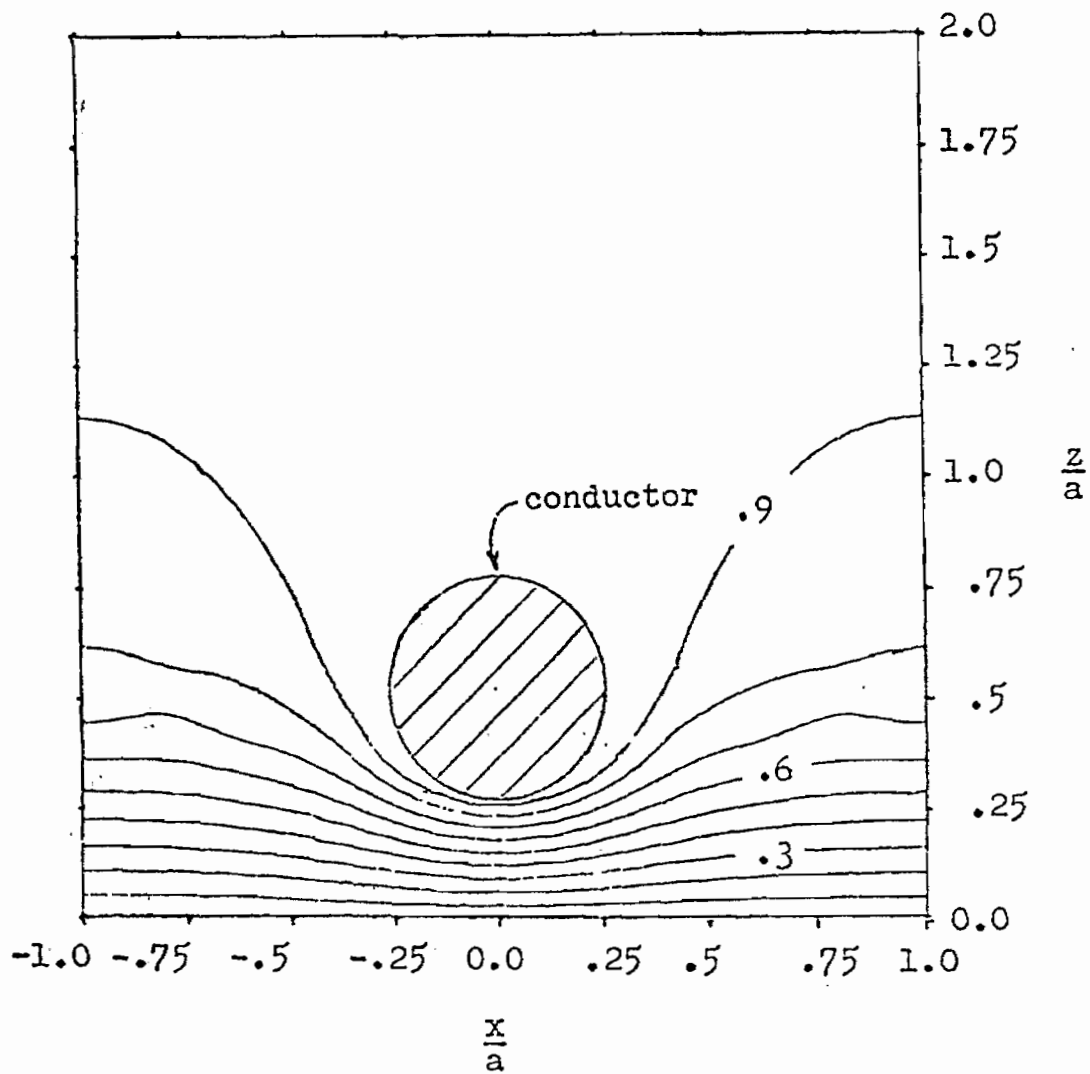


Figure IV-21c. Normalized Potential Contour Plot for $b/a = .5$, $c/a = .25$ and $z = a/2$

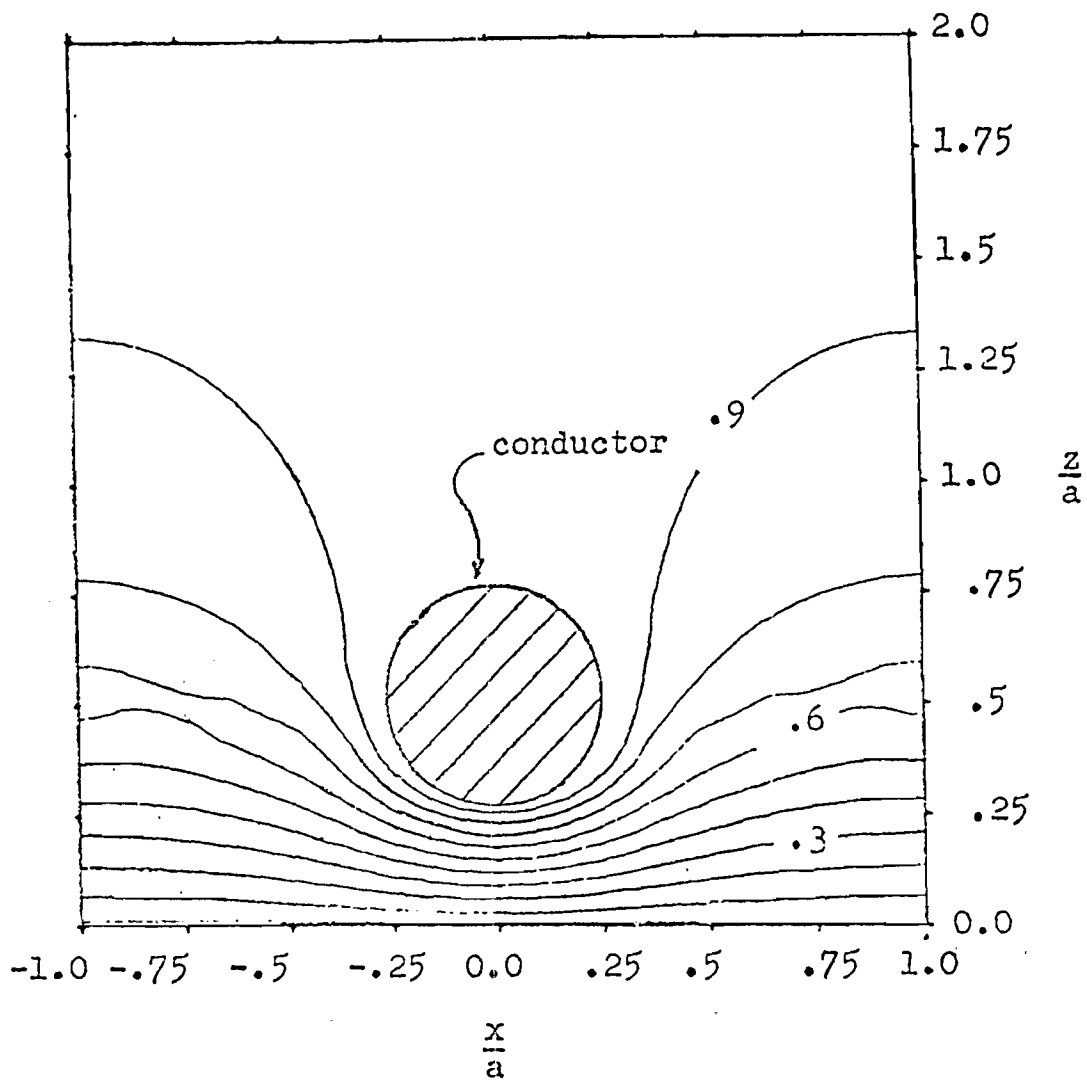


Figure IV-21d. Normalized Potential Contour Plot for $b/a = .5$, $c/a = .25$ and $z = 3a/4$

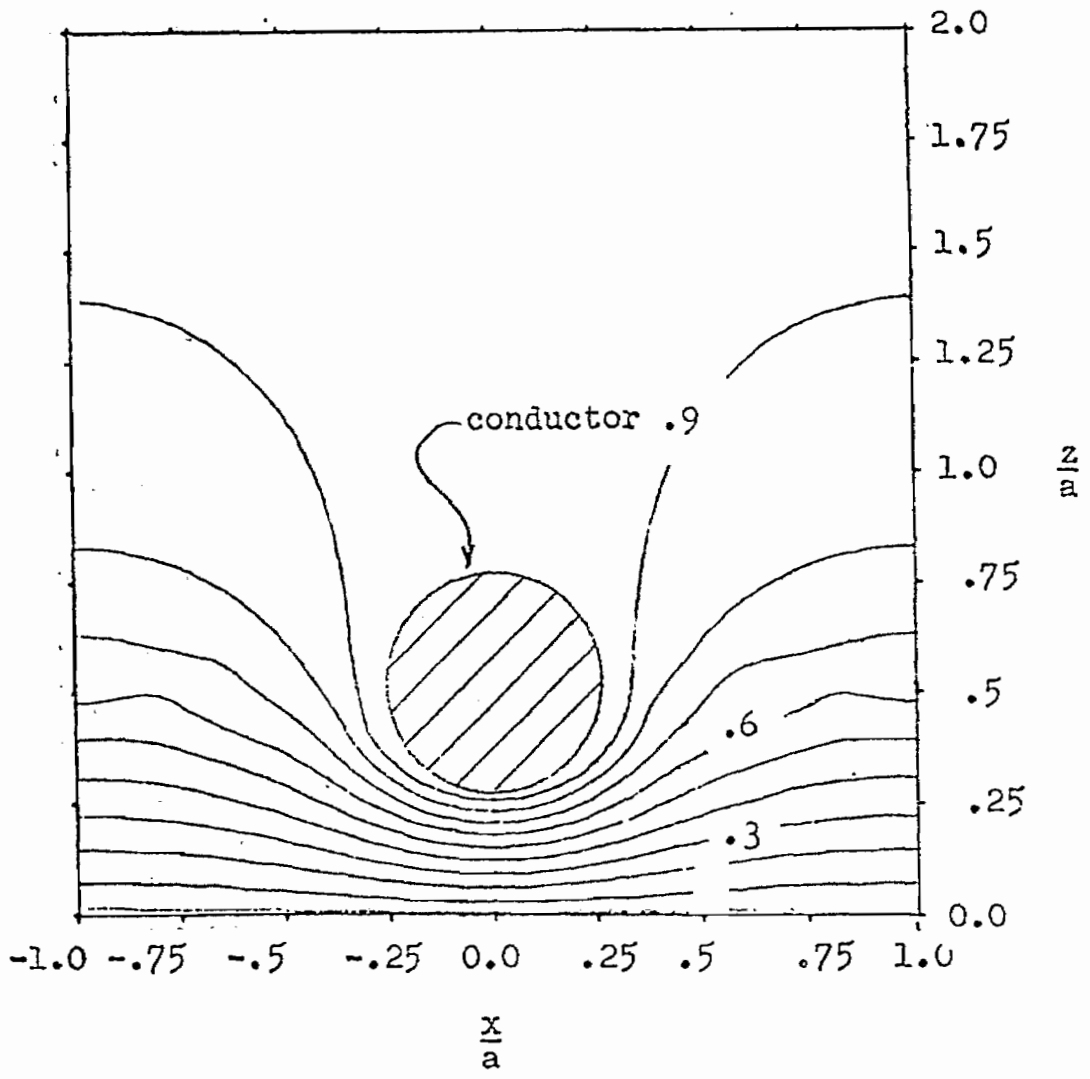


Figure IV-21e. Normalized Potential Contour Plot for $b/a = .5$, $c/a = .25$ and $z = a$

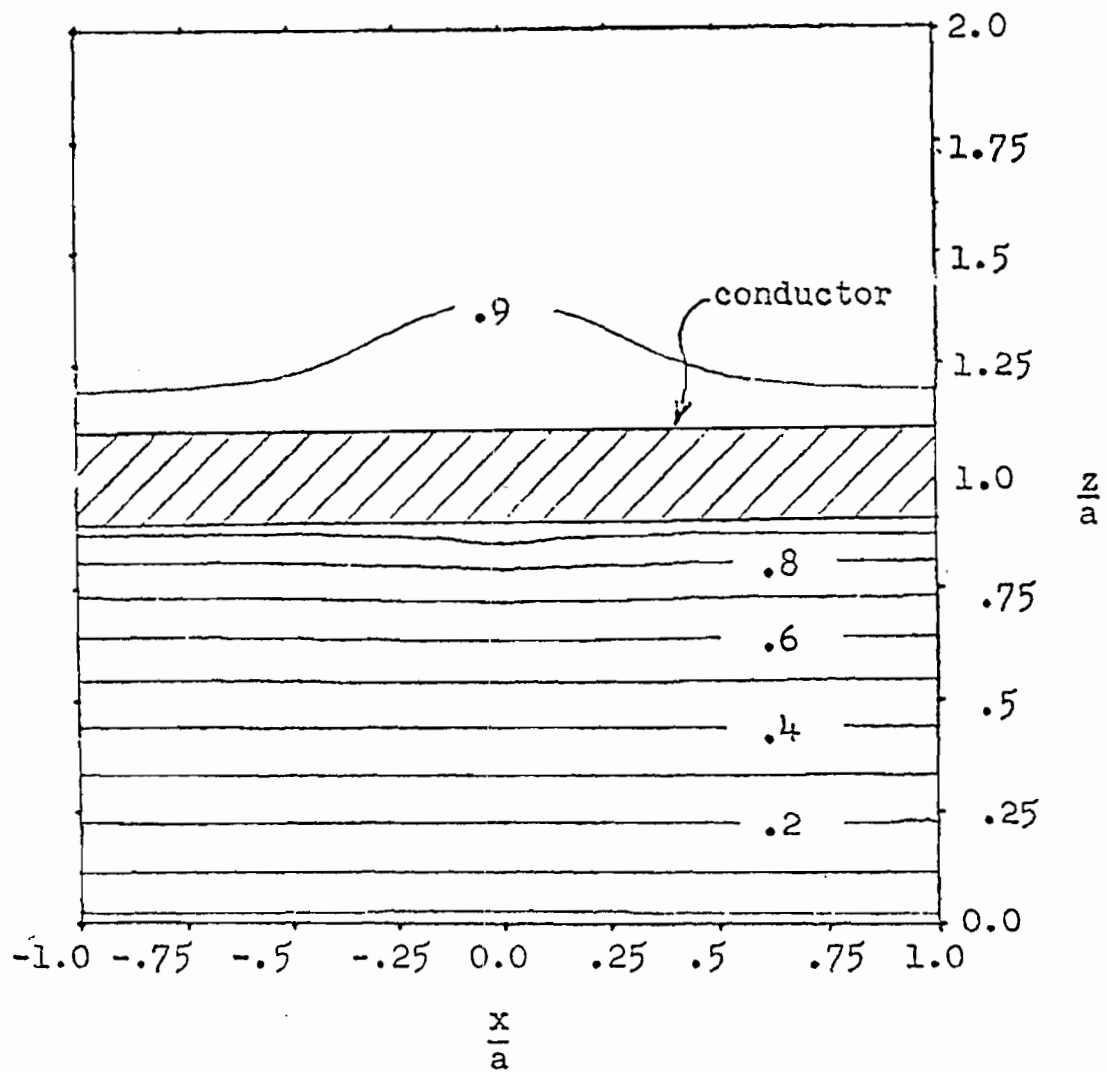


Figure IV-22a. Normalized Potential Contour Plot for $b/a = 1.0$, $c/a = .1$ and $z = 0$

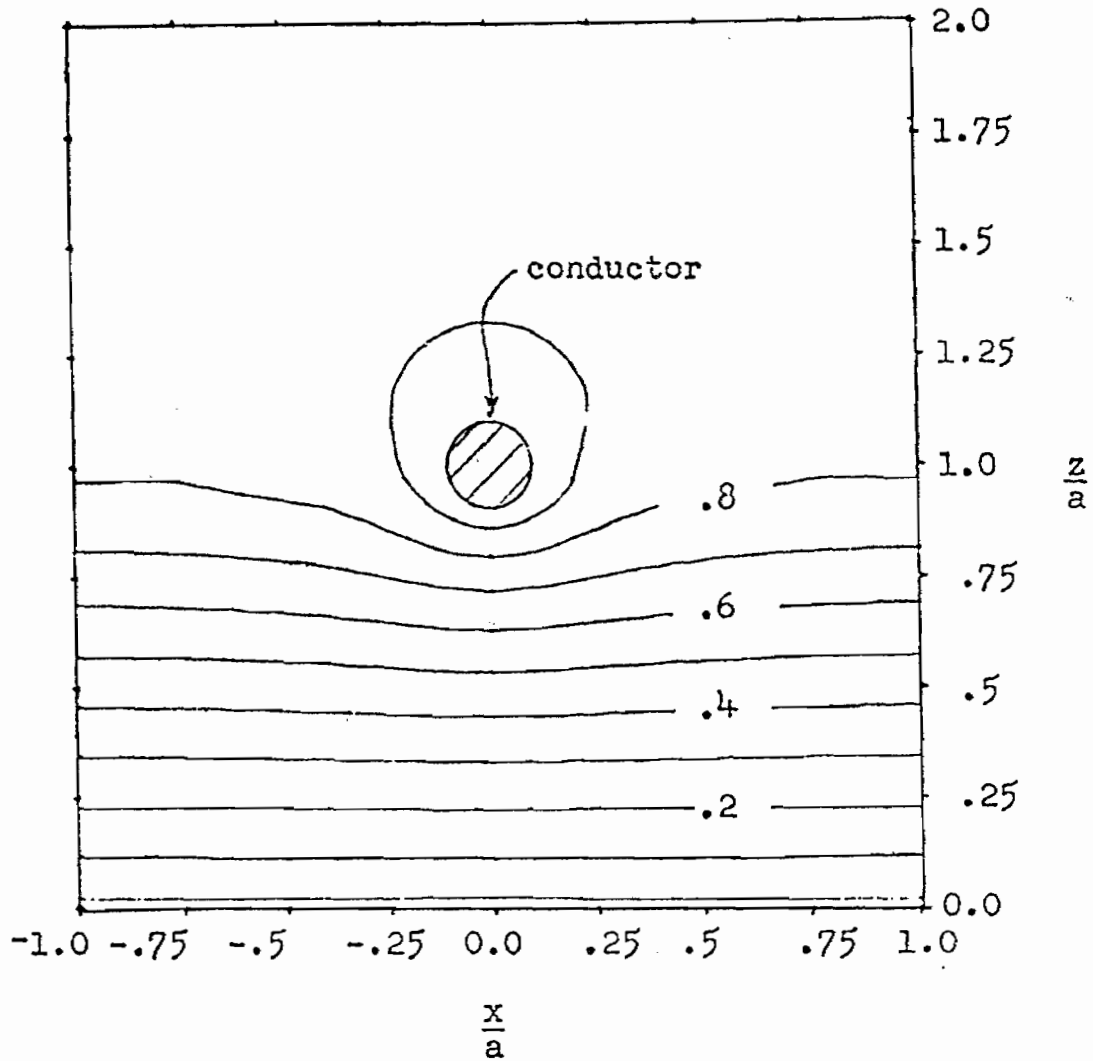


Figure IV-22b. Normalized Potential Contour Plot for $b/a = 1.0$, $c/a = .1$ and $z = a/4$

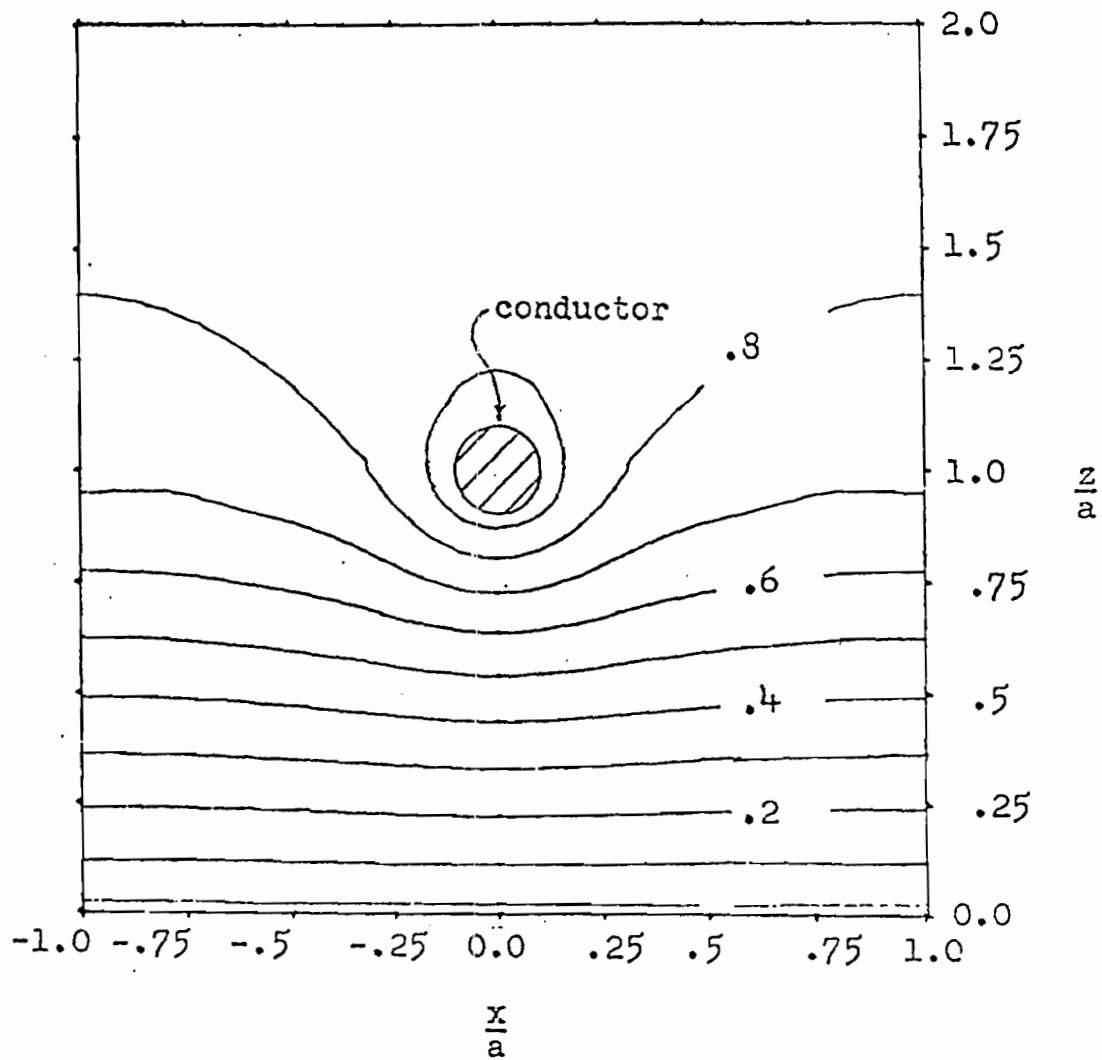


Figure IV-22c. Normalized Potential Contour Plot for $b/a = 1.0$, $c/a = .1$ and $z = a/2$

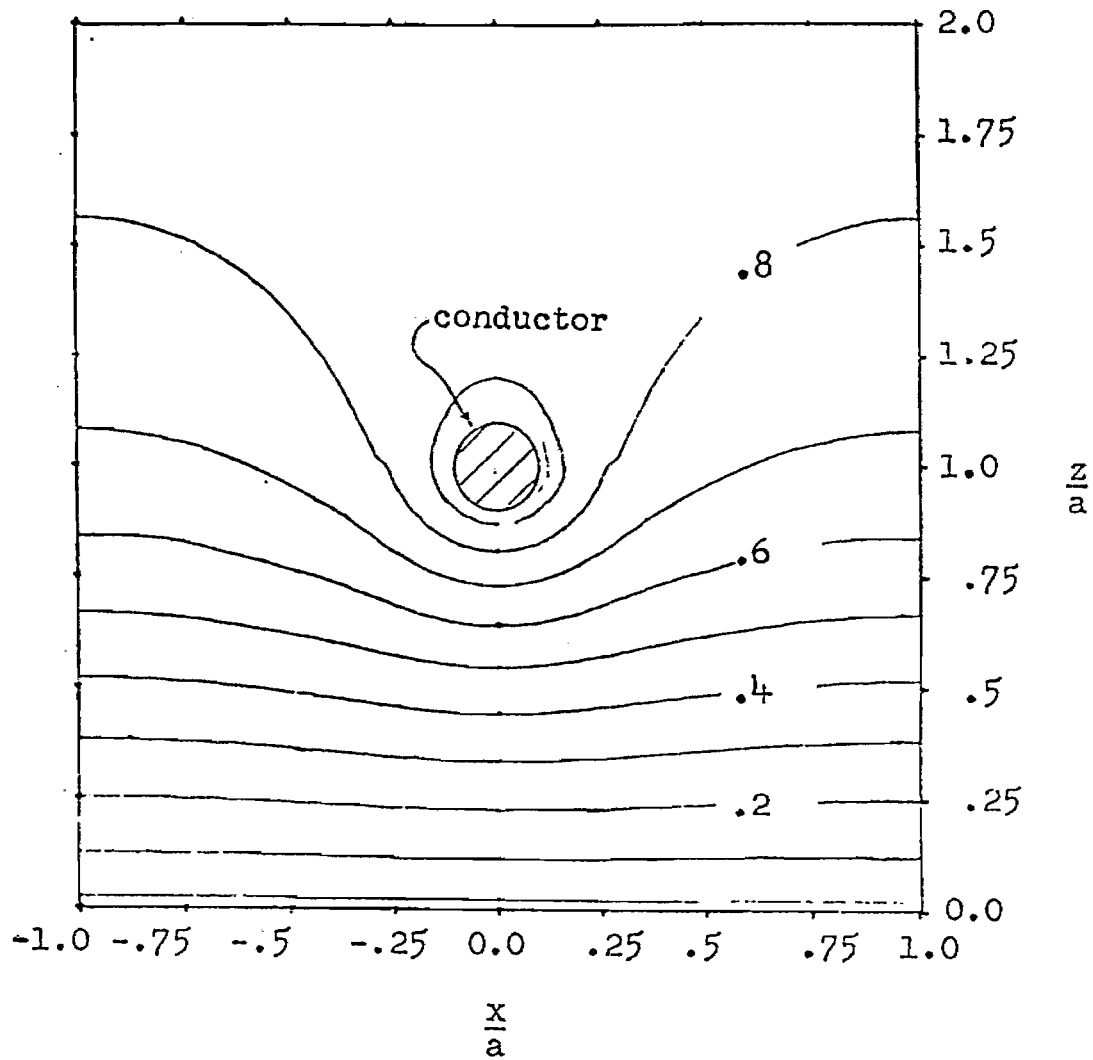


Figure IV-22d. Normalized Potential Contour Plot for $b/a = 1.0$, $c/a = .1$ and $z = 3a/4$.

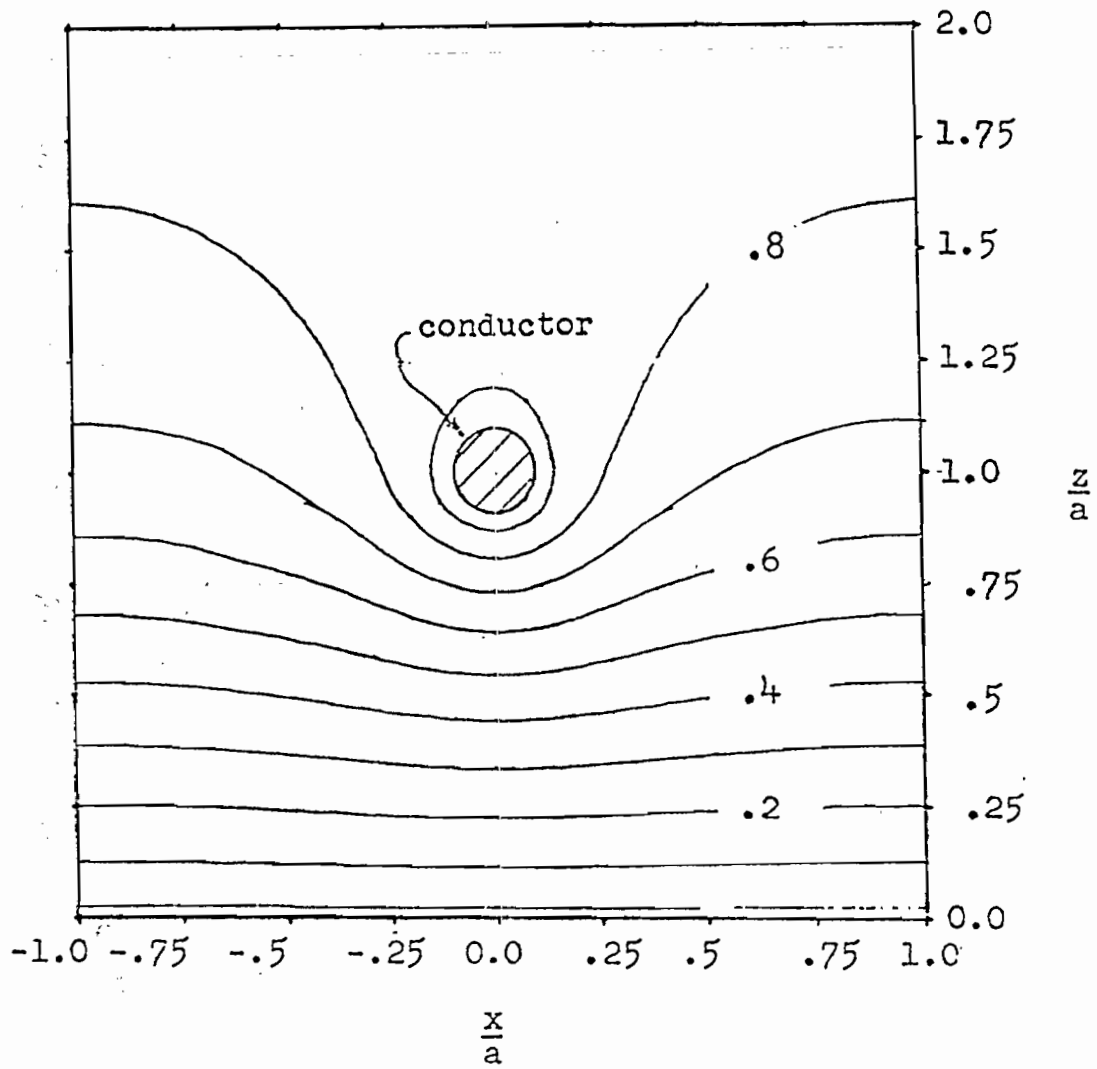


Figure IV-22e. Normalized Potential Contour Plot for $b/a = 1.0$, $c/a = .1$ and $z = a$

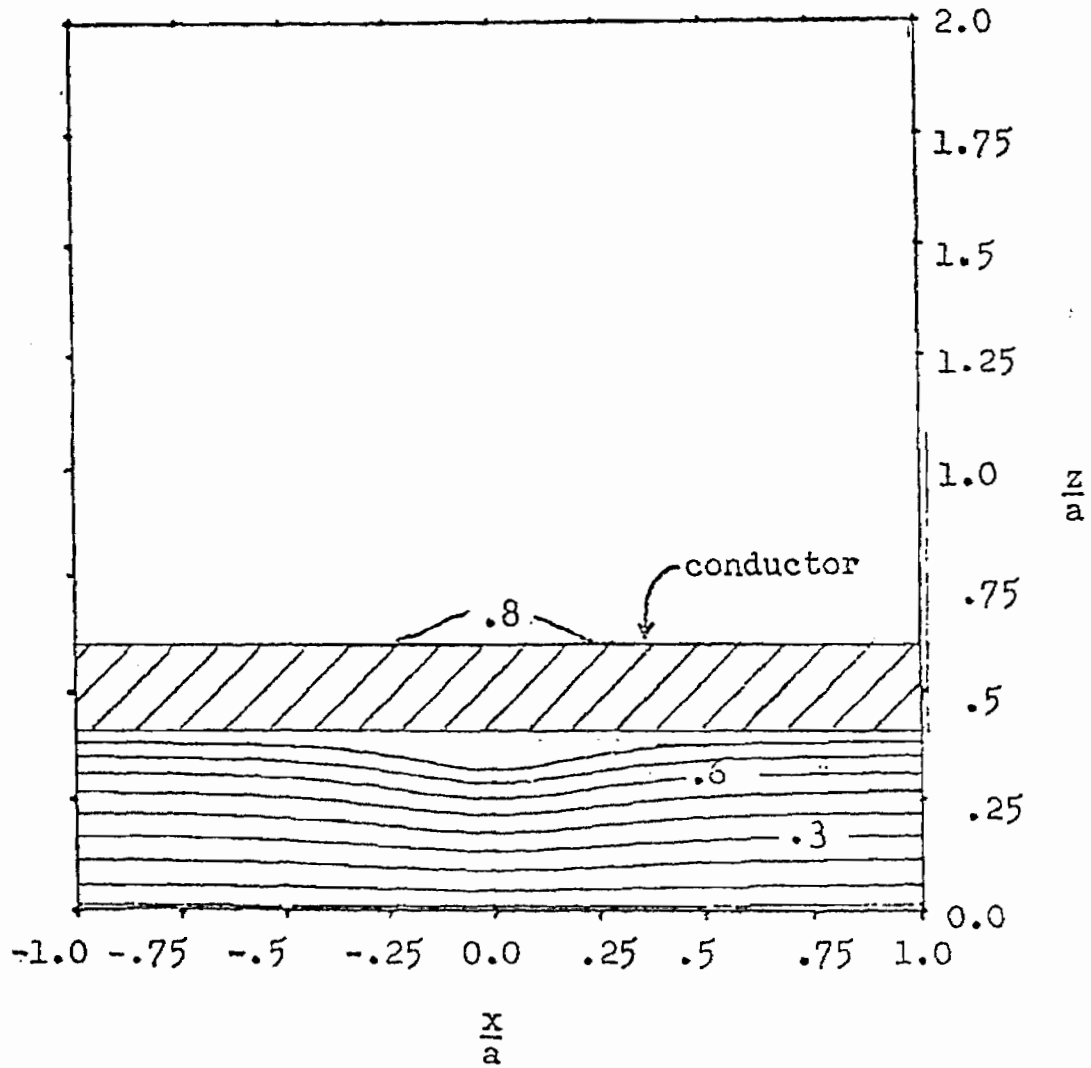


Figure IV-23a. Normalized Potential Contour Plot for $b/a = .5$, $c/a = .1$ and $z = 0$

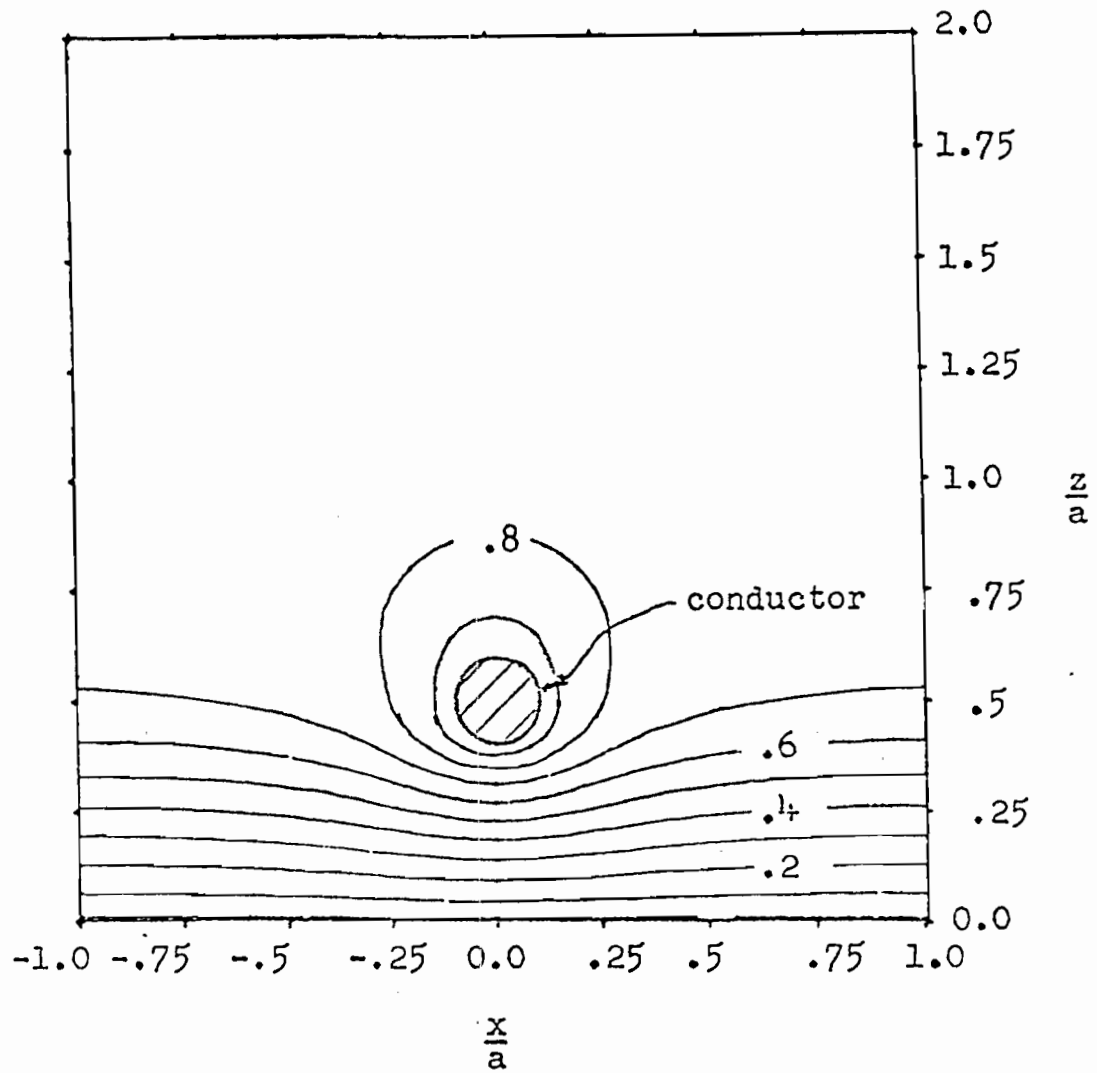


Figure IV-23b. Normalized Potential Contour Plot for $b/a = .5$, $c/a = .1$ and $z = a/4$

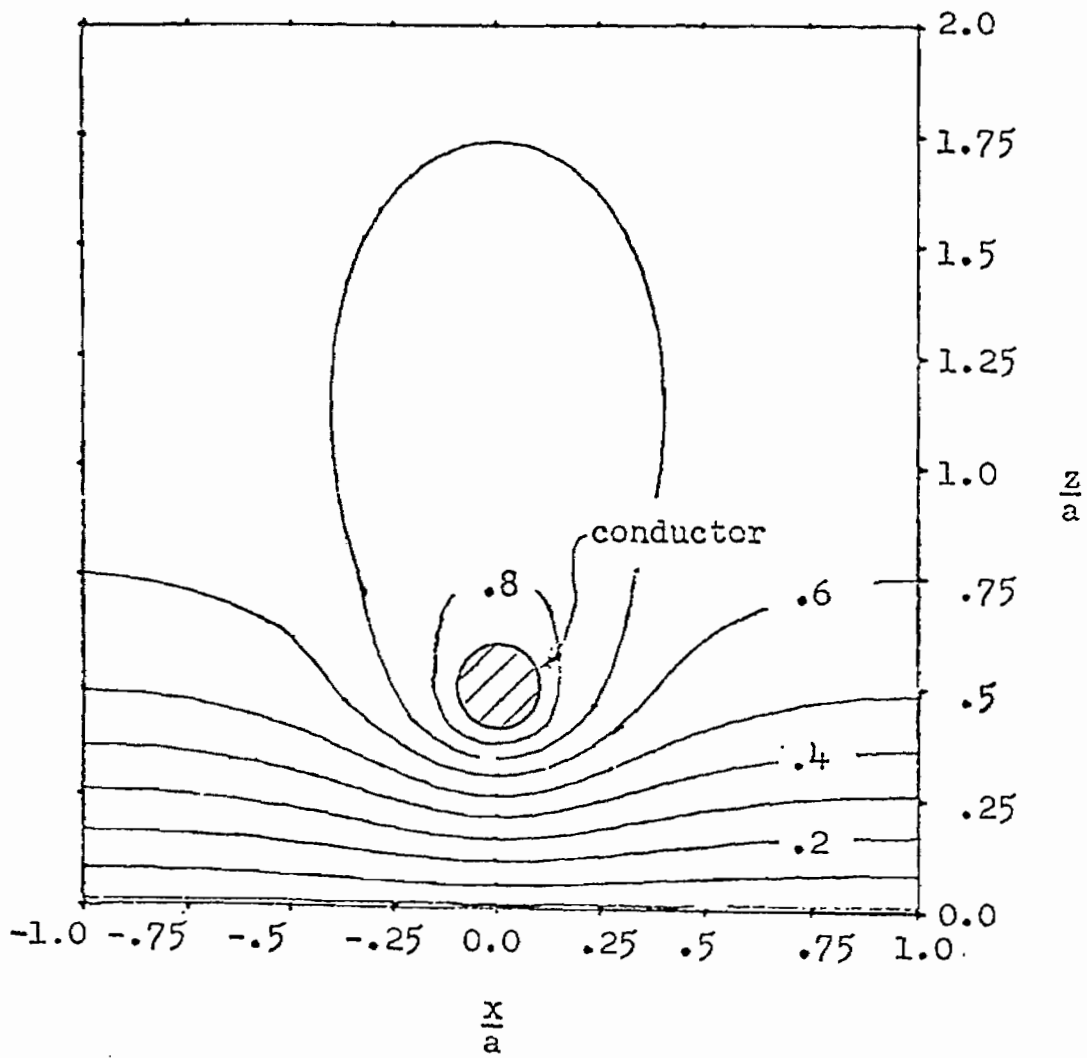


Figure IV-23c. Normalized Potential Contour Plot for $b/a = .5$, $c/a = .1$ and $z = a/2$

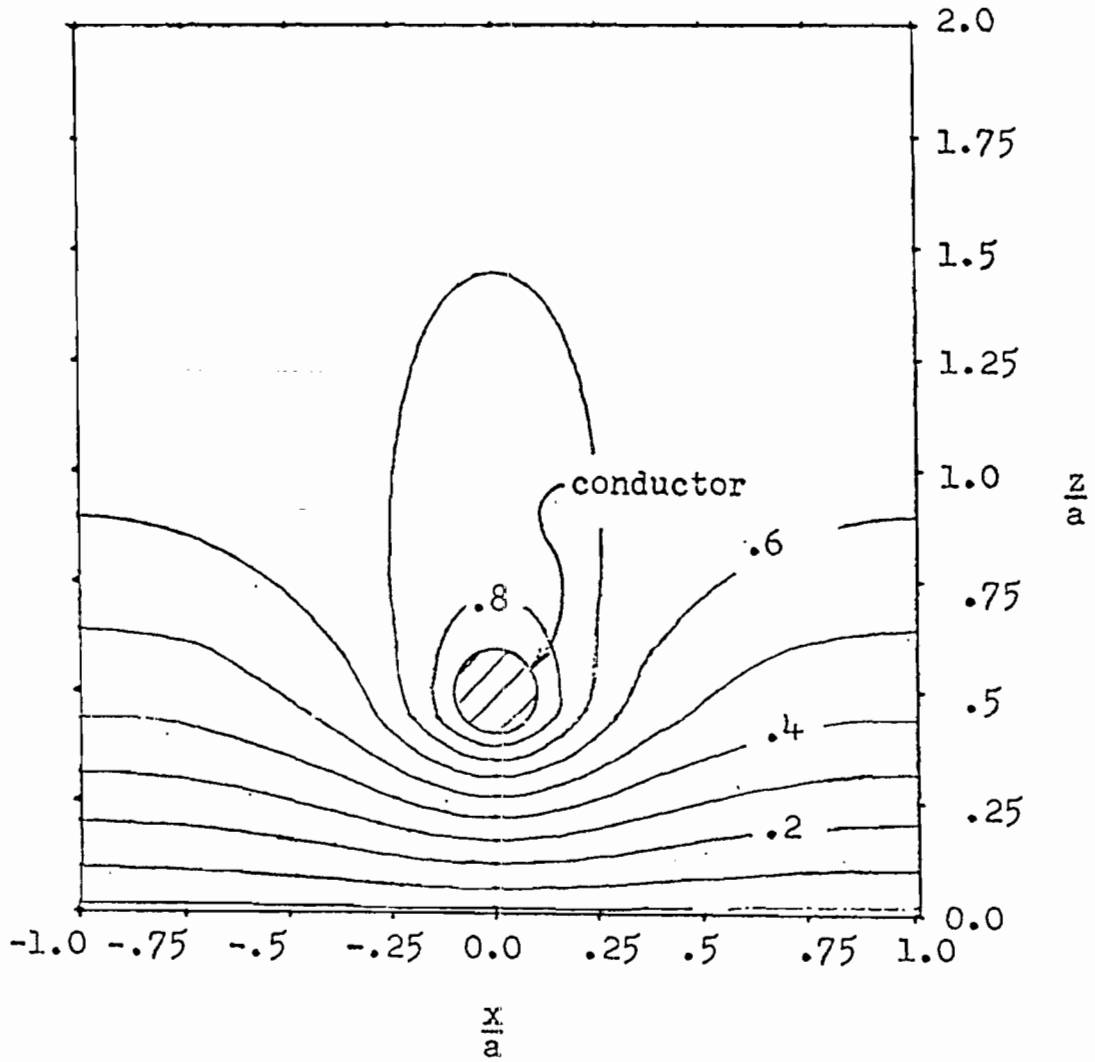


Figure IV-23d. Normalized Potential Contour Plot for $b/a = .5$, $c/a = .1$ and $z = 3a/4$

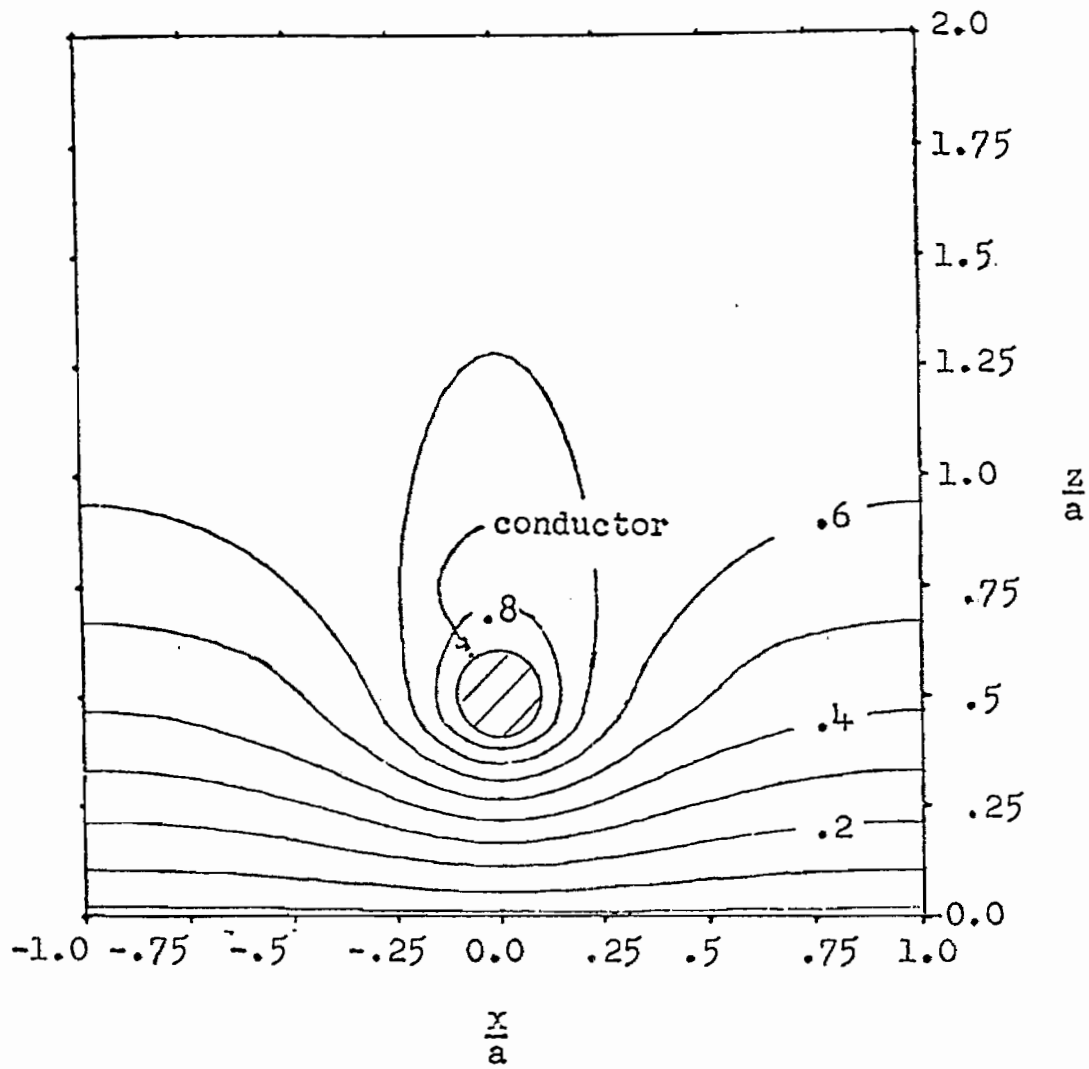


Figure IV-23e, Normalized Potential Contour Plot for $b/a = .5$, $c/a = .1$ and $z = a$

Electron trajectory calculations were performed for this case as was done for the other cases except that 25 initial positions for the electrons were used. The problems encountered due to the electrons striking the conductor are the same for this case as they are for the large radii parallel conductor case and the percentage of the electrons striking the conductors are shown. Energies of 1.1, 1.3 and 2.0 and values of β of 0 and $\pi/4$ radians were used for one spacing only but the 1.1 energy and β value of 0 radians was used for all spacings to provide comparison as was done in the parallel conducting cylinder case. The table below of V_0/V_∞ for the dimensions considered for this case is provided to determine if it is possible for an electron of a given energy to strike the conductors. V_0 is the potential of the conductors and V_∞ is the potential of $z \rightarrow \infty$.

b/a	c/a	V_0/V_∞
1.0	.25	1.039
1.0	.1	1.172
.5	.25	1.087
.5	.1	1.436

Table IV-5. V_0/V_∞ for Various Dimensions

6. High Energy Approximation

It was mentioned in Section III-3 that the approximation of Equation (103) was found to be good for high energy electrons for the line charge cases. To illustrate this, the graph of Figure IV-27 was produced.

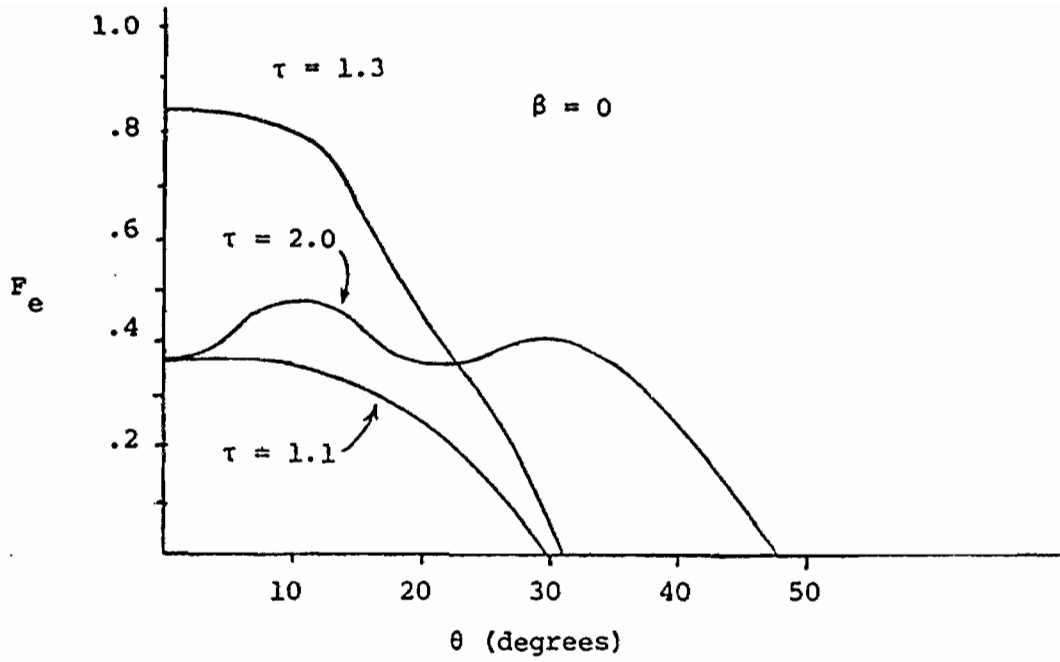


Figure IV-24a. Fraction of Electrons Escaping (F_e) for $b/a = 1.0$ and $c/a = .25$

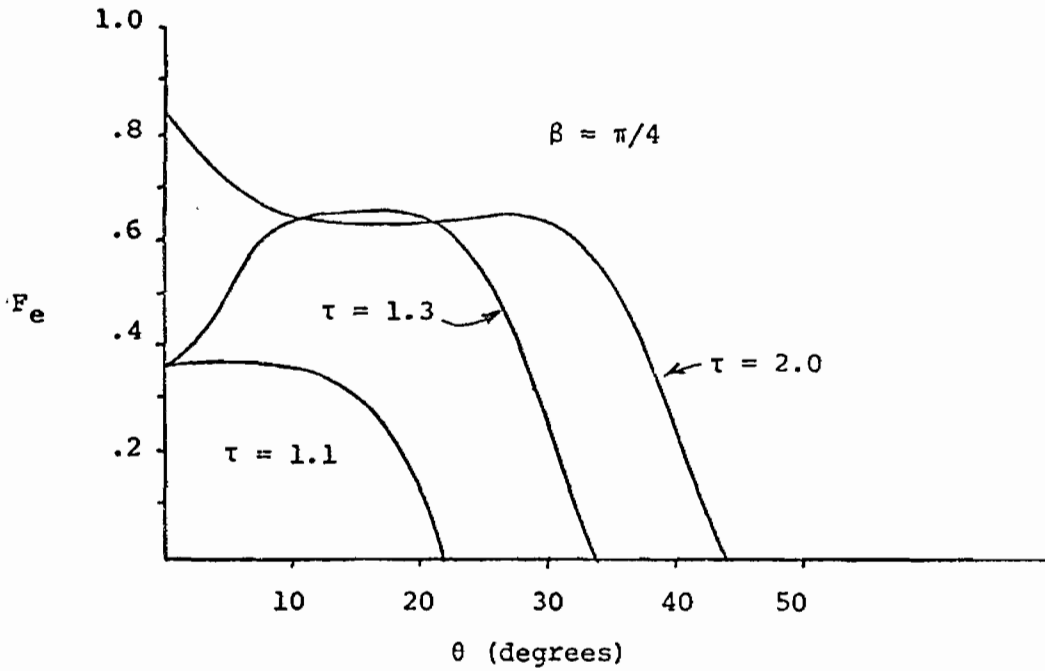


Figure IV-24b. Fraction of Electrons Escaping (F_e) for $b/a = 1.0$ and $c/a = .25$

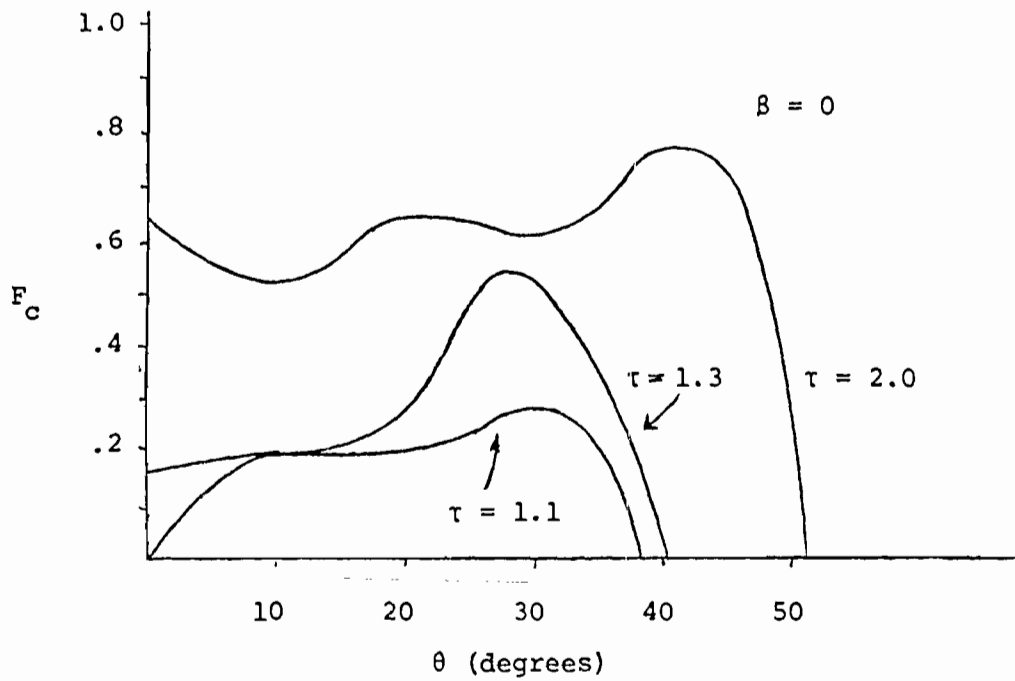


Figure IV-25a. Fraction of Electrons Striking the Conductors (F_c) for $b/a = 1.0$ and $c/a = .5$

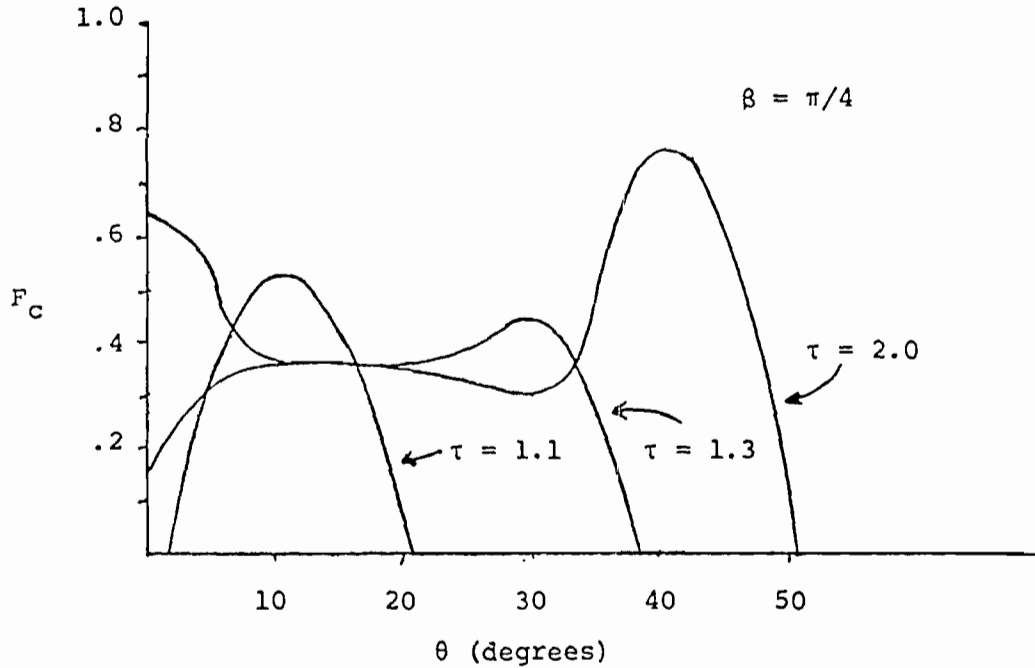


Figure IV-25b. Fraction of Electrons Striking the Conductors (F_c) for $b/a = 1.0$ and $c/a = .5$

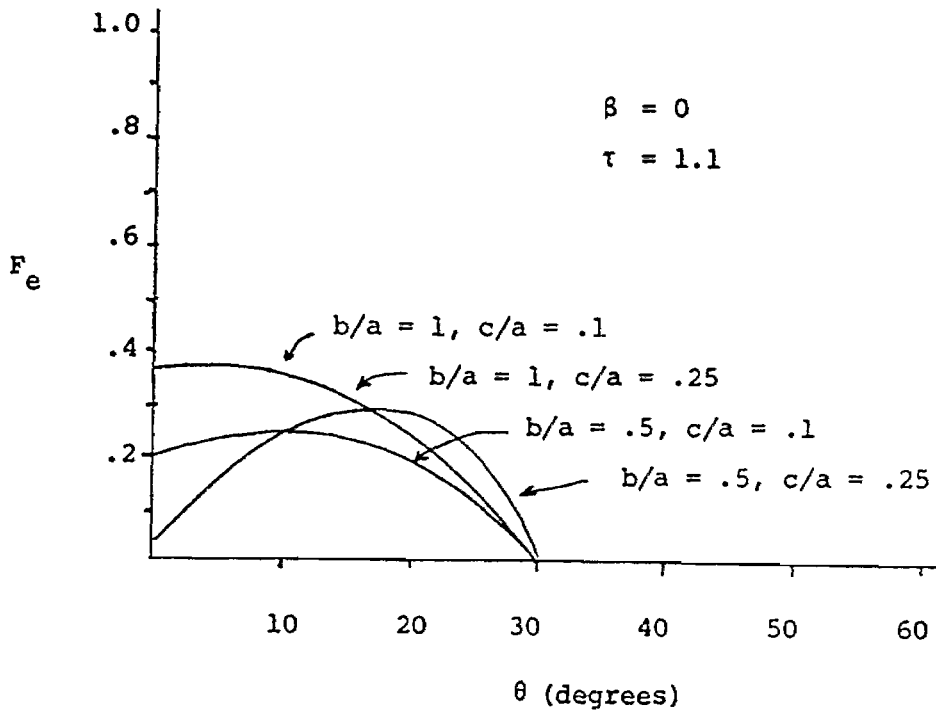


Figure IV-26a. Fraction of Electrons Escaping (F_e) for a Normalized Energy of 1.1

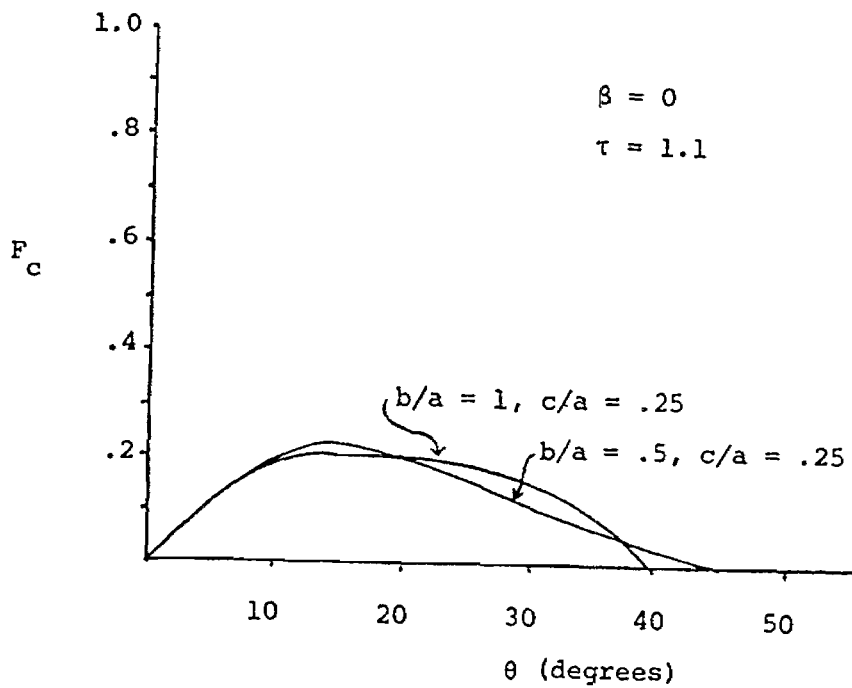


Figure IV-26b. Fraction of Electrons Striking Conductor (F_c) for a Normalized Energy of 1.1

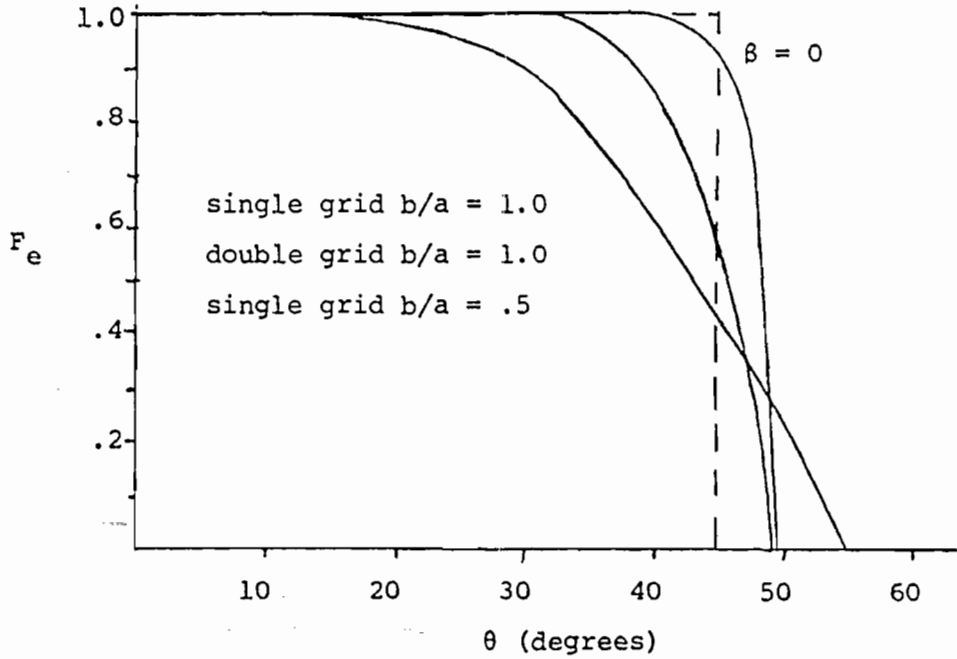


Figure IV-27. High Energy Approximation Comparison.

The dotted line represents the plot of the percentage of electrons that would escape according to Equation (103) for an energy of 2.0. The other lines are the percentage of electrons that escape from the electron trajectory data for the various line charge cases where the energy is 2.0. It can be seen that this approximation is quite good for a number of the cases and an investigation of this sort for higher energies shows that the agreement becomes better as the energy increases. It is not possible to compare this approximation to the large radii conductor cases due to the electrons that strike the conductors.

SECTION V

CONCLUSIONS AND FUTURE WORK

1. Conclusions

It has been found that the incoming radiation in an EMP simulator will produce Compton electrons on the wall of the simulator. In this paper techniques have been developed to determine the effectiveness of using a grid of wires parallel to the wall of the chamber in reducing the number of these electrons escaping to the working volume of the chamber. Several configurations have been studied and various radii of the conductors have been considered.

It is not the intention of this paper to present an exhaustive parametric study of the problem. The computer programs to do this have been written and a more complete study could be undertaken if sufficient computer time were available. In Section V-2 methods are suggested which, it is believed, would substantially reduce the time required for these calculations.

For those cases where the conductors could be approximated by line charges, the solution for the potential distribution was found in closed form. The single grid case was studied in some detail and data presented which characterizes the grids. A brief study was made of the double grid configuration but the results did not justify a more detailed investigation at this time. For each case, the normalized energies between 1.0 and about 2.0 or 3.0 were found to be the only ones for which actual calculations of the electron trajectories were required. For normalized energies greater than 2.0 or 3.0 the approximation of Equation (103) was found to be sufficiently accurate.

For cases of grids of conductors with large radii the potential

was found using the closed form line charge solution as a first approximation with a series solution added to improve the accuracy. A least squared error technique was used to match the boundary conditions. Electron trajectory calculations were performed for each of the cases.

In all cases, reducing the distance from the ground plane to the conductors resulted in a decrease in the number of electrons escaping for a given energy. As the conductors approach the ground plane their potential must increase in order to maintain the same potential at infinity. Thus, the electrons approaching close to the conductor encounter a higher potential gradient and are more likely to be repelled the closer the conductors are to the ground plane.

Significant differences are noted between the line charge cases and the corresponding large radii cases, especially when the comparison is made to the crossed conductor cases. The rather large radii of the conductor for which the most data was obtained makes these differences particularly apparent. More data was produced for this case to demonstrate the effects and problems which are encountered when using large radii conductors.

It is believed that the data presented in this paper provides insight into the features of the various configurations and shows the comparative effectiveness of the grids. As other design considerations arise, one may wish to more thoroughly investigate a particular case. The programs in Appendix B provide this capability and may be modified to include such effects as secondary Compton electrons produced on the grids, etc.

2. Future Work

It would be advisable to pursue a more detailed study of the problem

than was possible in this paper. To do this we suggest the following method for reducing the time necessary for the electron trajectory calculations. The programs as they are presently constituted recalculate the gradient of the potential for each iteration from the expression for the potential. It would appear to be faster to produce a table from which the gradient of the potential could be found by a "look up" procedure and a few algebraic manipulations. Since the series solutions are of the form of the product of functions each of which is a function of only one coordinate variable, this may be easily accomplished. A table could be made of the value of these functions in the x , y , and z directions and the potential at any point found by "looking up" the appropriate values and multiplying to find the potential. The gradient could be found in a similar manner. A similar table would reduce the time needed to calculate the line charge portion of the gradient. The symmetry of the problem helps to reduce the amount of storage necessary for this procedure.

The symmetry of the problem also could be used to reduce the number of electron trajectories it is necessary to calculate. For the $\beta = 0$ case, only those initial positions on the ground plane for which $0 \leq y \leq a$ need to be considered and for the $\beta = \pi/4$ case only those positions lying on and to one side of the line $x = y$ need be considered.

As mentioned previously, a further investigation into the effects of the electrons striking the wires and the effects of radiation incident on the wires should be undertaken.

REFERENCES

1. Baum, Carl E., "A Technique for Simulating the System Generated Electromagnetic Pulse Resulting from an Exoatmospheric Nuclear Weapon Radiation Environment," Sensor and Simulation Note 156, 18 September 1972.
2. Lapp, R. E., and Andrews, H. L., Nuclear Radiation Physics (4th ed.), Prentice-Hall, Inc., New Jersey, 1972, pp. 233-44.
3. Maxwell, James Clerk, A Treatise on Electricity and Magnetism (3rd ed.), Dover Publications, Inc., 1954, pp. 310-16.
4. Tesche, F. M., "Study of a Charged Wire Grid for Reducing Electron Backscatter in EMP Satellite Simulators," Sensor and Simulation Note 164, December 1972.
5. Marin, Lennart, "Effect of Replacing One Conducting Plate of a Parallel-Plate Transmission Line by a Grid of Rods," Sensor and Simulation Note 118, October 1970.
6. Chaffee, E. L., Theory of Thermionic Vacuum Tubes, McGraw-Hill Book Company, Inc., New York, New York, 1933.
7. Paszkowski, B., Electron Optics, American Elsevier Publishing Co., Inc., New York, New York, 1968.
8. Miller, E. K., Bevenssee, R. M., Poggio, A. J., Adams, R., Deadrick, F. J., and Landt, J. A., "An Evaluation for the Electromagnetic Analysis of Thin Wire Structures," Note 177, Interaction Notes, Lawrence Livermore Laboratory, March 1974.
9. Jonker, J. L. H., "Electron Trajectories in Multigrid Valves," Phillips Technical Review, Vol. 5, No. 5, May 1940, pp. 131-40.
10. Hashimoto, M., Kita, S., and Fujisawa, K., "The Mapping Theorem of Two Dimensional Electron Beam Trajectories," IEEE Transactions on Electron Devices, Vol. ED-20, No. 1, January 1973, pp. 60-62.
11. C. R. C. Standard Mathematical Tables (12th ed.), Chemical Rubber Publishing Co., Cleveland, Ohio, 1961.
12. Kraus, John D., Electromagnetics, McGraw-Hill Book Company, Inc., New York, New York, 1953.
13. Van Bladel, J., Electromagnetic Fields, McGraw-Hill Book Company, New York, New York, 1964.
14. Kelly, L. G., Handbook of Numerical Methods and Applications, Addison-Wesley Publishing Co., Reading, Massachusetts, 1967.
15. Dellin, T. A., and MacCallum, C. J., A Handbook of Photo-Compton Current Data, SCL-RR-720086, December 1972.
16. Longmire, C. L., "Direct Interaction Effects in EMP," Interaction Note 69, January 1971.

APPENDIX A

SERIES COEFFICIENTS

1. General

In this appendix are presented the series coefficients found in solving the potential distribution problem of the parallel and crossed cylindrical conductors cases. The forms of the equations used were modified by constant multipliers of the coefficients for ease of comparison. The form of the solution and the grid of points used for the fitting of the solutions are shown for each geometry. The coefficients are then tabulated. Unless otherwise specified, all solutions for which data is presented used 15 terms of the solution in each region.

2. Parallel Cylindrical Conductor Case

The form of the solutions used is

$$\phi_I(x,z) = \sum_{n=1}^N A_n \sinh(n\pi z/a) \cos(n\pi x/a) / \cosh(n\pi b/a) + A_0 z/b + (\text{pic}) \phi_{LC}(x,z) \quad (\text{A.1})$$

in region I and

$$\phi_{II}(x,z) = \sum_{n=0}^N B_n e^{\frac{-n\pi}{a}(z-b)} \cos(n\pi x/a) + (\text{pic}) \phi_{LC}(x,z) \quad (\text{A.2})$$

in region II, where $\phi_{LC}(x,z)$ is the line charge solution with leading constants omitted and is given by

$$\phi_{LC}(x,z) = \ln \frac{\cosh(\pi(z+b)/a) - \cos(\pi z/a)}{\cosh(\pi(z-b)/a) - \cos(\pi x/a)} \quad (\text{A.3})$$

The term pic is a constant adjusted to insure that the potential given by the line charge portion of the solution alone is 1.0 on the surface of the conductor at $x = c$. For this geometry the points used for the

matching of the boundary conditions were located on both the upper and lower surfaces of the conductor at $x < c(n-1)/20$, $n = 1, 2, \dots, 20$ and at $z < b$ between the conductors at $x = c + (a-c)(n-1)/20$, $n = 1, 2, \dots, 20$. The coefficients obtained for this case are shown in the following tables.

n	A_n	B_n
0	4.9658×10^{-2}	-4.1433×10^{-2}
1	.1124	-6.9864×10^{-2}
2	.1093	-7.2966×10^{-2}
3	.1097	-7.0768×10^{-2}
4	.1087	-6.6765×10^{-2}
5	.1040	-6.1244×10^{-2}
6	9.5263×10^{-2}	-5.4364×10^{-2}
7	8.2513×10^{-2}	-4.6168×10^{-2}
8	6.7190×10^{-2}	-3.7254×10^{-2}
9	5.0801×10^{-2}	-2.8161×10^{-2}
10	3.5376×10^{-2}	-1.9782×10^{-2}
11	2.2178×10^{-2}	-1.2608×10^{-2}
12	1.2272×10^{-2}	-7.1722×10^{-3}
13	5.5920×10^{-3}	-3.3997×10^{-3}
14	1.9014×10^{-3}	-1.2390×10^{-3}
pic = .1468		
Mean Squared Error = 1.064×10^{-5}		

Table A-1. Series Coefficients for $b/a = 1$ and $c/a = .25$.

n	A_n	B_n
0	5.1258×10^{-3}	-6.5851×10^{-3}
1	1.3061×10^{-2}	-9.7048×10^{-3}
2	1.2349×10^{-2}	-1.0518×10^{-2}
3	1.1540×10^{-2}	-1.0292×10^{-2}
4	1.1236×10^{-2}	-1.0259×10^{-2}
5	1.0367×10^{-2}	-9.5966×10^{-3}
6	9.833×10^{-3}	-9.2347×10^{-3}
7	8.8173×10^{-3}	-8.2912×10^{-3}
8	8.1487×10^{-3}	-7.7003×10^{-3}
9	6.9365×10^{-3}	-6.5783×10^{-3}
10	6.1690×10^{-3}	-5.8681×10^{-3}
11	4.9148×10^{-3}	-4.6860×10^{-3}
12	4.1624×10^{-3}	-3.9772×10^{-3}
13	2.9810×10^{-3}	-2.8539×10^{-3}
14	2.3538×10^{-3}	-2.2581×10^{-3}
pic = .1168		
Mean Squared Error = 7.480×10^{-5}		

Table A-2. Series Coefficients for $b/a = 1$ and $c/a = .1$.

n	A_n	B_n
0	.1203	-8.7278×10^{-2}
1	.2923	- .1248
2	.2868	- .1354
3	.2895	- .1356
4	.2896	- .1316
5	.2796	- .1248
6	.2578	- .1150
7	.2243	- .1015
8	.1833	-8.5127×10^{-2}
9	.1390	-6.6776×10^{-2}
10	9.7053×10^{-2}	-4.8622×10^{-2}
11	6.1043×10^{-2}	-3.2052×10^{-2}
12	3.3950×10^{-2}	-1.8861×10^{-2}
13	1.5586×10^{-2}	-9.2421×10^{-3}
14	5.3807×10^{-3}	-3.5041×10^{-3}
pic = .2767		
Mean Squared Error = 1.558×10^{-5}		

Table A-3. Series Coefficients for $b/a = .5$ and $c/a = .25$.

n	A_n	B_n
0	8.3083×10^{-3}	-1.2195×10^{-2}
1	2.4198×10^{-2}	-1.5803×10^{-2}
2	2.2805×10^{-2}	-1.7383×10^{-2}
3	2.1002×10^{-2}	-1.7381×10^{-2}
4	2.0258×10^{-2}	-1.7519×10^{-2}
5	1.8596×10^{-2}	-1.6503×10^{-2}
6	1.7653×10^{-2}	-1.5977×10^{-2}
7	1.5713×10^{-2}	-1.4369×10^{-2}
8	1.4484×10^{-2}	-1.3372×10^{-2}
9	1.2317×10^{-2}	-1.1451×10^{-2}
10	1.0933×10^{-2}	-1.0225×10^{-2}
11	8.7026×10^{-3}	-8.1817×10^{-3}
12	7.3616×10^{-3}	-6.9463×10^{-3}
13	5.2748×10^{-3}	-4.9956×10^{-3}
14	4.1563×10^{-3}	-3.9510×10^{-3}
pic = .1867		
Mean Squared Error = 2.465×10^{-5}		

Table A-4. Series Coefficients for $b/a = .5$ and $c/a = .1$.

3. Crossed Cylindrical Conductors Case

The forms of the solution used are

$$\begin{aligned} \phi_I(x,y,z) = & \sum_{n=0}^N \sum_{m=n}^N \{A_{n,m} [\cos(n\pi x/a) \cos(m\pi y/a) + \cos(m\pi x/a) \\ & \cos(n\pi y/a)] \sinh(\gamma_{n,m} z) / 2 \sinh(\gamma_{n,m} b)\} + A_{\infty} z/b \\ & + (\text{pic}) \phi_{LC}(x,y,z) \end{aligned} \quad (\text{A.4})$$

in region I and

$$\begin{aligned} \phi_{II}(x,y,z) = & \sum_{n=0}^N \sum_{m=n}^N \{B_{n,m} (.5) [\cos(n\pi x/a) \cos(m\pi y/a) \\ & + \cos(m\pi x/a) \cos(n\pi y/a)]\} e^{-\gamma_{n,m}(z-b)} + (\text{pic}) \phi_{LC}(x,y,z) \end{aligned} \quad (\text{A.5})$$

in region II where $\gamma_{n,m} = \sqrt{n^2 + m^2} \left(\frac{\pi}{a}\right)$ and $\phi_{LC}(x,y,z)$ is the line charge solution for a single crossed grid with the leading coefficients omitted and is given by

$$\begin{aligned} \phi_{LC}(x,y,z) = & \ln \frac{\cosh(\pi(z+b)/a) - \cos(\pi x/a)}{\cosh(\pi(z-b)/a) - \cos(\pi x/a)} \\ & + \ln \frac{\cosh(\pi(z+b)) - \cos(\pi y/a)}{\cosh(\pi(z-b)) - \cos(\pi y/a)} \end{aligned} \quad (\text{A.6})$$

The term pic is a constant whose value is adjusted to insure that the potential given by the line charge portion of the solution is 1.0 at $x = a$ and $y = c$ on the conductors. For this geometry the points used for the matching of the boundary conditions were located at $x = c(n-1)/8$ and $x = c + (a-c)n/9$ for $n = 1, 2, \dots, 9$ and at $y = c(m-1)/8$ and $y = c + (a-c)m/9$ for $m = 1, 2, \dots, 9$. If the x and y coordinates of a point corresponded to those of the conductors, points used were on the upper and lower surfaces of the conductor. If the x and y coordinates of a point corresponded to the aperture between conductors,

the point for the matching of the boundary conditions was located at $z = b$. Only those points for which $x \geq y$ were used. The coefficients obtained for this case are shown in the following tables.

n,m	$A_{n,m}$	$B_{n,m}$
00	4.0074×10^{-2}	- .1104
01	4.0260×10^{-2}	- .1997
02	.1052	- .1260
03	.1064	- .1101
04	6.272×10^{-2}	-7.1596×10^{-2}
11	- .1722	-7.8816×10^{-2}
12	- .1461	-4.8780×10^{-2}
13	-4.5895×10^{-2}	-5.2738×10^{-2}
14	-2.0106×10^{-2}	-3.9059×10^{-2}
22	-2.7186×10^{-2}	-1.1611×10^{-2}
23	5.7667×10^{-3}	-4.4008×10^{-2}
24	2.5202×10^{-3}	-3.2261×10^{-2}
33	1.5504×10^{-2}	-2.5466×10^{-2}
34	1.7077×10^{-2}	-3.4254×10^{-2}
44	5.1119×10^{-3}	-1.1367×10^{-2}
pic = 8.5354×10^{-2}		
Mean Squared Error = 6.275×10^{-4}		

Table A-5. Series Coefficients for $b/a = 1$ and $c/a = .25$.

n,m	$A_{n,m}$	$B_{n,m}$
0,0	-7.4821×10^{-2}	$-.1020$
0,1	-3.913×10^{-2}	-6.8826×10^{-2}
0,2	3.6006×10^{-3}	-2.3307×10^{-2}
0,3	8.7687×10^{-3}	-1.8746×10^{-2}
0,4	5.9525×10^{-4}	-1.4771×10^{-2}
1,1	-4.7650×10^{-2}	-4.2002×10^{-2}
1,2	-3.3415×10^{-2}	-2.5861×10^{-2}
1,3	-1.7365×10^{-2}	-1.4637×10^{-2}
1,4	-1.2492×10^{-2}	-1.1782×10^{-2}
2,2	-7.2520×10^{-3}	-3.8021×10^{-3}
2,3	-6.0480×10^{-3}	-5.8940×10^{-3}
2,4	-5.0636×10^{-3}	-6.0690×10^{-3}
3,3	-1.6965×10^{-3}	-9.3250×10^{-4}
3,4	-2.6606×10^{-3}	-2.6163×10^{-3}
4,4	-1.3321×10^{-3}	-3.0276×10^{-4}
pic = 7.6011×10^{-2}		
Mean Squared Error = 2.542×10^{-3}		

Table A-6. Series Coefficients for $b/a = 1$ and $c/a = .1$.

n,m	$A_{n,m}$	$B_{n,m}$
0,0	.1154	- .2314
0,1	.1755	- .4097
0,2	.2782	- .2726
0,3	.2662	- .2450
0,4	.1599	- .1639
1,1	- .3252	- .1526
1,2	- .2639	-9.2444×10^{-2}
1,3	-5.4500×10^{-2}	- .1117
1,4	-9.6815×10^{-3}	-9.0271×10^{-2}
2,2	-4.2613×10^{-2}	-2.2307×10^{-2}
2,3	4.2115×10^{-2}	-9.6293×10^{-2}
2,4	2.8580×10^{-2}	-7.4525×10^{-2}
3,3	4.6487×10^{-2}	4.2115×10^{-2}
3,4	$5,6085 \times 10^{-2}$	-7.9811×10^{-2}
4,4	1.8237×10^{-2}	-2.7425×10^{-2}
pic = .1833		
Mean Squared Error = 4.089×10^{-3}		

Table A-7. Series Coefficients for $b/a = .5$ and $c/a = .25$.

n,m	$A_{n,m}$	$B_{n,m}$
0,0	- .1051	- .1741
0,1	-6.5391×10^{-2}	- .1336
0,2	-1.9930×10^{-3}	-3.9764×10^{-2}
0,3	1.1666×10^{-2}	-3.3880×10^{-2}
0,4	7.4902×10^{-3}	-2.4173×10^{-2}
1,1	-7.7180×10^{-2}	-7.1494×10^{-2}
1,2	-5.5072×10^{-2}	-4.1261×10^{-2}
1,3	-2.7487×10^{-2}	-2.3332×10^{-2}
1,4	-1.9461×10^{-2}	-1.7427×10^{-2}
2,2	-1.2776×10^{-2}	-4.1782×10^{-3}
2,3	-1.0835×10^{-2}	-7.6550×10^{-3}
2,4	-7.3335×10^{-3}	-9.4613×10^{-3}
3,3	-4.7821×10^{-3}	-1.2948×10^{-3}
3,4	-5.6570×10^{-3}	-1.5460×10^{-3}
4,4	3.9989×10^{-3}	2.2703×10^{-3}
pic = .1385		
Mean Squared Error = 9.183×10^{-3}		

Table A-8. Series Coefficients for $b/a = .5$ and $c/a = .1$.

To illustrate the effect of using more terms in each solution region, a run was made using 21 terms in each region for the $b/a = 1$ and $c/a = .25$ crossed cylindrical conductor case. The coefficients obtained are shown in Table A-9. It can be seen that although the mean squared error was reduced substantially, the $B_{0,0}$ term changed by only $\approx .6\%$. Since this term, together with the line charge solution, specifies the potential as z becomes infinite, little improvement in the potential solution is to be expected by the use of the additional terms.

n,m	$A_{n,m}$	$B_{n,m}$
00	4.7666×10^{-2}	- .1120
01	3.6365×10^{-2}	- .2098
02	.1210	- .1206
03	.1222	- .1021
04	9.1829×10^{-2}	-8.6371×10^{-2}
05	6.5801×10^{-2}	-5.7384×10^{-2}
11	- .1948	-8.6447×10^{-2}
12	- .1645	-2.5389×10^{-2}
13	-5.5210×10^{-2}	-2.0104×10^{-2}
14	-1.4014×10^{-2}	-2.8432×10^{-2}
15	2.9949×10^{-2}	-4.1628×10^{-2}
22	3.0044×10^{-2}	1.0158×10^{-2}
23	2.3377×10^{-3}	-9.9481×10^{-4}
24	2.0358×10^{-2}	-2.7769×10^{-2}
25	3.8575×10^{-2}	-3.2589×10^{-2}
33	1.8698×10^{-2}	-8.8491×10^{-3}
34	3.6226×10^{-2}	-3.0328×10^{-2}
35	3.9910×10^{-2}	-2.9802×10^{-2}
44	1.6167×10^{-2}	-1.5809×10^{-2}
45	3.2051×10^{-2}	-2.6455×10^{-2}
55	1.2009×10^{-2}	-9.4318×10^{-3}
pic = 8.5354×10^{-2}		
Mean Squared Error = 3.6146×10^{-4}		

Table A-9. Series Coefficients for $b/a = 1$ and $c/a = .25$.

APPENDIX B

COMPUTER PROGRAMS

In this appendix are presented the computer programs used to obtain the data for this paper. These programs appear in pairs. The EMPEF programs calculated the series coefficients for the conducting cylinders cases. Program EMPEF #1 calculates the coefficients for the parallel conducting cylinders case and program EMPEF #2 calculates the coefficients for the crossed conducting cylinders case. Program BRPHI #1 was used to obtain the potential contour plots for all the line charge approximation cases and program BRPHI #2 was used to produce the potential contour plots for the series solution cases. Program ETRA #1 was used to calculate the electron trajectories for the line charge approximation cases and program ETRA #2 calculated the electron trajectories for the series solution cases. All the programs were run on the CDC 6600 computer located at Kirtland Air Force Base at Albuquerque, New Mexico.

EMPEF #1

```
EMPEF.P4.T777.CM60000.
TASK(GURRAX,46950106-5DH,ELE, )
DAFWL.
PUN(A,,TAPEZ)
PRESET.
MAP(PART)
LGO.
FXIT(S)
000000000000000000000000
CARDS
PROGRAM EMPEF(INPUT,OUTPUT)
DIMENSION IX(100),TRI(10000),AA(100,100),BB(100),XX(100)
EQUIVALENCE (A,TRI)
1000 FORMAT(3F7.3,3I4)
1001 FORMAT(1H .10G11.4)
1002 FORMAT(15H MATRIX AA N= ,I3)
1003 FORMAT(15H MATRIX BB )
1004 FORMAT(15H MATRIX X )
10 CONTINUE
READ 1000,A,B,C,LL,KK,NN
PRINT 1000,A,B,C,LL,KK,NN
IF(A.EQ.0.0) GO TO 400
READ 1000,VO,ETRM
C REMOVE THE CARDS BETWEEN THIS AND THE NEXT COMMENT CARD TO CHANGE PROG.
AC=0.0
IF(ETRM.EQ.1.0) GO TO 500
GO TO 30
20 AC=VO/PIC(C,B,A,R,C,1.0)
30 CONTINUE
IF(ETRM.EQ.1.0) GO TO 365
DO 250 J=1,NN
DO 200 N=1,NN
DO 100 L=1,LL
X=C*(1.0*LL-1.0)/(1.0*LL)
YN=R-SQRT(C**2-X**2)
YP=R-SQRT(C**2-X**2)
AA(J,N)=PI1(N,X,YN,A,B,C)*PI1(J,X,YN,A,B,C)+AA(J,N)
AA(J+NN,N+NN)=PI2(N,X,YP,A,B,C)*PI2(J,X,YP,A,B,C)+AA(J+NN,N+NN)
100 CONTINUE
DO 200 K=1,KK
```

```

X=C+(A-C)*(1.0*K-1.0)/(1.0*KK)
PJ1=PI1(J,X,B,A,B,C)
PJ2=PI2(J,X,B,A,B,C)
PJ2=-PJ2
DPJ1=DPI1(J,X,B,A,B,C)
DPJ2=DPI2(J,X,B,A,B,C)
DPJ2=-DPJ2
AA(J,N)=AA(J,N)+PI1(N,X,B,A,B,C)*PJ1+DPI1(N,X,B,A,B,C)*DPJ1
AA(J+NN,N)=AA(J+NN,N)+PI1(N,X,B,A,B,C)*PJ2+DPI1(N,X,B,A,B,C)*DPJ2
AA(J+NN,N+NN)=AA(J+NN,N+NN)-PI2(N,X,B,A,B,C)*PJ2-DPI2(N,X,B,A,B,C)
1*DPJ2
AA(J,N+NN)=AA(J,N+NN)-PI2(N,X,B,A,B,C)*PJ1-DPI2(N,X,B,A,B,C)*DPJ1
200 CONTINUE
DO 250 L=1,LL
X=C*(1.0*L-1.0)/(1.0*LL)
YN=R-SQRT(C**2-X**2)
YP=R+SQRT(C**2-X**2)
BR(J)=BR(J)+PI1(J,X,YN,A,B,C)*(VO-PIC(X,YN,A,B,C,AC))
BR(J+NN)=BR(J+NN)+PI2(J,X,YP,A,B,C)*(VO-PIC(X,YP,A,B,C,AC))
250 CONTINUE
C *****THIS IS THE NEXT COMMENT CARD *****
NSQ=VN*NN
NSQ=NSQ*4
N=NN*2
K=1
J=0
DO 325 I=1,NSQ
J=J+1
AA(I)=AA(J,K)
IF(J.EQ.N) K=K+1
IF(J.EQ.N) J=0
325 CONTINUE
PRINT 1002,N
IF(N.LT.30) PRINT 1001,(AA(I),I=1,NSQ)
PRINT 1003
PRINT 1001,(BR(I),I=1,N)
CALL MATSOLV(N,3,IX,TRI,AA,0,BR,XX)
PRINT 1004
PRINT 1001,(XX(I),I=1,N)
DO 350 I=1,10000
350 AA(I)=0.0
DO 360 I=1,100
BR(I)=0.0
360 CONTINUE
C ALSO REMOVE THE FOLLOWING CARDS TO CHANGE PROGRAM
365 CONTINUE
ERR1=0.0
ERR2=0.0
ERRS=0.0

```

```

DO 375 L=1,LL
X=C*(1.0*L-1.0)/(1.0*LL)
YN=R-SQRT(C**2-X**2)
YP=R+SQRT(C**2-X**2)
ERR1=VO-PIC(X,YN,A,B,C,AC)
ERR2=VO -PIC(X,YP,A,B,C,AC)
DO 370 N=1,NN
ERR1=ERR1-PI1(N,X,YN,A,B,C)*XX(N)
ERR2=ERR2-PI2(N,X,YP,A,B,C)*XX(N+NN)
370 CONTINUE
ERRS=ERRS+ERR1*ERR1+ERR2*ERR2
375 CONTINUE
ERR2=0.0
ERR1=0.0
DO 385 K=1,KK
X=C+(A-C)*(1.0*K)/(1.0*KK)
DO 380 N=1,NN
ERR1=ERR1+(XX(N)*PI1(N,X,B,A,B,C)-XX(N+NN)*PI2(N,Y,B,A,B,C))
ERR2=ERR2+(XX(N)*DPI1(N,X,B,A,B,C)-DPI2(N,X,B,A,B,C)*XX(N+NN))
380 CONTINUE
ERRS=ERRS+ERR1*ERR1+ERR2*ERR2
ERR1=0.0
ERR2=0.0
385 CONTINUE
ERRS=ERRS/(2.0*(LL+KK))
PRINT 1005, ERRS
1005 FORMAT(' MEAN SQUARED ERROR = ',G11.4)
500 CONTINUE
IF(AC.EQ.0.0) GO TO 20
C STOP REMOVING CARDS AT THIS POINT
GO TO 10
400 CONTINUE
STOP
END
NOLIST
FUNCTION DPI1(N,X,Y,A,B,C)
DPI1=(PI1(N,X,Y,A,B,C)-PI1(N,X,Y-R*.05,A,B,C))/(B*.10)
RETURN
END
FUNCTION DPI2(N,X,Y,A,B,C)
DPI2=(PI2(N,X,Y+B*.05,A,B,C)-PI2(N,X,Y,A,B,C))/(B*.10)
RETURN
END
FUNCTION PI1(N,X,Y,A,B,C)
PI=3.14159
AN=FLOAT(N)
FACT=(AN-1.0)*PI/A
IF(AN.EQ.1.0) GO TO 100
PI1= SINH(FACT*Y)*COS(FACT*X)/SINH(FACT*B)

```



```

GO TO 200
100 P11=Y/B
200 CONTINUE
RETURN
END
FUNCTION P12(N,X,Y,A,B,C)
PI=3.14159
AN=FLOAT(N)
FACT=(AN-1.0)*PI/A
P12=EXP(FACT*(B-Y))*COS(FACT*X)
RETURN
END
FUNCTION SINH(X)
SINH=(EXP(X)-EXP(-X))/2.0
RETURN
END
FUNCTION COSH(X)
COSH=(EXP(X)+EXP(-X))/2.0
RETURN
END
FUNCTION PIC(X,Y,A,B,C,AC)
PI=3.14159
T1=COSH(PI*(Y-B)/A)-COS(PI*X/A)
T2=COSH(PI*(Y-B)/A)-COS(PI*X/A)
PIC=AC*ALOG(T1/T2)
RETURN
END

```

```

LIBRARY
MATH000053
LAST
000000000000000000000000
+01.000+01.000+00.250+020+020+015
+01.000 +1.0
+01.000+01.000+00.100+020+020+015
+01.000 +1.0
+01.000+00.500+00.250+020+020+015
+01.000 +1.0
+01.000+00.500+00.100+020+020+015
+01.000 +1.0
+01.000+00.500+00.250+020+020+015
+01.000
+01.000+00.500+00.100+020+020+015
+01.000

```

```

000000000000000000000000
000000000000000000000000

```

EMPEF #2

```
-----  
-----  
-----  
-----  
-----  
EMPEF,PS,T177,CM60000.  
TASK(GURBAX,46950106-5DH,ELE,  
DAFWL.  
RUN(A,,TAPEZ)  
PPESET.  
MAP(PART)  
LGO.  
EXIT(S)  
000000000000000000000000  
CARDS  
PROGRAM EMPEF(INPUT,OUTPUT)  
DIMENSION IX(100),TRI(10000),AA(100,100),BB(100),XX(100)  
EQUIVALENCE (AA,TRI)  
1000 FORMAT(3F7.3,4I4)  
1001 FORMAT(2H ,LOG11.4)  
1002 FORMAT(15H MATRIX AA N= ,I3)  
1003 FORMAT(15H MATRIX BB )  
1004 FORMAT(15H MATRIX X )  
10 CONTINUE  
READ 1000,A,B,C,N1,N2,KK,NN  
PRINT 1000,A,B,C,N1,N2,KK,NN  
IF(A.EQ.0.0) GO TO 400  
READ 1000,VO  
C REMOVE THE CARDS BETWEEN THIS AND THE NEXT COMMENT CARD TO CHANGE PROG.  
AC=0.0  
LN=NN  
IF(NN.GT.0) AC=1.0/(PIC(C,B,A,B,C,1.0)+PIC(A,B,A,R,C,1.0))  
NN=KK  
DO 20 J=1,KK  
20 NN=NN+KK-J  
IF(LN.EQ.5) GO TO 370  
ISTEP=0.0  
IJ1=0  
IJ2=1  
DO 300 J=1,NN  
IJ1=IJ1+1  
IJ2=IJ1+ISTEP  
IF(IJ2.GT.KK) IJ1=1  
IF(IJ2.GT.KK) ISTEP=ISTEP+1  
IF(IJ2.GT.KK) IJ2=IJ1+ISTEP  
NSTEP=0.0  
IN1=0
```

```

IN2=1
DO 300 N=1,NN
  IN1=IN1+1
  IN2=IN1*NSTEP
  IF(IN2.GT.KK) IN1=1
  IF(IN2.GT.KK) NSTEP=NSTEP+1
  IF(IN2.GT.KK) IN2=IN1*NSTEP
  LL=N1+N2
  DO 300 L1=1,LL
    Y=FLOAT(L1-1)*C/FLOAT(N1-1)
    IF(Y.GT.C) Y=C+FLOAT(L1-N1)*(A-C)/FLOAT(N2)
    DO 300 L2=1,LL
      X=FLOAT(L2-1)*C/FLOAT(N1-1)
      IF(X.GT.C) X=C+FLOAT(L2-N1)*(A-C)/FLOAT(N2)
      IF(Y.GT.X) GO TO 300
      IF(Y.GT.C) GO TO 100
      ZP=R+SQRT(C**2-Y**2)
      ZN=R-SQRT(C**2-Y**2)
      GO TO 200
100 ZP=R
    ZN=R
200 CONTINUE
    PJ1=PI1(IJ1,IJ2,X,Y,ZN,A,B,C)
    PJ2=-PI2(IJ1,IJ2,X,Y,ZP,A,B,C)
    AA(J,N)=PI1(IN1,IN2,X,Y,ZN,A,B,C)*PJ1+AA(J,N)
    AA(J+NN,N+NN)=-PI2(IN1,IN2,X,Y,ZP,A,B,C)*PJ2+AA(J+NN,N+NN)
    IF(Y.LT.C) GO TO 250
    DPJ1=DP11(IJ1,IJ2,X,Y,ZN,A,B,C)
    DPJ2=DP12(IJ1,IJ2,X,Y,ZN,A,B,C)
    DPJ2=-DPJ2
    AA(J+NN,N)=AA(J+NN,N)+PI1(IN1,IN2,X,Y,ZN,A,B,C)*PJ2*DP11(IN1,IN2,
    IX,Y,ZN,A,B,C)*DPJ2
    AA(J,N)=AA(J,N)+DP11(IN1,IN2,X,Y,ZN,A,B,C)*DPJ1
    AA(J+NN,N+NN)=AA(J+NN,N+NN)-DP12(IN1,IN2,X,Y,ZN,A,B,C)*DPJ2
    AA(J,N+NN)=AA(J,N+NN)-PI2(IN1,IN2,X,Y,ZN,A,B,C)*PJ1-DP12(IN1,IN2,
    IX,Y,ZN,A,B,C)*DPJ1
250 CONTINUE
    IF(N.GT.1) GO TO 300
    IF(Y.GT.C) GO TO 300
    BB(J)=BB(J)+PI1(IJ1,IJ2,X,Y,ZN,A,B,C)*(VO-(PIC(X,ZN,A,B,C,AC)+
    IPIC(Y,ZN,A,B,C,AC)))
    BB(J+NN)=BB(J+NN)+PI2(IJ1,IJ2,X,Y,ZP,A,B,C)*(VO-(PIC(X,ZP,A,B,C,
    IAC)+PIC(Y,ZP,A,B,C,AC)))
300 CONTINUE
C *****THIS IS THE NEXT COMMENT CARD *****
  NSQ=NN*NN
  NSQ=NSQ*4
  N=NN*2
  K=1

```

```

J=0
DO 325 I=1,NSQ
J=J+1
AA(I)=AA(J,K)
IF(J.EQ.N) K=K+1
IF(J.EQ.N) J=0
325 CONTINUE
PRINT 1002,N
IF(N.LT.30) PRINT 1001,(AA(I),I=1,NSQ)
PRINT 1003
PRINT 1001,(BB(I),I=1,N)
CALL MATSOLV(N,3,IX,IRI,AA,0,BB,XX)
PRINT 1004
PRINT 1001,(XX(I),I=1,N)
DO 350 I=1,10000
350 AA(I)=0.0
DO 360 I=1,100
BB(I)=0.0
360 CONTINUE
C ALSO REMOVE THE FOLLOWING CARDS TO CHANGE PROGRAM
GO TO 366
370 CONTINUE
DO 365 I=1,100
365 XX(I)=0.0
366 CONTINUE
NPT=0
ERRS=0.0
DO 1600 L1=1,LL
Y=FLOAT(L1-1)*C/FLOAT(N1-1)
IF(Y.GT.C) Y=C*FLOAT(L1-N1)*(A-C)/FLOAT(N2)
DO 1600 L2=1,LL
X=FLOAT(L2-1)*C/FLOAT(N1-1)
IF(X.GT.C) X=C*FLOAT(L2-N1)*(A-C)/FLOAT(N2)
IF(Y.GT.X) GO TO 1600
IF(Y.GT.C) GO TO 2100
ZP=R+SQRT(C**2-Y**2)
ZN=R-SQRT(C**2-Y**2)
GO TO 2200
2100 ZP=R
ZN=B
2200 CONTINUE
NPT=NPT+1
NSTEP=0
IN1=0
IN2=1
ERR1=ERR2=0.0
IF(Y.LE.C) ERR1=-PIC(X,ZN,A,B,C,AC)-PIC(Y,ZN,A,B,C,AC)
IF(Y.LE.C) ERR2=-PIC(X,ZP,A,B,C,AC)-PIC(Y,ZP,A,B,C,AC)
DO 1500 I=1,NN

```

```

      IN1=IN1+1
      IN2=IN1+NSTEP
      IF(IN2.GT.KK) IN1=1
      IF(IN2.GT.KK) NSTEP=NSTEP+1
      IF(IN2.GT.KK) IN2=IN1+NSTEP
      IF(Y.GT.C) GO TO 1400
      ERP1=(VO/FLOAT(NN))-PI1(IN1,IN2,X,Y,ZN,A,B,C)*XX(I)+ERR1
      ERP2=(VO/(FLOAT(NN)))-PI2(IN1,IN2,X,Y,ZP,A,B,C)*XX(I+NN)+ERR2
1300 CONTINUE
      GO TO 1500
1400 ERR1=ERR1+PI1(IN1,IN2,X,Y,B,A,B,C)*XX(I)-PI2(IN1,IN2,X,Y,B,A,B,C)
      *XX(J+NN)
      ERR2=ERR2+DPI1(IN1,IN2,X,Y,B,A,B,C)*XX(I)-DPI2(IN1,IN2,X,Y,B,A,B,C)
      *XX(I+NN)
1500 CONTINUE
      ERRS=ERRS+ERP1*ERP1+ERR2*ERR2
1600 CONTINUE
      ERRS=ERRS/(FLOAT(NPT))
      ERRS=ERRS/2.0
      PRINT 1005,ERRS
      PRINT 1006,AC
1005 FORMAT(' MEAN SQUARED ERROR = ',G11.4)
1006 FORMAT(' PIC COEFFICIENT AC ',G11.4)
C STOP REMOVING CARDS AT THIS POINT
GO TO 10
400 CONTINUE
STOP
END
FUNCTION PI1(M1,M2,X,Y,Z,A,B,C)
N1=M1-1
N2=M2-1
IF((N1+N2).EQ.0) GO TO 100
PI=ACOS(-1.0)
FACT=PI*SQRT(((FLOAT(N1))**2+((FLOAT(N2))**2) )/A)
PI1=COS(PI*FLOAT(N1)*X/A)*COS(PI*FLOAT(N2)*Y/A)*SINH(FACT*Z)
1/SINH(FACT*B)
TEMP=N1
N1=N2
N2=TEMP
N2=TEMP
PI1=COS(PI*FLOAT(N1)*X/A)*COS(PI*FLOAT(N2)*Y/A)*SINH(FACT*Z)
1/SINH(FACT*B) *PI1
PI1=PI1/2.0
TEMP=N1
N1=N2
N2=TEMP
GO TO 200
100 CONTINUE
PI1=Z/B

```

```

200 CONTINUE
N2=N2+1
N1=N1+1
RETURN
END
FUNCTION PI2(N1,M2,X,Y,Z,A,B,C)
PI=ACOS(-1.0)
N1=M1-1
N2=M2-1
FACT=PI*SQRT((FLOAT(N1))*2+((FLOAT(N2))*2))
FACT=FACT/A
PI2=COS(PI*FLOAT(N1)*X/A)*COS(PI*FLOAT(N2)*Y/A)*EXP(FACT*(B-Z))
TEMP=N1
N1=N2
N2=TEMP
PI2=COS(PI*FLOAT(N1)*X/A)*COS(PI*FLOAT(N2)*Y/A)*EXP(FACT*(B-Z))
PI2=PI2/2.0
TEMP=N1
N1=N2
N2=TEMP
N2=N2+1
N1=N1+1
RETURN
END
FUNCTION DPI1(N1,N2,X,Y,Z,A,R,C)
DPI1=(PI1(N1,N2,X,Y,Z,A,B,C)-PI1(N1,N2,X,Y,Z-.05*R,A,B,C))/(.10*B)
RETURN
END
FUNCTION DPI2(N1,N2,X,Y,Z,A,B,C)
DPI2=(PI2(N1,N2,X,Y,Z+.05*B,A,B,C)-PI2(N1,N2,X,Y,Z,A,B,C))/(.10*B)
RETURN
END
NOLIST
FUNCTION COSH(X)
COSH=(EXP(X)+EXP(-X))/2.0
RETURN
END
FUNCTION SINH(X)
SINH=(EXP(X)-EXP(-X))/2.0
RETURN
END
FUNCTION PIC(X,Y,A,B,C,AC)
PI=3.14159
T1=COSH(PI*(Y+B)/A)-COS(PI*X/A)
T2=COSH(PI*(Y-B)/A)-COS(PI*X/A)
PIC=AC*ALOG(T1/T2)
RETURN
END

```

LIBRARY
MATH000053
LAST
000000000000000000000000
+01.000+00.500+00.250+009+009+005+005
+01.00
+01.000+00.500+00.100+009+009+005+005
+01.00
+01.000+01.000+00.250+009+009+005+005
+01.00
+01.000+01.000+00.100+009+009+005+005
+01.00
000000000000000000000000
000000000000000000000000

BRPHI #1

```
EMPEF,P4,T477,CM60000.
TASK(GURBAX,46950106-5DH,ELE, )
DAFWL.
RUN(A,,,TAPEZ)
PPESET.
MAP(PART)
LGO.
000000000000000000000000
CARDS
PROGRAM BRPHI(OUTPUT,FILMPL)
DIMENSION A(51,101),P(6),CU(20)
C CHANGE MADE TO NORMALIZE B AND MAKE A VARIABLE))))))))))
NV=20
CU(1)=.01
CU(2)=.05
DO 890 KK=3,NV
CU(KK)=CU(KK-1)+.05
880 CONTINUE
DO 881 KK=1,NV
CU(KK)=CU(KK)*2.
881 CONTINUE
C=1.
B=1.
DO 400 NN=1,4
DO 400 NNN=1,5
Z=(FLOAT(NNN)-1.0)/4.0
Z=AY*Z
AY=FLOAT(NN)
PRINT 101,AY
101 FORMAT(1H1,*A=*,F20.8,/)
XMAX=4.*AY
DX=XMAX/100.
YMAX=AY
DY=YMAX/50.
Y=-2.*AY-DY
DY=YMAX/25.
Y=-AY-DY
DO 20 J=1,51
Y=Y+DY
X=-DX
```



```

DO 10 I=1,101
X=X+DX
500 CALL PHI(AY,B,X,Y,PH)
APH=PH
CALL PHI(AY,B,X,Z,PH)
RPH=PH
CALL PHI(AY,2.*B,X,Y+AY,PH)
CPH=PH
CALL PHI(AY,2.*B,X,Z+AY,PH)
PH=(PH+APH+RPH+CPH)/4.
A(J,I)=PH
10 CONTINUE
200 FORMAT(1X,F20.8)
100 FORMAT(1X,11E12.4//)
20 CONTINUE
IZ=1
IZ1=IZ+10
DO 302 K=1,9
DO 301 J=1,51
301 CONTINUE
IZ=IZ+11
IZ1=IZ+10
PRINT 303
302 CONTINUE
303 FORMAT(//)
300 FORMAT(1X,11E12.4)
N=101
M=51
P(1)=0.
P(2)=DX*100.
P(3)=-AY
P(4)=AY
P(5)=.8
P(6)=P(5)
J=8
I=8
CALL BRIT(A,M,N,P,CU,NV,I,J)
41 CONTINUE
40 CONTINUE
700 CONTINUE
400 CONTINUE
STOP
END.
NOLIST
SURROUTINE BRIT (A,MM,NN,P,CU,NV,IL,J)          BRT
DIMENSION A(MM,NN), CU(NV), P(7)             BRT
COMMON /GOOP/ DX,DY,K,SAVEX(500),SAVEY(500)   BRT
CALL D4 (P(1),P(2),P(3),P(4),IL,J,P(5),P(6),1,SAVEX,SAVEY,1,-1) BRT
DY=(P(4)-P(3))/FLOAT(MM-1)                   BRT

```

```

DX=(P(2)-P(1))/FLOAT(NN-1)
NOMM1=MM-1
NONM1=NN-1
DO 45 I=1,NV
K=0
DO 5 N=1,NN
DO 5 M=1,NOMM1
IF ((A(M,N)-CU(I))*(A(M+1,N)-CU(I)).GT.0.) GO TO 5
K=K+1
IF (K.GT.500) GO TO 20
SAVEX(K)=FLOAT(N-1)*DX+P(1)
SAVEY(K)=FLOAT(M-1)*DY+P(3)+(DY/(A(M+1,N)-A(M,N)))*(CU(I)-A(M,N))
5 CONTINUE
DO 10 M=1,MM
DO 10 N=1,NONM1
IF ((A(M,N)-CU(I))*(A(M,N+1)-CU(I)).GT.0.) GO TO 10
K=K+1
IF (K.GT.500) GO TO 20
SAVEX(K)=FLOAT(N-1)*DX+P(1)+(DX/(A(M,N+1)-A(M,N)))*(CU(I)-A(M,N))
SAVEY(K)=FLOAT(M-1)*DY+P(3)
10 CONTINUE
15 FORMAT (1H0/1H0,20X,F10.6,9H CONTOUR/33X,13HNO. OF PTS. =,I4)
IF (K.LT.4) GO TO 45
GO TO 30
20 CONTINUE
25 FORMAT (1X,23H*** ARRAY OVERFLOW FOR ,F10.6,9H CONTOUR)
30 CALL ORDER (P)
DO 40 MISUM=1,3
LOAD=0
DO 35 JOY=1,K
IF (SAVEX(JOY).GE.1.E5) GO TO 35
LOAD=LOAD+1
SAVEX(LOAD)=SAVEX(JOY)
SAVEY(LOAD)=SAVEY(JOY)
35 CONTINUE
IF (LOAD.LT.5) GO TO 45
K=LOAD
40 CALL ORDER (P)
45 CONTINUE
CALL PLOT(FLOAT(IL)*P(5)+3.6,0.,-3)
RETURN
END
SURROUTINE ORDER (P)
COMMON /GOOP/ DX,DY,IPLLOT,SAVEX(500),SAVEY(500)
DIMENSION PX(500),PY(500),P(7)
V= DX*DX+DY*DY
CALL SORT (SAVEX,IPLLOT,SAVEY)
IMAX=0
TEMPX=SAVEX(1)

```

	TEMPY=SAVEY(1)	OR
	K6=0	OR
	IFD=0	OR
	I=1	OR
	IP=1	OR
	GO TO 10	OR
5	IP=2	OR
	I=JHOLD	OR
	PX(1)=SAVEX(I)	OR
	PY(1)=SAVEY(I)	OR
10	PX(IP)=SAVEX(I)	OR
	PY(IP)=SAVEY(I)	OR
15	KOUNT=0	OR
	DO 50 J=1,IPL0T	OR
	IF (SAVEX(J).GT.1.E5) GO TO 50	OR
	SX=SAVEX(J)-SAVEX(I)	OR
	SY=SAVFY(J)-SAVEY(I)	OR
	DEL= SX*SX+SY*SY	OR
	IF (DEL.LT.1.E-12) GO TO 50	OR
	KEEP=0	OR
	IF (DEL.GT.V) GO TO 30	OR
	KK=J+5	OR
	KK=MIN0(KK,IPL0T)	OR
	DELT=DEL	OR
	KEEP=-1	OR
	IF (J.EQ.IPL0T) GO TO 30	OR
	KB=J+1	OR
	DO 25 K=KB,KK	OR
	SXC=SAVEX(K)-SAVEX(I)	OR
	SYC=SAVFY(K)-SAVFY(I)	OR
	DELC= SXC*SXC+SYC*SYC	OR
	IF (DELC.LT.1.E-12) GO TO 25	OR
	IF (DELC-DELT) 20,25,25	OR
20	DELT=DELC	OR
	KEEP=K	OR
25	CONTINUE	OR
30	IF (KEEP) 80,35,75	OR
35	IF (IFD) 45,40,45	OR
40	JHOLD=J	OR
45	IFD=IFD+1	OR
50	KOUNT=KOUNT+1	OR
	IF (KOUNT.EQ.IPL0T.AND.IFD.NE.0) GO TO 55	OR
	IF (IP.GT.4) CALL D4 (P(1),D,P(3),D,M,4,P(5),P(6),IP,PX,PY,2,-1)	OR
	IF (K6.EQ.1) GO TO 100	OR
	IF (IP.EQ.IPL0T) GO TO 95	OR
	IMAX=IMAX+1	OR
	IF (IMAX.LT.(IPL0T+5)) GO TO 15	OR
	TSX=PX(IP)-TEMPX	OR
	TSY=PY(IP)-TEMPY	OR

```

15 M=M/2 SRT
IF (M.LT.1) RETURN SRT
K=NUM-M SRT
DO 25 J=1,K SRT
I=J SRT
20 IM=I+M SRT
IF (KEY(I).LE.KEY(IM)) GO TO 25 SRT
T2=KEY(I) SRT
T=KEY(IM) SRT
KEY(I)=KEY(IM) SRT
KEY(IM)=T2 SRT
KEY(I)=T SRT
I=I-M SRT
IF (I.GE.1) GO TO 20 SRT
25 CONTINUE SRT
GO TO 15 SRT
END SRT
SUBROUTINE D4 (XMIN,XMAX,YMIN,YMAX,IL,IH,SX,SY,NPTS,X,Y,KIND,LAST) D4
DIMENSION X(NPTS), Y(NPTS) D4
DATA IFT,JFT,FX,FY/4HF6.1,4HF6.2,0.6,0.59/ D4
IF (KIND-1) 10,15,5 D4
5 IF (KIND-2) 10,90,10 D4
10 RETURN D4
15 IF (10-2) 20,25,20 D4
20 CALL PLOTS (T,IB,10) D4
IO=? D4
25 CALL PLOT (FX,FY,3) D4
REALH=IH D4
REALL=IL D4
SCALEX=(XMAX-XMIN)/REALL D4
SCALEY=(YMAX-YMIN)/REALH D4
RSCALEX=1./SCALEX D4
RSCALEY=1./SCALEY D4
DO 35 I=1,4 D4
GO TO (30,35,30,35), I D4
30 NV=IH+1 D4
GO TO 40 D4
35 NN=IL+1 D4
40 DO 35 N=1,NN D4
REALN=N D4
GO TO (45,55,65,75), I D4
45 R=REALN-1. D4
CALL PLOT (-.05+FX,R*SY+FY,2) D4
CALL PLOT (FX,R*SY+FY,2) D4
YNUM=R*SCALEY+YMIN D4
IF (ABS(YNUM).LE.1.E-10) YNUM=0. D4
RR=(REALN-1.)*SY-.03 D4
CALL NUMBER (-.6+FX,RR+FY,.10,YNUM,0.,JFT) D4

```

```

..... CALL PLOT (FX,R*SY,FY,3) ..... D4
..... IF (N-NN) 50,85,50 ..... D4
50 ..... CALL PLOT (FX,REALN*SY,FY,2) ..... D4
..... GO TO 85 ..... D4
55 ..... R=RFALN-1. ..... D4
..... RR=REALH*.05 ..... D4
..... CALL PLOT (R*SX+FX,RR*SY,FY,2) ..... D4
..... CALL PLOT (R*SX+FX,REALH*SY,FY,2) ..... D4
..... IF (N-NN) 60,85,60 ..... D4
60 ..... CALL PLOT (REALN*SX+FX,REALH*SY,FY,2) ..... D4
..... GO TO 85 ..... D4
65 ..... R=RFALL*.05 ..... D4
..... RR=REALH-RFALN*1. ..... D4
..... CALL PLOT (R*SX+FX,RR*SY,FY,2) ..... D4
..... CALL PLOT (REALL*SX+FX,RR*SY,FY,2) ..... D4
..... IF (N-NN) 70,85,70 ..... D4
70 ..... CALL PLOT (REALL*SX+FX,(RR-1.)*SY,FY,2) ..... D4
..... GO TO 85 ..... D4
75 ..... R=RFALL-REALN*1. ..... D4
..... CALL PLOT (R*SX+FX,-.05*FY,2) ..... D4
..... CALL PLOT (R*SX+FX,FY,2) ..... D4
..... XNUM=R*SCALEX*XMIN ..... D4
..... IF (ABS(XNUM).LE.1.E-10) XNUM=0. ..... D4
..... RR=R*SX-.25 ..... D4
..... CALL NUMBER (RR+FY,-.25+FY,.10,XNUM,0.,IFT) ..... D4
..... CALL PLOT (R*SX+FX,FY,3) ..... D4
..... IF (N-NN) 80,85,80 ..... D4
80 ..... CALL PLOT ((R-1.)*SX+FX,FY,2) ..... D4
85 ..... CONTINUE ..... D4
90 ..... CALL PLOT ((X(1)-XMIN)*RSCALX*SX+FX,(Y(1)-YMIN)*RSCALY*SY,FY,3) ..... D4
..... DO 95 J=1,NPTS ..... D4
..... XX=(X(I)-XMIN)*RSCALX ..... D4
..... YY=(Y(I)-YMIN)*RSCALY ..... D4
95 ..... CALL PLOT (XX*SX+FX,YY*SY,FY,2) ..... D4
..... IF (LAST.LT.0) RETURN ..... D4
..... CALL PLOT ((RFALL+3.)*SX+FX,FY,-3) ..... D4
..... RETURN ..... D4
..... END ..... D4
..... SUBROUTINE PHI(A,R,X,Y,PH) .....
..... PH=0.0 .....
..... IF (X.EQ.0.0) RETURN .....
..... PI=ACOS(-1.) .....
..... X1=(X+R)*PI/A .....
..... COSH1=(EXP(X1)+EXP(-X1))*0.5 .....
..... X2=(X-R)*PI/A .....
..... COSH2=(EXP(X2)+EXP(-X2))*0.5 .....
..... COS1=COS(PI*Y/A) .....
..... IF ((COSH2-COS1).LT.0.001) RETURN .....
..... X1=(COSH1-COS1)/(COSH2-COS1) .....

```

PH=A/(2.*PI*B)*ALOG(X1)

RETURN

END

LIBRARY

PL0T000029

LAST

000000000000000000000000

000000000000000000000000

BRPHI #2

```

FMPEF,P4,T477,CM60000.
TASK(GURBAX,46950106-50H,ELE, )
DAFWL.
RUN(A,,TAPEZ)
PRESET.
MAP(PART)
LGO(LC=377777)
000000000000000000000000
CARDS
PROGRAM BRPHI(INPUT,OUTPUT,FILMPL)
DIMENSION A(51,101),P(6),CU(20),X1(100),X2(100)
C ***** SERIES SOLUTION -- COUNTOUR MAPS *****
EQUIVALENCE (V0,V0)
5 CONTINUE
READ 999,NX,AY,B,C,AA,V0,DIM
999 FORMAT(15,6F10.5)
IF(NX.EQ.0) GO TO 500
KK=NX
IF(DIM.EQ.0.0) GO TO 777
NX=0
DO 776 I=1,KK
776 NX=I+NX
777 CONTINUE
READ 888,(X1(N),N=1,NX)
PRINT 888,(X1(N),N=1,NX)
READ 888,(X2(N),N=1,NX)
PRINT 888,(X2(N),N=1,NX)
NX=KK
888 FORMAT(7G11.4)
AC=V0*AA/(PIC(C,B,AY,B,C,1.0)+DIM*PIC(AY,B,AY,B,C,1.0))
NV=20
CU(1)=.01
CU(2)=.05
DO 880 KK=3,NV
CU(KK)=CU(KK-1)+.05
880 CONTINUE
DO 881 KK=1,NV
CU(KK)=CU(KK)*2.
881 CONTINUE
NDIM=5*DIM

```

```

DO 400 NNN=1,NDIM
Z=AY*(FLOAT(NNN) -1.0)/4.0
PRINT 101,AY
101 FORMAT(1H1,*,A=*,F20.8,/)
XMAX=2.*AY
DX=XMAX/100.
YMAX=AY
DY=YMAX/25.
Y=-AY-DY
DO 20 J=1,51
Y=Y+DY
X=-DX
DO 10 I=1,101
X=X+DX
IF(J.LE.26) GO TO 50
A(J,I)=A(52-J,I)
GO TO 10
50 CALL PHI(NX,AY,B,C,Y,X,Z,X1,X2,PH,VO,DIM )
A(J,I)=PH+PIC(Y,X,AY,B,C,AC)/VO
A(J,I)=A(J,I)+DIM*PIC(Z,X,AY,B,C,AC)/VO
10 CONTINUE
200 FORMAT(1X,E20.8)
100 FORMAT(1X,11E12.4//)
20 CONTINUE
IZ=1
IZ1=IZ+10
DO 302 K=1,9
DO 301 J=1,51
301 CONTINUE
IZ=IZ+11
IZ1=IZ+10
PRINT 303
302 CONTINUE
303 FORMAT(//)
300 FORMAT(1X,11E12.4)
N=101
M=51
P(1)=0.
P(2)=DX*100.
P(3)=-AY
P(4)=AY
P(5)=.8
P(6)=P(5)
J=8
I=8
CALL BRUT(A,M,N,P,CU,NV,I,J)
41 CONTINUE
40 CONTINUE
700 CONTINUE

```



```

400 CONTINUE
GO TO 5
500 CONTINUE
STOP
END
SUBROUTINE PHI(N,A,B,C,X,Y,Z,X1,X2,PH,V0,DIM)
DIMENSION X1(100),X2(100)
V0=V0
PH=0.0
IF(DIM.EQ.1.0) GO TO 1000
IF(Y.GT.B) GO TO 200
DO 100 I=1,N
PH=PH+PI1(I,X,Y,A,B,C)*X1(I)/V0
100 CONTINUE
GO TO 400
200 CONTINUE
DO 300 I=1,N
PH=PH+PI2(I,X,Y,A,B,C)*X2(I)/V0
300 CONTINUE
400 CONTINUE
RETURN
1000 CONTINUE
KK=N
N=0
DO 1101 I=1,KK
1101 N=N+I
TEMP=Y
Y=Z
Z=TEMP
ISTEP=0
IJ1=0
IJ2=1
DO 1200 J=1,N
IJ1=IJ1+1
IJ2=IJ1+ISTEP
IF(IJ2.GT.KK) IJ1=1
IF(IJ2.GT.KK) ISTEP=ISTEP+1
IF(IJ2.GT.KK) IJ2=IJ1+ISTEP
IF(Z.GT.B) GO TO 1100
PH=PH+PI1(IJ1,IJ2,X,Y,Z,A,B,C)*X1(IJ1)/V0
GO TO 1200
1100 PH=PH+PI2(IJ1,IJ2,X,Y,Z,A,B,C)*X2(IJ1)/V0
1200 CONTINUE
N=KK
PH=PH/V0
TEMP=Y
Y=Z
Z=TEMP
RETURN

```

```

END
FUNCTION P111(M1,M2,X,Y,Z,A,B,C)
N1=M1-1
N2=M2-1
IF((N1+N2).EQ.0) GO TO 100
PI=ACOS(-1.0)
FACT=PI*SQRT((FLOAT(N1))**2+((FLOAT(N2))**2)) / A
PP1=COS(PI*FLOAT(N1)*X/A)*COS(PI*FLOAT(N2)*Y/A)*SINH(FACT*Z)
1/SINH(FACT*B)
TEMP=N1
N1=N2
N2=TEMP
N2=TEMP
PP1=COS(PI*FLOAT(N1)*X/A)*COS(PI*FLOAT(N2)*Y/A)*SINH(FACT*Z)
1/SINH(FACT*B) *PP1
PP1=PP1/2.0
TEMP=N1
N1=N2
N2=TEMP
GO TO 200
100 CONTINUE
PP1=Z/B
200 CONTINUE
N2=N2+1
N1=N1+1
P111=PP1
RETURN
END
FUNCTION P112(M1,M2,X,Y,Z,A,B,C)
PI=ACOS(-1.0)
N1=M1-1
N2=M2-1
FACT=PI*SQRT((FLOAT(N1))**2+((FLOAT(N2))**2))
FACT=FACT/A
PP2=COS(PI*FLOAT(N1)*X/A)*COS(PI*FLOAT(N2)*Y/A)*EXP(FACT*(B-Z))
TEMP=N1
N1=N2
N2=TEMP
PP2=COS(PI*FLOAT(N1)*X/A)*COS(PI*FLOAT(N2)*Y/A)*EXP(FACT*(B-Z))
1*PP2
PP2=PP2/2.0
TEMP=N1
N1=N2
N2=TEMP
N2=N2+1
N1=N1+1
P112=PP2
RETURN
END

```

```

FUNCTION PIC(X,Y,A,B,C,AC)
PIC=0.0
PI=3.14159
T1=COSH(PI*(Y+B)/A)-COS(PI*X/A)
T2=COSH(PI*(Y-B)/A)-COS(PI*X/A)
IF(ABS(T2).LT.0.001)GO TO 100
PIC=AC*ALOG(T1/T2)
100 RETURN
END
FUNCTION P11(I,X,Y,A,B,C)
PI=3.14159
AN=FLOAT(N)
FACT=(AN-1.0)*PI/A
IF(AN.EQ.1.0) GO TO 100
P11=SINH(FACT*Y)*COS(FACT*X)/SINH(FACT*B)
GO TO 200
100 P11=Y/B
200 CONTINUE
RETURN
END
FUNCTION P12(N,X,Y,A,B,C)
PI=ACOS(-1.0)
AN=FLOAT(N)
FACT=(AN-1.0)*PI/A
P12=EXP(FACT*(B-Y))*COS(FACT*X)
RETURN
END
FUNCTION COSH(X)
COSH=(EXP(X)+EXP(-X))/2.0
RETURN
END
FUNCTION SINH(X)
SINH=(EXP(X)-EXP(-X))/2.0
RETURN
END
NOLIST
SUBROUTINE BRIT (A,MM,NN,P,CU,NV,IL,J) BRT
DIMENSION A(MM,NN), CU(NV), P(7) BRT
COMMON /GOOP/ DX,DY,K,SAVEX(500),SAVEY(500) BRT
CALL D4 (P(1),P(2),P(3),P(4),IL,J,P(5),P(6),1,SAVFX,SAVEY,1,-1) BRT
DY=(P(4)-P(3))/FLOAT(MM-1) BRT
DX=(P(2)-P(1))/FLOAT(NN-1) BRT
NOMM]=MM-1 BRT
NONN]=NN-1 BRT
DO 45 I=1,NV BRT
K=0 BRT
DO 5 N=1,NN BRT
DO 5 M=1,NOMM] BRT
IF ((A(M,N)-CU(I))*(A(M+1,N)-CU(I)).GT.0.) GO TO 5 BRT

```

```

K=K+1 BRT
IF (K.GT.500) GO TO 20 BRT
SAVEX(K)=FLOAT(N-1)*DX*P(1) BRT
SAVEY(K)=FLOAT(M-1)*DY*P(3)+(DY/(A(M+1,N)-A(M,N)))*(CU(I)-A(M,N)) BRT
5 CONTINUE BRT
DO 10 M=1,MM BRT
DO 10 N=1,MM BRT
IF ((A(M,N)-CU(I))*(A(M,N+1)-CU(I)).GT.0.) GO TO 10 BRT
K=K+1 BRT
IF (K.GT.500) GO TO 20 BRT
SAVEX(K)=FLOAT(N-1)*DX*P(1)+(DX/(A(M,N+1)-A(M,N)))*(CU(I)-A(M,N)) BRT
SAVEY(K)=FLOAT(M-1)*DY*P(3) BRT
10 CONTINUE BRT
PRINT 15, CU(I),K BRT
15 FORMAT (1H0/1H0,20X,F10.6,9H CONTOUR/33X,13HNO. OF PTS. =,I4) BRT
IF (K.LT.4) GO TO 45 BRT
GO TO 30 BRT
20 PRINT 25, CU(I) BRT
25 FORMAT (1X,23H*** ARRAY OVERFLOW FOR ,F10.6,9H CONTOUR) BRT
30 CALL ORDER (P) BRT
DO 40 MISUM=1,3 BRT
LOAD=0 BRT
DO 35 JOY=1,K BRT
IF (SAVEX(JOY).GE.1.E5) GO TO 35 BRT
LOAD=LOAD+1 BRT
SAVEX(LOAD)=SAVEX(JOY) BRT
SAVEY(LOAD)=SAVEY(JOY) BRT
35 CONTINUE BRT
IF (LOAD.LT.5) GO TO 45 BRT
K=LOAD BRT
40 CALL ORDER (P) BRT
45 CONTINUE BRT
CALL PLOT(FLOAT(IL)*P(5)+3.6,0.,-3) BRT
RETURN BRT
END BRT
SUBROUTINE ORDER (P) OR
COMMON /GOOP/ DX,DY,IPLOT,SAVEX(500),SAVEY(500) OR
DIMENSION PX(500),PY(500),P(7) OR
V= DX*DX+DY*DY OR
CALL SORT (SAVEX,IPLOT,SAVEY) OR
I4X=0 OR
TEMPX=SAVEX(1) OR
TEMPY=SAVEY(1) OR
K6=0 OR
IFD=0 OR
I=1 OR
IP=1 OR
GO TO 10 OR
5 IP=2 OR

```

```

..... I=JHOLD ..... OR
..... PX(1)=SAVEX(I) ..... OR
..... PY(1)=SAVEY(I) ..... OR
10 ..... PX(IP)=SAVFX(I) ..... OR
..... PY(IP)=SAVEY(I) ..... OR
15 ..... KOUNT=0 ..... OR
..... DO 50 J=1,IPLOT ..... OR
..... IF (SAVFX(J).GT.1.E5) GO TO 50 ..... OR
..... SX=SAVEX(J)-SAVEX(I) ..... OR
..... SY=SAVEY(J)-SAVEY(I) ..... OR
..... DEL= SX* $SX$ +SY* $SY$  ..... OR
..... IF (DEL.LT.1.E-12) GO TO 50 ..... OR
..... KEEP=0 ..... OR
..... IF (DEL.GT.V) GO TO 30 ..... OR
..... KK=J+6 ..... OR
..... KK=MIN0(KK,IPLOT) ..... OR
..... DELT=DEL ..... OR
..... KEEP=-1 ..... OR
..... IF (J.EQ.IPLOT) GO TO 30 ..... OR
..... KB=J+1 ..... OR
..... DO 25 K=KR,KK ..... OR
..... SXC=SAVEX(K)-SAVEX(I) ..... OR
..... SYC=SAVEY(K)-SAVEY(I) ..... OR
..... DELC= SXC* $SXC$ +SYC* $SYC$  ..... OR
..... IF (DELC.LT.1.E-17) GO TO 25 ..... OR
..... IF (DELC-DELT) 20,25,25 ..... OR
20 ..... DELT=DELC ..... OR
..... KEEP=K ..... OR
25 ..... CONTINUE ..... OR
30 ..... IF (KEEP) 80,35,75 ..... OR
35 ..... IF (IFD) 45,40,45 ..... OR
40 ..... JHOLD=J ..... OR
45 ..... IFD=IFD+1 ..... OR
50 ..... KOUNT=KOUNT+1 ..... OR
..... IF (KOUNT.EQ.IPLOT.AND.IFD.NE.0) GO TO 55 ..... OR
..... IF (IP.GT.4) CALL 04 (P(1),D,P(3),D,M,Y,P(5),P(6),IP,PX,PY,2,-1) ..... OR
..... IF (K6.EQ.1) GO TO 100 ..... OR
..... IF (IP.EQ.IPLOT) GO TO 95 ..... OR
..... IMAX=IMAX+1 ..... OR
..... IF (IMAX.LT.(IPLOT+5)) GO TO 15 ..... OR
..... TSX=PX(IP)-TEMPX ..... OR
..... TSY=PY(IP)-TEMPY ..... OR
..... DEL= TSX* $TSX$ +TSY* $TSY$  ..... OR
..... IF (DEL.LT.V) GO TO 110 ..... OR
..... GO TO 100 ..... OR
55 ..... CONTINUE ..... OR
..... IF (K6.NE.0) GO TO 60 ..... OR
C ..... PRINT 105, (PX(L),PY(L),L,L=1,IP) ..... OR
..... SAVEX(IP)=SAVEX(IP)+10. ..... OR

```

```

IF (IP.GT.4) CALL D4 (P(1),D,P(3),D,M,M,P(5),P(6),IP,PX,PY,2,-1) OR
60 IF (K6) 70,70,65 OR
65 K6=0 OR
TSX=PX(2)-TEMPX OR
TSY=PY(2)-TEMPY OR
DEL= TSX*TSX+TSY*TSY OR
IF (DEL.GT.V) GO TO 100 OR
PX(1)=TEMPX OR
PY(1)=TEMPY OR
GO TO 100 OR
70 K6=1 OR
GO TO 5 OR
75 J=KEEP OR
80 IP=IP+1 OR
PX(IP)=SAVFX(J) OR
PY(IP)=SAVFY(J) OR
SAVEX(I)=SAVEX(I)+1.E6 OR
IF (J-JHOLD) 90,85,90 OR
85 IFD=0 OR
JHOLD=0 OR
90 I=J OR
IF (IP-IPL0T) 15,95,95 OR
95 TSX=PX(IP)-TEMPX OR
TSY=PY(IP)-TEMPY OR
DEL= TSX*TSX+TSY*TSY OR
IF (DEL.LE.V) GO TO 110 OR
100 CONTINUE OR
105 FORMAT (10X,7HFROM 75/(15X,2E15.5,I4)) OR
CALL D4 (P(1),D,P(3),D,M,M,P(5),P(6),IP,PX,PY,2,-1) OR
SAVEX(I)=SAVEY(I)+1.E6 OR
RETURN OR
110 IP=IP+1 OR
PX(IP)=TEMPX OR
PY(IP)=TEMPY OR
GO TO 100 OR
END OR
SUBROUTINE SORT (KEY,NUM,KEY1) SRT
INTEGER KEY(NUM),T,KEY1(NUM),T2 SRT
5 IF (NUM.LT.2) RETURN SRT
I=1 SRT
10 I=I+1 SRT
IF (I.LE.NUM) GO TO 10 SRT
M=I-1 SRT
15 M=M/2 SRT
IF (M.LT.1) RETURN SRT
K=NUM-M SRT
DO 25 J=1,K SRT
J=J SRT
20 IM=I+M SRT

```

	IF (KEY(I).LE.KEY(IM)) GO TO 25	SRT
	T2=KEY1(I)	SRT
	T=KEY(I)	SRT
	KEY1(I)=KEY1(IM)	SRT
	KEY(I)=KEY(IM)	SRT
	KEY1(IM)=T2	SRT
	KEY(IM)=T	SRT
	I=I-M	SRT
	IF (I.GE.1) GO TO 20	SRT
25	CONTINUE	SRT
	GO TO 15	SRT
	END	SRT
	SUBROUTINE D4 (XMIN,XMAX,YMIN,YMAX,IL,IH,SX,SY,NPTS,X,Y,KIND,LAST)	D4
	DIMENSION X(NPTS), Y(NPTS)	D4
	DATA JFT,JFT,FX,FY/4HF6.1,4HF6.2,0.6,0.59/	D4
	IF (KIND-1) 10,15,5	D4
5	IF (KIND-2) 10,90,10	D4
10	RETURN	D4
15	IF (I0-2) 20,25,20	D4
20	CALL PLOTS (TR,TR,10)	D4
	I0=2	D4
25	CALL PLOT (FX,FY,3)	D4
	REALH=IH	D4
	REALL=IL	D4
	SCALEX=(XMAX-XMIN)/REALL	D4
	SCALEY=(YMAX-YMIN)/REALH	D4
	RSCALX=1./SCALEX	D4
	RSCALY=1./SCALEY	D4
	DO 85 I=1,4	D4
	GO TO (30,35,30,35), I	D4
30	NN=IH+1	D4
	GO TO 40	D4
35	NN=IL+1	D4
40	DO 85 N=1,NN	D4
	REALN=N	D4
	GO TO (45,55,65,75), I	D4
45	R=REALN-1.	D4
	CALL PLOT (-.05+FX,R*SY+FY,2)	D4
	CALL PLOT (FX,R*SY+FY,2)	D4
	YNUM=R*SCALEY*YMIN	D4
	IF (ABS(YNUM).LE.1.E-10) YNUM=0.	D4
	RR=(REALN-1.)*SY-.03	D4
	CALL NUMBER (-.6+FX,RR+FY,.10,YNUM,0.,JFT)	D4
	CALL PLOT (FX,R*SY+FY,3)	D4
	IF (N-NN) 50,85,50	D4
50	CALL PLOT (FX,REALN*SY+FY,2)	D4
	GO TO 85	D4
55	R=REALN-1.	D4
	RR=REALH+.05	D4

```

CALL PLOT (R* $SX+FX$ ,RR* $SY+FY$ ,2) D4
CALL PLOT (R* $SX+FX$ ,REALH* $SY+FY$ ,2) D4
IF (N-NN) 60,85,60 D4
60 CALL PLOT (REALN* $SX+FX$ ,REALH* $SY+FY$ ,2) D4
GO TO 85 D4
65 R=RFALL+.05 D4
RR=REALH-REALN*1. D4
CALL PLOT (R* $SX+FX$ ,RR* $SY+FY$ ,2) D4
CALL PLOT (REALL* $SX+FX$ ,RR* $SY+FY$ ,2) D4
IF (N-NN) 70,95,70 D4
70 CALL PLOT (REALL* $SX+FX$ , (RR-1.)* $SY+FY$ ,2) D4
GO TO 85 D4
75 R=REALL-REALN*1. D4
CALL PLOT (R* $SX+FX$ , -.05* $SY+FY$ ,2) D4
CALL PLOT (R* $SX+FX$ ,  $SY+FY$ ,2) D4
XNUM=R*SCALEX*XMIN D4
IF (ABS(XNUM).LE.1.E-10) XNUM=0. D4
RR=R* $SX$ -.25 D4
CALL NUMBER (RR* $SY$ , -.25* $SY$ , .10, XNUM, 0., IFT) D4
CALL PLOT (R* $SX+FX$ ,  $SY$ ,3) D4
IF (N-NN) 80,85,80 D4
80 CALL PLOT ((R-1.)* $SX+FX$ ,  $SY$ ,2) D4
85 CONTINUE D4
90 CALL PLOT ((X(1)-XMIN)*RSCALX* $SX+FX$ , (Y(1)-YMIN)*RSCALY* $SY+FY$ ,3) D4
DO 95 I=1,NPTS
XX=(X(I)-XMIN)*RSCALX
YY=(Y(I)-YMIN)*RSCALY D4
95 CALL PLOT (XX* $SX+FX$ ,YY* $SY+FY$ ,2) D4
IF (LAST.LT.0) RETURN D4
CALL PLOT ((RFALL+3.)* $SX+FX$ ,  $SY$ , -3) D4
RETURN D4
END D4
LLIBRARY
PLOT000029
LAST
00000000000000000000000000000000
00000000000000000000000000000000
00000000000000000000000000000000

```


ETRA #1

```
FMPEF.P4.T777.CM40000.
TASK(GURRAX,46950106-5DH,ELE, )
DAFWL(.DUM)
RUN(A.,,TAPEZ)
PRESET.
MAP(PART)
LGO.
EXIT(S)
000000000000000000000000
CARDS
PROGRAM ETRA(INPUT,OUTPUT,FILMPL)
DIMENSION P(9),XPTS(10001),YPTS(1001)
1000 FORMAT(9(5X,F7.3))
1001 FORMAT(5X,10HCONTAINED ,5X,F7.3,5X,F7.3,5X,F7.3)
1002 FORMAT(5X,10HESCAPED ,5X,F7.3,5X,F7.3,5X,F7.3)
1003 FORMAT(8F7.3,4I3)
1004 FORMAT(10H I=1000 ,3(5X,F7.3))
1005 FORMAT(31H NUMBER OF ESCAPED FLECTRONS = ,I3)
1006 FORMAT(33H NUMBER OF CONTAINED ELECTRONS = ,I3)
1007 FORMAT (11X,°A°,11X,°R°,11X,°C°,9X,°DT°,9X,°ZMAX°,9X,°ENG°,9X,°THETA°
1TA°,9X,°RETA°,7X,°NX°,1X,°NY°)
1008 FORMAT(8(5X,F7.3),2I3)
90 READ 1003,A,B,C,DT,ZMAX,ENG,THETA,RETA,NX,NY,NB,NT
IF(A,FO,0.0) GO TO 170
READ 1003,RHO1,RHO2,AA,RB,CC,XSHIF,YSHIF,START
RHO2=RHO1/2.0
START=AA
BB=R*2.0
AA=A
CC=C
XSHIF=C
YSHIF=A
ABET=RETA
ATET=THETA
DO 165 MR=1,NB
DO 165 MT=1,NT
NE=0
NC=0
RETA=ARFT*FLOAT(MR-1)
THETA=ATET*FLOAT(MT-1)
THETA=THETA+START*.1745
IF((THETA.EQ.0.0).A.(BETA.GT.0.0)) GO TO 165
PI=3.14159
R=1.0
```

```

XMAX=ZMAX
IF(NX.GT.5) GO TO 12
DO 10 I=1,25
YPTS(I)=B
XPTS(I)=(2.0*C/25.0)*(FLOAT(I)-1.0)
XPTS(I+25)=2.0*C+(2.0*A/25.0)*.86603*(FLOAT(I)-1.0)
YPTS(I+25)=B+(A/25.0)*(FLOAT(I)-1.0)
XPTS(I+50)=2.0*C+2.0*A*.86603-(2.0*C/24.0)*(FLOAT(I)-1.0)
YPTS(I+50)=B+A
XPTS(I+75)=(2.0*A/25.0)*.86603*(25.0-FLOAT(I))
YPTS(I+75)=B+(A/25.0)*(25.0-FLOAT(I))
10 CONTINUE
CALL DRAW4(0.0,4.0,0.0,5.0,8,10,100,XPTS,YPTS,1,-1)
IF(RHO2.EQ.0.0) GO TO 13
DO 8 I=1,50
YPTS(I)= RR+YSHIF*.5
XPTS(I)=XSHIF+YSHIF*.86603-AA*(25.5-FLOAT(I))/25.5
8 CONTINUE
CALL DRAW4(0.0,4.0,0.0,5.0,8,10,50,XPTS,YPTS,2,-1)
DO 9 I=1,50
XPTS(I)=XSHIF+YSHIF*.86603-.86603*CC*(25.5-FLOAT(I))/24.5
YPTS(I)=YSHIF*.5+BB-.5*CC*(25.5-FLOAT(I))/24.5
9 CONTINUE
CALL DRAW4(0.0,4.0,0.0,5.0,8,10,50,XPTS,YPTS,2,-1)
13 CONTINUE
DO 11 I=1,25
XPTS(I)=2.0*.86603*(FLOAT(I)-1.0)/25.0
YPTS(I)=(FLOAT(I)-1.0)/25.0
11 CONTINUE
CALL DRAW4(0.0,4.0,0.0,5.0,8,10,25,XPTS,YPTS,2,-1)
12 CONTINUE
PRINT 1007
PRINT 1008,A,B,C,DT,ZMAX,ENG,THETA,BETA,NX,NY
PRINT 1008,RHO1,RHO2,AA,BB,CC,XSHIF,YSHIF
DO 160 KK=1,NY
DO 160 K=1,NX
I=0
Y=(FLOAT(KK)-.5)/(FLOAT(NY))
Y=Y*2.0*A
X=(FLOAT(K)-.5)/FLOAT(NX)
X=X*2.0*C
Z=0.0
V=SQRT(2.0*ENG)
VZ=V*COS(THETA)
VX=V*SIN(THETA)*COS(BETA)
VY=V*SIN(THETA)*SIN(BETA)
J=0
100 CONTINUE
J=J+1

```

```

I=I+1
CALL FIELD(A,B,C,RHO1,X,Y,Z,EE,EEY,EEZ)
CALL FIELD(AA,BB,CC,RHO2,X-XSHIF,Y-YSHIF,Z,EX,EY,FZ)
TERM1=RHO1*R*(1.0/A)+(1.0/C)
TERM2=RHO2*RB*(1.0/AA)+(1.0/CC)
TERM=-1.0/(2.0*PI)*(TERM1+TERM2)
EX=RHO1*TERM*EX+RHO2*TERM*EX
EY=RHO1*TERM*EY+RHO2*TERM*EY
EZ=RHO1*TERM*EZ+RHO2*TERM*EZ
X=X+VX*DT+EX*.5*(DT**2)
Y=Y+VY*DT+EY*.5*(DT**2)
Z=Z+VZ*DT+EZ*.5*(DT**2)
VX=VX+EX*R*DT
VY=VY+EY*R*DT
VZ=VZ+EZ*R*DT
P(3*J-2)=X
P(3*J-1)=Y
P(3*J)=Z
XPTS(I)=X+Y*.86603
YPTS(I)=Z+Y*.5
IF(XPTS(I).GT.4.0) XPTS(I)=4.0
IF(YPTS(I).GT.5.0) YPTS(I)=5.0
C IF(J.EQ.3) PRINT 1000,P
IF(J.EQ.3) J=0
IF(I.EQ.1000) PRINT 1004,X,Y,Z
IF(I-1000)110,150,150
110 IF(Z-XMAX)130,130,120
120 CONTINUE
NE=NE+1
GO TO 150
130 IF(Z)140,140,100
140 CONTINUE
NC=NC+1
150 CONTINUE
IF(NX.GT.5) GO TO 160
IF(NX.GT.5) GO TO 164
CALL DRAW4(0.0,4.0,0.0,5.0,8.10,I,XPTS,YPTS,2,-1)
164 CONTINUE
160 CONTINUE
CALL DRAW4(0.0,4.0,0.0,5.0,8.10,1,0.0,0.0,2,1)
PRINT 1006,NC
PRINT 1005,NE
165 CONTINUE
GO TO 90
170 CONTINUE
STOP
END
SUBROUTINE FIELD(A,B,C,RHO,X,Y,Z,EX,EY,EZ)
REAL N1,N2

```

```

IF (RHO.EQ.0.0) GO TO 100
PI=ACOS(-1.0)
D1=(COSH(PI*(Z-B)/A)-COS(PI*Y/A))
N1=(COSH(PI*(Z+B)/A)-COS(PI*Y/A))
D2=(COSH(PI*(Z-B)/C)-COS(PI*X/C))
N2=(COSH(PI*(Z+B)/C)-COS(PI*X/C))
TERM=1.0
EX=TERM*(PI/C)*((1.0/N2)-(1.0/(D2)))*SIN(PI*X/C)
EY=TERM*(PI/A)*((1.0/N1)-(1.0/(D1)))*SIN(PI*Y/A)
EZ1=(PI/A)*((SINH(PI*(Z+B)/A))/N1-(SINH(PI*(Z-B)/A))/(D1))
EZ2=(PI/C)*((SINH(PI*(Z+B)/C))/N2-(SINH(PI*(Z-B)/C))/(D2))
EZ=TERM*(EZ1+EZ2)
100 CONTINUE
RETURN
END
NOLIST
FUNCTION COSH(X)
COSH=(EXP(X)+EXP(-X))/2.0
RETURN
END
FUNCTION SINH(X)
SINH=(EXP(X)-EXP(-X))/2.0
RETURN
END
SUBROUTINE DRAW4 (XMIN,XMAX,YMIN,YMAX,IL,IH,NPTS,X,Y,KIND,LAST) 49
COMMON /DU/DU
COMMON /R22/ SX,SY,FX,FY
DIMENSION X(NPTS), Y(NPTS)
DATA JFT,JFT,FX,FY,SX,SY/4HF8.3,4HF6.2,0.6,0.59,.80,.80/
XM=XMAX-XMIN
YM=YMAX-YMIN
REALH=IH
REALL=IL
SCALEX=XM/REALH
SCALEY=YM/REALH
RSCALX=1./SCALEX
RSCALY=1./SCALEY
IF (KIND-1) 10,20,5
5 IF (KIND-2) 10,110,10
10 PRINT 15, KIND
15 FORMAT (41H THE KIND OF GRAPH ASKED FOR IS IN ERROR,F8.2)
RETURN
20 IF (I0-2) 25,30,25
25 CALL PLOTS (T9,TR,10)
I0=2
30 CALL PLOT (FX,FY,3)
DO 90 I=1,4
GO TO (35,40,35,40), I
35 NN=IH+1

```

```

GO TO 45
40 NN=IL+1
45 DO 90 N=1,NN
REALN=N
GO TO (50,60,70,80), I
50 R=REALN-1.
CALL PLOT (-.05*FX,R*SY+FY,2)
CALL PLOT (FX,R*SY+FY,2)
YNUM=R*SCALEY+YMIN
IF (ABS(YNUM).LE.1.E-10) YNUM=0.
RR=(REALN-1.)*SY-.03
CALL NUMBER (-.6*FX,RR*FY,.10,YNUM,0.,JFT)
CALL PLOT (FX,R*SY+FY,3)
IF (N-NN) 55,90,55
55 CALL PLOT (FX,REALN*SY+FY,2)
GO TO 90
60 R=REALN-1.
RR=REALH+.05
CALL PLOT (R*SX+FX,RR*SY+FY,2)
CALL PLOT (R*SX+FX,REALH*SY+FY,2)
IF (N-NN) 65,90,65
65 CALL PLOT (REALN*SX+FX,REALH*SY+FY,2)
GO TO 90
70 R=REALN+.05
RR=REALH-REALN+1.
CALL PLOT (R*SX+FX,RR*SY+FY,2)
CALL PLOT (REALN*SX+FX,RR*SY+FY,2)
IF (N-NN) 75,90,75
75 RRR=RR-1.
CALL PLOT (REALN*SX+FX,RRR*SY+FY,2)
GO TO 90
80 R=REALN-1.
CALL PLOT (R*SX+FX,-.05*FY,2)
CALL PLOT (R*SX+FX,FY,2)
XNUM=R*SCALEX+XMIN
IF (ABS(XNUM).LE.1.E-10) XNUM=0.
RR=R*SX-.25
CALL NUMBER (R*FX,-.25*FY,.10,XNUM,0.,IFT)
CALL PLOT (R*SX+FX,FY,3)
IF (N-NN) 85,90,85
85 RRR=R-1.
CALL PLOT (RRR*SX+FX,FY,2)
90 CONTINUE
YY=-YMIN*RSCALY
XX=-XMIN*RSCALX
IF (YMIN) 95,100,100
95 CALL PLOT (FX,YY*SY+FY,3)
CALL PLOT (REALN*SX+FX,YY*SY+FY,2)
100 IF (XMIN) 105,110,110

```

```

105 CALL PLOT (XX*SX+FX,FY,3) ..... 04
CALL PLOT (XX*SX+FX,REALH*SY,FY,2)
110 XX=(X(1)-XMIN)*RSCALX
YY=(Y(1)-YMIN)*RSCALY
CALL PLOT (XX*SX+FX,YY*SY,FY,3)
DO 115 I=1,NPTS
XX=(X(I)-XMIN)*RSCALX
YY=(Y(I)-YMIN)*RSCALY
CALL PLOT (XX*SX+FX,YY*SY,FY,2)
115 CONTINUE
IF (LAST) 120,125,125
120 RETURN
125 R=RFALL+3.
CALL SYMBOL(6.4,7.0,.14,DU4,0,.13)
CALL PLOT (R*SX+FX,FY,-3)
RETURN
END

```

```

LIBRARY .....
PLOT000029 .....
LAST .....
000000000000000000000000 .....
+01.000+01.000+01.000+00.030+03.000+02.000+00.174+00.393+10+10+03+04 .....
+01.000+00.000 3.0 .....
000000000000000000000000 .....
000000000000000000000000 .....

```

ETRA #2

```

PROGRAM ETRA(INPUT,OUTPUT,FILMPL)
DIMENSION P(9),XPTS(1001),YPTS(1001) ,X1(100),X2(100)
EQUIVALENCE (V0,V0)
1000 FORMAT(9(5X,F7.3))
1001 FORMAT(5X,10HCONTAINED ,5X,F7.3,5X,F7.3,5X,F7.3)
1002 FORMAT(5X,10HESCAPED ,5X,F7.3,5X,F7.3,5X,F7.3)
1003 FORMAT(8F7.3,4I3)
1004 FORMAT(10H I=1000 ,3(5X,F7.3))
1005 FORMAT(31H NUMBER OF ESCAPED ELECTRONS = ,I3)
1006 FORMAT(33H NUMBER OF CONTAINED ELECTRONS = ,I3)
1007 FORMAT (11X,*A*,11X,*B*,11X,*C*,9X,*D*,9X,*ZMAX*,8X,*ENG*,9X,*THETA*
11A*,9X,*BETA*,7X,*NX*,1X,*NY*)
1008 FORMAT(8(5X,F7.3),2I3)
P1=ACOS(-1.0)
90 READ 1003,SKIP,AA
READ 1003,A,B,C,D1,ZMAX,ENG,THETA,BETA,NX,NY,NB,NI
IF(A.EQ.0.0) GO TO 170
READ 1010,CRAD,VO,NN
1010 FORMAT(2F7.3,I3)
IF(SKIP.EQ.1.0) GO TO 80
DIM=1.0
IF(NY.LE.1) DIM=0.0
AA=V0*AA/(PIC(CRAD,B,A,D,CRAD,1.0)+DIM*PIC(A,B,A,B,CRAD,1.0))
KK=NN
IF(NY.EQ.1) GO TO 777
NN=0
DO 776 I=1,KK
776 NN=I*NN
777 CONTINUE
READ 1011,(X1(I),I=1,NN)
PRINT 1011,(X1(I),I=1,NN)
READ 1011,(X2(I),I=1,NN)
PRINT 1011,(X2(I),I=1,NN)
PINF=P1*2.0*(1.0+DIM)*AA*B/A+X2(1)
NN=KK
80 CONTINUE
ABET=BETA
ATEI=THETA
DO 165 MB=1,NB
DO 165 MT=1,NI
NE=0
NWRITE=0
1011 FORMAT(7G11.4)
NC=0
BETA=ABET*FLOAT(MB-1)
THETA=ATEI*FLOAT(MT-1)
IF((THETA.EQ.0.0),A.(BETA.GT.0.0)) GO TO 165
PI=3.14159
K=1.0
XMAX=ZMAX
IF(NX.GT.5) GO TO 12
IF(NY.EQ.1) CALL DRAW4 (0.0,4.0,0.0,5.0,9.10,1.0,0.0,0.0,1,-1)
IF(NY.EQ.1) GO TO 14
DO 10 I=1,25
YPTS(I)=B
XPTS(I)=(2.0*C/25.0)*(FLOAT(I)-1.0)
XPTS(I+25)=2.0*C+(2.0*A/25.0)*.86603*(FLOAT(I)-1.0)
YPTS(I+25)=B+(A/25.0)*(FLOAT(I)-1.0)

```

```

XPTS(I+50)=2.0*C+2.0*A*.86603-(2.0*C/24.0)*(FLOAT(I)-1.0)
YPTS(I+50)=B+A
XPTS(I+75)=(2.0*A/25.0)*.86603*(25.0-FLOAT(I))
YPTS(I+75)=B+(A/25.0)*(25.0-FLOAT(I))
10 CONTINUE
CALL DRAW4(0.0,4.0,0.0,5.0,8.10,100,XPTS,YPTS,1,-1)
DO 11 I=1,25
XPTS(I)=2.0*.86603*(FLOAT(I)-1.0)/25.0
YPTS(I)=(FLOAT(I)-1.0)/25.0
11 CONTINUE
CALL DRAW4(0.0,4.0,0.0,5.0,8.10,25,XPTS,YPTS,2,-1)
14 CONTINUE
12 CONTINUE
PRINT 1007
PRINT 1008,A,B,C,DI,MAX,ENG,THETA,BETA,NX,NY
PRINT 1010,CRAD,VO,WA
ENG=ENG*PI*NF
DO 160 KK=1,NY
DO 160 K=1,NX
I=0
Y=(FLOAT(KK)-.5)/FLOAT(NY)
Y=Y*2.0*A
IF(NY.EQ.1) Y=0.0
X=(FLOAT(K)-.5)/FLOAT(NX)
X=X*2.0*C
Z=0.0
V=SQRT(2.0*ENG)
VZ=V*COS(THETA)
VX=V*SIN(THETA)*COS(BETA)
VY=V*SIN(THETA)*SIN(BETA)
J=0
100 CONTINUE
J=J+1
I=I+1
CALL FIELD(A,B,C,X,Y,Z,DT,VX,VY,VZ,NV,EX,EY,EZ,X1,X2,NY,AA)
EX=EX/VO
EY=EY/VO
EZ=EZ/VO
EX=-EX
EY=-EY
EZ=-EZ
X=X+VX*DT*EX*.5*(0.0**2)
Y=Y+VY*DT*EY*.5*(0.0**2)
Z=Z+VZ*DT*EZ*.5*(0.0**2)
VX=VX+EX*R*DT
VY=VY+EY*R*DT
VZ=VZ+EZ*R*DT
XWIRE=Y
XWIRE=X
P(3*J-2)=X
P(3*J-1)=Y
P(3*J)=Z
XPTS(I)=X+Y*.86603
YPTS(I)=Z+Y*.5
IF(XPTS(I).GT.4.0) XPTS(I)=4.0
IF(YPTS(I).GT.5.0) YPTS(I)=5.0
IF(J.EQ.3) J=0
200 IF(ABS(XWIRE).GT.A) XWIRE=XWIRE-SIGN(A*.2,XWIRE)

```



```

IF (ABS(XWIRE).GT.A) GO TO 200
IF (N1.LE.1) GO TO 215
IF (ABS(YWIRE).GT.A) YWIRE=YWIRE-SIGN(A*.YWIRE)
IF (ABS(YWIRE).GT.A) GO TO 210
F=CRAD
IF ((XWIRE**2+(Z-B)**2).LE.(F**2)).OR.((YWIRE**2+(Z-B)**2)
1.LE.(CRAD**2)) GO TO 220
GO TO 230
215 IF (XWIRE**2+(Z-B)**2).LE.(CRAD**2) GO TO 220
GO TO 230
220 NWIRE=NWIRE+1
GO TO 150
230 CONTINUE
IF (I.EU.100) PRINT 1004,X,Y,Z
IF (I-100) 110,150,150
1004 FORMAT(* NUMBER OF ELECTRONS HITTING WIRE = *,I3)
110 IF (Z-XMAX) 130+130+120
120 CONTINUE
NE=NE+1
GO TO 150
130 IF (Z) 140,140+100
140 CONTINUE
NC=NC+1
150 CONTINUE
IF (NA.GT.5) GO TO 160
IF (NA.GT.5) GO TO 164
CALL DRAM4(0.0,4.0,0.0,5.0,8.10,1.0,0.0,0.2,1)
164 CONTINUE
160 CONTINUE
CALL DRAM4(0.0,4.0,0.0,5.0,8.10,1.0,0.0,0.2,1)
PRINT 1006,NC
PRINT 1005,NE
PRINT 1009,NWIRE
165 CONTINUE
GO TO 90
170 CONTINUE
STOP
END

```

```

SUBROUTINE FELD(A, C, X, Y, Z, D1, V, V, V, V, V, L, E, Y, E, L, X), M, Z, NY, AA)
DIMENSION X1(100), X2(100)
EX=ET=ELZ=0.0
UX=VX*DT
UY=VY*DT
UZ=VZ*DT
DIM=1.0
IF(NY.LE.1) DIM=0.0
IF(UX.LE.0.01) DX=.01
IF(UY.LE.0.01) DY=.01
IF(UZ.LE.0.01) DZ=.01
POT1=PIC(X,Z+A*B,C+A)
POT2=DIM*PIC(Y,Z+A*B,C+AA)
POT=PO11*PO12
EX=(PIC(X,DX,Z+A*B,C+AA)-POT1)/DX
EY=(DIM*PIC(Y,DY,Z+A*B,C+AA)-POT2)/DY
EZ=(PIC(X,Z+DZ+A*B,C+AA)+DIM*PIC(Y,Z+DZ+A*B,C+AA)-POT1)/DZ
IF(NY.LE.1) GO TO 300
ISTEP=0
IJ1=0
IJ2=1
KK=NM
N=0
DO 1101 I=1, KK
1101 M=N+1
DO 200 J=1, N
IJ1=IJ1+1
IJ2=IJ1+1STEP
IF(IJ2.GT.KK) IJ1=1
IF(IJ2.GT.KK) ISTEP=1STEP+1
IF(IJ2.GT.KK) IJ2=1IJ1+1STEP
IF(Z.G1.R) GO TO 100
POT=PI1(IJ1,IJ2,X,Y,Z+A*B,C)
EX=(PI1(IJ1,IJ2,X+DX,Z+A*B,C)-POT1)*X1(J)/DX*EX
EY=(PI1(IJ1,IJ2,X,Y,Z+A*B,C)-POT1)*X1(J)/DY*EY
EZ=(PI1(IJ1,IJ2,X,Y,Z+DZ+A*B,C)-POT1)*X1(J)/DZ*EZ
GO TO 200
100 CONTINUE
POT=PI2(IJ1,IJ2,X,Y,Z+A*B,C)
EX=(PI2(IJ1,IJ2,X+DX,Z+A*B,C)-POT1)*X2(J)/DX*EX
EY=(PI2(IJ1,IJ2,X,Y,Z+A*B,C)-POT1)*X2(J)/DY*EY
EZ=(PI2(IJ1,IJ2,X,Y,Z+DZ+A*B,C)-POT1)*X2(J)/DZ*EZ
200 CONTINUE
RETURN
300 CONTINUE
DO 500 J=1, NM
IF(Z.G1.H) GO TO 400
POT=PI1(IJ1,IJ2,X,Z+A*B,C)
EX=(PI1(IJ1,IJ2,X+DX,Z+A*B,C)-POT)*X1(J)/DX*EX
EZ=(PI1(IJ1,IJ2,X,Z+DZ+A*B,C)-POT)*X1(J)/DZ*EZ
GO TO 500
400 CONTINUE
POT=PI12(IJ1,IJ2,X,Z+A*B,C)
EX=(PI12(IJ1,IJ2,X+DX,Z+A*B,C)-POT)*X2(J)/DX*EX
EZ=(PI12(IJ1,IJ2,X,Z+DZ+A*B,C)-POT)*X2(J)/DZ*EZ
500 CONTINUE
RETURN
END

```

```

FUNCTION P11(M1,N2,(Y,Z),A,B,C)
N1=M1-1
N2=N2-1
IF((Y1,N2).EQ.0) GO TO 100
P1=ACOS(-1.0 )
FACT=P1*SQRT((FLUAT(11))**2.+(FLUAT(N2))**2) /A
P11=COS(P1*FLUAT(Y1)*X/A)*COS(P1*FLUAT(N2)*Y/A)*SINH(FACT*Z)
1/SINH(FACT*B)
TEMP=N1
N1=N2
N2=TEMP
P11=COS(P1*FLUAT(N1)*X/A)*COS(P1*FLUAT(N2)*Y/A)*SINH(FACT*Z)
1/SINH(FACT*B)
TEMP=N1
N1=N2
N2=TEMP
GO TO 200
100 CONTINUE
P11=Z/B
200 CONTINUE
N2=N2+1
N1=N1+1
RETURN
END

```

```

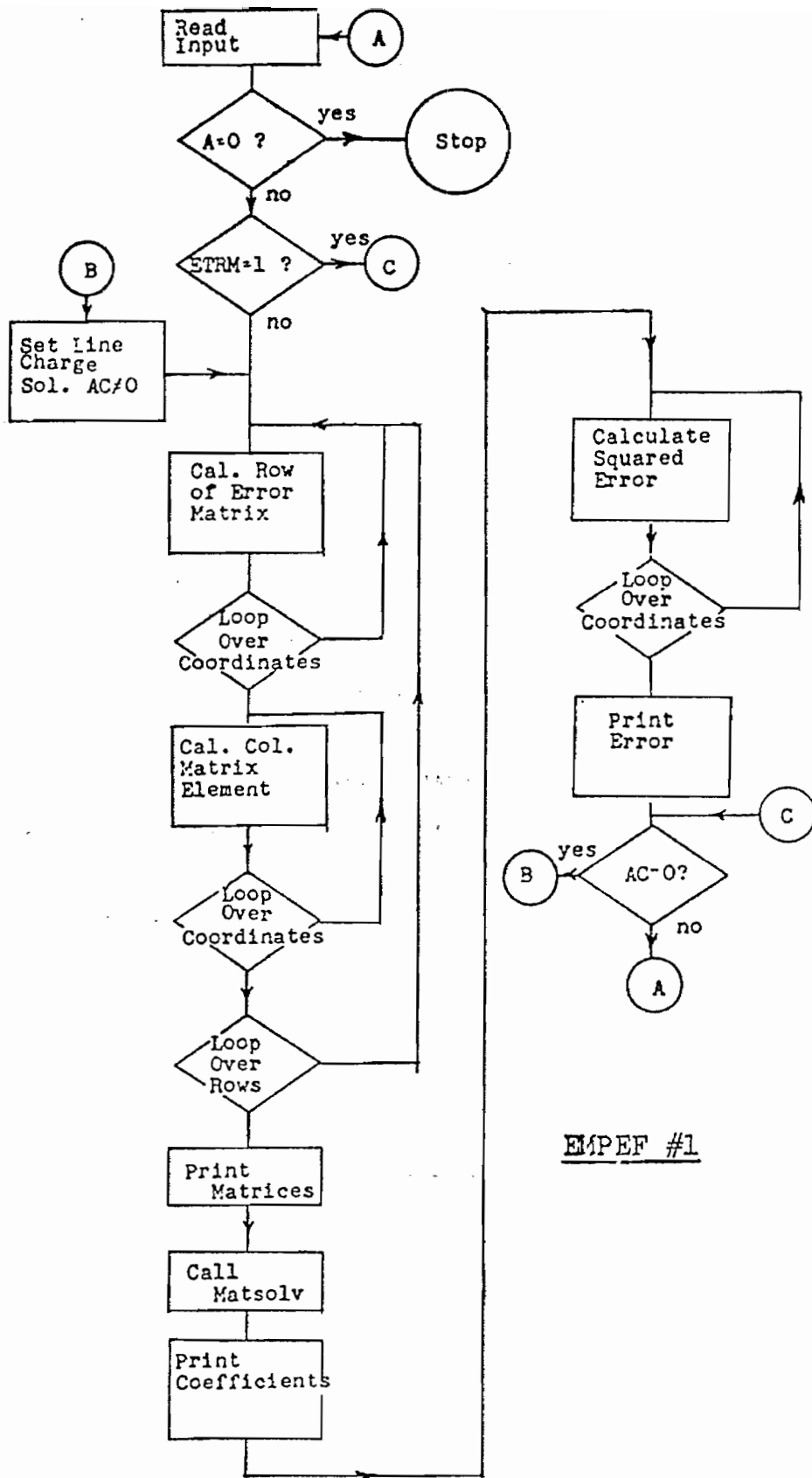
FUNCTION P12(M1,N2,X,Y,Z),A,B,C)
P1=ACOS(-1.0)
N1=M1-1
N2=N2-1
FACT=P1*SQRT((FLUAT(11))**2.+(FLUAT(N2))**2)
FACT=FACT/A
P12=COS(P1*FLUAT(N1)*X/A)*COS(P1*FLUAT(N2)*Y/A)*EXP(FACT*(B-Z))
TEMP=N1
N1=N2
N2=TEMP
P12=COS(P1*FLUAT(N1)*X/A)*COS(P1*FLUAT(N2)*Y/A)*EXP(FACT*(B-Z))
1*P12
P12=PI/2.0
TEMP=N1
N1=N2
N2=TEMP
N2=N2+1
N1=N1+1
RETURN
END

```

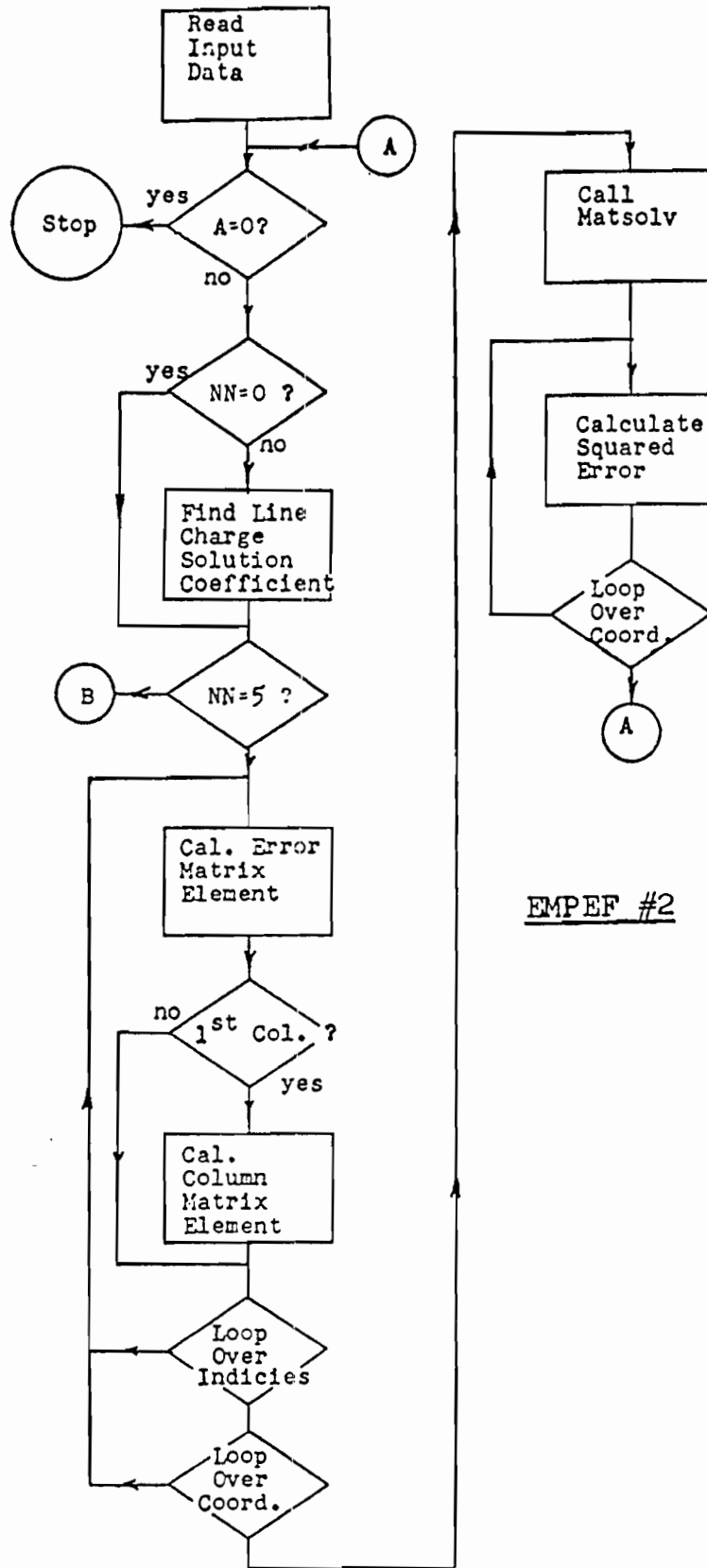
```

FUNCTION PIC(X,Y,A,B,C,AC)
PIC=0.0
P1=3.14159
I1=COSH(P1*(Y+B)/A)-COS(P1*X/A)
I2=COSH(P1*(Y-B)/A)-COS(P1*X/A)
IF(ABS(I2).LT).0.0001)GO TO 100
PIC=AC*ALOG(I1/I2)
100 RETURN
END

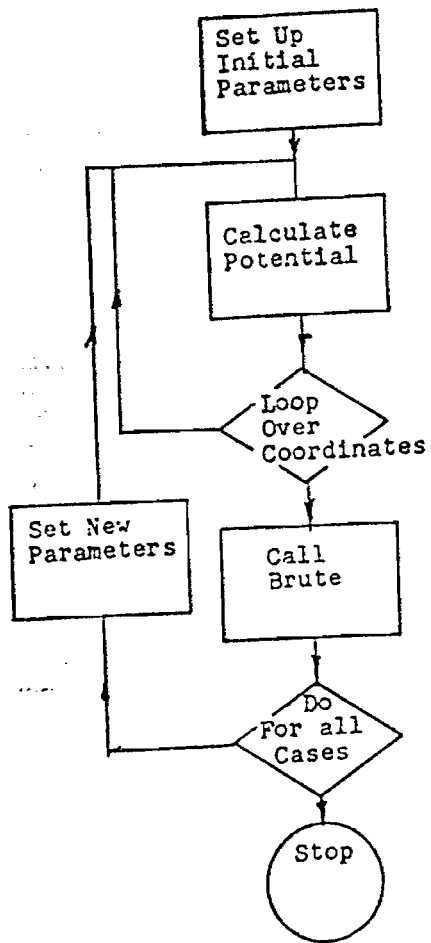
```



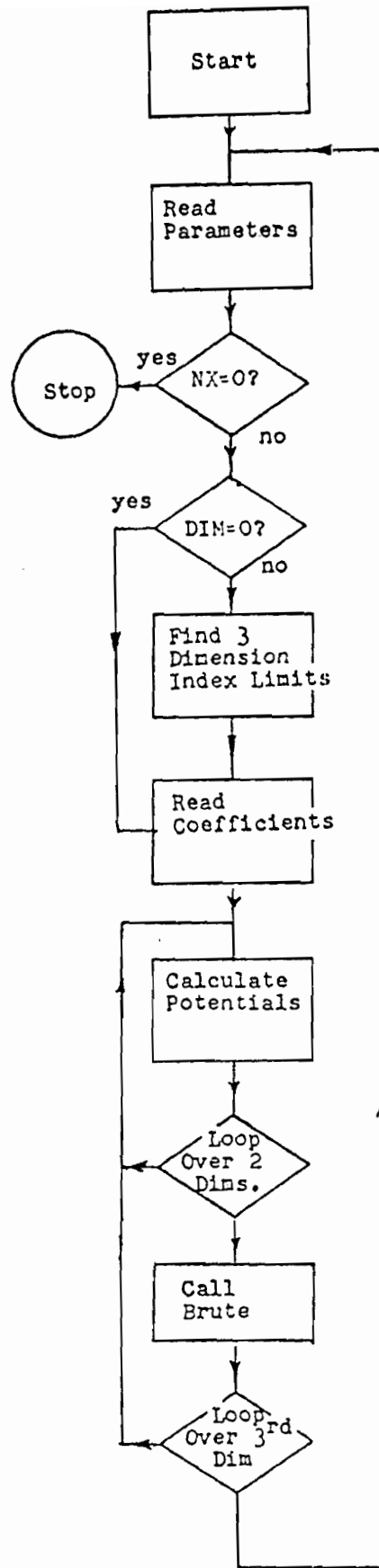
EMPEF #1



EMPEF #2



BRPHI #1



BRPHI #2

7/2/85

